DOKUZ EYLUL UNIVERSITY
GRADUTAE SCHOOL OF NATURAL AND APPLIED SCIENCES

FLOODPLAIN MANAGEMENT BASED ON THE HEC-RAS MODELING SYSTEM

by

Gülay ONUŞLUEL

September, 2005
IZMIR

FLOODPLAIN MANAGEMENT BASED ON THE HEC-RAS MODELING SYSTEM

A Thesis Submitted to the
Graduate School of Natural and Applied Sciences of Dokuz Eylul University
In Partial Fulfillment of the Requirements for the Degree of Doctor of Philosophy in
Civil Engineering, Hydraulics Hydrology and Water Resources Program

by
Gülay ONUŞLUEL

September, 2005
IZMIR

CONTENTS

Page

ACKNOWLEDGMENTS

The author would like to express her gratitude to her advisor, Prof. Dr. Nilgun Harmancioglu, who has always been very supportive of her work. She is also grateful to all her colleagues who have helped her throughout this research.

A special thank also goes to Mr. Ali Gul, her colleague, for his invaluable help on the GIS analyses and for his great moral support. His expertise and support throughout her research made this project possible.

Additionally, she feels herself indebted to Prof. Dr. Ertugrul Benzeden due to the fact that the results of her work would have been less than desirable without his assistance during some trying times.

Finally, she would sincerely like to thank her family. They have always been there to set her on the right path and for that she is eternally grateful.

Gülay ONUŞLUEL

FLOODPLAIN MANAGEMENT
BASED ON
THE HEC-RAS MODELING SYSTEM

ABSTRACT

The aim of this study is to determine floodplains based on the HEC-RAS modeling system by using Geographic Information Systems (GIS).

Since floods are still among the major causes of serious damages in many regions throughout the world, the relationship between flood characteristics and the surrounding area they inundate should be examined in depth to cope with flood related disasters.

An in-depth study on floods and floodplains requires the analysis of hydrologic, hydraulic, topographic, and other related components in temporal and spatial scales. Most of the floodplain delineation methods used about a decade ago were manual applications, rather than technologically supported ones, and required a significant amount of time and effort. Recently, a more complicated but a more robust technique, commonly named as "the automated floodplain determination technique", has been used to determine more accurately where and when flooding may occur. By using this technique, it is possible to reduce the computation time while improving the accuracy of flood rate estimation and the determination of flood inundation boundaries. Hydrologic/hydraulic models and Geographic Information System (GIS) tools offer an ideal environment for this type of work.

In this study, the hydraulic model HEC-RAS is applied to a critical location within the Bostanli Basin in Izmir both for steady and unsteady flow simulations. Flood peaks and hydrographs are extracted from the hydrologic model, HEC-HMS, and its outputs are utilized as HEC-RAS inputs. Water depths extracted from HEC-RAS are then transferred into ArcView software using its compatible extensions to identify and visualize floodplains in a spatial framework.

Keywords : Floods, floodplain management, HEC-RAS, HEC-HMS, GIS.

HEC-RAS MODELLEME SİSTEMİNE DAYALI TAŞKIN ALANI YÖNETİMİ

ÖZ

Bu çalışmada, taşkın alanlarının HEC-RAS modelleme sistemi ve Coğrafi Bilgi Sistemleri (CBS) kullanılarak belirlenmesi ve görsel olarak ortaya konması amaçlanmıştır.

Taşkınlar hala dünyanın birçok bölgesinde meydana ciddi hasarların nedenleri arasında bulunduğundan, taşkın karakteristikleri ve taşkın altında kalan alanlar arasındaki ilişkinin taşkın nedenli felaketlerle baş etmek için detaylı bir şekilde araştırılması gerekmektedir.

Taşkın ve taşkın alanları üzerine yapılacak detaylı bir çalışma; hidrolojik, hidrolik, topoğrafik ve diğer ilişkili unsurların zaman ve alan boyutunda analizini gerekli kılmaktadir. Yaklaşık on yıl öncesine kadar kullanılan taşkın alanı belirleme yöntemlerinin çoğu, teknoloji desteğinden uzak ve önemli oranda zaman ve emek gerektiren manuel uygulamalar şeklinde olmuştur. Son zamanlarda, "otomatize taşkin yatağı belirleme tekniği" olarak bilinen biraz daha karmaşık ama daha dayanıklı bir teknik, taşkınların nerede ve ne kadar bir süre sonra olacağının daha doğru tahmini için kullanılmaya başlanmıştır. Bu yöntem sayesinde, taşkın tahmini ve taşkın alanı belirlenmesinin daha doğru ve daha kısa sürede yapılması mümkün olmaktadır. Bu türden bir çalışma için, hidrolojik/hidrolik modeller ile Coğrafi Bilgi Sistemleri ideal bir destek oluşturmaktadır.

Bu çalışmada, HEC-RAS hidrolik modeli Izmir Bostanlı Havzası'ndaki kritik yerlere kararlı ve kararsız akım simülasyonlarının oluşturulması amacıyla uygulanmıştır. Taşkın pik değerleri ve taşkın hidrografları HEC-HMS hidrolojik modeli ile elde edilmiş ve bu model çıktıları HEC-RAS modelinde girdi olarak kullanılmıştır. HEC-RAS modelinden elde edilen su derinlikleri daha sonra ArcView sistemine uygun ArcView yardımcı programları ile aktarılmış ve böylece taşkın altında kalabilecek olan alanlar belirlenerek görsel hala getirilmiştir.

Keywords: Taşkınlar, taşkın alanı yönetimi, HEC-RAS, HEC-HMS, CBS.

CHAPTER ONE
INTRODUCTION

1.1 Problem Statement

Since floods are still among the major causes of serious damages in many regions throughout the world, the relationship between flood characteristics and the surrounding area they inundate should be examined in depth to cope with flood related disasters. Various types of flooding events may be identified on the basis of their causes and the environment they impact. Fluvial floods can occur as flash floods or plain floods. Other types of flooding can also be identified as: coastal flooding due to waves and surges, floods resulting from the catastrophic failures of hydraulic structures like dams, groundwater floods due to long term accumulation of precipitation, and pluvial floods where local drainage systems cannot evacuate intense storm rainfall. Flash floods are indeed a real problem in densely populated urban areas, regarding their economic impacts and infrastructure failures in metropolitan areas. A number of flood disasters, especially in the form of flash floods, have occurred throughout the city of Izmir, Turkey, which is a highly urbanized and industrial city.

An in-depth study on floods and floodplains requires the analysis of hydrologic, hydraulic, topographic, and other related components in temporal and spatial scales. Most of the floodplain delineation methods used about a decade ago were manual applications, rather than technologically supported ones, and required a significant amount of time and effort. Recently, a more complicated but a more robust technique, commonly named as “the automated floodplain determination technique”, has been used to determine more accurately where and when flooding may occur. By using this technique, it is possible to reduce the computation time while improving the accuracy of flood rate estimation and the determination of flood inundation boundaries. Hydrologic/hydraulic models and Geographic Information System (GIS) tools offer an ideal environment for this type of work.

Peak flows associated with an extreme storm event can cause flooding. In order to anticipate this flooding risk, hydrologic modeling is often used to calculate the quantity of runoff that is generated for each rainfall event that occurs in a particular watershed. Hydraulic modeling, on the other hand, is used to determine the water surface profiles that can be expected from the runoff estimated by hydrologic modeling. Evaluation of the resulting floodplain is a time-consuming process which, in the past, had been accomplished by manually plotting the extent of the floodplain on paper maps. Automating this process with the aid of GIS can indeed result in significant savings on time and resources in the design process.

The following steps are often used to determine floodplain maps in an effective way supported by information technologies:

1) derivation of geospatial data to be used in the model(s);
2) hydrologic modeling where the rainfall-runoff process is simulated by using a design storm or historic storm event;
3) hydraulic modeling by which the flood runoff along stream channels is routed for the determination of water surface profiles;
4) floodplain mapping and visualization (Shrestha, 2000).

Geographic information tools, in the form of a variety of professional software applications, have a widespread use in many fields of science. In particular, these tools proved to be very effective in studies related to hydrology and water management due to the distributed spatial character of water related processes. GIS tools have also been used effectively in many floodplain management studies. A number of GIS- based automated floodplain delineation tools have been developed by several organizations in different countries. Although the lack of good quality digital data and poor inter-disciplinary cooperation between these organizations and decision makers lead to some difficulties on the use of these tools, the increased number of qualified engineers involved in both GIS and modeling studies facilitated the widespread use of automated floodplain delineation tools (Benavides, 2001).

In general, the automated floodplain delineation procedure is similar to the traditional approach, but there are some significant differences. Automated floodplain delineation requires special software and digital maps to derive basin parameters and water surface profiles more accurately. It is evident that the outcomes are more reliable as the accuracy of estimates is increased by the use of geospatial data. On the other hand, the accuracy of floodplain delineation depends also on the modeler's judgment so that engineering experience is very important in automated floodplain studies.

The new programs released by the U.S. Army Corps of Engineers, Hydrologic Engineering Center (HEC) are quickly replacing their predecessors in the analysis of geospatial data. HEC's recently released HEC-HMS and HEC-RAS, along with their geospatial counterparts, HEC-GeoHMS and HEC-GeoRAS, are mainly designed to work with a wide variety of recently available digital data (HEC, 2001a; HEC, 2001b). With respect to flood studies, the River Analysis System (HEC-RAS) hydraulic model and the Hydrologic Modeling System (HEC-HMS) hydrologic model are accepted as valid modeling tools by Federal Emergency Management Agency (FEMA) (FEMA, 2004). These tools, when used jointly with GIS, can help to develop the relationship between flood characteristics and the inundated areas in an automated framework.

It follows from the above that the basic problem addressed in the presented study is to improve the accuracy of flood rate estimation and that in the determination of flood inundation boundaries, thereby reducing the computational time and efforts required for such a study. To this end, the use of automated techniques comprising HEC-RAS and HEC-HMS modeling tools along with GIS is investigated.

1.2 Objectives and Scope of the Study

The objectives of the presented study are twofold and, thereby, include two components: a research component and an application component. These components can be summarized as the following:

A) Research component, where the basic objective is to address the basic problem identified in Section 1.1, i.e., to improve the accuracy of flood rate estimation and that in the determination of flood inundation boundaries. This component comprises the use of "automated floodplain determination techniques" which, not only improve the accuracy of the analysis, but also reduce the computational time and manual efforts in floodplain identification;

B) Application Component, where the techniques investigated with the Research Component, is applied to the case of the Bostanli basin in Izmir, which has suffered significant flood damages for years within its densely populated and urbanized boundaries.

To realize the study components, the hydraulic model HEC-RAS is applied to a critical location within a study area for unsteady flow simulation. Flood peaks and hydrographs are extracted from the hydrologic model HEC-HMS, and its outputs are utilized as HEC-RAS inputs. Water depths extracted from HEC-RAS are then transferred into ArcView software using suitable ArcView extensions to identify and visualize floodplains in a spatial framework.

The following steps are accomplished to achieve the objectives of the study:

1. Evaluating the overall flooding problem in the case basin, while determining a suitable area for research purposes and a detailed analysis;
2. Creating Digital Elevation Model (DEM) and Triangular Irregular Network (TIN) to digitally represent the topography within the case study area;
3. Delineating the basin boundaries, and developing input files, which include basin properties and a schematic diagram to be used in HEC-HMS by running its HEC-GeoHMS extension on a GIS software platform (ArcView);
4. Running the HEC-HMS model;
5. Importing HMS Results in the form of peak discharges and/or flood hydrographs into HEC-RAS;

6. Running the HEC-RAS model to obtain water surface profiles under the already defined conditions;
7. Developing a visual floodplain representation by transferring the HEC-RAS model results through a postprocessing step;
8. Creating two and three-dimensional flood animations under current and expected future conditions.

1.3 Research Outline

The study presented comprises 11 chapters. This chapter provides an introduction to the study and identifies the objectives of the research. Chapter 2 investigates literature related to hydrologic and hydraulic modeling for floodplain management. Chapters 3, 4, and 5 focus on methods of hydrologic and hydraulic modeling and floodplain management. Chapter 6 gives detailed information about the tools used in this research, including HEC-HMS, HEC-GeoHMS, HEC-RAS, and HEC-GeoRAS. Chapter 7 provides an overview of the case study area. Chapter 8 and Chapter 9 present model applications, and Chapter 10 describes results of the study. Finally, conclusions are given in Chapter 11.

CHAPTER TWO
LITERATURE REVIEW ON AUTOMATED FLOODPLAIN DETERMINATION

Flood analyses have become more effective by transferring hydraulic model outputs into a GIS environment. Numerous studies have been used to link a hydraulic model to a spatial visualization model in order to find an optimum combination of various methods. As the number of studies on improvement of the linkage between hydraulic models and GIS software increased, the application of these tools on problem solving has become more effective and feasible.

Djokic et al. (1994) developed an interface known as ARC/HEC2 between the 1-D steady-state hydraulic model HEC-2 of the Hydrologic Engineering Center and the ArcInfo GIS software. This interface was used to export terrain data from ArcInfo into HEC-2 and convert HEC-2 water surface elevations into GIS coverages compatible with ArcInfo.

In the following years, due to the increased use of Windows-based software, HEC released a Windows-compatible counterpart to HEC-2, called the River Analysis System (RAS). The Graphical User Interface (GUI) of the HEC-RAS was programmed in Visual Basic programming language while flow computation algorithms were compiled in the FORTRAN language.

Evans (1998) developed pre- and post-processor tools for the HEC-RAS package. These tools were designed to transfer physical element properties mutually between hydrologic/hydraulic models and the GIS software. The preprocessor tool creates a data exchange file that consists of channel and reach geometry extracted from terrain models. After the hydraulic computation is accomplished, HEC-RAS exports the output data back to a GIS using postprocessor tool. In 1998, Environmental Research Institute in the USA (ESRI) developed the Arcview GIS extension, AVRas, by improving Evans' tools and adding new features to promote the use of HEC-RAS.

Tate (1999) developed the Avenue scripts to build a connection between the HEC-RAS model and ArcView GIS, providing an advanced analysis of floodplain data and visualization (Figure 2.1).

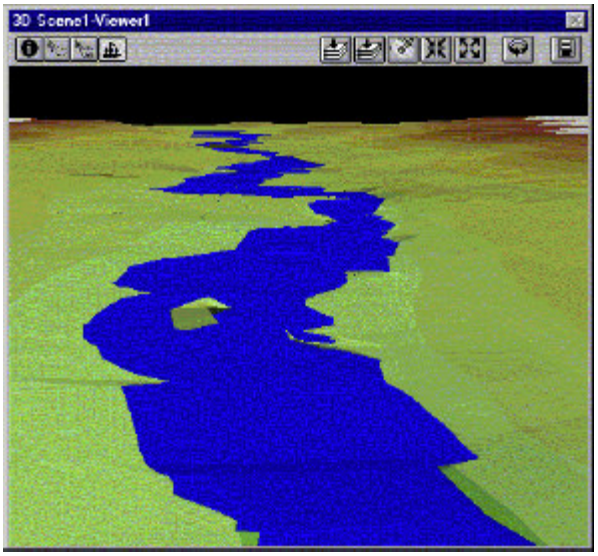

Figure 2.1 Channel geometry incorporated into a digital terrain model (Tate, 1999).

Gonzales (1999) used the SMS (FESWMS) model and the one dimensional HEC-RAS hydraulic model to develop a calibrated two dimensional finite element model of the Red River Floodway, which is very valuable in providing flood protection for the City of Winnipeg in Canada. In this improved study, it was also intended to determine the maximum capacity, of the floodway channel, to find possible means to increase the channel capacity and to identify the location and magnitude of spills associated with flows larger than the maximum capacity.

Olivera and Maidment (1999) developed a GIS to facilitate the design of highway drainage facilities by reducing the analysis time and improving hydraulic computations and analyses. In the first step of this research, a spatial database of the hydrologic system was developed. Afterwards, CRWR-PrePro was introduced at the Center for Research in Water Resources (CRWR) to model the hydrologic phenomena and then to obtain flood

discharges using the HEC-HMS model. The HEC-RAS model was used to compute water levels by using HEC-HMS outputs. Finally, computed water levels were mapped on the spatial data, using AVRas to generate floodplains.

Azagra et al. (1999) selected a smaller study area, the Waller Creek watershed in Austin, Texas, to validate the existing floodplain determination and visualization tools that use terrain data from a Triangulated Irregular Network (TIN), obtained as a result of processing aerial images of the project area (Figure 2.2). Following the creation of the TIN, validation of the information was performed, using the available field data; and this information was then transferred to the HEC-RAS model to derive channel and stream geometry. Two and three dimensional flood inundation maps and animations were developed in ArcView GIS. Since Azagra and Olivera used the steady state HEC-RAS model, the process of developing flood animations was tiresome. Furthermore, the HEC-RAS model may not have been sufficient to give accurate outputs, since the cross-section data based on the terrain information from aerial photography did not account for existing water surfaces in the stream channel when the photographs were taken.

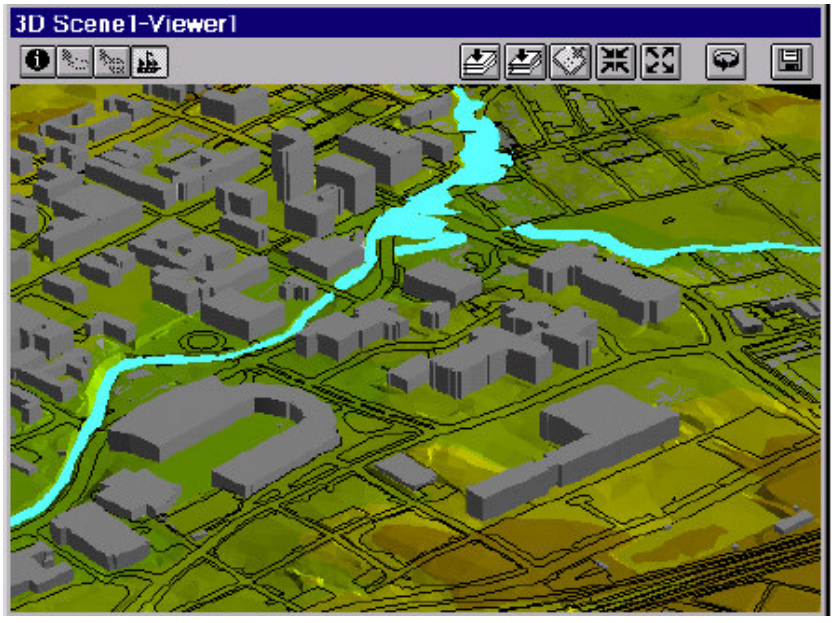

Figure 2.2 Flood visualization using AVRAS and a TIN (Azagra, 1999).

Andrysiak and Maidment (2000) carried out an application project to determine floodplain areas for the Mill Creek Basin in Hamilton County in southwestern Ohio by using floodplain determination and visualization tools developed at the Center for Research in Water Resources at the University of Texas in Austin. They used a digital elevation model (DEM) with 30-meter accuracy as the terrain model. They depicted in their project that the most important problem in modeling studies is the calibration of the model. In addition, it was emphasized that terrain model refinement is limited to the accuracy of the data and that accuracy in geo-referencing of the surveyed cross-sections and control structures is imperative as well in the development of an optimum terrain model.

Anderson (2000) carried out floodplain delineation analyses, using modified ArcView GIS scripts and software along with the HEC-HMS hydrologic model, HEC-RAS hydraulic model and HEC-GeoRAS ArcView extension. The latter is used to develop geometric data to be imported into HEC-RAS and allows the user to view exported water surface profile data. Anderson fulfilled the study on two case areas: Castleman Creek Watershed in Robinson and Pecon Bayou Watershed in Brownwood, both located in Texas. Anderson concluded that the type and resolution of the data are the most important factors to affect accurate floodplain delineation activities. In addition, the number of cross-sections required for the hydraulic modeling of a channel with its corresponding overbanks may not be equal to the number of cross-sections required for floodplain delineation in GIS. Thus, Anderson suggested that the effects of intersecting cross-sections on terrain development activities may not be significant as originally thought.

Snead (2000) applied two unsteady models, the Danish Hydraulic Institute's (DHI) MIKE 11 hydrodynamic model and HEC-RAS model, to the Mill Creek Watershed in Ohio to determine the advantages and limitations of the models.

Alamilla et al. (2001) used the HEC-1 and the HEC-RAS models in combination with GIS to analyze the direct effects of urbanization, allowing for the suitable planning and controlled development of Oak Creek Watershed in southeastern Wisconsin.

Noman (2001) suggested the Floodplain Delineation Integrated System (FDIS), which comprises the Cross Section Data Management (CSDM), the Hydraulic Model Interface (HMI), and the Flood Delineation Process (FDP). These three components of the FDIS offered benefits in managing cross-sections, creating hydraulic models, and delineating floodplains from DTMs, using georeferenced water levels.

Later in 2001, Benavides used HEC-HMS hydrologic model with Next Generation Radar (NEXRAD) rainfall estimates, HEC-RAS for hydraulic modeling, and HEC-GeoRAS and ArcView to develop digital floodplains in the Clear Creek Watershed, located to the south of Houston, Texas. He combined these models to investigate the effectiveness of the proposed flood control alternatives including limited channelization and floodplain property buyouts.

CHAPTER THREE
THE STUDY AREA

Bostanli River Basin, located in the Karsiyaka Municipality of metropolitan Izmir is selected as the study area for this study (Figure 3.1). The basin assumes the coordinates of 38 27 27 N-38 33 49 N and 27 05 32 E-27 10 14 E, with a total area of about 29.6 km^2. The area is partially urbanized, especially in the southern parts. The main stream with a length of 14.28 km originates from Buyukcamlar Hill at the elevation of 997 m and discharges to the Izmir Bay with a major flow direction of northwest-southeast. Three major tributaries contribute to the Bostanli River. Kartalkaya River, the most important one to cause several floods in Elit city-state in the past, originates from the Kartalkaya Ridge. The second one, Eskisekikoy River, originates from Eskikoy while the last, Dallik River, confluences the Bostanli River at the left over bank (Tempo Altyapi, 2000).

The bed slope of the Bostanli River is about 11 % upstream of the river. In the area with elevations more than 30 meters, the slope becomes 1 % indicating a smooth topography. The average slope is 0.4 % at about the elevation of 10 m for the area which lies between the Anadolu Street and the Bay of Izmir.

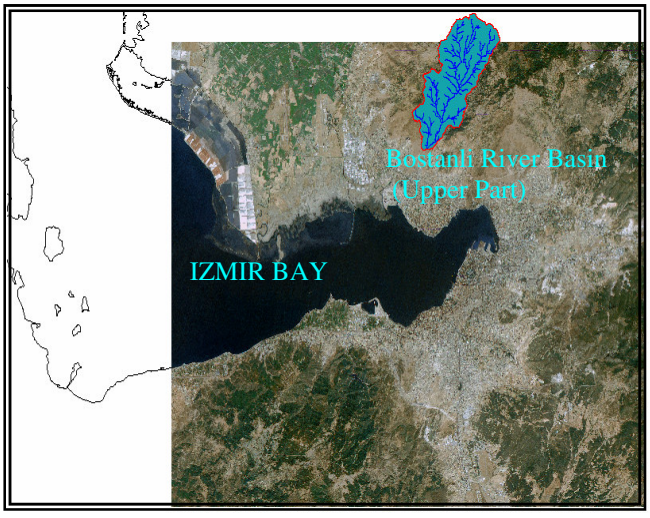

Figure 3.1 Bostanli River Basin.

Pilav Hill, Kartalkaya Ridge, Asagigol Hill, Yukarigol Hill, and Yaylabasi Hill constitute the west boundary of the Bostanli Basin at elevations of 127 m, 385 m, 594 m, 618 m, and 670 m, respectively.

Bostanli Dam, which is planned to be built in the case area, will be 2.5 kilometers far from the southeast of Sancakli Village in Karsiyaka County, Bostanli. The main purposes of the Bostanli Dam are flood control and drinking water supply.

The study area and its surroundings are located in the regional tectonic zone, the so-called Izmir-Ankara Ocean within the theory of Slab Tectonic of Turkey.

Being in the Mediterranean climatic zone, the city of Izmir has hot and arid summer seasons, and warm and rainy winter seasons. Rainfall generally occurs between the months of November and March, being fairly rare in the summer. Since the city is settled around the Bay with surrounding mountains, humidity rates are very high (Tempo Altyapi, 2000). Since there is no meteorological station in the case basin, Bornova, Guzelyali and Menemen meteorological stations in close proximity are used for hydrologic computations.

Lemur with a Mediterranean climatic feature is the major vegetation in the study area.

Bostanli River Basin is selected for this study for two reasons: first, it is located within an urban area in the City of Izmir, making a floodplain study inevitable to prevent damage. Second, it provides a branched stream network (a feature desirable to test the procedure) with enough simplicity to allow rapid computations during the modeling processes. Bostanlı River is an urban stream that flows through Ornekkoy, Elit development, Cumhuriyet, Dedebasi, Fikri Altay, Demirkopru, Goncalar and Bostanli districts.

Due to its proximity to numerous school buildings, homes, and businesses, the location of Bostanli River’s floodplain is of great interest to city planners,

developers, and property owners. Since Bostanli River has threatened both settlements and fertile lands for years, several administrations have tried to reduce flood dangers through local flood control studies, which have provided temporary solutions for these kinds of serious dangers. Thus, effective solutions could not have been obtained for the flood problem of Bostanli River Basin (Tempo Altyapi, 2000).

Because of the urban development in the 90s, increased illegal housing along the main river course as a result of the expansion of settlements up to the upstream of Anadolu street on the way from Izmir to Canakkale, waste dumping on the edges of the river, insufficient capacities of the hydraulic structures built along the stream, and insufficient efforts for solving problems; the flood disaster of November 4, 1995 took place. After this flood event in Izmir, which resulted in 69 deaths, a bridge failure occurred near the Yamanlar College. The first floors of the buildings along Bostanli River were flooded, and flood water passing over the Anadolu Street caused high water elevations which reached the third floors of the downstream buildings (Tempo Altyapi, 2000).

Since reconstruction of settlements in the floodplain areas, improper urbanization, heavy and discursive constructions in the river bed, construction of hydraulic structures with insufficient cross sections, and construction of sewer systems in the river bed increase flood peaks, all these factors have to be examined in a flood study. It is intended in this study to investigate whether measures, such as channel improvements and building of hydraulic structures for flood prevention, are adequate or not (Figure 3.2-3.4). For this purpose, 100 and 500-year hypothetical storms are taken into consideration, together with the 1995 flood event hyetograph observed in the neighborhood basin.

(a) (b)

Figure 3.2 Former (a) and present (b) views near the basin outlet.

(a) (b)

Figure 3.3 Former (a) and present (b) views of the Kartalkaya River.

(a) (b)

Figure 3.4 Former (a) and present (b) views beyond the Canakkale highway.

(a) (b)

Figure 3.5 Former (a) and present (b) views upstream of the Eskisekikoy junction.

CHAPTER FOUR
HYDROLOGIC MODELING

This chapter describes the methods used in hydrologic modeling of the Bostanli Basin. Since no record was available on precipitation data in the study area, a design storm was used as precipitation input to the HEC-HMS model. On the other hand, other input parameters of HMS, such as Soil Conservation Service (SCS) Curve Number (CN) and Clark's unit hydrograph, were estimated via GIS techniques.

4.1 Design Storms

Design storm is a hyetograph which defines the precipitation volume, intensities and duration. The following factors are used to define a design storm:

- a value of precipitation depth at a point
- a hyetograph specifying the time distribution of precipitation during a storm
- an isohyetal map specifying the spatial pattern of the precipitation

Design storm is used as an input for rainfall-runoff modeling studies to compute the design hydrograph for the design or evaluation of hydraulic sufficiency of a drainage system. Since the more recently developed methods that include unsteady flow analysis require reliable estimates to obtain the design hydrograph, mainly two methods have become eminent, i.e., Alternating Block Method and Instantaneous Intensity Method.

4.1.1 Point Precipitation

Point precipitation is the precipitation measured at a meteorological station while areal precipitation is defined over a region. Analysis of point precipitation is generally realized, using point precipitation frequency analysis. The annual maximum precipitation for a given duration of time is determined, using all storms in a year of historical record. The point precipitation estimate of a design storm of

duration T_d and return period T is calculated by using the frequency analysis of annual maximum precipitation records of duration T_d, measured at a meteorological station (Benzeden, 2000). This means that when T_d is the duration and T is the return period of a design storm, the point precipitation estimate can be calculated by using the following equation:

$$P_T = \mu_D + \sigma_D K_T \tag{4.1}$$

Various probability distribution models, such as the Gumbel, 2-parameter Log Normal (LN2), Normal, 2-parameter Gamma (G2), 3-parameter Log Normal (LN3), 3-parameter Gamma (G3), and Log Pearson Type 3 (LP3) can be applied in the frequency analysis of precipitation for a given duration (Benzeden, 2000). This computation is realized on each of a series of durations for which the frequency analysis is fulfilled on the data to obtain the design precipitation values for different return periods. Next, the design precipitation values are converted into precipitation intensities, through dividing them by the precipitation duration (Chow, 1988).

4.1.2 Areal Precipitation

Following the frequency analysis of point precipitation, the next step covers the frequency analysis of areal precipitation. Since the real probability distribution of areal precipitation is not known, the determination of the average areal precipitation can be achieved by extending point precipitation values. The areal estimate is classified as storm centered and location fixed estimates. For the latter one, precipitation stations can be near the storm center, on the outer edges, and in between two. An averaging process results in location fixed depth area curves relating areal precipitation to point measurements. Depth-area curves are used for the determination of areal depths as a percentage of point precipitation values.

Depth-area-duration relationships are derived by using a depth-area-duration analysis. In this method, isohyetal maps are constructed for each rainfall duration, using maximum n-hour rainfall recorded in the project area. The areas bordered by

isohyets are determined on the maps, and the average precipitation depth-area graph is drawn for each of the rainfall durations (Chow, 1988).

4.1.3 Triangular Hyetograph Method

Using a triangular shape is the simplest way to represent a design hyetograph. If the design precipitation value P and the duration T_d are known, the base length and height of the triangle can be computed easily. As shown in Figure 4.1, if the base length is T_d and the height is h, the total depth of precipitation in the hyetograph is given by $P = \frac{1}{2} T_d h$, from which the maximum rainfall intensity can be derived as.

$$h = \frac{2P}{T_d} \tag{4.2}$$

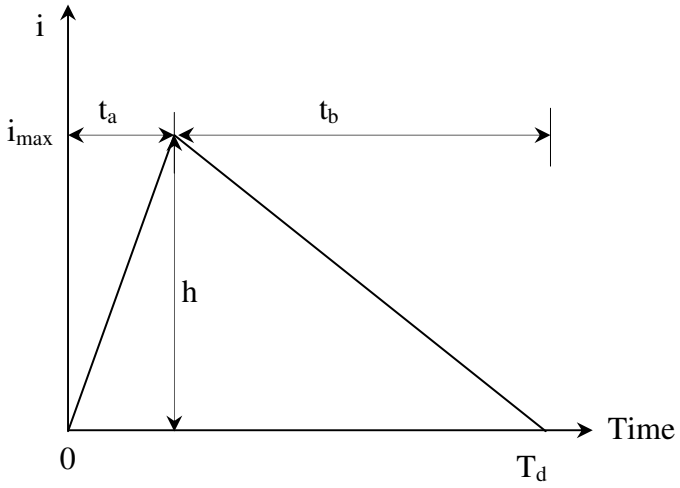

Figure 4.1 A general triangular design hyetograph.

A storm advancement coefficient r is defined as the ratio of the time before the peak t_a to the total duration:

$$r = \frac{t_a}{T_d} \tag{4.3}$$

Then the recession time t_b is given by:

$$t_b = T_d - t_a$$
$$= (1-r)T_d \tag{4.4}$$

A value of 0.5 corresponds to the peak intensity occurring in the middle of the storm such that a value less than 0.5 will have the peak earlier and a value greater than 0.5 will have the peak later than the midpoint (Chow, 1988).

4.1.4 Design Precipitation Hyetograph Derived from Intensity-Duration-Frequency (IDF) Relations

Formerly, only the peak discharge value had been considered in the hydrologic design studies. Neither the discharge hydrograph, which represents the temporal variation of discharge, nor the precipitation hyetograph was used. On the other hand, current methods applied in hydrologic studies need reliable estimates of the design hyetograph to derive design hydrographs. Methods used for derivation of design hyteographs are given in the following sections.

4.1.4.1 Alternating Block Method

In the first step of this method, the precipitation depth that occurs in n successive time intervals of Δt over a total duration T_d, which is equal to $n.\Delta t$, is calculated. Next, the design return period is selected, and the intensity is determined by using intensiy-duration-frequency (IDF) curve for each of the durations. Then, the precipitation depth is found by multiplying the intensity by the duration. Next, the incremental depths, called blocks, are determined by taking differences between successive precipitation values and rearranging them so that the maximum precipitation value is at the center of the duration T_d, while the other blocks are set up in descending order first to the right and then to the left of the central block to obtain the design hyetograph (Chow, 1988).

4.1.4.2 Instantaneous Intensity Method

With the use of a known IDF curve function, the equations to describe the temporal variation of the intensity in design hyetograph can be easily obtained.

The principle of the method is very similar to the alternating block method such that the precipitation depth for a duration T_d around the peak of the storm equals the value given by the IDF curve or function. However, the fact that the precipitation intensity here varies continuously throughout the storm is not the case for the alternating block method.

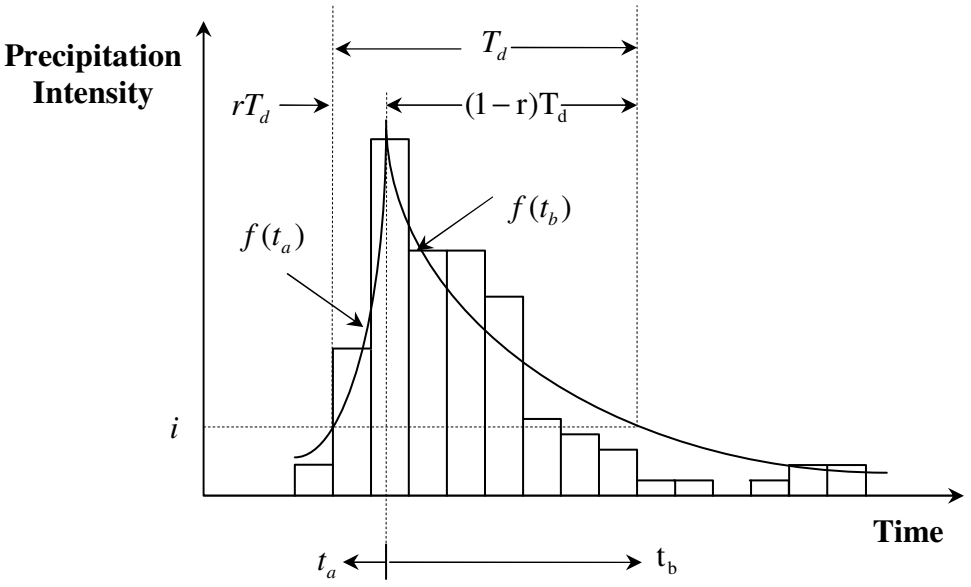

Figure 4.2 Fitting a hyetograph by curves (Chow, 1988).

When a horizontal line is drawn for a specific intensity i on the hyetograph, it will have two intersections with the hyetograph curve on either side of the peak intensity. The time duration from the peak to the left intersection point is called t_a, while the one to the right intersection point is called t_b (Figure 4.2) (Chow, 1988).

The sum of these two time durations gives the total time, T_d, as given below:

$$T_d = t_a + t_b \tag{4.5}$$

A storm advancement coefficient *r* is defined as the ratio of the time before the peak t_a to the total time:

$$r = \frac{t_a}{T_d} \tag{4.6}$$

From Equations (4.5) and (4.6) it follows that

$$T_d = \frac{t_a}{r} = \frac{t_b}{1-r} \tag{4.7}$$

The rising limb and the recession limb of the ideal rainfall hyetograph shown in Figure 4.2 are defined by the following functions:

$$f(t_a) = i_a \ , \ 0 \le t_a \le rT_d \tag{4.8}$$

$$f(t_b) = i_b \ , \ 0 \le t_b \le (1-r)T_d \tag{4.9}$$

The total amount of rainfall P within time T_d equals the area under these curves:

$$P = P_a + P_b \tag{4.10}$$

$$P = \int_0^{rT_d} f(t_a)dt_a + \int_0^{(1-r)T_d} f(t_b)dt_b \tag{4.11}$$

However, if i_{ave} is the average intensity for durationT_d, then:

$$P = T_d i_{ave} \tag{4.12}$$

Differentiating Equation (4.12) with respect to T_d, it is obtained the following.

$$\frac{dP}{dT_d} = i_{ave} + T_d \frac{di_{ave}}{dT_d} \tag{4.13}$$

When Equation (4.11) is differentiated with respect to T_d, with the resulting derivative being equal to $f(t_a) = f(t_b)$, it can be written as follows, and noting that $f(t_a) = f(t_b)$ for any horizontal line.

$$\frac{dP}{dT_d} = f(t_a) = f(t_b) \tag{4.14}$$

Hence, Equation (4.13) and Equation (4.14) yield:

$$\frac{dP}{dT_d} = i_{ave} + T_d \frac{di_{ave}}{dT_d} = f(t_a) = f(t_b) \tag{4.15}$$

In 1957, Keifer and Chu used the following equation to develop a synthetic hyetograph to design the sewer system of Chicago, where the average intensity is defined as:

$$i_{ave} = \frac{c}{T_d^e + f} \tag{4.16}$$

with i_{ave} being the average intensity; and c, e, and f, representing coefficients that vary with location and the return period.

Keifer and Chu (1957) gave the general intensity-duration curve as:

$$i = \frac{c\left[(1-e)T_d^e + f\right]}{(T_d^e + f)^2} \tag{4.17}$$

Equation (4.17) can be used for determining the intensity of the rising limb and of the recession limb which are found by substituting T_d given in Equation (4.7). Results are given in Equation (3.18) and Equation (3.19), respectively (Chow, 1988):

$$i_a = f(t_a) = \frac{c\left[(1-e)(t_a / r)^e + f\right]}{\left[(t_a / r)^e + f\right]^2} \tag{4.18}$$

$$i_b = f(t_b) = \frac{c\left[(1-e)(t_b /(1-r))^e + f\right]}{\left[(t_b /(1-r))^e + f\right]^2} \tag{4.19}$$

4.2 Preparation of Input Parameters via GIS

The estimation of spatially variable hydrologic parameters such as SCS Curve Numbers, subbasin area and lag time can be accomplished by using a GIS software like ArcView. In the following sections, the extraction of SCS Curve Numbers and the application of Clark's synthetic hydrograph methods are discussed in detail.

SCS Curve Number methodology is a standard hydrologic analysis technique that has been applied in a variety of different settings all over the world, and the development and application of the curve number are well documented (SCS, 1985). As the curve is a function of the soil and land use properties of a drainage basin, estimation of a curve number requires mapping the soil conditions and land use within the drainage basin, together with specification of unique soil types and land use categories. The manual calculation of curve numbers for large areas or many drainage basins can be cumbersome and time-consuming, therefore, GIS can be an appropriate tool to be used for such an application (Halley et al., 2000).

On the other hand, the determination of basin unit hydrographs is one of the most important issues in flood studies. Particularly in ungauged watersheds, the computational steps required for reliable solutions in the determination of flow rates are pretty difficult and time consuming. To perform hydrologic and/or hydraulic design analyses in ungauged areas, synthetic unit hydrographs have been commonly used. Synthetic unit hydrographs are estimated, based on the relationships between the unit hydrograph model parameters and the physical characteristics of the basin. However, most of these relationships have not found a common use in many related studies since most of them are empirically derived relationships. Clark's method is

quite different from the other synthetic methods since its parameters can be computed in a series of more rapid and accurate analyses with the help of GIS. Originally, it has been shown to provide better representations of unit hydrographs (Halley et al., 2000).

4.3 Estimation of the SCS Curve Number

The SCS Curve Number is based on the ability of soils to infiltrate water, land use, and the soil water conditions at the beginning of a rainfall event (antecedent soil water conditions). As mentioned before, it is not an easy process to calculate CNs manually for large areas or for many drainage basins. Therefore, a GIS tool may be required for such an application. For this purpose, the user provides drainage areas, land use and soil maps in digital forms, and the curve number for a drainage basin is estimated by using the combined information on land use, soil type and antecedent soil moisture conditions (AMC). Soil surveys list soil types, which are based on certain physical characteristics of the soils. However, the information needed to determine a curve number is the hydrologic soil group, which indicates the amount of infiltration the soil will allow. Significant infiltration occurs in sandy soils while no infiltration occurs on heavy clay or rock formations. Most published soil surveys present a listing of the soil types and corresponding hydrologic soil groups. The original soil type map must be converted to a map of hydrologic soil groups, using these published conversions (Ward, 1995). There are four hydrologic soil groups: A, B, C and D, which define the infiltration characteristics of soils as:

A. Soils of Group A, with a low runoff potential, have high infiltration rates even when thoroughly wetted. They are deep, well-drained sands and gravels. This type of soils has a high rate of water transmission.

B. Soils of Group B have moderate infiltration rates when thoroughly wetted. They are moderately deep to deep, moderately well to well-drained soils with moderately fine to moderately coarse textures. Group B soils have a moderate rate of water transmission.

C. Soils of Group C have slow infiltration rates when thoroughly wetted. They are soils with a layer that impedes downward movement of water or soils with moderately fine to fine texture. These soils have a slow rate of water transmission.

D. Soils of Group D, with a high runoff potential, have very slow infiltration rates when thoroughly wetted. They are clayey soils with high swelling potential, soils with a permanent high water table, soils with a claypan or clay layer at or near the surface, and shallow soils over nearly impervious materials. Group D soils have a very slow rate of water transmission (Ward, 1995).

The land use distribution map for the area of interest is derived from zoning, parcel boundary maps, and aerial photography. Land use categories are defined, based on the level of detail required for the study. Standard SCS curve numbers are assigned to each possible land use-soil group combination. Table 4.1 presents an example of typical land use categories used for hydrologic analysis, along with corresponding curve numbers for each land use-soil group combination. The land use categories shown in this table are derived from the standard categories typically used for hydrologic analyses using the SCS methodology (Halley et al, 2000). Table 4.1 shows standard values of CN for antecedent moisture condition II (AMC II) for various land uses and soil types. The AMC is defined as the initial wetness of the soil and is classified into in three groups. These are dry, average, and wet conditions represented by AMC I, AMC II, AMC III, respectively (Pilgrim & Cordery, 1993). As a general application, firstly CNs are calculated for AMC II, afterwards adjusted up to simulate AMC III or down to simulate AMC I. More detailed information on AMC I and AMC III are given in U.S. Soils Conservation Service (1985).

Table 4.1 Land use categories and associated curve numbers CN (Pilgrim & Cordery, 1993).

		CN			
		Hydrologic soil group			
Land Use Description		**A**	**B**	**C**	**D**
Cultivated land:					
Without conservation treatment		72	81	88	91
With conservation treatment		62	71	78	81
Pasture or range land:					
Poor condition		68	79	86	89
Good condition		39	61	74	80
Meadow: Good condition		30	58	71	78
Wood or forest land:					
Thin stand, poor cover, no mulch		45	66	77	83
Good cover		25	55	70	77
Open spaces, lawns, parks, golf courses, cemeteries, etc.:					
Good condition: grass cover on 75% or more of the area		39	61	74	80
Fair condition: grass cover on 50 to 75% of the area		49	69	79	84
Commercial and business areas (85% impervious)		89	92	94	95
Industrial districts (72% impervious)		81	88	91	93
Residental:					
Average lot size	Average % impervious				
1/8 acre or less	65	77	85	90	92
1/4 acre	38	61	75	83	87
1/3 acre	30	57	72	81	86
1/2 acre	25	54	70	80	85
1 acre	20	51	68	79	84
Paved parking lots, roofs, driveways, etc.		98	98	98	98
Street and roads:					
Paved with curbs and storm sewers		98	98	98	98
Gravel		76	85	89	91
Dirt		72	82	87	89

Once the data are gathered, the typical process given in Figure 4.3 is followed to estimate CN for a drainage area by using GIS tools. As can be seen from the figure, the derivation of CN comprises of a number of steps. The first step is to define and delineate the boundaries of the basin or subbasins for which CN values are to be computed. This step precedes the delineation of the drainage area and is followed by mapping the land use and soil type information. These soil types are then converted into hydrologic soil groups to be used in an overlay analysis with the land use map. Prior to the computation of polygonal areas, each unique land use-soil group polygon is identified and assigned a CN, based on the standard SCS curve number tables. Then, the basin map is overlaid on the land use-soil group polygons. The final step is the calculation of an average curve number for each basin from the land use–soil group polygons by performing a method based on weighting by areas. The basic equation for curve number calculation is as follows:

$$CN_{aw} = \frac{\sum_{i=1}^{n} (CN_i * A_i)}{\sum_{i=1}^{n} A_i} \tag{4.20}$$

where CN_{aw} is the area-weighted curve number for the drainage basin; CN_i is the curve number for each land use-soil group polygon; A_i is the area for each land use-soil group polygon; and n is the number of land use-soil polygons in each drainage basin (Halley et al, 2000).

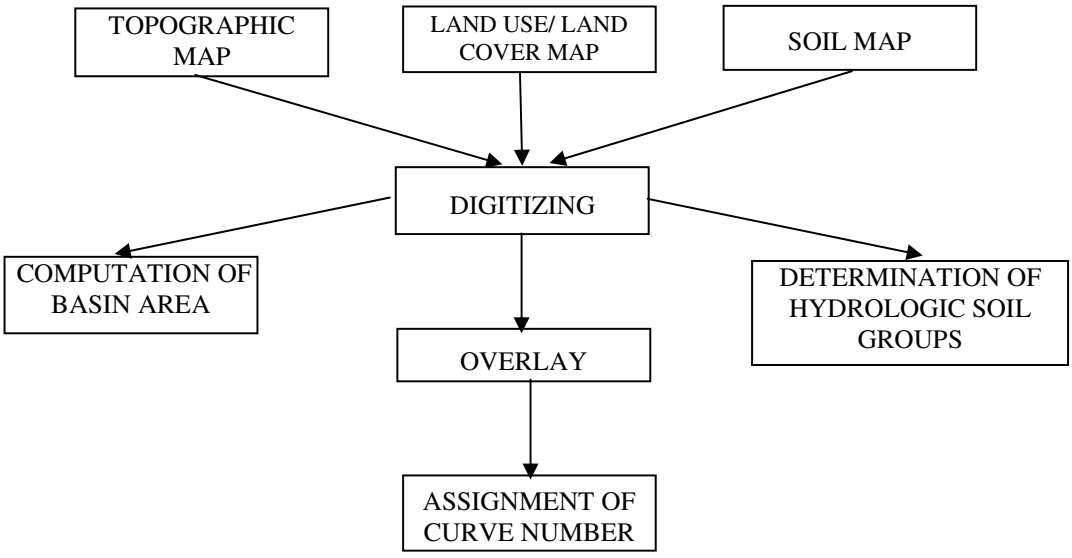

Figure 4.3 Curve number estimation process using GIS tools.

4.4 Estimation of the Clark's Unit Hydrograph

4.4.1 Clark's unit hydrograph method

Unit hydrographs for gauged basins are derived by using observed hydrographs and hyetographs. Though there are lots of catchments where recorded data are not available, it is preferred to define a relationship between the physical characteristics of the watershed and the resulting hydrographs, since the derivation of unit hydrographs for such catchments is highly significant. There are three approaches used for this purpose: formulas relating hydrograph features to basin characteristics, transportation of unit hydrographs, and storage routing (Linsley et al, 1998).

When inflow and outflow are considered to be excess rainfall (or runoff) and hydrograph, respectively, the problem of storage routing arises; and, in this case, Clark's synthetic unit hydrograph method is utilized as a derivation technique for the analysis of storage routing. In Clark's unit hydrograph method, the basin time-area diagram is combined with a linear reservoir at the basin outlet (Clark, 1945). The shape of Clark's unit hydrograph is determined by the travel time through the basin, as well as by the basin shape and storage characteristics.

On the other hand, when the nature of the problem is evaluated, the use of lag and route methods needs to be considered. Lagging inflow is derived by dividing the basin into zones through isochrones of travel time from the outlet. After this process, the areas between alternate isochrones are measured, and a time-area diagram is formed, based on these measurements. The resulting time-area diagram is regarded as an inflow to a hypothetical reservoir located in the basin, where the characteristics of both the reservoir and the basin are the same. Therefore, routing the time-area diagram with the use of any suitable method (such as the Muskingum Method with x = 0) finally gives the outflow hydrograph with a special adjustment for units. This feature differentiates the Clark's unit hydrograph from other synthetic unit hydrograph methods (Linsley et al, 1998).

It is also possible to utilize the same methodology above to estimate, for each time zone, the average runoff for a storm of duration equal to the interval between isochrones, which is to be expressed in cubic meters per second. The resulting time-runoff diagram is then routed through storage to give the actual outflow hydrograph. If rain lasts for several time periods, the time-runoff diagrams are lagged and superimposed, and the summation is routed. The method utilized here takes two factors into consideration, i.e., time-intensity variations and areal distributions of rainfall, which are not readily considered in the unit hydrograph theory (Linsley et al, 1998).

When compared to other methods, another distinctive feature of Clark's unit hydrograph method is that it can be used with GIS tools which support modelers and scientists by facilitating data management, spatial analyses and visualization of the results (Onusluel and Gul, 2004).

4.4.1.1 Parameters of Clark's unit hydrograph

For derivation of Clark's unit hydrograph, the parameters of the hydrograph are first determined. By using these parameters, which are mainly the time-area diagram and the storage attenuation coefficient (R), the translation hydrograph is created, and the instantaneous unit hydrograph is obtained by means of linear reservoir routing.

The time-area diagram simply gives the fraction of the area contributing to the flow at the basin outlet at a certain instance in time. As this diagram reflects the shape and drainage properties of the basin, it is considered to be the most important parameter for derivation of the translation hydrograph (Usul and Yilmaz, 2002). In order to obtain the time-area diagram, flow lengths are first calculated within each subbasin, based on the flow directions obtained from the digital elevation model; and travel times of flow are determined through the use of GIS analyses. "Travel time" is the time required for rainwater to follow the flow length between a point in the basin and the basin outlet so that the travel time from the farthest cell gives the time of concentration (T_C), which is required to produce the translation hydrograph (Wanielista et al, 1997). The time of concentration is simply the maximum value

used in the time-area relationship. The time-area curve may be broken into smaller time intervals, representing percentages of the time of concentration. There are several equations for the determination of T_C. Considering the available data and the necessary parameters of these equations, the Soil Conservation Service (SCS) has proposed a lag equation for the computation of T_C, which requires the main channel length, average Curve Number and the slope of the basin. Equation (4.21) gives the formulation of T_C (SCS, 1985):

$$T_C = 0.6T_{lag} \tag{4.21}$$

in which T_{lag} is the lag time of the watershed in hours, which is computed from:

$$T_{lag} = \frac{2.587 * L^{0.8}\left(\frac{1000}{CN} - 9\right)^{0.7}}{1900 * H^{0.5}} \tag{4.22}$$

where L is the longest flow path of the basin in meters; CN is the hydrologic area-weighted curve number; and H, the average watershed land slope (%) (SCS, 1985).

The travel times for a subbasin can be calculated by using the following equation in which FlGrid is the grid representation of flow lengths, T_C is the time of concentration, and Max(FlGrid) is the maximum of the travel lengths in the grid data format. An average velocity is assumed here to be constant over the whole subbasin so that travel times proportional to the travel lengths are calculated for each unit area (for each cell in GIS terminology) within the basin.

$$\text{TtGrid} = \frac{T_C}{\text{Max(FlGrid)}} * \text{FlGrid} \tag{4.23}$$

Having obtained the time-area diagram, for which the area is the accumulated area from the basin outlet, and the time is the travel time as defined by isochrones (contours of constant time of travel), the required translation hydrograph can be

conveniently derived by using the above relation. Such a relationship can be expressed in dimensionless form with area expressed as a percent of the total basin area and time as a percent of the total time of concentration. The translation hydrograph can be obtained by determining from a time-area relation the portion of the basin that contributes runoff at the basin outlet during each time interval after the occurrence of the instantaneous burst of unit excess. The contributing area associated with a time interval (times the unit depth and divided by the time interval) yields an average discharge. This is the ordinate of the translation hydrograph for that interval.

Naturally, a difference exists between the time-area translation hydrograph and the basin outflow hydrograph simply because of the fact that the resulting hydrograph is attenuated under the effect of basin storage. In order to represent this attenuation, the Muskingum storage coefficient, K (or termed R in most references to the Clark method), is used in the Clark UH method. Clark used the Muskingum technique to investigate hydrographs for a number of gauged basins. It is demonstrated that a hydrograph or a flood wave, routed 5 times at 2-hour intervals with a Muskingum weighting coefficient of x = 0.5, could be approximated by the same original hydrograph or floodwave being translated 9 hours and then routed for a short time interval through a reservoir with a Muskingum weighting coefficient of x = 0.0. This is one of the basic concepts of the Clark's unit hydrograph. Beside the "x" weighting coefficient, the Muskingum routing technique requires a second coefficient, "K", which has units of time and is often presented as the travel time for a reach. Actually, Clark referred to this parameter as the storage parameter, thus indicating the storage in terms of units of time. References to the Clark unit hydrograph often denote the Muskingum K value, or the R value used by Clark. Beyond different naming, Muskingum "K" represents storage effects in a routing reach, while Clark "R" represents the same effects for a basin. The Clark storage coefficient can be calculated by the following formula, which is based on the use of information at the point of inflection on the recession limb of a measured hydrograph (Wanielista et al., 1997, Yu, 2002):

$$K = -\frac{Q}{dQ/dt} \tag{4.24}$$

K is computed from an observed storm hydrograph if it is available, or it may be computed by formulas (suggested by Clark and Linsley) which depend on basin characteristics.

Clark also suggested that K (in hours) can be estimated by using the equation (Linsley et al, 1998):

$$K = \frac{cL}{\sqrt{s}} \tag{4.25}$$

where L denotes the length of the main stream in kilometers; s ,the mean channel slope; and c, a constant that varies from about 0.5 to 1.4.

Following this proposal by Clark, Linsley suggested the same formula in a different form as follows:

$$K = \frac{bL\sqrt{A}}{\sqrt{s}} \tag{4.26}$$

where A is the drainage area in square kilometers, and b is a constant that varies from about 0.01 to 0.03 for the basins tested (Linsley et al, 1998).

The translation hydrograph and linear reservoir routing are jointly used to transfer the instantaneous unit excess rainfall, which is uniformly distributed over the basin, to the basin outlet. The translation hydrograph is the representation of the rainfall-runoff relationship for surface runoff. Linear reservoir routing, where Muskingum x is equal to 0.0, represents how the stream channel storage affects the hydrograph.

The IUH ordinates are determined by Equation (4.27) considering time steps equal to the time-area increment:

$$Q(t) = \frac{\Delta t}{K + 0.5\Delta t} I(t) + (1 - \frac{\Delta t}{K + 0.5\Delta t}) Q(t-1) \quad (4.27)$$

where Q(t) are the ordinates of the IUH; I(t) are the translation hydrograph ordinates, K is the storage attenuation coefficient; and Δt is the time step chosen for the time-area relationship.

The final unit hydrograph is derived by averaging two instantaneous unit hydrographs which are the time step Δt (Wanielista et al., 1997). Figure 4.4 summarizes the methodology based on GIS tools, which results in the final computation of the unit hydrograph.

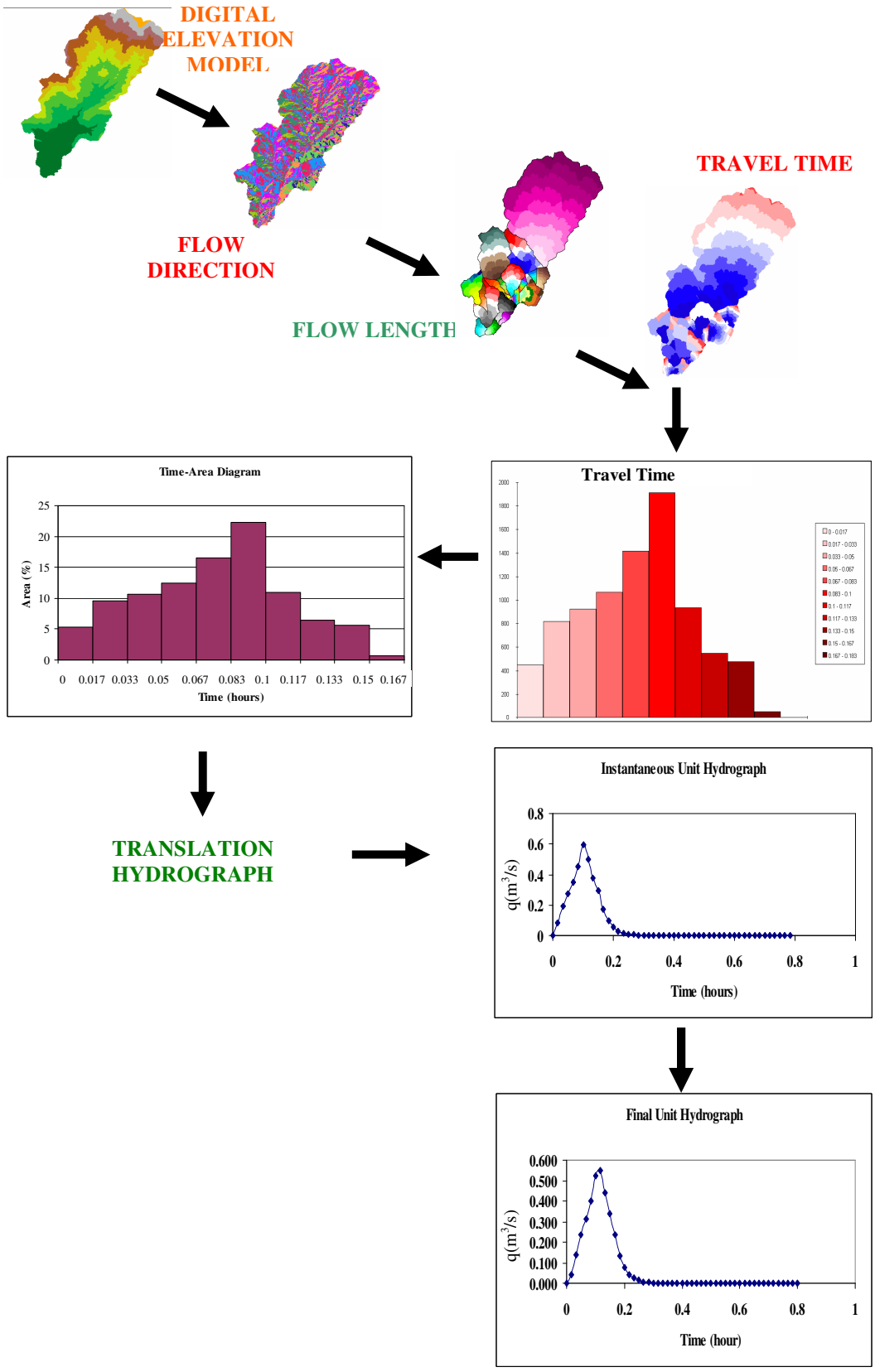

Figure 4.4 Derivation of Clark's unit hydrograph by the use of GIS tools.

CHAPTER FIVE
HYDRAULIC MODELING

5.1 Open Channel Flow

Open channel flow is defined as the flow of a free surface fluid, such as the flow in natural streams, constructed drainage canals, and storm sewers. The pressure at the free surface is atmospheric, and shear forces across the open channel are negligible. Since problems in open channel flow are more complex than those in pipe flow, and the solutions are more varied, especially in effective floodplain management studies, open channel flow hydraulics should be reviewed prior to any modeling studies (Chow, 1959).

5.1.1 Classification of Open Channel Flow

The following classification of open channel flow is made, regarding the change in flow depth with respect to time and space.

5.1.1.1 Classification based on time

When time is regarded as a criterion, the flow is said to be *steady* when the flow depth and flow velocity do not change within a time interval. On the other hand, if depth and velocity at a point vary with time, the flow is classified as *unsteady flow* (Figure 5.1). For example, floods and surges are common examples of unsteady flow where the flood level changes instantaneously as the flood wave passes. In the design of control structures, time becomes an important factor (Chow, 1959, Klotz et al., 2003).

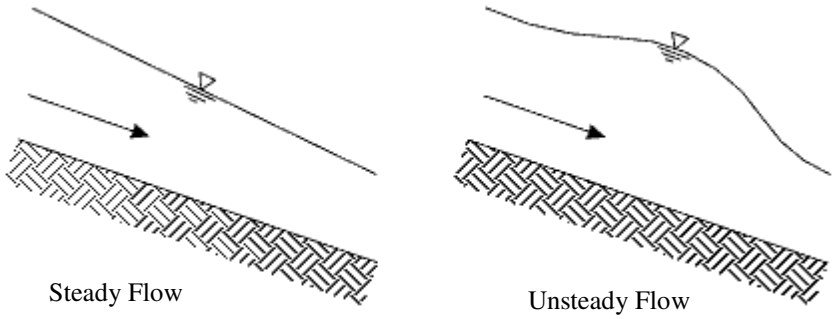

Figure 5.1 Steady versus unsteady flow (Klotz et al., 2003).

The discharge is constant along the channel reach in applications of steady flow, which means that the flow is continuous. This phenomenon is expressed with the continuity equation.

The continuity equation is not used when water runs in or out of the channel along the course of flow. In this case, discharge of a steady flow is *varied* along the channel, and it is called *spatially varied* or *discontinuous flow*. Roadside gutters, side-channel spillways, the washwater troughs in filters, the effluent channels around sewage-treatment tanks, main drainage channels, and feeding channels in irrigation systems are examples of spatially varied flow (Chow, 1959).

5.1.1.2 Classification based on space

When space is considered as a criterion, the flow is said to be *uniform* if the depth of the flow is constant at every section along the channel. Uniform flow conditions require the channel to be straight, with constant cross-sectional geometry, and a water surface that is parallel to the base of the channel. Uniform flow becomes unsteady or steady depending on the existence, or non-existence, of a change in depth with time. In the condition of steady uniform flow, the depth of the flow does not change during the time interval; on the other hand, in unsteady uniform flow, the water surface changes from time to time while remaining parallel to the channel bottom.

Flow is said to be “varied” when the depth of flow changes through the river channel (Figure 5.2).

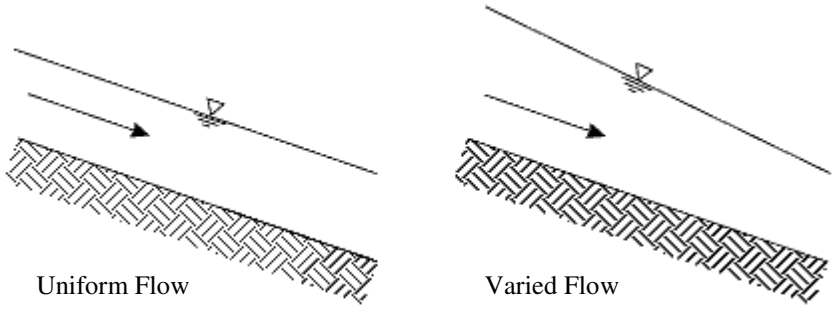

Figure 5.2 Uniform flow versus varied (Nonuniform) flow (Klotz et al., 2003).

Varied flow may also be unsteady or steady, and it may be classified as *rapidly* or *gradually varied flow*. If the flow changes abruptly in a very short distance, the *rapidly varied flow* occurs; otherwise, it becomes *gradually varied flow* (Figure 5.3).

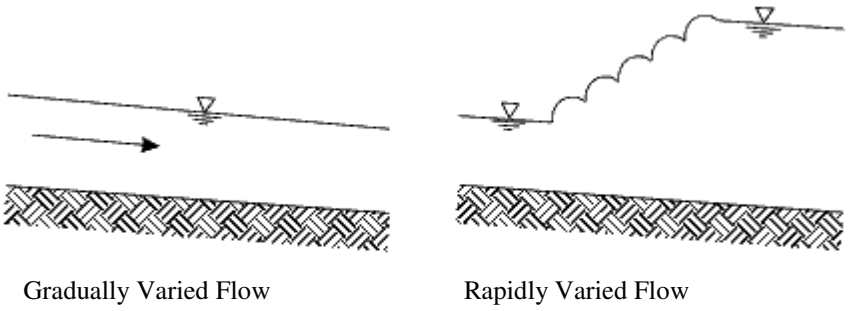

Figure 5.3 Gradually varied flow versus rapidly varied flow (Klotz et al., 2003).

Rapidly varied flow typically occurs at hydraulic structures such as dam spillways. Bridge openings that severely constrict flow may also cause rapidly varied flow through the bridge opening. The occurrence of a hydraulic jump is the most notable example of rapidly varied flow (Chow, 1959, Klotz et al., 2003).

The above classification of open channel flow is summarized below:

- **Steady Flow**
  - Uniform Flow
  - Varied Flow
    - Gradually Varied Flow
    - Rapidly Varied Flow
- **Unsteady Flow**
  - Unsteady Uniform Flow
  - Unsteady Flow (i.e., Unsteady Varied Flow)
    - Gradually Varied Unsteady Flow
    - Rapidly Varied Unsteady Flow (Chow, 1959)

5.1.2 Flow Regime

Flow can also be classified as *subcritical* or *supercritical* with respect to the Froude number, which is the ratio of inertial forces to the gravitational forces.

The dimensionless Froude number is calculated by using Equation (5.1).

$$Fr = \sqrt{\frac{V}{gY}} \tag{5.1}$$

where

Fr : Froude number
V : mean fluid velocity (m/s)
g : gravitational acceleration (m/s^2)
Y : water depth (m)

If Fr > 1, the flow is said to be *supercritical flow*. In this case, the flow velocity is extremely high, and the flow depth is low. Supercritical flow generally occurs in the case of steeper slopes, and most often in man-made channels; however, the flow in steep mountain streams may also be supercritical, especially during floods. Flow in a

street gutter can be given as an example of supercritical flow since the flow velocity is about 0.3-0.6 m/s while the depths are several centimeters.

The flow with a relatively low velocity and high depth occurs when Fr < 1, resulting in a *subcritical flow*. Subcritical flow generally occurs in channels with small channel slopes and is the most common type of flow in natural channels.

Critical flow, at which the depth and the velocity are critical, occurs at the point where the total energy head is a minimum and the corresponding Froude Number is equal to 1 (Chow, 1959, Klotz et al., 2003).

5.1.3 Relevant Equations

There are four most commonly used equations in open channel hydraulic problems; namely, continuity, energy, momentum, and Manning equations.

5.1.3.1 Continuity Equation

The continuity equation states that flow must be conserved but that its properties may change between adjacent cross-sections:

$$Q = V_1 A_1 = V_2 A_2 \tag{5.2}$$

where

Q : flow rate/discharge (m^3/s)

V_n : average velocity at cross-section n (m/s)

A_n : area at cross-section n (m^2)

5.1.3.2 The energy equation

The theory of the conservation of energy underlies the energy equation, which is also called Bernoulli equation. Daniel Bernoulli's equation is a special form of

Euler's equations of motion. Bernoulli developed the energy equation for pressure conduits as the following:

$$z_2 + \frac{p_2}{\gamma} + \frac{V_2^2}{2g} = z_1 + \frac{p_1}{\gamma} + \frac{V_1^2}{2g} + h_{L_{1-2}} \tag{5.3}$$

where

z : the elevation of the conduit centerline, datum (m)
p : the pressure in the conduit (N/m^2)
γ : the specific weight of the fluid (N/m^3)
V : the flow velocity in the pipe (m/s)
h_L : energy losses between downstream point 1 and upstream point 2 (m)

While datum plus pressure head represent the potential energy of the water, the velocity head term represents the kinetic energy of the water. The sum of the potential and the kinetic energy is the total energy head at a given point. h_L is the head loss which includes the friction loss and the expansion or contraction loss between locations 2 and 1 (Figure 5.4). The total energy head at upstream location 2 becomes:

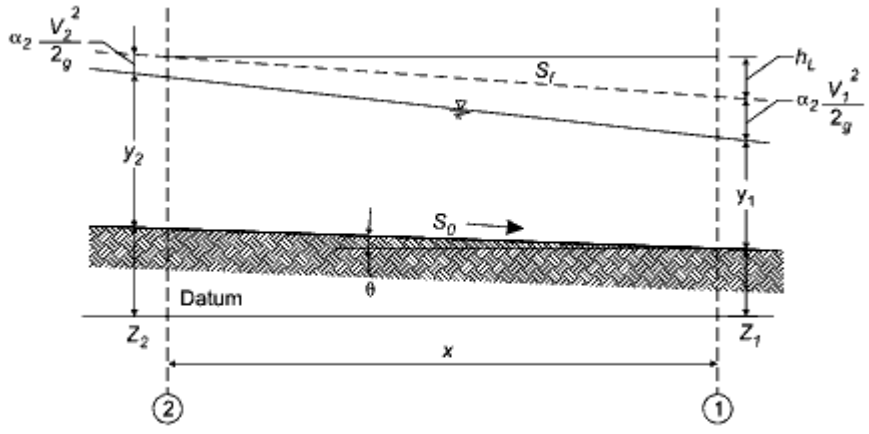

Figure 5.4. Key variables used in open channel hydraulics (Klotz et al., 2003).

$$H_2 = H_1 + h_{L_{1-2}} \tag{5.4}$$

where

H_2 : the total energy head (m)

5.1.3.3 The Momentum Equation

In open channel flow, the momentum equation states that the sum of forces acting on an isolated system is equal to the system's mass times its acceleration.

Figure 5.5 shows the forces which act on a volume of fluid, and Equation 5.5 describes these forces. The mass is the mass flow rate (ρQ), and the acceleration is the difference in velocity in the direction of flow at the system boundaries. Momentum computations are accomplished only in the downslope direction in steady flow analysis.

$$F_2 - F_1 + W\sin\theta - F_f - F_0 = \frac{\gamma}{g}Q(\beta_2 V_2 - \beta_1 V_1) \quad (5.5)$$

where

F_1 and F_2 : the hydrostatic forces at the system boundaries (N)

$W \sin\theta$: the component of the weight of the liquid (F_g) (N)

F_f : the friction force along the sides and bottom of the channel (N)

F_0 : the force of any internal obstruction (N)

β : the momentum coefficient (dimensionless)

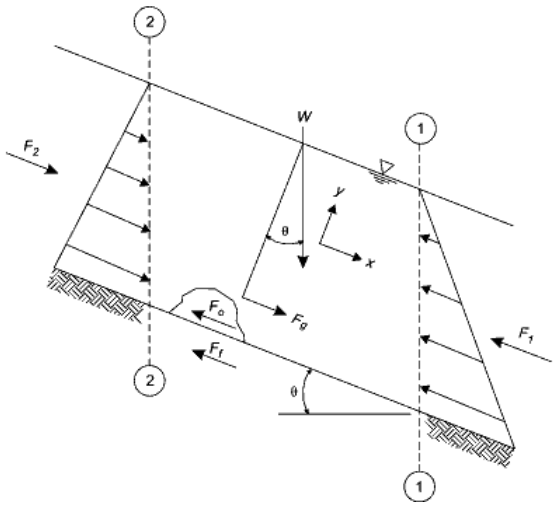

Figure 5.5. Forces in the momentum equation (Klotz et al., 2003).

5.1.3.4 The Chézy and Manning Equations

The Chézy equation commonly used in open channel hydraulics is:

$$V = C\sqrt{RS_0} \tag{5.6}$$

where

V : average velocity (m/s)
C : The Chézy roughness coefficient
R : hydraulic radius (m)
S_0 : slope of the channel invert (m/m)

In the SI system, the Chézy roughness coefficient can take on any value in the range from 5 to 77 for the same type of surfaces. Flow depth, hydraulic radius, and other variables affect the C value. Since Chézy's equation was developed for uniform flow, the S_0 term equals S_f, the friction slope. Late in the nineteenth century, Robert Manning used available prototype data from actual canals and channels and compared measured velocities to the computed Chézy velocities. After comparing the computed average velocity with that derived from available data, he proved that better results can be obtained by using $R^{2/3}$ instead of $R^{1/2}$. The Manning's equation is thus:

$$V = \frac{k}{n} R^{2/3} S_0^{1/2} \tag{5.7}$$

where

k : 1.486 for the English system and 1.0 for the SI system
n : Manning's roughness coefficient (same in the English or the SI system)

The discharge, Q, can be obtained as follows by substituting Q/A for velocity:

$$Q = \frac{k}{n} A R^{2/3} S_0^{1/2} \tag{5.8}$$

where

A : the cross section area (m^2)

Since Manning's equation is based on uniform flow, the friction slope can replace the channel invert slope in the equation. Moreover, the equation can also be used in the case of gradually varied flows. The values of the Manning's n vary, based on channel terrain and are given in all hydraulic engineering books. Some typical values of the Manning coefficient are shown in Table 5.1 (Prasuhn, 1992).

Table 5.1. Manning's n values for open channels (Chow, 1959).

Channel Type and Description	**Value**
Smooth Concrete	0.012 - 0.013
Unfinished Concrete	0.013 - 0.016
Earthen, smooth, no weeds	0.02
Firm gravel	0.02
Earthen, some stones & weeds	0.025
Earthen, unmaintained, winding natural streams	0.035
Mountain streams	0.04 - 0.05

Equation 5.8 may be rearranged as in Equation 5.9.

$$Q = K\sqrt{S_f} \tag{5.9}$$

where

K : conveyance ($m^{5/3}$)

S_f : friction slope

and K is

$$K = \frac{1}{n} AR^{2/3} \tag{5.10}$$

To determine conveyance, the cross-section is subdivided, based on the Manning coefficient (Figure 5.6), into the left overbank, main channel, and the right overbank. The conveyance for each subdivision is then calculated by using Equation 5.10. The total conveyance for the cross-section is obtained by summing the individual subdivision conveyances (HEC, 1997).

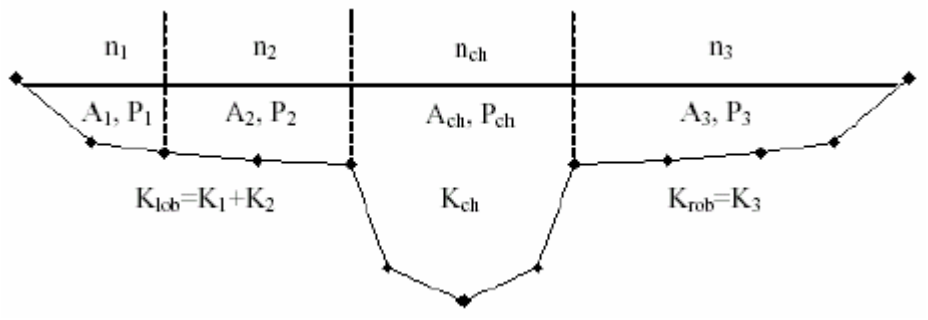

Figure 5.6. Parameters used in the calculation of conveyance.

For prismatic river channels, the flow rate is known, based on either hydrologic modeling or flood frequency analyses. With the flow and conveyance known, the average friction slope between two adjacent cross-sections can be calculated as follows:

$$\overline{S}_f = \left(\frac{Q_1 + Q_2}{K_1 + K_2} \right)^2 \tag{5.11}$$

Q_n : flow rate/discharge at cross-section n(m^3/s)

K_n : conveyance at cross-section n ($m^{5/3}$)

5.2 Computational Methods for Steady Flow

The methods of direct step and standard step are the most frequently used methods among several graphical and analytical techniques in steady flow calculation. The aim of the computation is to obtain the water depth or the water surface elevation for any given location along a channel.

5.2.1 Direct Step Method

Since an engineer generally wants to find the depth at a specific location, such as at a bridge, this method can be used only to solve for distance when the depth is known or to solve for a change in depth. In addition, the method is often used only for prismatic channels. such as a storm sewer, culvert, or small drainage channel of constant slope.

The distance between location 1 and location 2 can be computed as in the following, recognizing that $E = y + V^2/2g$ and assuming that $\alpha = 1$:

$$\Delta x = \frac{E_2 - E_1}{S_0 - \overline{S}_f} \tag{5.12}$$

where

Δx : the distance from location 1 to location 2 for the depth selected (m)

E_2 : specific energy at upstream location 2 (m)

E_1 : specific energy at downstream location 1 (m)

S_0 : the channel invert slope (m/m)

$\overline{S}_f$: the average friction slope between the two locations (m/m)

Figure 5.7 shows the variables used in Equation 5.12.

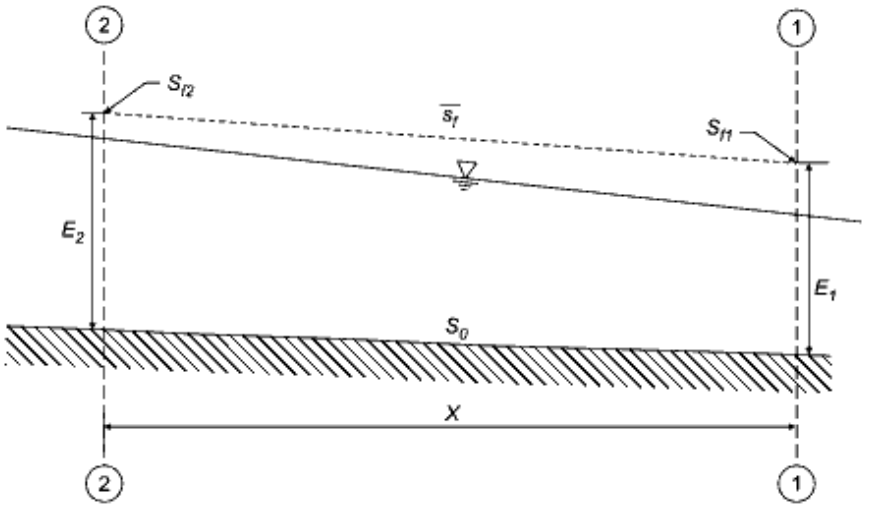

Figure 5.7 Variables used in the direct step method (Klotz et al., 2003).

The initial conditions, provided as depth or water surface elevation at the downstream cross section, cross-section geometry, Manning's n, and the discharge are the required parameters for this method. As a first step in the computation, the velocity, specific energy, and friction slope at Section 1 and Section 2 are computed. The next step is to obtain a value for S_f from the rearranged form of the Manning equation below:

$$S_f = \frac{n^2 V^2}{k^2 R^{4/3}} \tag{5.13}$$

where

S_f : the energy grade line slope (m/m)
n : Manning's roughness coefficient (dimensionless)
V : average velocity (m/s)
k : 1.0 for SI units (constant)
R : hydraulic radius (m)

The HEC-RAS program uses the direct step method to compute an open channel flow profile through a culvert.

5.2.2 Standard Step Method

This method is applicable for both prismatic and nonprismatic channels, including the adjacent floodplains. It is used in most computer programs that compute steady, gradually varied flow profiles and can be applied for both subcritical and supercritical flow. The continuity, energy, and Manning equations are used to obtain water depth or water surface elevations at selected locations along the stream.

The basic equation for the standard step solution is given in Equation 5.14:

$$WSEL_2 + \frac{\alpha_2 V_2^2}{2g} = WSEL_1 + \frac{\alpha_1 V_1^2}{2g} + h_{L_{1-2}} \tag{5.14}$$

where

$WSEL_{1,2}$: the water surface elevation (z + y) at the indicated location (m)

$h_{L_{1-2}}$: the friction loss plus expansion or contraction loss between the two points (m)

Figure 5.8 illustrates the variables used in standard step computations.

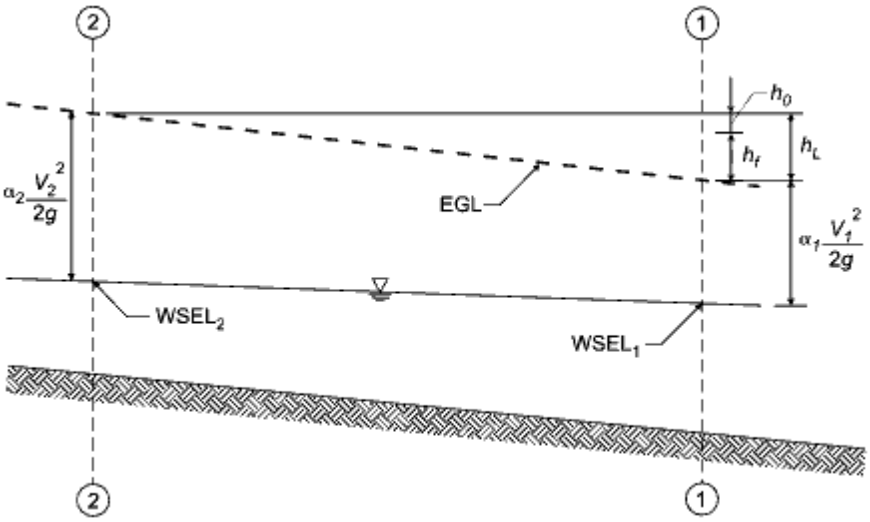

Figure 5.8. Variables used in the standard step method (Klotz et al., 2003).

The head loss, which is a combination of friction and expansion/contraction losses, is computed by using Equation 5.15:

$$h_{L_{1-2}} = h_f + h_0 \tag{5.15}$$

where

h_f : energy loss due to friction between the two locations (m)

h_0 : energy loss due to expansion or contraction between the two locations (m)

5.3 Unsteady Flow

In unsteady flow modeling, two equations are required to compute stage and flow variables. Unsteady flow modeling is also concerned with how these parameters change with time and distance downstream. This is reflected in the partial differential terms in the relevant equation.

Equation 5.16, which is also known as the continuity equation, is the first equation required for unsteady flow modeling (Chow, 1959):

$$\frac{\partial Q}{\partial x}+\frac{\partial A}{\partial t}=\frac{\partial (VA)}{\partial x}+\frac{\partial A}{\partial t}=q \tag{5.16}$$

The second equation is the momentum equation (or the St Venant equation), given in Equation (5.5) in its conservation form:

$$\frac{\partial V}{\partial t}+V\frac{\partial V}{\partial x}+g\frac{\partial y}{\partial x}-g(S_0-S_f)=0 \tag{5.17}$$

where

y : hydraulic depth (m)
g : acceleration due to gravity (9.81 m/s^2)
S_0 : bed slope (m/m)
S_f : Friction slope (m/m)

In Equation 5.17, the terms indicate local acceleration, convective acceleration, presssure force, gravity force, and friction force in the corresponding order.

The local and convective acceleration terms are called the inertial terms. The friction slope is defined in the same way as in steady flow modeling. For this purpose, Manning, Chezy or Colebrok-White equations may be needed.

The difficulty in solving the above equations has led to some simplifications. Even if a software is used to solve the full set of equations, the simplified methods are preferred for particular situations simply because of data limitations. Figure 5.9 shows a summary of the various solutions for St Venant Equations.

5.3.1 Solution Methods

5.3.1.1 Steady State Approximation

Since the variables do not change under steady state assumption, the momentum equation of Equation 5.17 can be expressed in a different way to give the steady state momentum expression as follows:

$$\frac{dV(V)}{dx} + \frac{dy}{dx} - S_0 = S_f \tag{5.18}$$

This steady state approximation assumes that the flow is steady but gradually varied over space.

5.3.1.2 Level Pool Routing

This method uses only the continuity equation. Inflow, outflow, and stored water volume are balanced, and the water surface slope is zero, making the approach useful only for lakes and reservoirs.

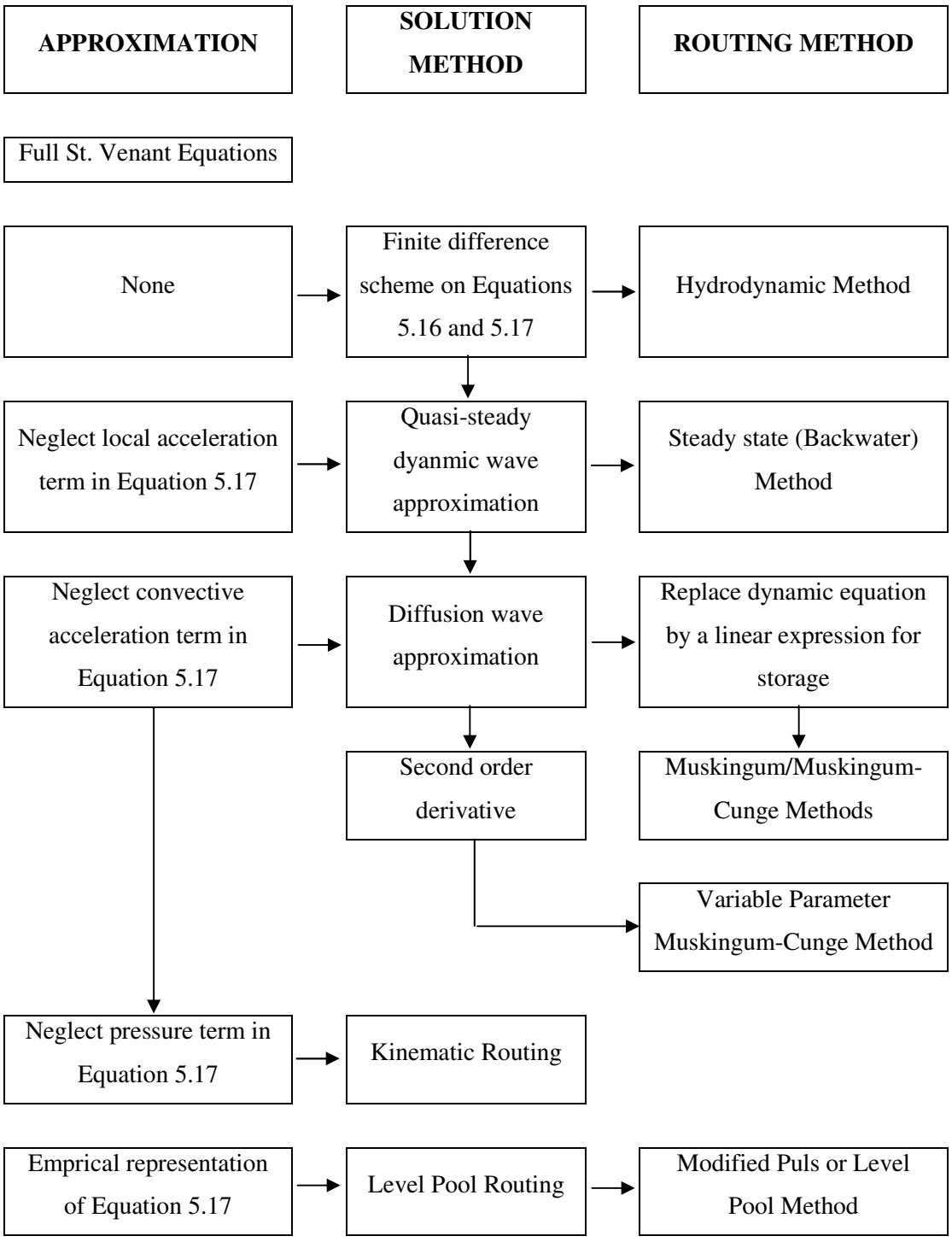

Figure 5.9. Summary of solution methods for the St. Venant Equations (Klotz et al., 2003).

5.3.1.3 Kinematic Wave Approximation

In the kinematic wave approximation, inertial and friction forces are ignored while considering the change of flow with distance and time. Accordingly, this method can develop rapid propagation of changes downstream.

When the terms of d/dx and d/dt are neglected in Equation 5.16, the momentum equation becomes:

$$S_f = S_0 \tag{5.19}$$

This equation is the description of a steady, uniform flow and indicates that there is a single-value relationship between channel storage (or stage) and flow. This relationship could take a number of forms, and a functional relationship of the considered form can be expressed as in the following:

$$Q = f(A) \text{ such that } \frac{dQ}{dA} = c \tag{5.20}$$

where

c : wave celerity (m/s)

Kinematic wave equation is obtained by combining Equation 5.20 and Equation 5.16 as:

$$\frac{\partial Q}{\partial t} + c\frac{\partial Q}{\partial x} = a\frac{\partial^2 Q}{\partial x^2} \tag{5.21}$$

where a is a function of discharge.

The kinematic wave equation describes the propagation of a flood wave along a river reach but does not account for any backwater effects. This implies that water may only flow downstream.

5.3.1.4 Diffusion Wave Approximation

In the diffusion wave approximation, the dy/dx term is kept and the inertial terms are dropped from the momentum equation. The watersurface slope is not equal to the bed slope. The momentum equation is defined as:

$$\frac{dy}{dx} = S_0 - S_f \tag{5.22}$$

If the simplified momentum given in Equation (5.22) is combined with the continuity equation, the diffusion wave equation is obtained as:

$$\frac{\partial Q}{\partial t} + b(Q)\frac{\partial Q}{\partial x} = a\frac{\partial^2 Q}{\partial x^2} \tag{5.23}$$

where $b(Q)$ is related to an attenuation parameter that can be derived, and b is a function of discharge and must be evaluated over a range of depths and discharges.

5.3.1.5 Other Approximations

If assumptions given above are not significantly violated, solutions with the relevant equations can be sought. However, a more theoretical assessment of the applicability of these equations may be attempted. Henderson (1996) derived the following expressions for the relative magnitude of the various terms in the momentum equation that balance the friction slope (S_f). Altough these analytical solutions are for a wide rectangular channel, similar relationships can also be used for more complex channel shapes:

$$\frac{\partial y}{\partial x} \propto S_0^{-2/3} \times (\text{terms characteristic of the inflow hydrograph}) \tag{5.24}$$

$$\frac{V}{g}\frac{\partial V/\partial x}{\partial y/\partial x} = O(Fr^2) \tag{5.25}$$

and

$$\frac{1}{g}\frac{\partial V}{\partial t} = O\left(\frac{V}{g}\frac{\partial V}{\partial x}\right) \tag{5.26}$$

where

Fr : Froude number

O : means "order of magnitude of"

The following application areas are suggested for the various unsteady flow equations:

- For high slopes (3.8-5.7 m/km) but largely subcritical streams, the s_o term is the only significant term, and kinematic wave approximation is appropriate.
- For low slopes (< 0.19 m/km and Fr is significantly less than 1), the acceleration terms are small, so that the diffusion wave approximation is appropriate.
- For intermediate slopes, in order to furnish an accurate solution, the full St. Venant equations become necessary. Depending on data accuracy and the required exact solution, the use of one of the simpler approximations is suggested.

5.3.2 Solving the Diffusion Wave Equation

5.3.2.1 Muskingum Method

The continuity equation is used between upstream and downstream points in a reach or a storage unit. The question is to determine the outflow when the inflow

hydrograph flowing into the storage unit is known. The principle of continuity provides the basic equation for solving the problem as

(Inflow volume in time dt) - (outflow volume in time dt) = (change in volume of water stored)

The differential form of this expression is given as:

$$I - O = \frac{dS}{dt} \tag{5.27}$$

where

I : inflow to the reach (m^3/s)
O : outflow from the reach (m^3/s)
S : storage (m^3)

By using the average inflow and outflow, Equation 5.27 can be written as given in Equation 5.28 to obtain a more suitable form:

$$\frac{I_1 + I_2}{2}\Delta t - \frac{O_1 + O_2}{2}\Delta t = S_2 - S_1 \tag{5.28}$$

The subscripts 1 and 2 indicate the values at the start and end, respectively, of the time period Δt.

Since it is presumed that the hydrograph shape is a straight line during Δt, the choice of the time step requires more attention to preserve the important features of the hydrograph, such as flow peak. In particular, the routing period must be less than the travel time of the flood wave through the reach.

The Muskingum method models the storage volume of flooding in a river channel by a combination of the volume beneath a line parallel to the stream bed (prism

storage), and the volume of water between that line and the water surface (wedge storage) (Figure 5.10) (Chow et al., 1988; Klotz et al., 2003)

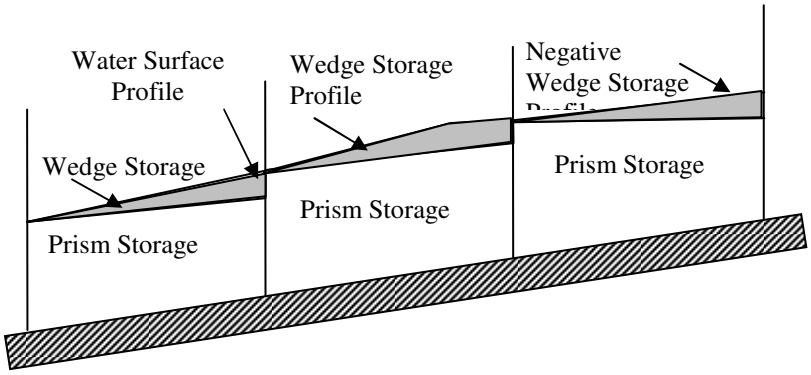

Figure 5.10 Storage in a river channel.

The water surface slope can often be assumed to be horizontal; but in rivers, the water surface does not have a horizontal shape so that a relationship for the wedge storage is required. This relationship can be derived by assuming that the cross sectional area of flood flow is directly proportional to the discharge at the section (Equation 5.29) (Chow et al., 1988; Klotz et al., 2003).

$$S_t = KO_t + KX(I_t - O_t) = K(XI_t + (1-X)O_t) \quad (5.29)$$

where

K : travel time of the flood wave through the routing reach (s)

X : a dimensionless weight ($0.0 \le X \le 0.5$)

S_t : Storage at time t (m^3)

In Equation 5.29, KO_t indicates the volume of prism storage, and $KX(I_t-O_t)$ shows the volume of wedge storage. The quantity $(XI_t + (1-X)O_t)$ is a weighted discharge. If storage in the channel is controlled by downstream conditions such that storage and outflow are highly correlated, then X becomes zero and Equation 5.29 is rearranged as:

$$S = KO \quad (5.30)$$

The value X = 0.0 yields a similar result to that of a large reservoir producing significant attenuation, while X = 0.5 is representative of a prismatic channel with little or no attenuation. For most streams where the Muskingum method is applied, the value of X is commonly between 0.05 and 0.2.

In order to determine the outflow at time $t+\Delta t$, S_2 and S_1, expressed by Equation 5.29, are substituted into Equation 5.28 to obtain:

$$O_{t+\Delta t} = \frac{\frac{I_{t+\Delta t} + I_t}{2}\Delta t - \frac{O_t}{2}\Delta t - XK(I_{t+\Delta t} - I_t) + (1-X)KO_t)}{\frac{\Delta t}{2} + (1-K)X} \tag{5.31}$$

Successive reaches can be simulated by noting that outflow from an upstream reach provides inflow to the downstream reach.

5.3.2.2 Muskingum-Cunge Method

Since the Muskingum model was developed, depending on some assumptions that are often violated in natural channels (such as uniform distribution of velocity and a fixed wave speed with depth and flow), estimation of parameters for this method becomes very difficult. Muskingum-Cunge model solves some of these limitations. Continuity equation and the diffusion form of the momentum equation are both used in the solution of the method so that it becomes possible to examine not only a change in volume, but also change in flow with distance and change in flow area with time. Equation 5.32 shows the form of the diffusion wave equation used in the computations:

$$\frac{\partial A}{\partial t} + c\frac{\partial Q}{\partial x} = \mu\frac{\partial^2 Q}{\partial x^2} + cq_L \tag{5.32}$$

c : wave celerity (speed) (m/s)

μ : hydraulic diffusivity (m^2/s)

q_L : lateral inflow (m^3/s)

Standard configuration and eight-point cross-section configuration are two forms of the Muskingum-Cunge model. In the former, a representative channel cross section is provided as principal dimensions, channel roughness, energy slope, and length. In the latter, the "average" section is described as eight pairs of distance and elevation values.

5.3.2.3 Variable Parameter Muskingum-Cunge Method (VPMC)

The VPMC method was developed, based on a second-order derivation of Equation 5.32. This method has been widely applied in Europe. The equation used in the computations is:

$$\frac{\partial Q}{\partial t} + c\frac{\partial Q}{\partial x} = \frac{\alpha}{L}Q\frac{\partial^2 Q}{\partial x^2} + cq_L \qquad (5.33)$$

where

α : an attenuation parameter

c : a parameter which is a function of the flow, Q

The difference between the Muskingum-Cunge and VPMC methods is that, in the VPMC method the attenuation and wave celerity parameters (a and c) are functions of the flow rate. Hence, the degree of attenuation and wave celerity may vary during the passage of a hydrograph.

5.3.2.4 Solving the Full St. Venant Equations

Since St. Venant equations (Equation 5.16 and 5.17) are partial differential equations, their solution is furnished by a numerical method. The numerical schemes include both explicit and implicit schemes. Implicit schemes have superior numerical stabilities and computational efficiencies so that they have become mainstream numerical techniques in solving the unsteady flow equations for rivers. Discretization

and iteration are the two main stages to derive the numerical solution for St. Venant equations.

Discretization

Though the differential terms, $\partial/\partial t$ and $\partial/\partial x$, vary continuously, numerical solutions evaluate them only at discrete points in space or moments in time in an approach called discretization. Many software packages use the method of finite differences, and the solution is obtained at a number of discrete points (with distance interval Δx) and a number of discrete times (Δt) for which derivatives are approximated by their finite differences. The simplest form of a finite difference is the forward-difference method, which uses only the discrete point and the one next to it to evaluate a differential; such as:

$$\frac{\partial y}{\partial x} = \frac{y_2 - y_1}{\Delta x} \tag{5.34}$$

Common implicit finite-difference schemes include the six-point Abbott-Ionescu scheme (Abbott, 1979), and the four-point Priessmann scheme, which is used in HEC-RAS (Klotz et.al., 2003).

Iteration

The solution of the implicit discretized equations requires an iterative approach. This means that, at a given time step, successive solutions of flow and stage are obtained until the difference between the value in the latest iteration and that in the previous iteration is small enough to provide convergence on the correct value. In software packages, the definitions on how close the values have to be for convergence are usually set by the user as tolerances. For example, the default value in HEC-RAS is 0.006 m for water-level convergence.

In some cases, however, the values within each iteration change remarkably, and convergence can be time-consuming or even unachievable. Most software packages have a maximum number of iterations that is also defined by the user. For example, the default number of iterations is 20, and the maximum number of iterations is 40 in HEC-RAS. If convergence has not been achieved after a given number of iterations, the solution with minimum error is used and nonconvergence is flagged.

CHAPTER SIX
FLOODPLAIN MANAGEMENT

6.1 Floods

Flooding is accounted as one of the most common environmental hazards (Smith, 1992). Changes in hydrology and topography of a floodplain can be considered as causes of floods (Yang& Tsai, 2000). In particular, widespread geographical distribution of river valleys and low-lying coasts, together with their long-standing attractions for human settlement, cause these changes (Smith, 1992).

The estimation of flooding and the delineation of inundated areas are important for floodplain management, flood-damage mitigation, engineering design, and site planning (Chang et al., 2000). Some flood-prone environments present a higher risk than others. Smith (1992) defined the most vulnerable landscape settings in five categories:

1. *Low-lying parts of active floodplains and river estuaries*. These environments encounter flood hazards frequently.

2. *Small basins subject to flash floods*. Flash floods generally occur in arid and semi arid areas, where steep topography, sparse vegetation, and high intensity-short duration rainfall are eminent. In addition, intensively developed urban areas are affected by flash floods as a result of rapid runoff.

3. *Areas downstream of unsafe or inadequate dams.* Dam break related floods are both natural and technological hazards. There is often restricted time for warning and evacuation for such a flood type as for flash floods.

4. *Low-lying inland shorelines.* The main problem in these areas is the change in lake levels. After a wet season, lake levels rise to risky levels. There is often enough time for warning people, but if erosion, sand dunes or bluffs exists, buildings and facilities may be destroyed.

5. *Alluvial fans*. These environments lead to a special type of flash flood, especially in semi-arid areas when the fans support urban development. Alluvial fans are risk-prone environments as the drainage channels may meander unpredictably across relatively steep slopes, leading to high velocity flows (commonly reaching speeds of 5-10 ms-1) which are highly charged with sediment (Smith, 1992).

There are two main measures to cope with floods, structural and nonstructural measures. Yevjevich (1992) presented five classes of these measures:

- adjustment to natural hazards
- flood damage prevention
- flood damage reduction
- flood policy making
- basic categories of individual measures.

Structural measures are taken to alter several parameters of a flood event, such as runoff volume, peak flow, time of peak, and velocity to protect urban settlements and to use floodplain areas for agriculture and transportation network locations (Correia et al., 1999, Rossi, 1992).

Since non-structural measures have gained more importance in the last decades, warning systems based on real-time flood forecasting techniques, floodplain zoning to limit the illegal uses of the plain, local flood proofing, and flood insurance programs have been used to reduce flood risk in floodplains. After the use of non-structural measures, public awareness on environmental matters and the obligatory assessment of environmental impacts opened the way to a more systematic consideration of non-structural measures. The ecological and cultural values and functions of wetlands are often threatened by structural measures and are increasingly recognized as values that are worth protecting (Rossi, 1992, Correia et al., 1999).

Platt and Mc Mullen (1980) defined three periods of floodplain management practices; a fourth period is also added to start in the 90s:

1) Structural measures era (1930s-1960s): in this period, hydraulic structures such as reservoirs, channel improvements, dikes, levees and floodwalls, high flow diversions, spillways, retention basins and storm water management facilities were designed to control floods as structural measures with exclusive reliance.

2) Integrated floodplain management era (1960s-1980s): although this period combined structural and nonstructural measures, the latter such as flood warning, land use regulation programs and insurance, found a wider area of application.

3) Post-flood hazard mitigation era (1980s-1990s): this period, which is still in effect, covered measures, such as property acquisition and land use controls, realized in the immediate post-flood period.

4) Broader approach era (1990s-): it is the current period in which structural and non-structural measures for flood mitigation are incorporated with the preservation and restoration of environmental resources (Smith, 1992, Correia et al., 1999).

Since institutional aspects and public participation play an important role, a comprehensive approach is required for non-structural measures. These measures are very important for fast growing urban areas, particularly in coastal zones where flood risk is increased by sea level rise. Land use planning procedures are still important in floodplain management (Burby and French, 1981; Handmer, 1995; Muckleston, 1972; Parker, 1981; Fordham, 1992; Saraiva, 1995). Burby and French (1981) discuss the so-called ‘land-use management paradox’, where factors that stimulate the adoption of land-use programmes in hazard-prone areas can also promote encroachment, which in turn limits their effectiveness. Therefore, the consideration of the local context is essential in evaluating the aims and effectiveness of floodplain management programmes. Relevant stakeholders and conflicts between development interests and regulatory restrictions should be taken into consideration (Correia et al., 1999).

6.2 Floodplain Modeling Methods

Mainly there are three floodplain modeling methods:

- Engineering experience – In flood modeling studies, engineer's experience and judgment, with minimal consideration of hydraulic computations, were used about 100 years ago. In levee design or determination of roadway embankment heights, highwater marks indicating a flood level were the records used as inputs. Today, all floodplain modeling problems are approached by using hydrologic and hydraulic modeling tools even by engineers who have valuable experiences.

- Physical modeling – Most of the physical modeling studies were implemented in the late 1800s and early 1900s, especially in the hydraulic laboratories of universities to examine flume related problems. These models were not used directly in floodplain modeling studies. Nowadays, physical models are only constructed at large hydraulic laboratories, and they are simply used in cases where numerical models do not give sufficient results. Physical models are expensive to construct and operate, require special engineering expertise, and are typically only practical for major river systems or large river structures.

- Numerical modeling – While, in the initial studies, analytical procedures were carried out through manual computations, afterwards, computer programs have replaced them efficiently. Today, computer programs with GIS integration are the most appropriate techniques used in floodplain modeling studies.

6.3 Floodplain Delineation Process

Since flooding is a dynamic process, watershed, channel and floodplain characteristics vary in time. This means that the conditions which cause floods change over time. A floodplain map prepared, based on the today’s conditions, cannot be used for tomorrow since it does not reflect the current conditions.

Floodplain maps should be updated by using new data available over time. It is possible to obtain floodplain maps that are more accurate and represent more area at less cost by using new techniques. Accuracy depends on the purpose for which it is prepared and the data used in it. Some floodplain maps are prepared just to show general areas subject to flooding. Others are done for a flood control project, which need to be more accurate and are, therefore, more expensive (Wahl et al., 2000).

The traditional floodplain mapping procedure involves marking the observed water level points on a topographic map and extending water levels over the map until a contour of a higher elevation is reached. The water-land intersection points are then connected together by following the contours to get the extent of inundation. This process requires an understanding of flow dynamics over the floodplain, topographic relationships, and sound judgment by the draft person (Noman, 2001).

Nowadays, computer modeling techniques have been widely used in water related studies. Engineers may determine where and when floods occur through the use of these modeling tools. Computer modeling techniques have assisted engineers with determining more accurately where and when flooding may occur (Snead, 2000).

The same procedure mentioned above is followed for every computer based automated floodplain delineation process, where the determination of water surface profiles associated with different flow conditions is accomplished. Automated floodplain mapping supplies significant advantages when compared to traditional floodplain mapping, such as saving of both time and resources, providing more speed and efficiency, and developing flood depths in addition to flood extents (Noman, 2001, Snead, 2000).

6.4 The Role of Tools in Floodplain Determination

There are four computational steps in floodplain determination based on computer models (Figure 6.1):

1) Preprocessing: The geospatial data to be used in both the hydrologic and the hydraulic models is extracted via GIS tools such as ArcView and ArcInfo systems.

2) Hydrologic Modeling: A rainfall-runoff model is used for a design storm or historic storm event to obtain flood peak value, or flood hydrograph, depending on the scope of the study.

3) Hydraulic Modeling: A hydraulic model routes the runoff through stream channels to determine water surface profiles at specific locations along the stream network.

4) Postprocessing: Floodplain mapping and visualization are accomplished with GIS tools.

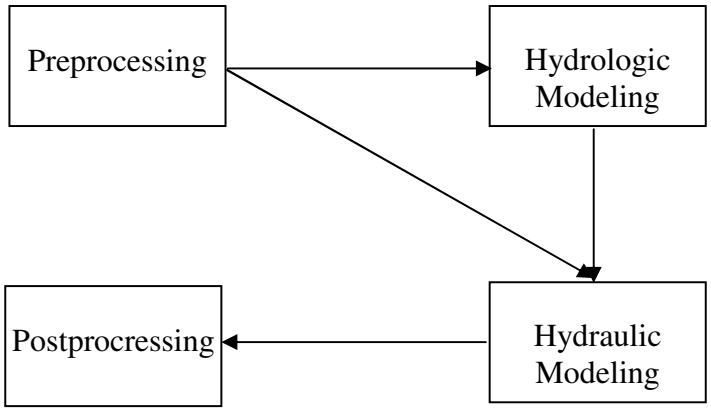

Figure 6.1 Flow chart for floodplain determination via computer models and GIS.

Since flows in streambeds are naturally random and unsteady, steady-state methods often do not accurately depict water surface profiles. The steady-state modeling technique is also limited by how the modeler spatially synchronizes the rainfall-runoff routing for multiple drainage basins at a specified point in time. Such methods are subject to human error and can be very time consuming. Developments in fully dynamic, unsteady models have provided engineers with highly accurate hydraulic modeling methods that result in two- and three-dimensional graphics (Snead, 2000).

The application of a standard riverine numerical model, such as HEC-RAS, enables the engineer to simulate the hydraulics of the floodplain, evaluate existing conditions, determine proper design of hydraulic structures, and assess the effects of these structures. Performed by a competent engineer, floodplain modeling is an

objective and defensible method to determine river hydraulic information (Klotz et al., 2003).

The use of a hydraulic model in simulation of river hydraulics offers many advantages:

1) Hydraulic models, which are properly written and documented, are preferred because they are scientific and defensible analytical tools.

2) Hypothetical flood events can also be simulated by using a hydraulic model. It means that one does not have to wait for the occurrence of any flood event to perform a simulation. Engineers can attain optimal solutions by using recorded floods, as well as larger or smaller events to design hydraulic structures. A flood record can represent the "once-in-a-million" event, while, in many cases, it may not represent a very rare event. In the first case, a very rare event can lead to a significantly overdesigned and expensive structure; whereas the latter case can lead to unsafe projects.

3) Prior to the design of major hydraulic structures, an economic analysis is often required to determine project feasibility. A key component of this analysis is the determination of net benefits and the benefit-cost ratio of the project. A hydraulic model is used to determine the water surface elevation versus frequency relationship, which is then linked to the elevation-damage data collected by the economist. The combined relationship (damage versus frequency) may be integrated to obtain an average annual damage value for the no-project alternative. The elevation-versus-frequency relationship is then established for the designed project and the average annual damage for this case is computed. The difference between the average annual damage values with and without the project represents the reduction in flood damages realized by the project, or the average annual project benefits due to reduced flooding. These benefits must exceed the average annual costs for the project to be economically viable.

4) A hydraulic model allows for quick modification of key variables, such as Manning's n, to develop scenarios for the determination of the most appropriate solutions on flood problems (Klotz et al., 2003).

Another tool widely used in floodplain delineation studies is the Geographic Information Systems (GIS) which offer the ideal environment for this type of work. GIS offers hydrologists and planners the powerful capability to analyze and visually express flood control measures.

Although GIS is an excellent tool to accomplish the requirements of maintaining, acquiring, and utilizing a spatially referenced database, it is limited in its ability to perform floodplain modeling and flood damage calculations. Thus, GIS have been incorporated with hydrologic and hydraulic models to delineate floodplain areas. There are several advantages of using GIS with these models: 1) it is possible to integrate data from different sources, 2) GIS can create spatial relationships that are important in floodplain modeling studies, 3) the display and data organizing capabilities of GIS are powerful tools for visualizing insights of the physical process of storm water transport (Shrestha, 2000). Therefore, the GIS-based Flood Information System (GFIS) was developed for floodplain modeling, analysis of project feasibility, and informational support (Yang & Tsai, 2000).

Developments in fully dynamic, unsteady models have provided engineers with highly accurate hydraulic modeling techniques that result in two-and three-dimensional graphical visualizations for flood analysis. The key to graphical visualizations in dynamic modeling is the inclusion of time-series data within a spatial interface (Snead, 2000).

6.5 Steps in Floodplain Modeling

Floodplain modeling studies should follow the 10 steps given below for a complete analysis (Figure 6.2):

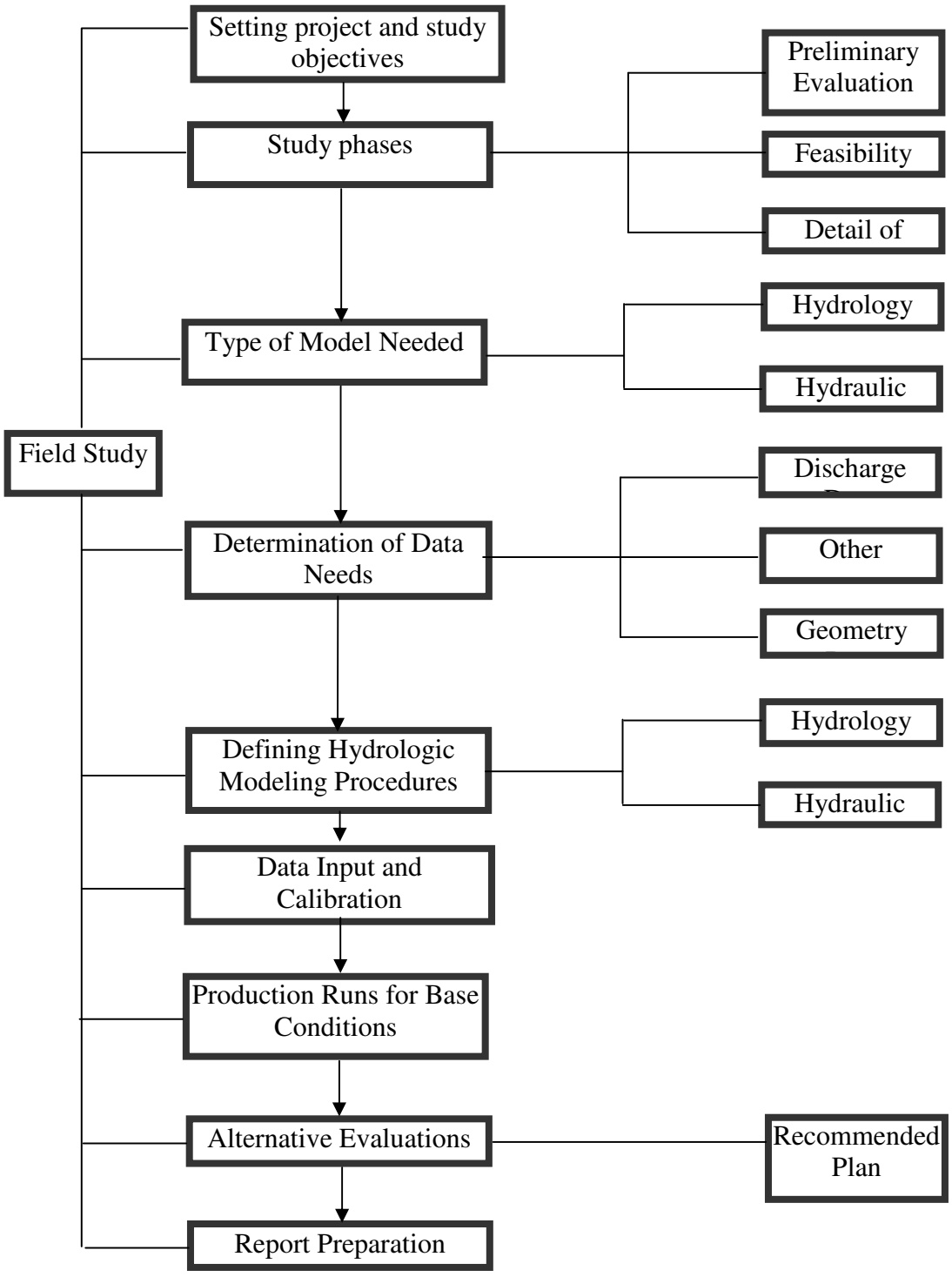

Figure 6.2 Steps of floodplain modeling studies (Klotz et al., 2003).

1) Setting project and study objectives
2) Study phases
3) Field study
4) Determination of the hydrologic and hydraulic simulation types needed
5) Determination of data needs
6) Defining hydrologic modeling procedures
7) Preparing input data and calibration
8) Performing production runs for base conditions
9) Performing project evaluations
10) Preparing the report (Klotz et al., 2003).

1) Setting project and study objectives: The main objective of floodplain modeling studies is the analysis of flood damage reduction. The other objectives considered may be the analysis of flood impacts on navigation, hydropower, irrigation, water supply, environmental concerns, and permits.

2) Study phases: There are three main phases in a flood study; preliminary evaluation phase, feasibility phase, and detailed design.

A preliminary evaluation is made when it is uncertain whether there is an economic interest in further pursuing a project. Rough designs with associated costs and benefits are developed. This information is then used to ascertain if it is likely that more-detailed studies will lead to a feasible and desirable solution. Since there is limited time and money for this phase, evaluations are often based on available hydraulic data and engineering judgement.

In the feasibility phase, the scope and magnitude of the project are specified. Here, floodplain hydrology and hydraulic analyses are performed for base conditions. For this purpose, hypothetical frequency flood profiles are determined, and then final hydrologic and hydraulic studies are performed to determine potential flood damages along the analyzed stream (Klotz et al., 2003).

The detailed design phase covers the structural and hydraulic design of a flood control scheme.

3) Field Study: Field studies are needed for all modeling studies. The hydraulic engineer should take photographs of representative reaches of the river, bridges and culvert crossings of the main channel, and the adjacent floodplains. The channel bed material should also be surveyed at different locations. Bed material grain size is an important factor in estimating Manning's n for the channel.

The river banks should also be surveyed as well. Leaning or fallen trees in the channel, exposed root wads in the channel bank, large deposits of material, scour around bridge footings, and vertical banks with sloughed material at the toe give information on changes in channel geometry. These changes may need to be included in the floodplain modeling process (Klotz et al., 2003).

Highwater marks can be obtained from interviews with local residents to collect calibration data.

4) Determination of hydrologic and hydraulic simulation types needed: This is another important step in floodplain modeling. The most appropriate method for floodplain modeling will always be a one-dimensional model, coupled with either steady, quasi-unsteady, or fully unsteady hydraulics (Klotz et al., 2003).

5) Determination of data needs: Flow and geometry related data are the main requirements for floodplain modeling. If the study reach is short and uncomplicated, only a peak discharge value may be necessary. On the other hand, a full hydrograph is required if the reach is long with several tributaries, or if there are ongoing changes in the watershed.

Channel and floodplain cross-sectional data must be collected at a sufficient number of locations to accurately define the water surface profile. Stream locations that have an effect on flood elevations should also be surveyed or estimated. These locations include sharp breaks in the channel slope, large expansions or contractions of the floodplain width, and significant changes in land use or vegetation (Klotz et al., 2003).

Cross sections should extend across the entire width of the floodplain, if possible. The geometry data of hydraulic structures should also be obtained either from new surveys of old structures or by getting sections of structures from the agency responsible.

6) Defining hydrologic and hydraulic modeling procedures: This step is an important part of the planning process. The hydrologic model to be used in the modeling process should be the acceptable and accurate for the project area.

The modeling procedures can be selected on the basis of the following criteria for steady flow modeling:

- Precipitation Data: Depth, temporal distribution, or mean areal precipitation.
- Infiltration modeling technique: Uniform and initial, SCS curve numbers, Green-Ampt, Holtan, Horton, or other methods.
- Runoff Modeling: Kinematic wave or synthetic unit hydrographs (SCS, Clark, Snyder, or other methods).
- Hydrograph Routing: Straddle-Stagger, Muskingum, Modified Puls, Muskingum-Cunge, or other methods.
- Calibration Data: If a flood has produced known highwater marks or if stream gage data are available, gaged rainfall data should also be obtained. Rainfall maps are prepared, using the Theissen or isohyetal techniques. If discharge gages are available, the recorded flood events should be obtained from the agency in charge or from a reliable web site. If several actual storm-flood events are available, all should be used in the calibration and verification process (Klotz et al., 2003).

For unsteady flow modeling, modeling procedures should also include the following:

- Boundary conditions at upstream and downstream locations and for each major tributary: Such data as stage and/or discharge hydrographs, rating

curves, normal depth, lateral inflows, and gate opening settings are needed at each boundary location.

- Although a single hydrograph is often sufficient, some studies require a full period of record for unsteady flow routing. The discharge data come from gage records or from simulation with runoff models. A "warm–up" period featuring a constant flow for a specified time is typically included as an initial condition for the model operation (Klotz et al., 2003).

7) Preparing input data and calibration: Preparation of input data, debugging and model calibration require significant amounts of time and effort to enter all cross-sections, bridges, culverts, dams, diversions, and other structures affecting water surface profiles into HEC-RAS model. If storage-discharge data are needed, ineffective flow areas should be specified in the HEC-RAS cross-sectional data for hydrologic routing. Historic discharges and highwater marks can be used to calibrate the output from HEC-RAS. Following calibration, a series of steady flow discharges is used to obtain a storage-discharge relationship for each routing reach in the hydrologic simulation. Following calibration and verification of the model input, an independent technical review of the output should be made for quality assurance/quality control (QA/QC) purposes (Klotz et al., 2003).

8) Performing production runs for base conditions: Model calibration and verification processes are the most important steps in modeling studies. Actual representation of the floodplain depends on calibration, but data availability is generally the most problematic issue for modelers. Further adjustment to model parameters during the model runs may be required, based on available local data and engineering experience (Klotz et al., 2003). In the simulation of large and rare events, the following actions may be required:

- Modification of infiltration parameters to reflect more runoff
- Modification of peaking coefficients to increase the peak discharge of the unit hydrograph
- Modification on routing of travel times to reflect a faster movement of the hydrograph through a routing reach

- Reduction of Manning's n to reflect a more efficient channel during rare flood events
- Simulation of the buildup of trash and debris during a major flood.

9) Performing project evaluations: When modeling process is completed, the engineer has several water surface profiles, indicating the flood levels from actual or hypothetical floods at any location in the study area. These water surface profiles and inundated areas are obtained by examining a number of scenarios which deal with flood reduction studies or changes in the basin. For example, land use changes such as urbanization or reservoir construction may be possible in the future. Since both the hydrologic and the hydraulic model will change in these cases, they should be run for the expected changes; and, thus, new profiles are computed. Such additional runs are recommended in order to show possible future developments that will affect floodplains. In addition to potential damage costs, a benefit/cost analysis is prepared for the future conditions as well. This effort should commence well in advance of a detailed design of flood control measures by other civil engineering disciplines, so that the overall study effort is not delayed (Klotz et al., 2003).

Although all possible alternatives are examined in initial planning activities, only adequate solutions with respect to effectiveness and costs are analyzed in detail. Pre-project versus post-project profiles and inundated areas are assessed.

Unlike the case of small-scale projects, the reduction in flooding for each scenario is expressed as an annual project economic benefit for large-scale projects. Appropriateness of the project in economic terms depends on the benefit-cost ratio and the least cost condition. In the former, the suitable relation is the one for which the average annual costs are less than the annual benefits; while in the latter, a least cost solution is selected to satisfy a design criterion. The hydraulic engineers, economists, and project managers are work together in the project evaluation phase (Klotz et al., 2003).

10) Preparing the report: In the planning stage, a report, which includes the estimates on time and costs spent on the project, is essential. Acceptance of the

technical work generally depends on the adequacy of the technical report. Thus, sufficient time and budget should be allocated to the report which should be brief, clear, and well-written (Klotz et al., 2003).

CHAPTER SEVEN
HYDROLOGIC AND HYDRAULIC MODELING TOOLS

Hydrologic and hydraulic modeling studies play an important role in floodplain management studies. These studies, which include the estimation of flood peaks and/or flood hydrographs and the determination of flood inundation maps, have been realized first to save human lives, and then to protect people's property, agricultural areas, animals, etc. (Olivera & Maidment, 2000). Thus, hydrologic and hydraulic models have become essential tools in prediction of floods and the investigation of flood management alternatives. This chapter discusses the modeling capabilities of the computer programs utilized in this study.

7.1 Basic Concepts in Hydrologic Modeling Studies

Available stream flow and rainfall records, high water marks, etc. are required for simulations of historic or hypothetical frequency events. If the project area is a gauged basin, runoff parameters are first estimated by using monitoring data. Then the calibration process is carried out on both the rainfall and the runoff parameters for each of the selected historic flood events. The model has to be calibrated also by using the hypothetical events for gauged frequency statistics. If the analyzed basin has no stream gauge, it may be possible to take advantage of nearby or similar gauged basins. Hypothetical frequency storm data and synthetic unit hydrograph methods can be conveniently used if there is no monitoring data in the basin (HEC, 1996).

7.2 Hydrologic Modeling by HEC-HMS

7.2.1 General

Hydrologic modeling is mainly performed to develop discharge values over a river basin for floodplain modeling studies. Discharge hydrographs must be computed to investigate the effects of changes due to urbanization, to evaluate potential flood mitigation projects, or to perform quasi-unsteady or full unsteady

flow analyses. Full discharge hydrographs can be obtained only by watershed modeling, and these hydrographs are then translated through the watershed, regarding the effects of timing, tributary inflows, reservoirs, channel modifications, and other flood mitigation components.

In the hydrologic modeling process, an actual or hypothetical design storm is developed, and the runoff hydrograph is computed together with the peak discharge value for the selected event (Klotz et al., 2003). Flood hydrographs are developed at key locations to define the magnitude and timing of flood flows. The relationship between rainfall and runoff helps to define warning times. Hydrologic models, such as HEC-1 and HEC-HMS, are widely used in the computation of flood hydrographs.

The U.S Army Corps of Engineers' Hydrologic Modeling System (HEC-HMS) is a rainfall-runoff simulation model. In 1968, HEC released the HEC-1 computer model to aid engineers in hydrologic analysis. HEC-HMS, the windows-based modified version of HEC-1 model was released in 1998. It is drafted to assist in planning, designing, and operating projects in which current and future runoff from watersheds, with or without water control structures, are computed with the help of the model. HEC-HMS has been designed to be compatible with GIS technology and to facilitate the use of advanced GIS data in civil engineering. The advantage of using GIS in hydrologic modeling is to provide spatially derived hydrologic parameters (such as watershed area, curve number, gridded precipitation, flow length in each watershed, and slope) as input into more powerful hydrologic models.

The HEC-HMS model simulates a rainfall runoff response of a watershed system to precipitation input by representing the entire watershed as an interconnected system of hydrologic and hydraulic components, such as subbasins, streams, reservoirs, diversions, etc. The outputs of the HEC-HMS model can become input to many hydraulic models.

7.2.2 Components of the HEC-HMS Model

In HEC-HMS model, each project consists of three components (Figure 7.1): Basin Model, Meteorologic Model, and Control Specifications.

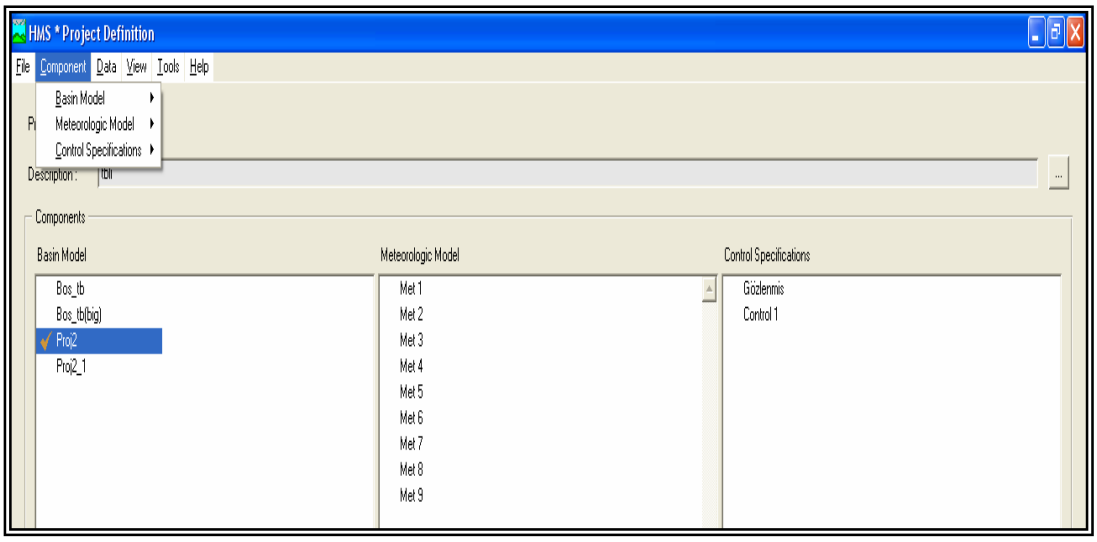

Figure 7.1 Components of the HEC-HMS model.

Each component also has several elements as shown in Figure 7.2.

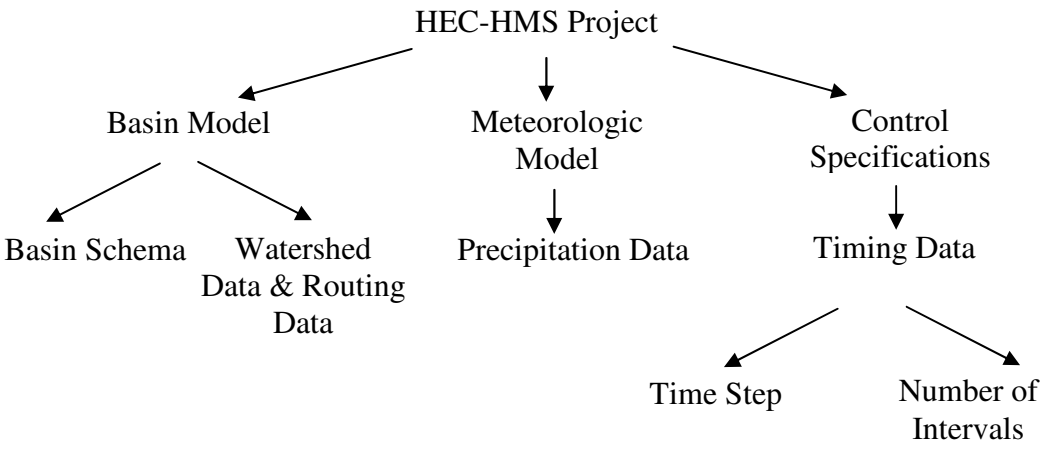

Figure 7.2 Elements of HEC-HMS components.

7.2.2.1 Basin Model

Within the basin model, the physical system is represented by using the available hydrologic elements. There are seven types of hydrologic elements in a basin

schema: subbasin, routing reach, junction, reservoir, diversion, source, and sink. A basin schema may be configured by using “dragging-and-dropping” icons on a schematic display; or it may be prepared by analyzing spatial data in HEC Geospatial Hydrologic Model Extension (HEC-GeoHMS) and then by transferring them into the HEC-HMS model (Figure 7.3). The element data can be edited with editors one by one or globally. Each element can be given a name and a description. The computation methods may be selected by the user and, the data on the basin model elements may be entered again by the user. Some data can be imported directly from GIS, but basically the user himself adds this information. Such data include specification of the hydrologic elements which the basin model comprises, information on how the hydrologic elements are connected, and values of parameters for the hydrologic elements. The basin model is simply used to visualize the locations and sizes of each element for representing the actual basin. As a rule, multiple elements can connect downstream to one element, but one element cannot have multiple downstream connections. The correct direction of flow should be checked by the flow direction option in the toolbar (Bedient & Huber, 2002).

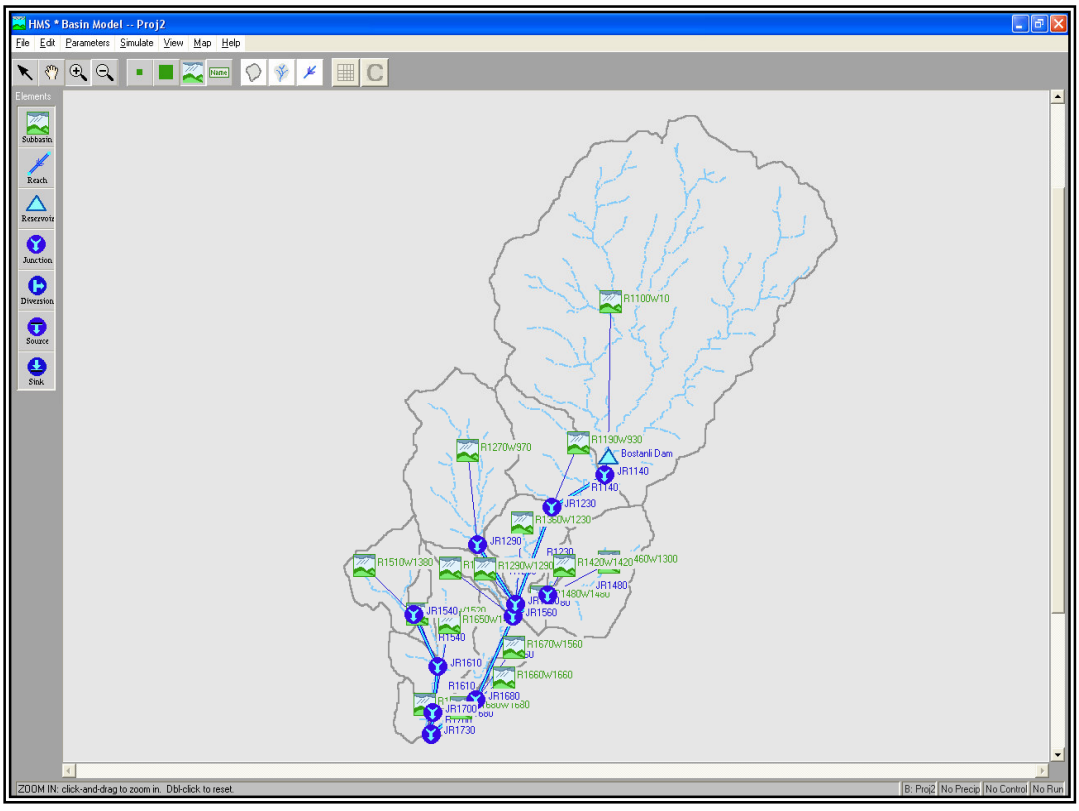

Figure 7.3 HEC-HMS basin model.

Subbasin Element. The subbasin element in the basin component requires three input tables which are used in the computation of subbasin hydrograph. As shown in Figure 7.4, each subbasin element comprises the loss rate, transform, and base flow input tables.

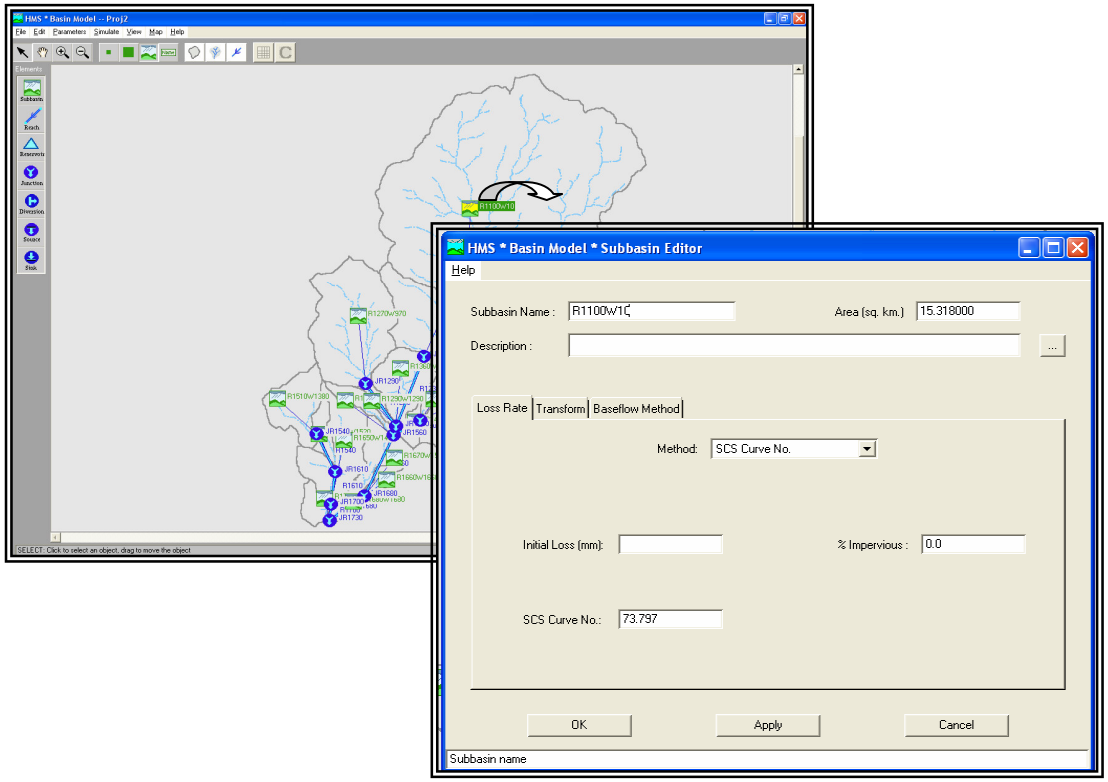

Figure 7.4 Subbasin elements.

Loss Rates

The following assumptions are taken into consideration in the calculation of loss rates:

- Losses include interception, depression storage, infiltration, and evaporation
- Losses leave the hydrologic system.

In the HEC-HMS model, several options are available to simulate loss rates depending on data availability or the aim of the study. These methods and their classifications in modeling theory are given below:

- Green-Ampt (event-based, distributed, empirical, fitted parameter)
- Initial/Constant Loss (event-based, lumped, empirical, fitted parameter)
- Deficit/Constant Loss (continuous, lumped, empirical, fitted parameter)
- SCS-Runoff Curve Number (event-based, lumped, empirical, fitted parameter)
- Gridded SCS Curve Number (event-based, distributed, empirical, fitted parameter)
- Soil Moisture Accounting Loss Method (continuous, lumped, empirical, fitted parameter)
- Gridded Soil Moisture Accounting Loss Method (continuous, lumped, empirical, fitted parameter) (HEC, 2001a)

The one-layer deficit/constant method model can be used for simple continuous modeling, while the five-layer soil moisture accounting model can be used for modeling of complex infiltration and evapotranspiration environments (Bedient & Huber, 2002).

Transform

After the loss rate is computed, the rainfall excess is converted to surface runoff by using the following four methods:

Synthetic Unit Hydrograph Methods:

- Clark, Snyder, SCS, (event-based, lumped, empirical, fitted parameter)

User-Inputs:

- User-specified S Graph (event-based, lumped, empirical, fitted parameter)
- User-specified UH (event-based, lumped, empirical, fitted parameter)

Distributed Parameter Methods:

- Kinematic Wave (Muskingum-Cunge Channel Option) (event-based, lumped, conceptual, measured parameter)

Grid-Based Methods:

- ModClark (event-based, distributed, empirical, fitted parameter)

Spatially distributed runoff can be computed by the ModClark method for which gridded precipitation data is required (HEC, 2001a).

Baseflow Method

Baseflow takes into account normal flow through a channel or the effects of groundwater. Baseflow can be calculated by using the following four methods:

- Recession (event-based, lumped, empirical, fitted parameter)
- Bounded Recession (continuous, lumped, empirical, fitted parameter)
- Constant Monthly (continuous, lumped, empirical, fitted parameter)
- Linear Reservoir (event, lumped, empirical, fitted parameter) (HEC, 2001a).

Reach Element. The stream routing process is accomplished within stream reaches. When a reach element is edited, the screen given in Figure 7.5 appears.

The HEC-HMS model comprises seven stream routing options:

- Semi-Hydraulic Methods (Based on Equations)
  - Kinematic Wave Method
  - Muskingum-Cunge Method (St.)
  - Muskingum-Cunge Method (8 points)
  - Straddle-Stragger
- Hydrologic Methods (Based on Field Data)
  - Muskingum Method
  - Storage Method (Modified Puls)
  - Lag Method

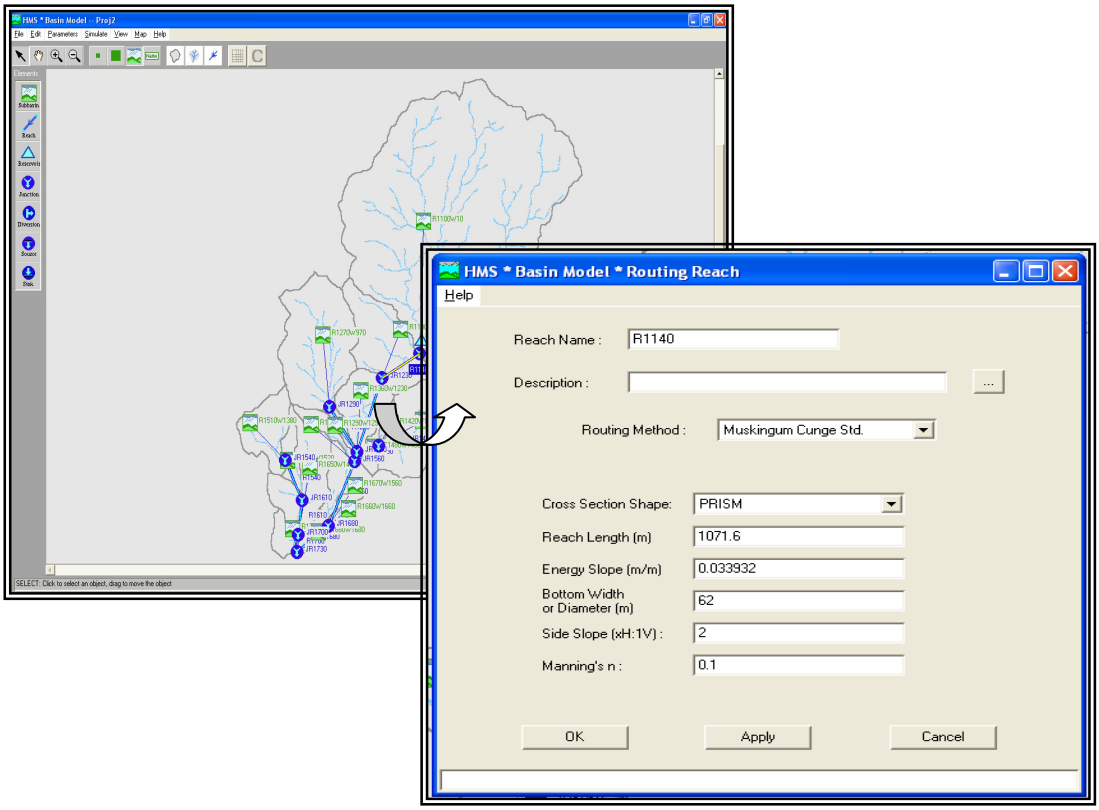

Figure 7.5 Input table for a reach element.

Reservoir Element. The effects of reservoir storage, reservoir performance/design, dam safety and dam failure are analyzed with reservoir routing methods. When "reservoir element" is edited, an input table including the reservoir characteristics such as storage, outflow, spillway and overflow, and options of dambreak analysis appears (Figure 7.6). The available reservoir routing options in the HEC-HMS model can be grouped as follows:

- Simple Storage vs. Discharge or Elevation vs. Discharge Relationship:
  Developed Outside of HEC-HMS
- Storage Specification Alternatives:
  Storage vs. Elevation
  Surface Area vs. Elevation
- Discharge Specification Alternatives:
  Spillways, Low-Level Outlets, Pumps
  Dam Safety: Embankment Overflow, Dam Breach

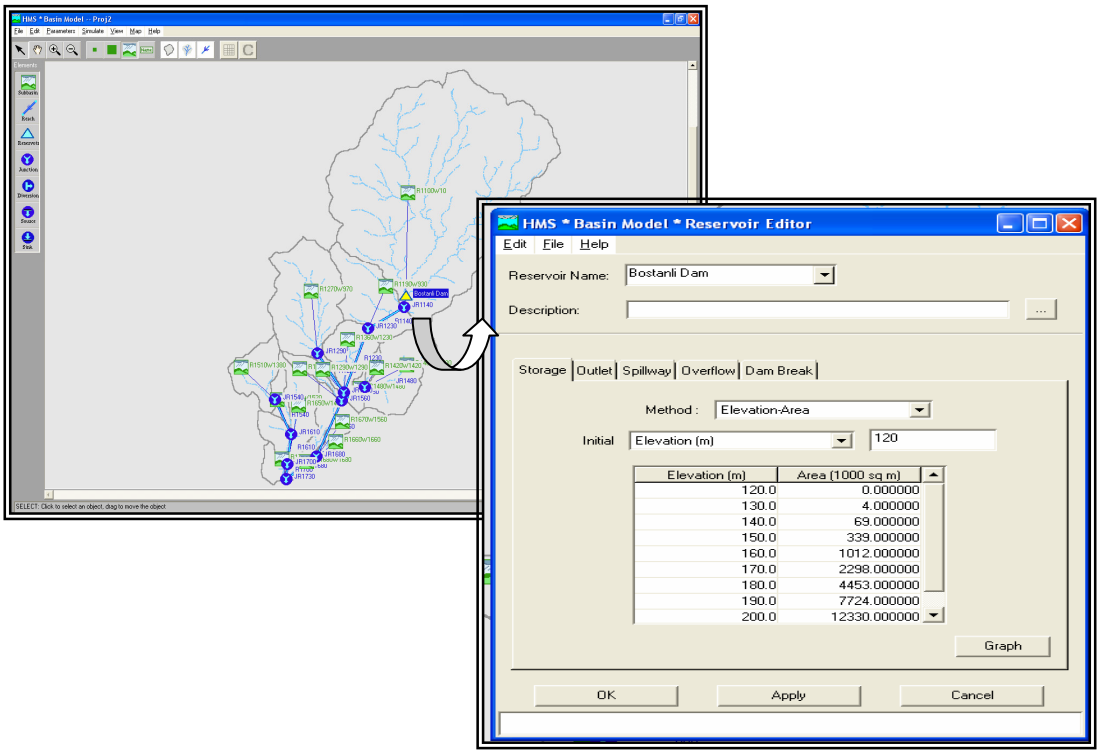

Figure 7.6 Reservoir element table.

7.2.2.2 Meteorologic Model

Another part of the HEC-HMS model is the Meteorologic Model, which contains information required to define historical or hypothetical precipitation data. Types of hypothetical storms used in the model include:

- Hypothetical Frequency Storm Events: Standard Facility Design
- SCS Hypothetical Rainfall Distributions
- Corps Standard Project Storm: Major Facility Design

To specify historical precipitation, several commonly used options are available in the meterologic model:

- Basin-Average Precipitation: One Gage Record
- Composite Precipitation: Weighted Average of Multiple Gage Records (Theissen Polygon Method)
- Inverse-Distance Weighting

- Gridded Precipitation (Weather Radar Data): this allows the inclusion of spatial and temporal distribution of rainfall. Currently, GIS can be used to combine radar data and provide a fairly accurate temporal distribution of rainfall for individual subareas in a watershed (Hydro GIS CD, 2001).

Figure 7.7 shows a view of the meterologic model chosen for the method of frequency storm.

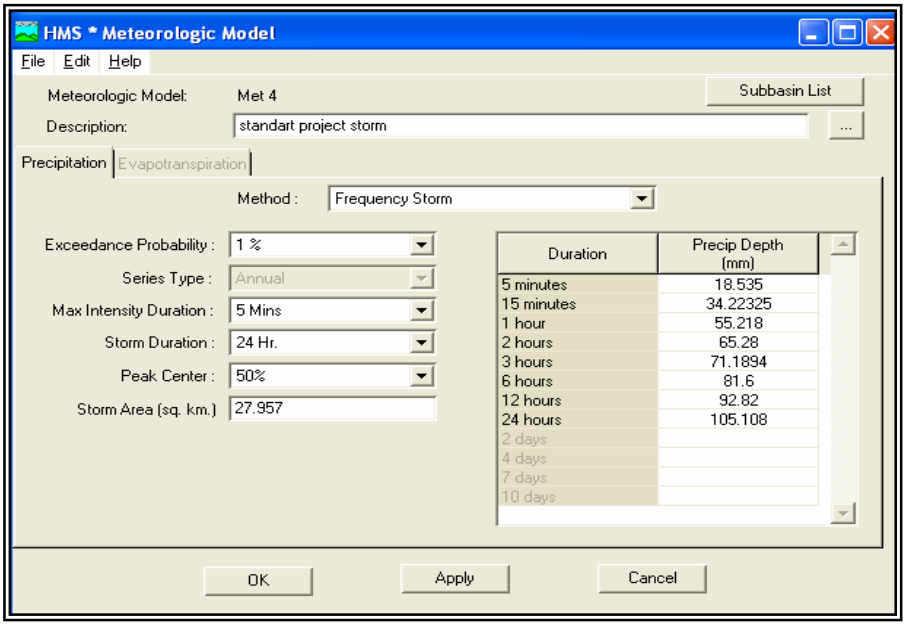

Figure 7.7 View of the frequency storm method in Meterologic Model.

7.2.2.3 Control Specifications

Start and end dates/times, and the computational time step for the model is defined in the part of control specifications, as time related information used in a simulation (Figure 7.8) (HEC, 2001a).

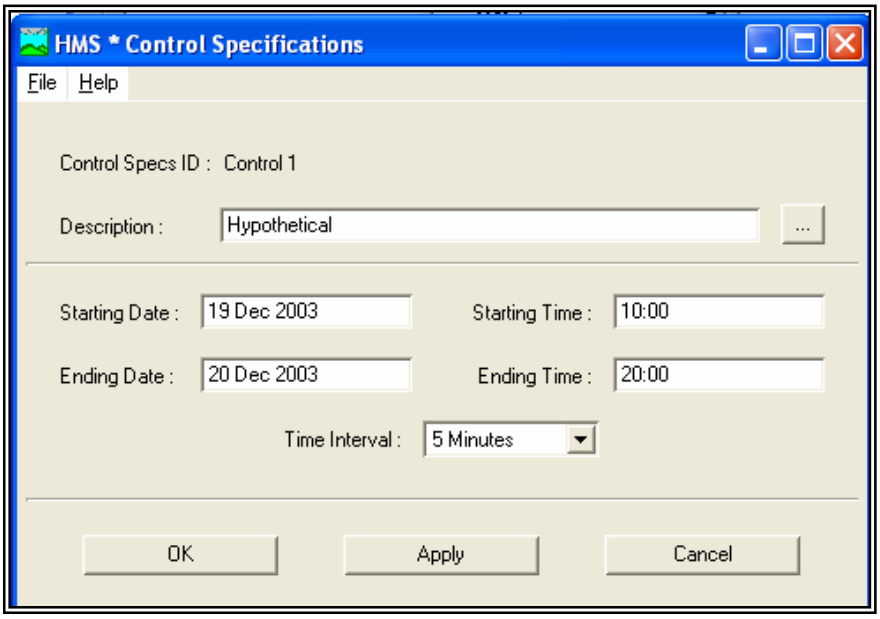

Figure 7.8 Control specifications.

7.2.3 Calibration of HEC-HMS

HEC-HMS automatically estimates the parameters in order to find the best fit of the simulated to the observed hydrograph for one element. The user sets the initial values for the parameters of each element along with maximum and minimum values so that the parameter values must fall within a reasonable range. There are two methods in HEC-HMS for parameter estimation:

- Univariate Gradient Method
- Nelder & Mead Method

In the Univariate Gradient Method, only one parameter is changed at a time, leaving the rest constant, so that the computation is faster than the latter method, namely Nelder & Mead Method. This second method runs more slowly than the former since every parameter value is changed while iterating according to the greatest potential effect on the objective function (Bedient & Huber, 2002).

The type of the optimization function is based on six possible alternatives: peak-weighted RMS error, sum of squared residuals, sum of absolute values, percent error in peak flow, percent error in volume, and time weighted RMS error (Figure 7.9).

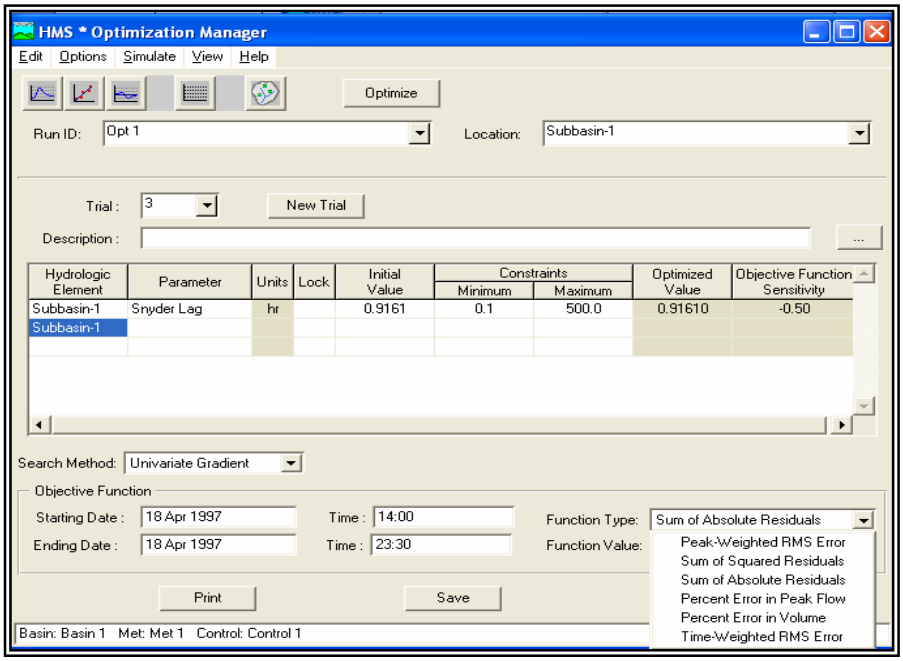

Figure 7.9 HEC-HMS optimization manager.

7.3 HEC-GeoHMS Geospatial Hydrologic Modeling Extension

With the recent advances in GIS, spatial data preparation required by hydrologic models has been enhanced, and the GIS tools on data preparation have been utilized frequently for this purpose. By identifying lumped hydrologic parameters via spatial analysis, one can save time and effort, and the outcomes become more feasible compared to those of early methods. Additionally, radar rainfall data and advanced techniques, which require cell by cell computation, has proved to be useful for basin hydrologic modeling on a grid level.

HEC-GeoHMS has been developed to assist engineers and modelers on deriving geospatial data with the use of GIS. It combines the functionality of some advanced GIS programs into a package that is easy to be used within a specialized interface. Visualization of spatial information and documentation of watershed characteristics

are possible by using this tool. It also allows the user to perform spatial analysis, delineate subbasins and streams, construct inputs to hydrologic models, and assist with report preparation. The fundamental data comprising, digital geospatial data should be available to set up hydrologic models (Hydro GIS CD, 2001, HEC, 2000).

7.3.1 Menu Options in HEC-GeoHMS

The following contents describe the major steps in starting a project and taking it through the GeoHMS process.

- Terrain Preprocessing
- Hydrologic Processing
- Hydrologic Parameters and HEC-HMS

7.3.1.1 Terrain Preprocessing

The 8-pour point approach is used to process and examine the terrain information in order to obtain flow paths. Since this analysis depends on the data size and the data processing capacity of the computer, it may take several minutes/hours to complete the work. The spatial analysis is carried out after the terrain preprocessing is completed. Appropriate data sets, which then become inputs for hydrologic models, can be derived from the spatial database by using the analysis. It is recommended that comparisons are made between the delineated features and the published information in order to find possible errors in the terrain model. If any error in the terrain model is noticed, the DEM should then be corrected outside the program. Afterwards, the spatial database should be processed once again.

In the HEC-GeoHMS model, a step-by-step process is applied for the terrain analysis so that the user may check the outputs and make corrections to the data. However, if the user has performed the terrain preprocessing a number of times, then batch processing will allow terrain preprocessing to be performed unattended (HEC, 2000).

Steps in Terrain Preprocessing

Eight data sets are derived by using a terrain model to describe the drainage patterns of the watershed and allow for stream and subbasin delineation. These data sets become inputs for basin processing.

Flow direction, flow accumulation, stream definition, stream segmentation, and watershed delineation data sets are in grid format. The next two data sets are watershed polygons and stream segments, and they are vector representations of the watersheds and streams. The aggregated watersheds data set is used mainly to improve the performance of the watershed delineation operation.

The steps in the analysis include filling depressions or pits, calculating flow directions and flow accumulations, delineating streams with an accumulation threshold, defining streams, stream segmentation, watershed delineation, watershed polygon processing, stream processing, and watershed aggregation.

- **Data Management**

GeoHMS needs a depressionless DEM for ensuing steps in terrain preprocessing. Hence, the depressionless DEM must first be created in the beginning of a study. The depressionless DEM may be created from the original DEM by using either an external program or the Fill command in the Terrain preprocessing menu.

If the user has developed the flow direction and accumulation grid in another program, he can bring in these data as themes and assign their roles.

- **Flow Direction**

The direction of flow for each cell in a DEM is computed in this step. The eight-point pour algorithm specifies the following eight possible directions:

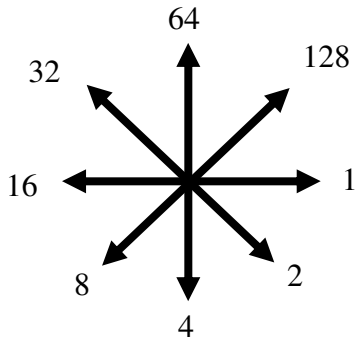

1= east	2= southeast	4= south	8= southwest
16= west	32=northwest	64= north	128= northeast

- **Flow Accumulation**

The accumulated flow, or the number of up-slope cells is computed in this step, based on a flow direction grid. Upstream drainage area at a given cell can be calculated by multiplying the flow accumulation value by the area of a single cell.

- **Stream Definition**

All cells that belong to the stream network are classified with flow accumulations, based on a user-defined threshold. Typically, cells with high flow accumulation, which is greater than a user-defined threshold value, are considered part of a stream network. The threshold value may be assigned as an area in distance units squared, e.g., square kilometers/miles, or as a certain number of cells. The flow accumulation value of a particular cell must exceed the user-defined threshold for a stream to be initiated. The default is one percent of the largest drainage area in the entire basin. The smaller the threshold chosen, the greater the number of subbasins delineated by Geo-HMS.

- **Stream Segmentation**

In this step, the stream is divided into segments. Connection of two successive junctions, a junction and an outlet, or a junction and the drainage divide are provided by stream segments or links.

- **Watershed Delineation**

A subbasin or the whole watershed for every stream segment is delineated by the watershed delineation process. This step delineates a subbasin or a watershed for every stream segment.

- **Watershed Polygon Processing**

The grid representations of subbasins are converted into the vector representations by using this step.

- **Stream Segmentation Processing**

This step converts the grid representation of the stream into a vector representation.

- **Watershed Aggregation**

This step has no importance hydrologically and is only needed to improve the computational performance of interactive subbasin delineation and also to enhance data extraction.

- **Full Processing Setup**

Full Processing Setup is used when terrain processing is executed in batch mode. The depressionless DEM is an input for this process. Therefore, the DEM must be filled first to run full the delineation process. The names of output files are specified (Figure 7.10).

- **Hydrologic Model Setup**

The required information for this step is derived from the spatial database by using the HMS Project Setup menu on the MainView of HEC-GeoHMS. For this purpose, control points at the downstream outlet specifying the tributary of the HMS basin should be defined.

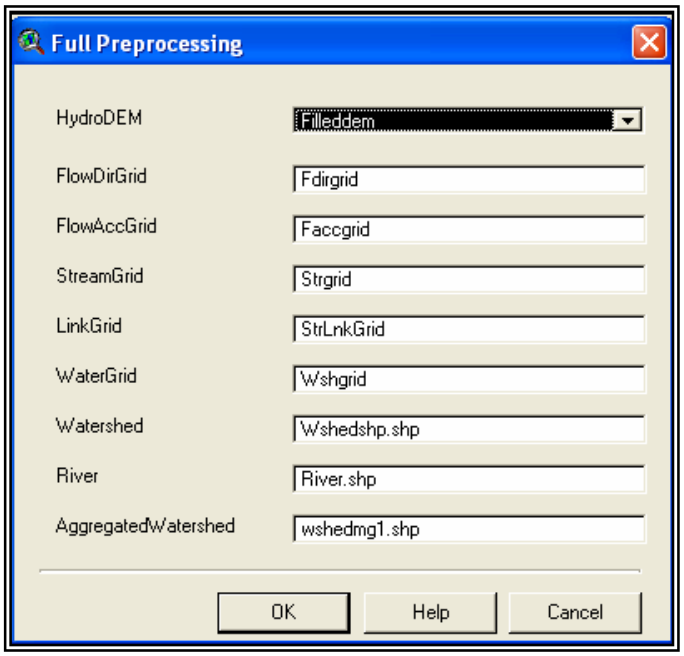

Figure 7.10 Full processing setup.

The following data sets are extracted for the specified study area in the ProjView:

"FilledDEM" representing the depressionless DEM.
"FdirGrid" representing the flow direction grid.
"LinkGrid" representing the stream segments grid.
"SmallStrGrid" containing denser stream representation for visualization purposes.
"WaterShd.shp" representing the subbasins.
"River.shp" representing the stream segments.
"Bostanli.shp" containing the project outlet point that defines the study area.

7.3.1.2 Hydrologic Processing

Terrain processing is carried out in the MainView, and then the derived information, that will be used in the HMS model, is transferred into the ProjView to execute subbasin processes.

Basin Processing

The Basin Processing tool includes Basin Merge, Basin Subdivision, River Merge, River Profile, Basin Split at Confluences and Batch Subbasin Delineation operations.

Multiple basins can be merged by using the Basin Merge menu, or a single basin can be subdivided into several subbasins, following the rules and methods necessary to obtain the desired modeling area.

Stream & Watershed Characteristics

Topographic characteristics of streams and watersheds are also computed by using the HEC-GeoHMS extension. The computational results should first be compared with the published information before the hydrologic parameters are estimated. The characteristics given in Table 7.1 may be used to compare basins and to estimate hydrological parameters.

Table 7.1 Physical characteristics of streams and subbasins.

	Physical Characteristics
Stream	Length
	Upstream elevation
	Downstream elevation
	Slope
	Stream Profile
Watershed	Area
	Centroid Location
	Centroid elevation
	Longest Flow Path
	Longest Flow Length
	Upstream elevation
	Downstream elevation
	Slope between endpoints
	Slope between 10%-85%
	Centroidal Path
	Centroidal Length

- **River Length**

This step computes the river length for all subbasins and routing reaches in the "River.shp", river shape file. In the attribute table, the river length is computed, using the grid representation of the stream. This step computes the river length more accurately, based on the vector representation of the stream.

- **River Slope**

The upstream and downstream elevations of a river reach are derived, and the river slope is then computed by using these values.

- **Basin Centroid**

Four methods are available in GeoHMS for specifying the place of the basin centroid: bounding box, ellipse, flow path, and user-specified methods. Since there is a possibility that the centroid may lie outside a U-shaped or other similar odd-shaped subbasins, the momentum calculation around an X and Y axis, that is commonly used in engineering applications, is not performed here.

- **Longest Flow Path**

It is possible to have information on the longest flow length, upstream elevation, downstream elevation, slope between the endpoints, and slope between 10% and 85% of the length, that are computed with the longest flow path operation. These characteristics are visualized on the "Watershd.shp" theme.

- **Centroidal Flow Path**

The length of the centroidal flow path, which is the length between the centroid and the outlet of the subbasin, is computed by using this Menu tool, such that the centroid lies on the longest flow path.

Hydrologic Modeling System

The input files used in the HEC-HMS model, such as background-map file, lumped-basin schematic model file, grid-cell parameter file, and distributed-basin

schematic model file, are created by HEC-GeoHMS. In this part, reaches and subbasins are designated; possible errors in the basin and/or stream connections are determined; a schematic diagram is developed for HMS, and finally HMS related inputs are generated.

- **Reach AutoName**

In this process, stream reaches are named, starting upstream by using the index "R" together with a corresponding number. The user can further change these reach names by more descriptive ones.

- **Basin AutoName**

Similar to the reach autoname process, the basin autoname process provides a naming convertion for subbasins in the upstream - downstream order simply by adding "W+10, 20, etc." to the receiving reach name. It is possible to alter the names given by the program with real or more descriptive ones.

HMS Model Files

- **Map to HMS Units**

Although the map unit is the unit of the ArcView data, the physical characteristics of the reaches and subbasins in map units are to be transformed into the HMS units since the terrain is described typically in meters.

- **HMS Data Check**

This option is used on the data sets in order to make a consistency check for the hydrologic structure of the model. A track of the relationship between the stream segments, subbasins, outlet points, and other entities is kept by the program. Since these relationships may have been disrupted because of the improper use of the tools, it is also suggested here to check the data before continuing the process for the next step.

- **HEC-HMS Basin Schematic**

In the HEC-HMS basin schematic, the hydrologic basin model with basin elements and their connectivity are shown in GIS visual format. Hence, two files are to be created in this step: a point shape file, so-called HMSPoint.shp, in which a number of point features, such as icon location, outlets, and junctions are available; and a line shape file, called HMSConnect.shp, that includes some interconnected line features, such as subbasin connectors and reaches.

- **HMS Legend**

HMS Legend process applies the symbols of the HMS model to represent point and line features for hydrologic elements.

- **Background Map File**

The background map is simply used to show the boundaries of the basin, subbasins, and stream reaches analyzed. It is in an ASCI text file readable by HEC-HMS.

7.4 HEC-RAS Hydraulic Simulation Model

HEC-RAS hydraulic model developed again by HEC is designed for interactive use in a multi-tasking and multi-user network environment. In 1964, HEC released the HEC-2 computer model to analyze flows in stream channels and to determine floodplain areas (Beavers, 1994). Since Windows-based software is more user-friendly, it has become one of the widely used tools. At the beginning of 1990, HEC developed a Windows-compatible counterpart to HEC-2, the River Analysis System (RAS). In April 2000, the Center also developed the *HEC-GeoRAS* extension for the Arcview GIS system as a tool to be used for pre-and post-processing of the data in the HEC RAS model and as an upgrade to the previously used AvRAS extension.

The biggest difference between the HEC-RAS and the HEC-2 model is that the former has a graphical user interface (GIU) programmed in Visual Basic to allow the user to enter, edit, and display data and graphics easily. This capability allows to

better visualize the stream and its condition, and a three-dimensional plotting of the stream geometry (Tate, 1999). In addition to hydraulic design features, HEC-RAS has several hydraulic computation capabilities, such as flow water surface profile computations, unsteady flow simulation, and movable boundary sediment transport computations (HEC, 2001b).

7.4.1 Steady and Unsteady Flow Computations in HEC-RAS

Steady Flow Computation: This option is used for the computation of water surface profiles for steady gradually varied flow in floodplain management and flood insurance studies to assess floodway encroachments. The system may have a single river reach, a dendritic system, or a full network of channels. Not only subcritical but also supercritical and mixed flow regime water surface profiles can be modeled in HEC-RAS. The one dimensional energy equation is used in the basic computational procedure. Two kinds of energy losses are considered. These are the friction losses that are computed by using Manning's equation and the contraction/expansion losses for which the loss coefficient is multiplied by the change in velocity head. The momentum equation is applied if the water surface profile is in rapidly varied conditions, which comprise mixed flow regime computations (i.e., hydraulic jumps), hydraulics of bridges, and evaluation of profiles at river confluences (stream junctions). It is also possible to see how bridges, culverts, weirs, spillways and other structures affect water surface profile computations. The options of multiple plan analyses, multiple profile computations, multiple bridge and/or culvert opening analysis, and split flow optimization at stream junctions and lateral weirs and spillways are available in the steady flow component so that it is possible to evaluate changes in water surface profiles due to channel improvements and levees.

Unsteady Flow Computation: The one dimensional unsteady flow computation is based on Barkau's UNET model which was developed primarily for subcritical flow regime computations. In this model, the hydraulic computations for cross-sections and hydraulic structures that were developed for the steady flow component were incorporated into the unsteady flow module. Storage areas, hydraulic connections

between storage areas, and stream reaches can also be modeled in the unsteady flow component.

Sediment Transport/Movable Boundary Computations: Another component of the HEC-RAS model is the simulation of one-dimensional sediment transport/movable boundary computations, resulting from scour and deposition over moderate time periods. The grain size fraction is used for computation of the sediment transport potential. There are several significant features in this computation, such as the ability to model a full network of streams, channel dragging, various levee and encroachment alternatives, and the use of similar other equations. The model is designed to simulate long-term trends of scour and deposition in a stream channel, that mayt result from modified frequency and duration of water discharge and stage, or modified channel geometry. These computations are very useful in order to assess deposition in reservoirs, to design channel contractions required to maintain navigation depths, to predict the influence of dredging on the rate of deposition, to estimate the maximum possible scour during large flood events, and to evaluate sedimentation in fixed channels (HEC, 2001b).

The following hydraulic situations are evaluated in HEC-RAS:

- Simultaneous subcritical and supercritical flow computations, including the determination of flow regime
- Ice hydraulics
- Channel modification analysis
- Levee modeling
- Current bridge and culvert modeling, using Federal Highway Administration (FHWA) HDS-S techniques
- Scour analysis at bridges
- Floodway analysis
- Split flow optimization
- Inline and lateral weirs and gates
- Multiple bridge and culvert opening analysis
- Multiple reach analysis

- Geographic Information System (GIS) integration (Klotz et al., 2003).

7.4.2 Data Required for HEC-RAS Simulations

The data files for a HEC-RAS simulation can be summarized as plan data, geometric data, flow data (steady flow data, unsteady flow data), sediment data, and hydraulic design data (Figure 7.11). Detailed information on these data groups is given in the following subsections.

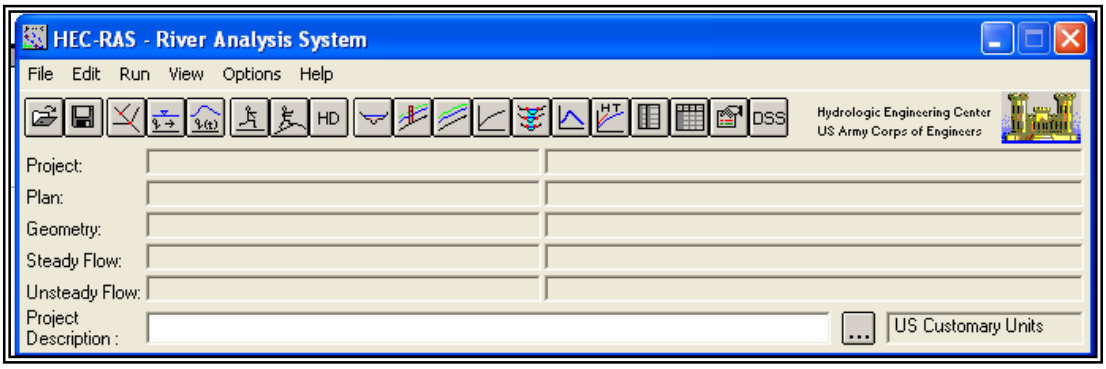

Figure 7.11 Required data of HEC-RAS.

7.4.2.1 Plan Data

Usually, the first step in performing a simulation is to put together a so-called *Plan*. The *Plan* defines which geometry and flow data are to be used and provides a description and a short identifier for the run, as well. If the geometry and flow data do not exist, then this action is performed later, following their creation. Also included in the plan information are the selected flow regime and the simulation options (Andrysiak, 2000).

7.4.2.2 Geometric Data

All physical and topographical data are entered into the modelwith the help of the Geometric Data Editor. Figure 7.12 shows the editors and tools in the Geometric Data Editor. While tools are used to develop the system comprising river reaches, storage areas, pumps, etc., data and parameters of the river reaches and hydraulic

structures such as bridges, culverts, and levees, are entered into the HEC-RAS by using editors. As a first step, a river reach is drawn to create a river network. After creating the river reaches, the cross sections which represent the geometric boundary are formed. The distance between the cross sections along the stream should be short enough to characterize the flow carrying capacity of the stream and its adjacent floodplain (Bedient & Huber, 2002). Cross sections should also be provided at the representative nodes where changes occur in discharge, slope, shape, and roughness; at locations where levees begin and end; and at hydraulic structures such as bridges, culverts, and weirs. The information required for a cross section includes the river, reach and river station identifiers; a brief description; X - Y coordinates (station and elevation points); downstream reach lengths; Manning's roughness coefficients; main channel bank stations; and contraction and expansion coefficients (Figure 7.13).

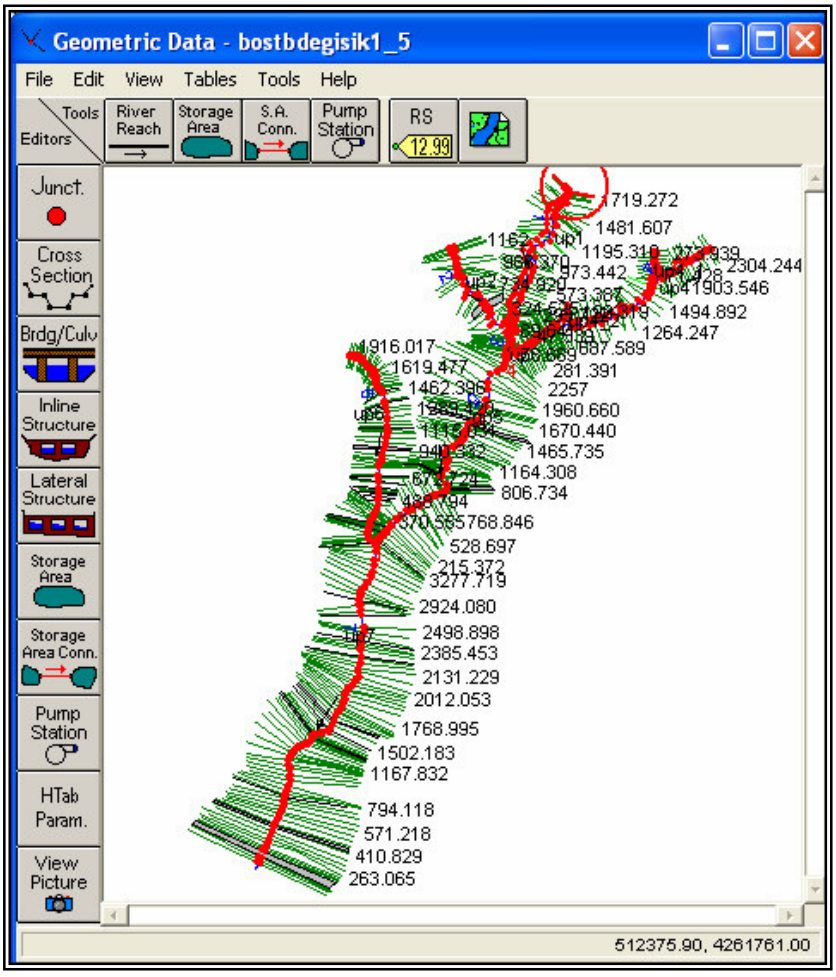

Figure 7.12 Editors and tools in Geometric Data Editor.

These are used to show a series of cross-sections along the stream. In each cross-section, HEC-RAS subdivides the cross sections as the left floodway, the main channel and the right floodway because of the differences in their corresponding hydraulic parameters.

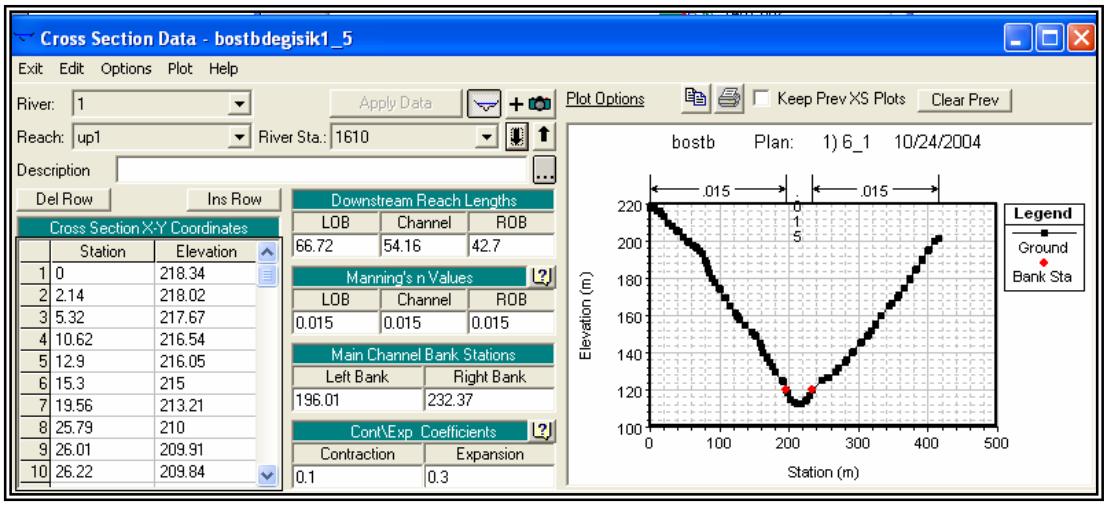

Figure 7.13 Cross Section Data Editor.

7.4.2.3 Flow Data

The necessary flow data are entered, depending on options of steady or unsteady computations. Flow data can be entered manually or may be imported directly from the HEC-HMS run. The HMS flow data computed at the junctions are generally used for this purpose (HEC, 2001b). HEC-RAS allows simultaneous modeling of multiple profiles so that the model can easily compare the results, e.g., 10-yr, 25-yr, 50-yr, and 100-yr floods can be shown on one graph.

Boundary conditions must be specified to indicate the starting water surface at both ends of the river system, and HEC-RAS uses this information to begin the simulation.

The computation of subcritical flow requires boundary conditions only for the downstream end of the river system; whereas for supercritical flow, only upstream boundary conditions are required. In the case of a mixed flow regime, boundary conditions for all ends of the river system are to be provided.

Connections to junctions are considered internal boundary conditions. They are automatically listed, and the modeler enters the necessary external boundary conditions (HEC, 2001b).

The steady flow data file includes the number of profiles for computation of flow values and the boundary conditions for each reach (Figure 7.14).

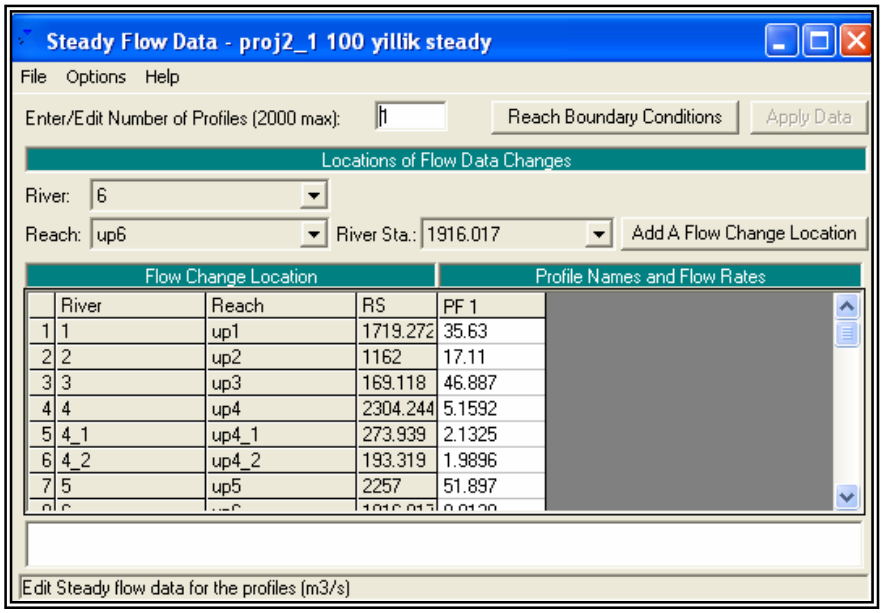

Figure 7.14 Steady Flow Data Editor.

Unsteady Flow Data Editor consists of two main conditions: Boundary and Initial Conditions (Figure 7.15).

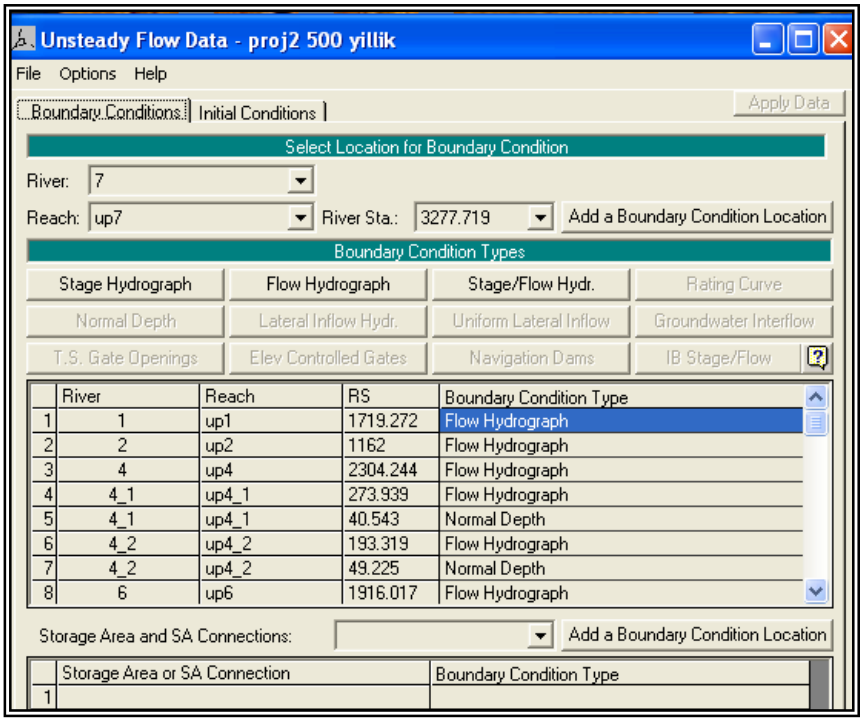

Figure 7.15 Unsteady Flow Data Editor (boundary conditions).

In the first box, it is possible to define boundary conditions for certain cross-sections which are originally river stations automatically populated in the table. This tool gives several alternatives for boundary conditions, depending on the station properties and the existing conditions. Such properties are stage hydrograph, flow hydrograph, stage/flow hyd., rating curve, normal depth, lateral inflow, uniform lateral inflow, groundwater inflow, TS gate openings, elevation controlled gates, navigation dams, and IB stage/flow. The user can then enter the flow hydrograph manually or use DSS (data storage system) files, which include flow rates obtained from the HEC-HMS model.

Considering the initial conditions, the initial flow distribution method is defined either with the help of a *restart file* or by entering an *initial flow distribution*. Initial flow values for appropriate river stations are entered, using appropriate fields in the window (Figure 7.16). Similar to boundary conditions, HEC-RAS gives an alternative to enter additional flow change locations for initial conditions.

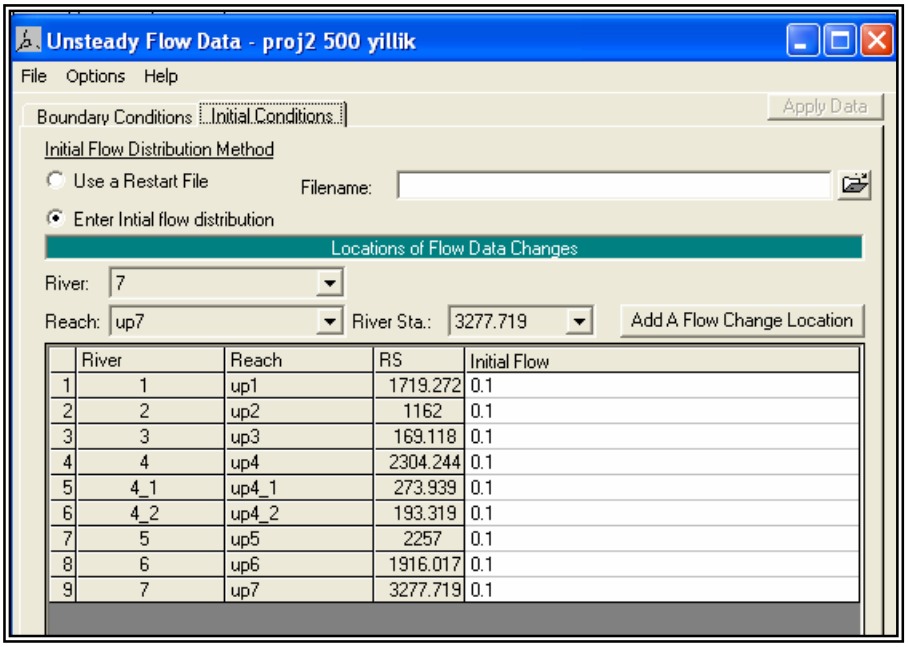

Figure 7.16 Unsteady Flow Data Editor (initial conditions).

7.4.2.4 Sediment Data

Sediment data are required conditions where sediment transport modeling is expected. This type of data includes flow data, boundary conditions for each reach, and sediment data.

7.4.2.5 Hydraulic Design Data

Input data for hydraulic structures depend on the hydraulic design data files that contain information on the type of requested hydraulic design computations.

7.4.3 Viewing, Reporting and Plotting the Results

The user can view the computational results in forms of cross section plots, water surface profile plots, general profile plot, rating curve plots, X-Y-Z perspective plots, stage and flow hydrographs, hydraulic property plots, detailed output tables, profile summary tables, and the summary of errors, warnings, and notes (Figure 7.17).

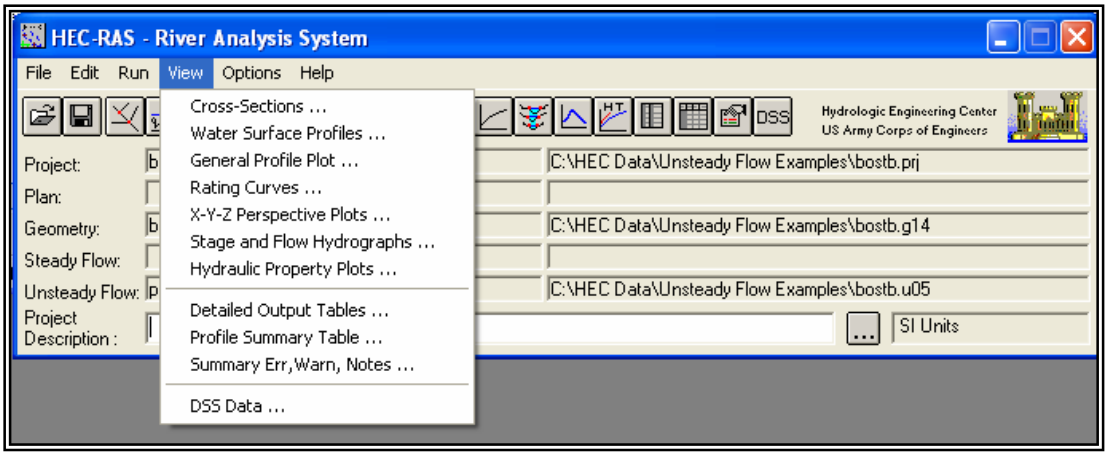

Figure 7.17 Viewing options in HEC-RAS.

Hydraulic structures can also be viewed and plotted by using the bridge/culvert data button and then by selecting the appropriate river stations on the river reaches from the list box at the top of the Bridge/Culvert Data Editor (Figure 7.18).

A desired cross section can also be plotted on the same graphic window which is originally used for the hydraulic structures.

3D multiple cross section plot is also available, so that the user can define the start and end points on the river reaches; the points rotate the plot left and right or up and down to obtain different views of the selected river reaches (Figure 7.19). The computed water surface profiles can be superimposed with the cross section data to visualize the inundated areas (HEC, 2001b).

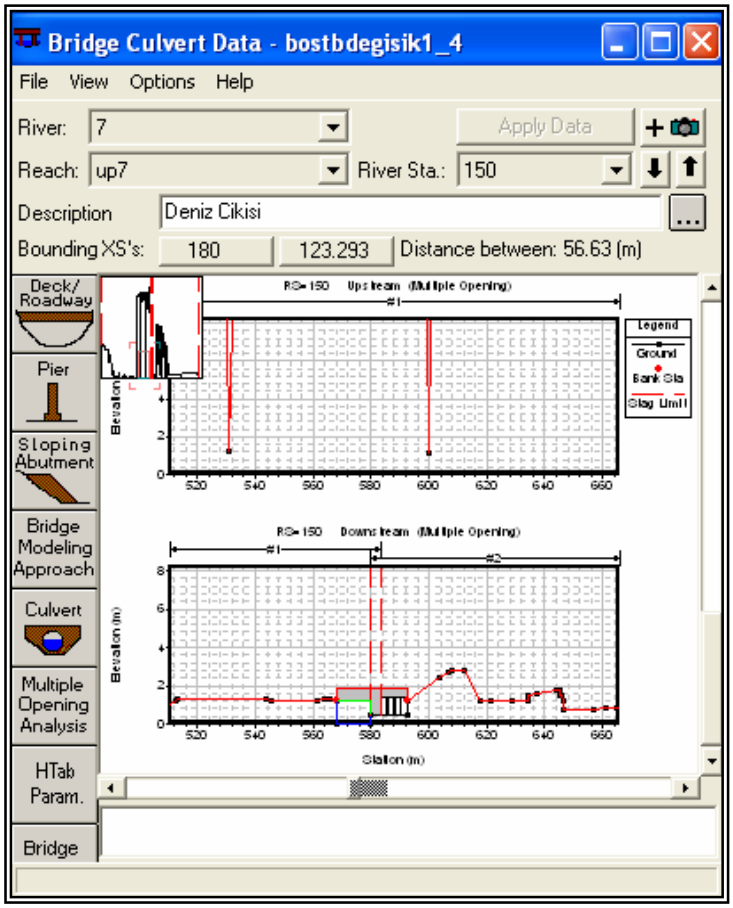

Figure 7.18 View and plot options for hydraulic structures.

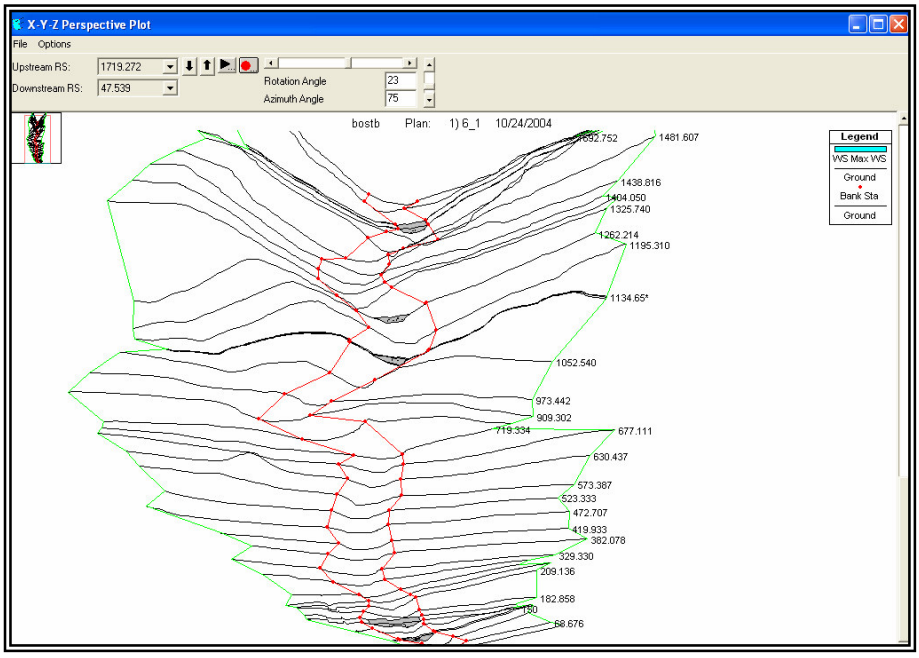

Figure 7.19 X-Y-Z perspective plot.

There are three formats for tabular outputs in HEC-RAS. Detailed hydraulic results at required cross sections are provided by the first tabular type called Cross Section Output Table (Figure 7.20). The second one, Profile Summary Table, shows a limited number of hydraulic variables for several cross sections and multiple profiles (Figure 7.21). Finally, the last one summarizes the errors, warnings and notes (Figure 7.22).

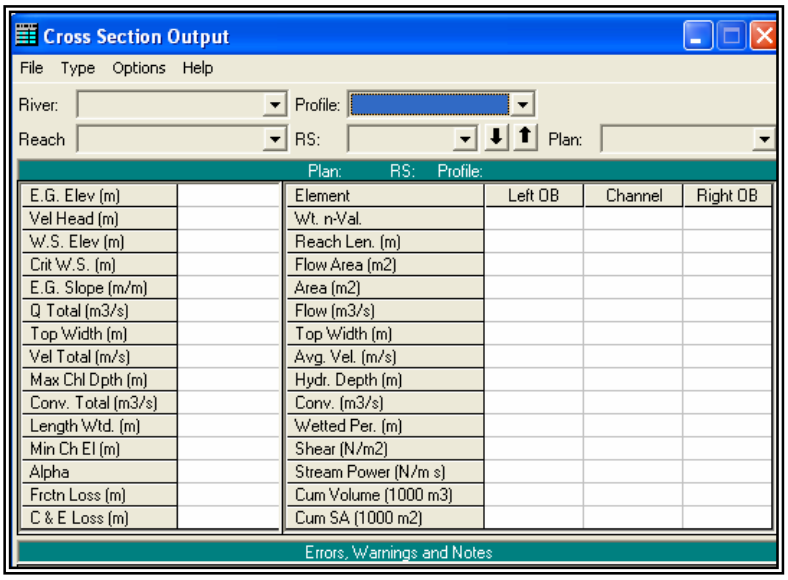

Figure 7.20 Cross section output table.

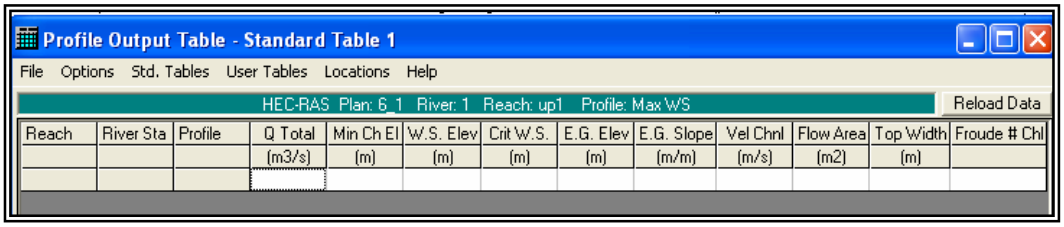

Figure 7.21 Profile output table.

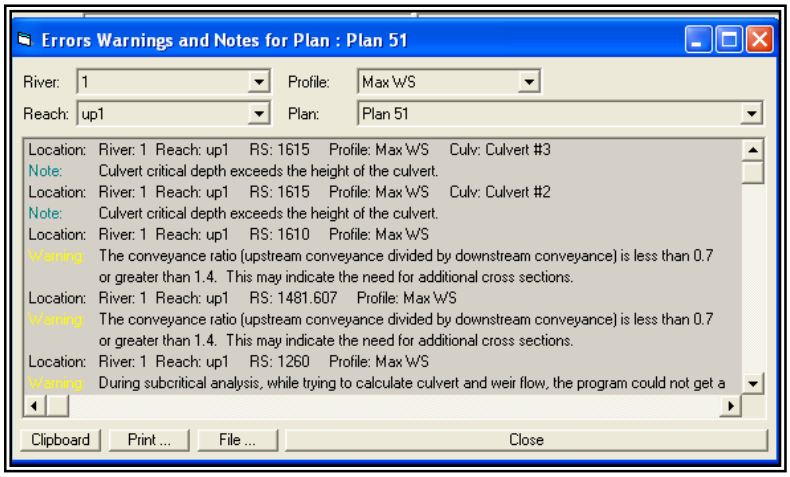

Figure 7.22 Warnings and notes.

7.4.4 Performing a Steady Flow Analysis

Performing a steady flow computation is carried out in two steps as follows:

- Data entering for steady flow computations
- Execution of steady flow computation

7.4.4.1 Data Entering for Steady Flow Computations

In the first step, the peak flow data (at least one flow for every river reach and every profile) must be entered for the profiles to be computed. For this purpose, the number of profiles is first entered prior to the flow data for each river reach, which should follow an order in the upstream to downstream direction. Flow value is assumed to be constant along the river reach up to the confluence where another river reach is connected to the system. This value may vary at any cross section within a reach (Figure 7.14).

Boundary Conditions

Boundary conditions are required for initializing the computation of water surfaces upstream and/or downstream of the river system, depending on the selected flow regime. Since the program begins with the initial values, a starting water surface must be defined. Boundary conditions are used only at the downstream ends of the river system in the computation of a subcritical flow regime. For a supercritical flow regime computation, boundary conditions become necessary only for the upstream ends of the river system. When a mixed flow regime computation is selected boundary conditions are used at both ends of the river system (Figure 7.15) (HEC, 2001b).

There are four types of boundary conditions for the steady flow computation in the HEC-RAS model (Figure 7.23):

- Known Water Surface Elevations
- Critical Depth

- Normal Depth
- Rating Curve

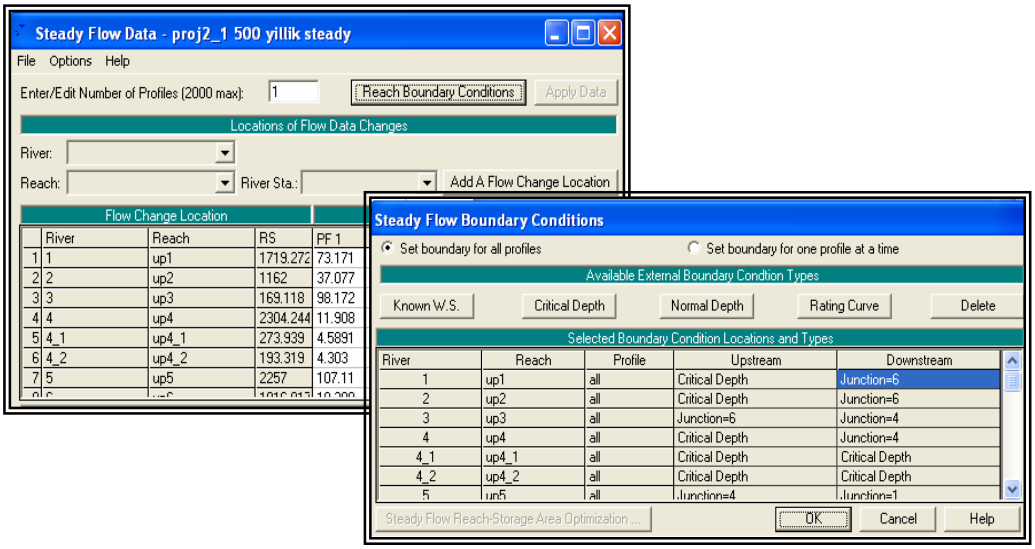

Figure 7.23 Steady flow data and boundary conditions.

7.4.4.2 Performing Steady Flow Computation

Having provided all the required data, including the ones about the geometry and the flow, steady flow analysis is initialized with the help of the **Run** button on the main window. From this editor, the geometry file, the steady flow file, and the type of flow regime are selected properly (Figure 7.24).

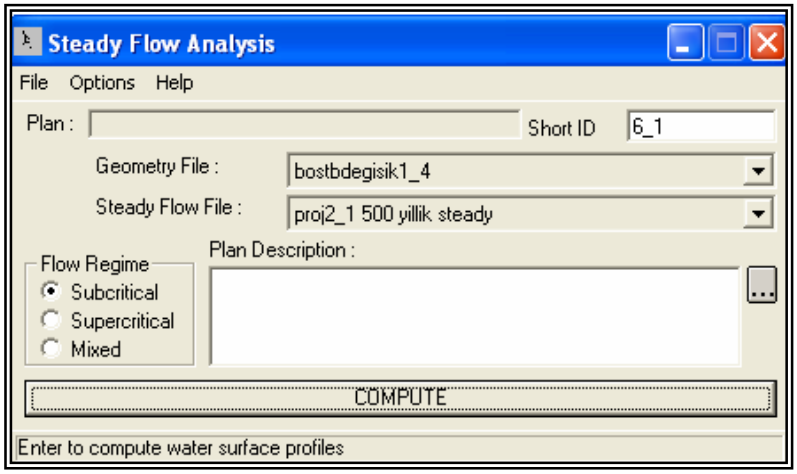

Figure 7.24 Steady flow computation.

7.4.5 Performing an Unsteady Flow Analysis

Unsteady flow analysis consists of two main steps:

- Data Entry for Unsteady Flow
- Execution of the Unsteady Flow Computation

7.4.5.1 Data Entry for Unsteady Flow

Unsteady Flow Data

In unsteady flow computation, boundary conditions should be defined for all external boundaries and for any desired internal locations. Initial flow values should also be set in the system at the beginning of the simulation. HEC-RAS fills the external bounds of the system into the corresponding table automatically (Figure 7.15).

Boundary Conditions

There are several different types of boundary conditions (Figure 7.15):

- Flow Hydrograph
- Stage Hydrograph
- Stage and Flow Hydrograph
- Rating Curve
- Normal Depth
- Lateral Inflow Hydrograph
- Uniform Lateral Inflow Hydrograph
- Groundwater Interflow
- Time Series of Gate Openings
- Elevation Controlled Gate
- Internal Observed Stage Hydrograph
- Internal Observed Stage and Flow Hydrograph

Initial Conditions

Initial conditions are needed in addition to boundary conditions. They include flow and stage information at each cross section; and elevations are also required if storage areas are available in the described system (HEC, 2001b).

7.4.5.2 Execution of Unsteady Flow Computation

After all geometry and unsteady flow data are entered, one can start the unsteady flow computation. The Unsteady Flow Analysis Computation Editor appears by pressing the **Run** button on the main window (Figure 7.25). First, the geometry and unsteady files must be selected on this screen. There are Geometry Preprocessor, Unsteady Flow Simulation and Post Processor options in the **Programs to Run** window**.** Geometry Preprocessor is used to detect any geometry errors in the developed system; and it is adequate to run this processor once if the geometry is not changed. Post Processor prepares the output files. **Simulation Time** window includes starting date, ending date, starting time and ending time. In the **Computation Settings** window, the computational interval should be stated. In addition, the hydrograph output interval and the detailed output interval are needed. If the user is sure that the system has mixed flow regime, the box at the bottom of the screen is selected. Finally, unsteady flow analysis is started by pressing the **Compute** button (HEC, 2001b).

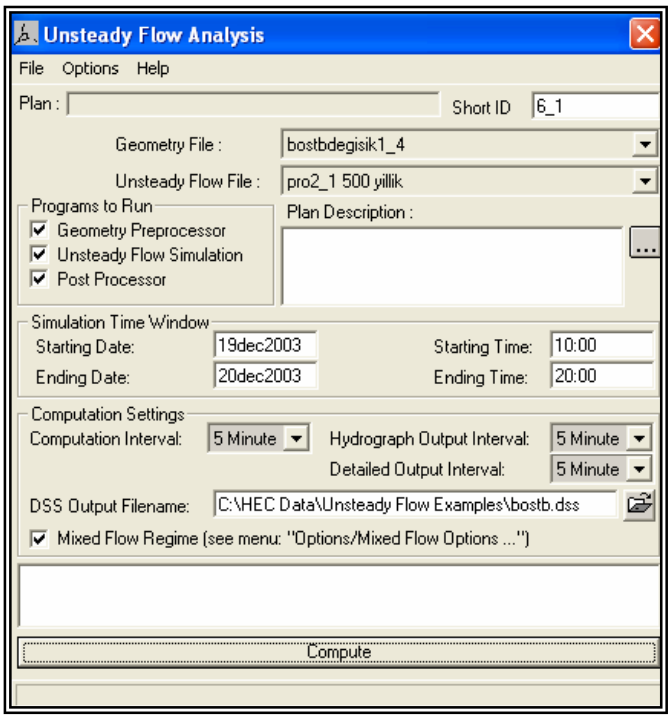

Figure 7.25 Unsteady flow analysis computation editor.

7.5 HEC-GeoRAS

HEC-GeoRAS is an extension which supports the use of geospatial data in HEC-RAS through the ArcView system. HEC-GeoRAS is developed to assist users with less GIS knowledge in constituting an HEC-RAS import file, where geometric attribute data from an existing digital terrain model (DTM) and complementary data are available. The HEC-RAS model results can be imported into the HEC-GeoRAS extension to obtain more meaningful outputs by visualization techniques. The import file of the current version of HEC-GeoRAS includes river, reach and station identifiers; cross-sectional cut lines; cross-sectional surface lines; cross-sectional bank stations; downstream reach lengths for the left overbank, main channel, and right overbank; and cross-sectional roughness coefficients. Data on hydraulic structures must be entered manually. Water surface profile data and velocity data exported from HEC-RAS may be processed into GIS data sets (ESRI, 1999).

An overview of the HEC-GeoRAS process is shown in Figure 7.26.

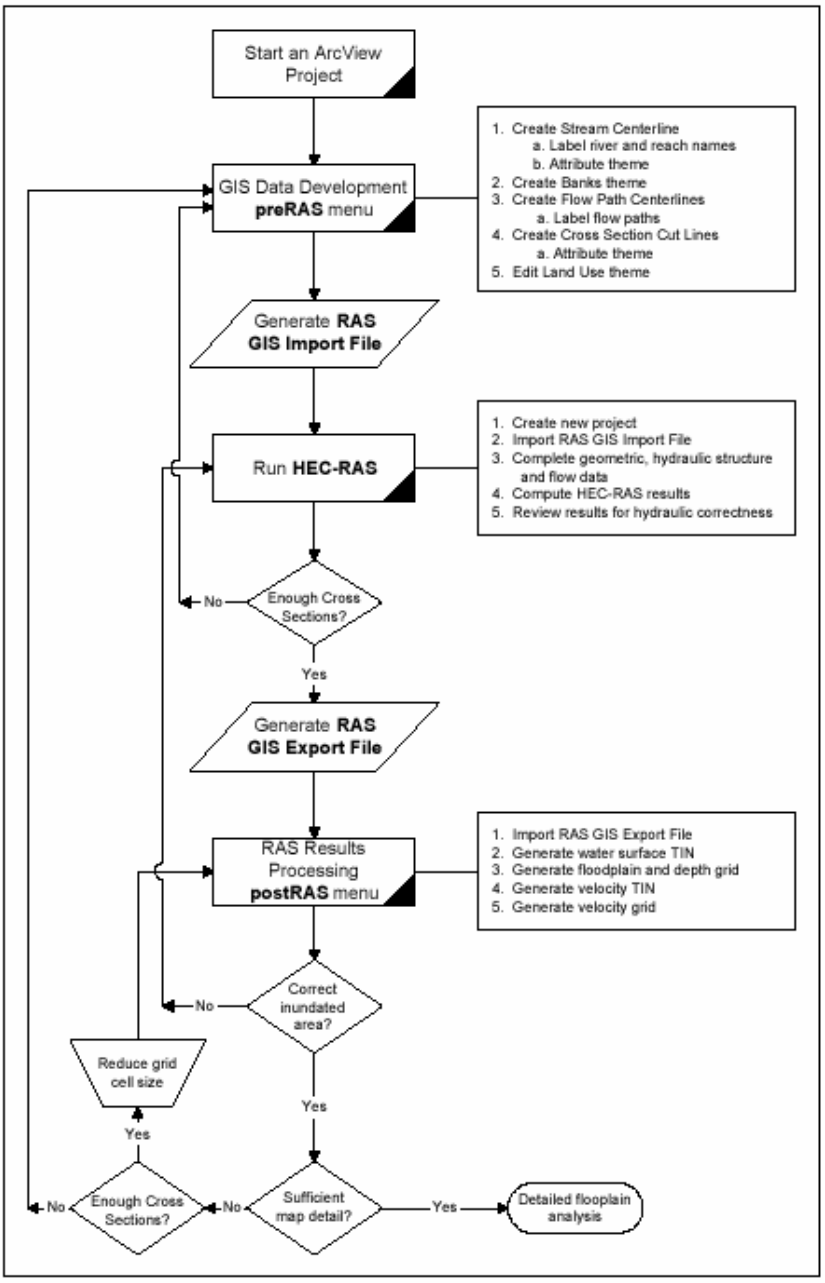

Figure 7.26 Process Flow Diagram For Using HEC-GeoRAS (HEC, 2002).

Menu options include HEC-GeoRAS preRAS, postRAS and GeoRAS Util options. The preRAS option is used for geometric data preprocessing to import them into the HEC-RAS model.

By using the postRAS option, it is possible to export HEC-RAS results.

The GeoRAS Util option supplies utilities to be used in editing and managing themes. The procedures in GeoRAS Util are required to assist the user with various functions (HEC, 2002).

7.5.1 Development of the Import File

Development of the import file requires two main steps:

- Creating RAS Themes
- Generating the RAS GIS Import File

7.5.1.1 Creating RAS Themes

RAS themes that are used for geometric data development and extraction are developed in this step. The Stream Centerline, the Main Channel Banks *(optiona*l), the Flow Path Centerlines *(optiona*l), and the Cross Section Cut Lines are called "line themes". These line themes are created by using ArcView tools. Land cover from which Manning's *n* values can be obtained is a polygon theme. It is possible to use existing shapefiles or ArcInfo coverages for each RAS theme, but they must have the same attributes as those of the created themes by GeoRAS (Figure 7.27).

Stream Centerline Theme

The river network is created by using the Stream Centerline theme. If the user has an existing river network, this theme does not have to be created again; simply, the existing one is defined as the stream centerline theme to be used in the following steps. The river network creation is realized on a reach by reach basis and follows some important rules. It starts upstream and finalizes at the downstream end following the channel thalweg. Junctions act as a connection supplier among the river reaches. Each reach should have a River Name and a Reach Name. The Stream Centerline Theme is mainly used to assign river stationing to cross sections and to display the river network schematically. It may also be used to define the main channel flow path.

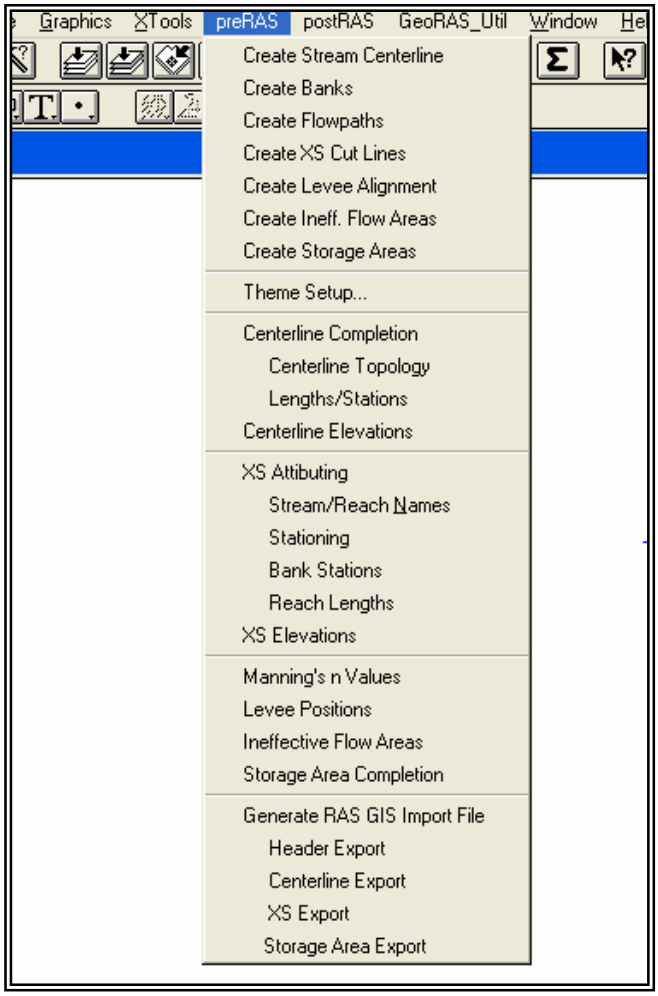

Figure 7.27 RAS themes.

Main Channel Banks Theme

The banks are separated from the main channel by the Main Channel Banks Theme, and the bank stations located on the intersection of the banks with the cross-sectional cut lines are determined by following this intersection. There are some requirements in defining these bank lines, i.e., exactly two bank lines may cross each cross section cut line, bank lines may be broken, and orientation of bank lines is not important.

Flow Path Centerlines Theme

The lines representing the hydraulic flow paths along the two overbanks (left and right) and the main channel are stored in the Flow Path Centerlines theme. Here, it should be noted that the flow lines are drawn towards the downstream direction; each line must have only a single intersection with each cross-sectional cut line while no intersection is allowed between the flow path lines themselves.

Cross-Sectional Cut Lines Theme

The Cross-Sectional Cut Lines Theme defines the features of cross sections, such as location, position and extent. The station-elevation data set is obtained from the DTM on the cut line. The cut lines must be perpendicular to the flow direction and drawn starting from the direction of left overbank. It should be noted that the cut lines must not pass over themselves.

Land Use Theme

By using this optional process, it is possible to obtain Manning's *n* values for left bank, right bank, and the main channel areas if the user has a digital land use data set. Land use theme must be polygon data and must have a field which indicates the *n* value.

Theme Setup

Theme Setup defines themes that constitute input data and intermediate data before executing computations on them. The window shown in Figure 7.28 is filled in for this process. RAS GIS Import File name is required to complete this step.

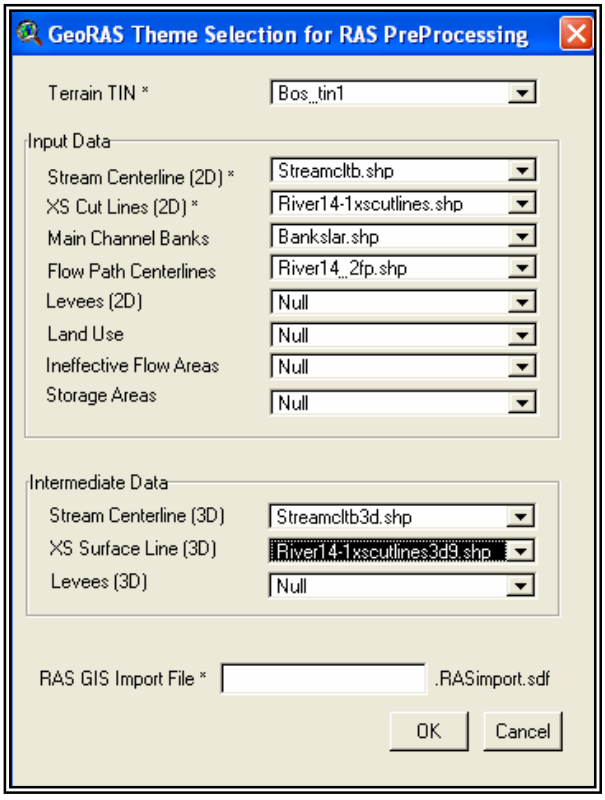

Figure 7.28 Pre-Processing theme setup.

Centerline Completion

Centerline Completion process includes the computation of river lengths, setting up the connectivity of the river network, and derivation of the 3D shapefile. These processes are carried out by using the items of Lengths/Station, Centerline Topology and Centerline Z Extract, respectively.

- Lengths/Stations

Each river length is computed along the stream centerline to the most downstream and the most upstream point with Lengths/Stations function.

- Centerline Topology

River network connectivity and orientation are formed using the Centerline Topology.

- Centerline Z Extract

This function produces a 3D Stream Centerline shapefile by using the 2D Stream Centerline theme.

XS Attributing

The features of stream and reach names, stationing, bank stations, and reach lengths are exported into the Cross Section Cut Lines Theme by using XS Attributing.

XS Elevations

3D shapefile is created from the 2D Cross Section Cut Line Theme by using TIN, from which station-elevation data are drawn. The Cross Section Cut Line (2D) theme should be completely processed before converting it into a 3D shapefile.

7.5.1.2 Generating the RAS GIS Import File

3D Stream Centerline and 3D Cross Section Surface Line are required for the generation of the Import File in order to export the geometric data (such as the identifiers of river, reach and station; cross section cut lines; cross section surface lines, etc.) into the RAS GIS Export Theme, which will be used to export the results of the HEC-RAS model later.

7.5.2 Development of the Export File

HEC-GeoRAS also has the visualization property to be employed for the HEC-RAS model results. In addition to velocities, inundated areas may be shown under different conditions or scenarios after exporting the simulation results into HEC-GeoRAS (Figure 7.29).

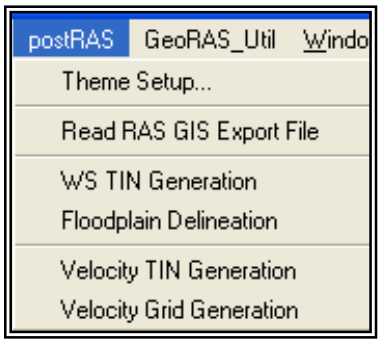

Figure 7.29 PostRAS steps.

7.5.2.1 Generation of the Water Surface TIN

Water surface TIN, which is different from the terrain TIN, is created as a first step of this process, by using water surface elevations computed at all cross sections. Water Surface TIN is clipped by the bounding polygon which limits the water surface to the areas modeled by HEC-RAS, and it should be scrutinized around meandering portions of the river model.

7.5.2.2 Floodplain Delineation

The floodplain is determined as the area where the water surface grid value is equal to the terrain grid value. Water depth grid is calculated by subtracting the water surface TIN from the Terrain TIN.

It is possible to obtain floodplain areas which do not exist in the real case so that the user should be aware of all possible errors, and that these errors are removed in the GIS or modeled behind levees. Another caution is about the cases where the cross sections are placed improperly. The problem of incorrect floodplain limits is expected in such situations. Delineation of floodplains is the process which requires more attention and iterative computations to obtain reasonable results.

7.5.2.3 Velocity TIN Generation

In generation of the Velocity TIN, the themes of velocity points, cut lines, bank lines, and floodplain polygon for the corresponding water surface profile are needed.

It should be kept in mind that the velocities computed in HEC-RAS are the results of one dimensional hydraulic model.

7.5.2.4 Velocity Grid Generation

Velocity Grid is developed by using the Velocity TIN. The user should be careful on velocity results and must control them at the locations where the velocities are unreasonable when compared to the expected results.

CHAPTER EIGHT
APPLICATION OF THE HEC-HMS MODEL USING THE HEC-GEOHMS EXTENSION

This chapter presents the application of the hydrologic processing steps described in Chapter Three for the case of Bostanli Basin. First, storm hyetographs are obtained by the use of the instantaneous intensity hyetograph method. Second, terrain processing is carried out on the HEC-GeoHMS, and finally, prior to the hydraulic modeling for floodplain delineation, the actual hydrologic modeling is performed.

8.1 Application of the Instantaneous Intensity Hyetograph Method

Bukey (2000) has suggested the use of the following intensity-duration-frequency (IDF) curve equation for maximum precipitation values with standard durations, observed at precipitation stations in the Aegean Region of Turkey:

$$\hat{I}_{ort}(t,T) = \frac{\hat{A}(T)}{(t+d)^{b}} \tag{8.1}$$

where,

A, b, and d are constants in the equation. In addition, Hacisuleyman (2003) studied the relationships between these constants and recurrence intervals, T, using precipitation stations in the Aegean Region. The relationships were determined for several recurrence intervals in order to allow their particular use in the city of Izmir. Equations 8.2 and 8.3 show these relationships for A, b, and d constants, respectively, as suggested for the IDF curve equation.

$$A = 203.84T^{0.4727} \tag{8.2}$$

$$b = 0.6186T^{0.063} \tag{8.3}$$

$$Ln\ \ d = 1.065Ln(Ln\ \ T) + 0.391 \tag{8.4}$$

By using the above equations whose determination coefficient (D) are given as the following, A, b, and d are computed in this study for several recurrence intervals as shown in Table 8.1.

LnA-LnT D = 0.9986
LnB-LnT D = 0.9999
Lnd-Ln(LnT) D = 0.9860

In addition, a computer program is developed in the Visual Basic programming language to compute instantaneous intensity hyetograph for a given recurrence interval, T, storm duration, T_d, time interval of hyetograph, Δt, and the computation interval, Δt_i. This program was also used in an undergraduate research work for estimating hyetographs with given durations and recurrence intervals in the case of Izmir (Lopcu, 2004). Source-codes of the program are given in Appendix I.

Table 8.1 Values of constants A, b, and d in the intensity-duration-frequency curve equation for Izmir.

$I = \frac{A}{(t+d)^b}, mm/hour$			
T	**b**	**d**	**A**
2	0.646212	0.51058	282.870
5	0.684613	2.45424	436.207
10	0.715171	3.59392	605.326
25	0.75767	5.134688	933.460
50	0.791489	6.319994	1295.366
100	0.826818	7.519098	1797.585
500	0.91505	10.34653	3846.737

Input variables required by the program are recurrence interval (in years), storm duration (in hours), constants of the IDF curve, time interval of the hyetograph, computational interval, and the storm advancement coefficient, which are donated as T, T_d, A, b, d, Δt, Δt_i, and r, respectively.

The above computer program computes instantaneous intensity functions, $f(t_a)$ and $f(t_b)$, together with minimum and maximum intensities. It also gives incremental precipitation values and ordinates of the hyetograph by using a minimum computational time interval. The input files used to draw the intensity-duration functions and the hyetographs with time interval Δt are created in this way.

To use the outputs of the above program in the HEC-HMS hydrologic model, precipitation values with 100-year and 500-year recurrence intervals are estimated for T_d=6 hours by using the r coefficient of 0.3. Resulting hyetographs for two different recurrence intervals are given in Figures 8.1 and Figure 8.2.

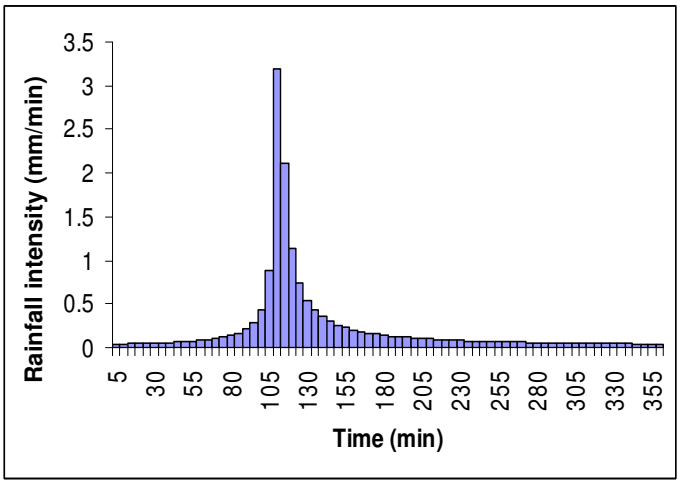

Figure 8.1 Instantaneous intensity hyetograph for T=100 years and Td=6 hours.

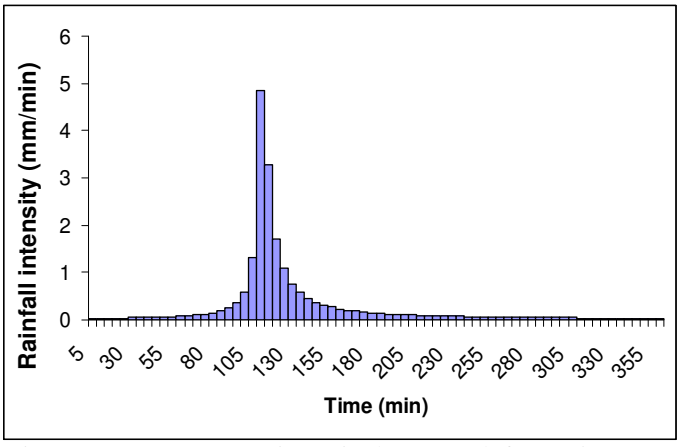

Figure 8.2 Instantaneous intensity hyetograph for T=500 years and Td=6 hours.

8.2 Derivation of Input Files by Using HEC-GeoHMS

In the case of the Bostanli River Basin, the HEC-GeoHMS extension is used for generation of the geospatial data files to be entered into the HEC-HMS model. For this purpose, the steps given in Chapter Three are followed. The following stages are performed in the MainView of the ArcView program:

- filling depressions or pits in the DEM,
- computation of flow directions,
- calculating flow accumulation,
- delineation of streams with an accumulation threshold,
- stream definitions,
- stream segmentation,
- watershed delineation,
- watershed polygon processing,
- stream processing, and
- watershed aggregation.

8.2.1 Terrain Processing

Depressionless DEM

Considering the need for identification of flood-prone places, especially in highly populated areas, the river segments that extend through the built-up portion of the whole river basin is extracted from the entire drainage network. Before proceeding to the next step of hydraulic modeling, it is necessary to compute the inflows for the selected river portion in a series of hydrologic modeling analyses. In this respect, a Digital Elevation Model (DEM) is needed, that is mainly utilized for gathering the geospatial information about some of the basin drainage characteristics. In the beginning of the process of

obtaining such an elevation model, the elevation data in the form of elevation contours are extracted from the available digital map layers and controlled against any kind of data irregularity or deficiency. After determining these inefficiencies with the available data set, the data are defined by further editing, especially on the visible contour lines without any attribute value related to the elevation. Having performed the most necessary corrections on the available digital data, the DEM is automatically created on the ARC/INFO platform by using the linear features of the elevation data as well as some point features that correspond to the peaks and sinks over the land surface (Figure 8.3).

Flow Direction

By using the above-described depressionless DEM, the flow directions to represent the actual directions through which the water flows over the land surface due to gravitational forces are obtained in the form of a separate raster file called “Fdirgrid”. The resulting flow directions are presented in Figure 8.4.

Flow Accumulation

The theme of “Faccgrid” is obtained in a separate process, based on accumulating flows through cells through the flow directions derived in “Fdirgrid” (Figure 8.5).

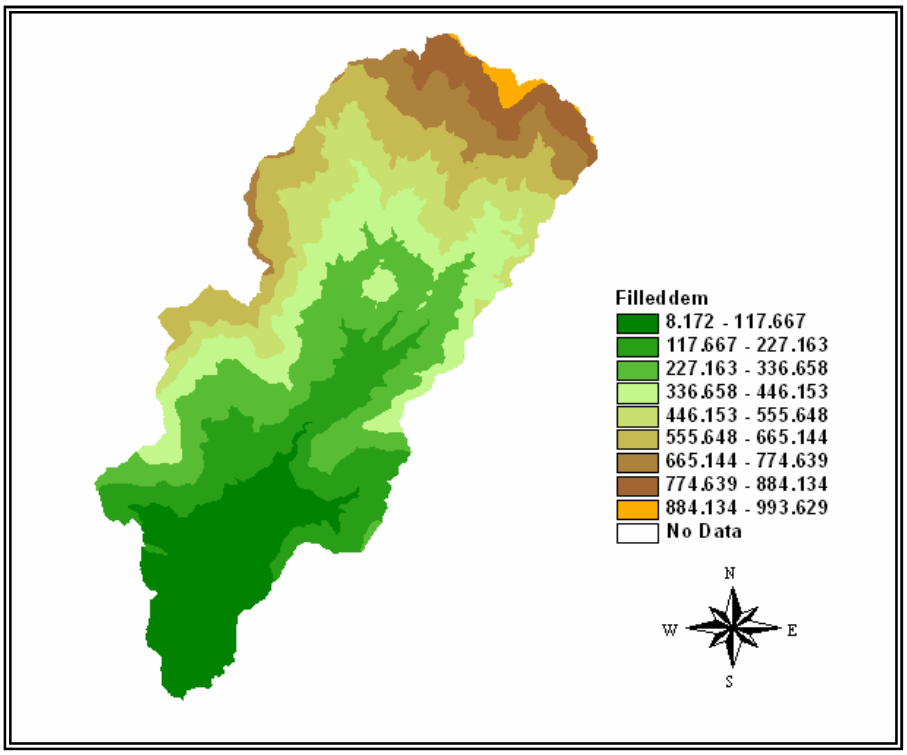

Figure 8.3 DEM for the upstream part of the Bostanli River Basin.

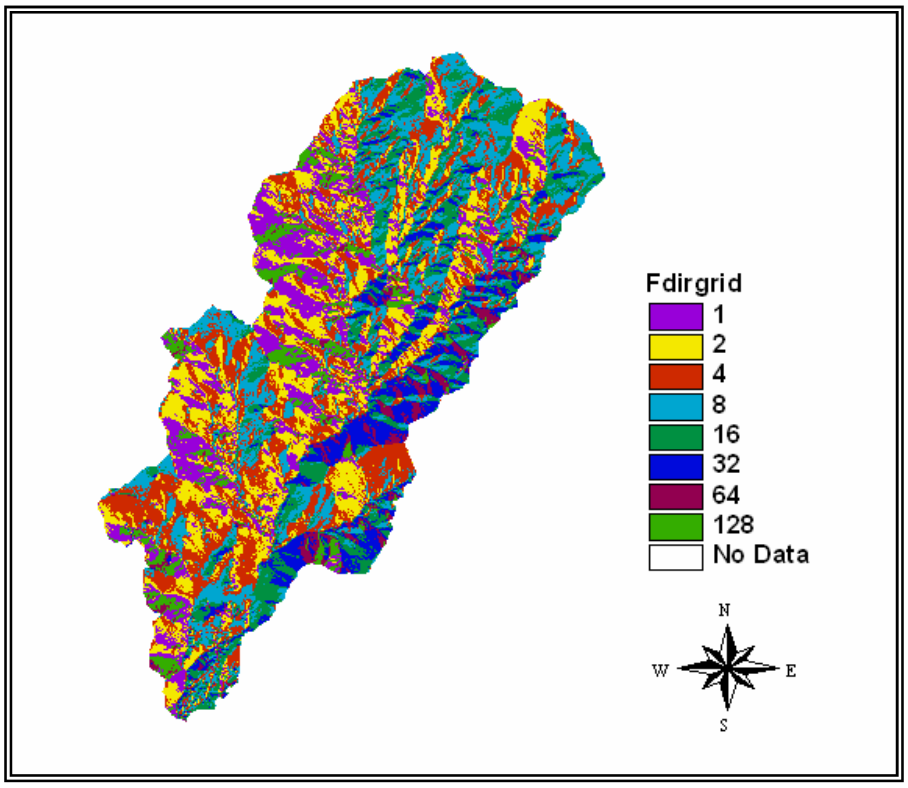

Figure 8.4 Flow direction grid.

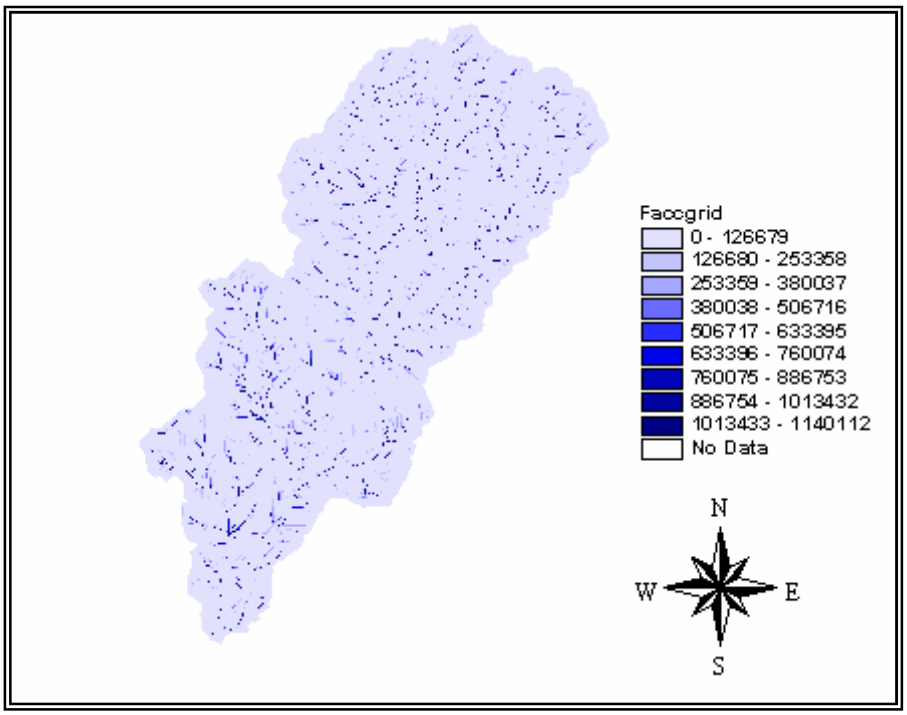

Figure 8.5 Flow accumulation grid.

Stream Definition

In order to define the streams on the basis of flow directions, a threshold value is assigned as the minimum number of cells sufficient to create channeling along the way water moves. The result of the Stream Definition procedure is the "StrGrid23", as shown in Figure 8.6.

Stream Segmentation

The use of the stream segmentation operation provides a stream-link-grid, as in the example of "StrLnkGrid14" theme of Figure 8.7, where the links are the sections of a stream channel connecting two successive junctions, a junction and the outlet, or a junction and the drainage divide.

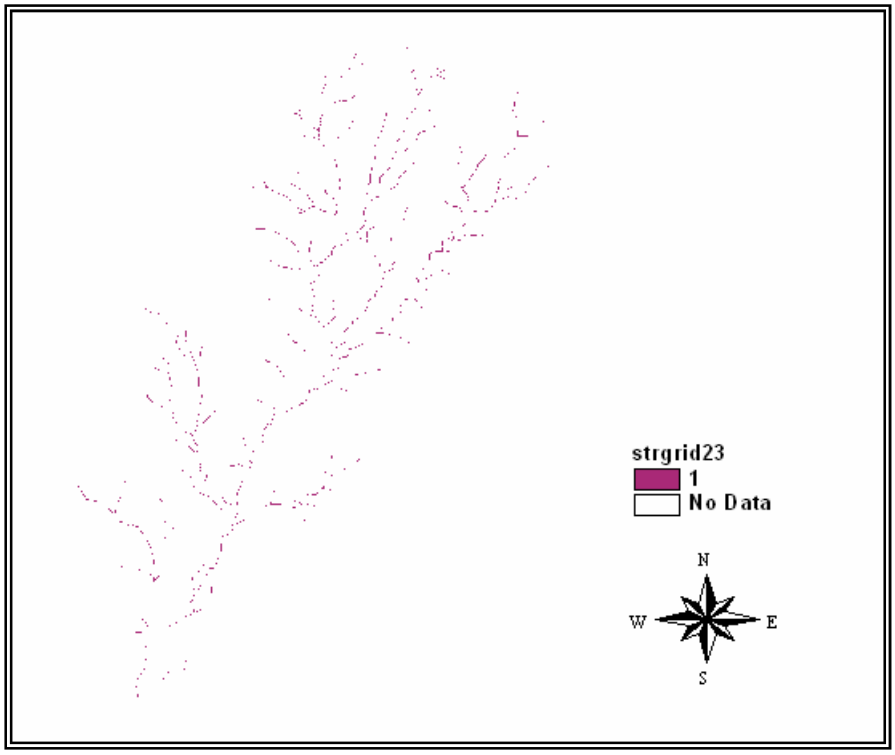

Figure 8.6 Resulting for the Bostanli River stream definition.

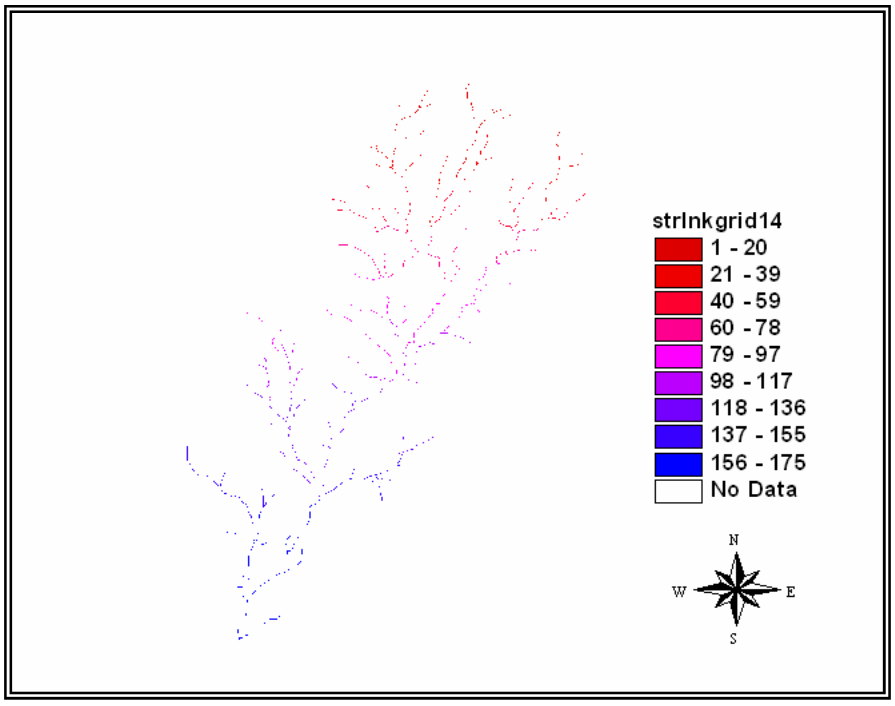

Figure 8.7 Stream segmentation for the Bostanli River.

Watershed Delineation

In this step, subbasins are delineated for every stream segment, and "Wshgrid14" theme is obtained (Figure 8.8).

Watershed Polygon Processing

Through the use of the watershed polygon processing procedure, the grid-based subbasins are transformed into polygonal vector areas as shown in the "Wshshp14.shp" theme in Figure 8.9.

Stream Segmentation Processing

The stream segmentation processing is utilized to convert the grid-based streams into linear vector objects that represent the stream network, as shown in the "River14.shp" theme of Figure 8.10.

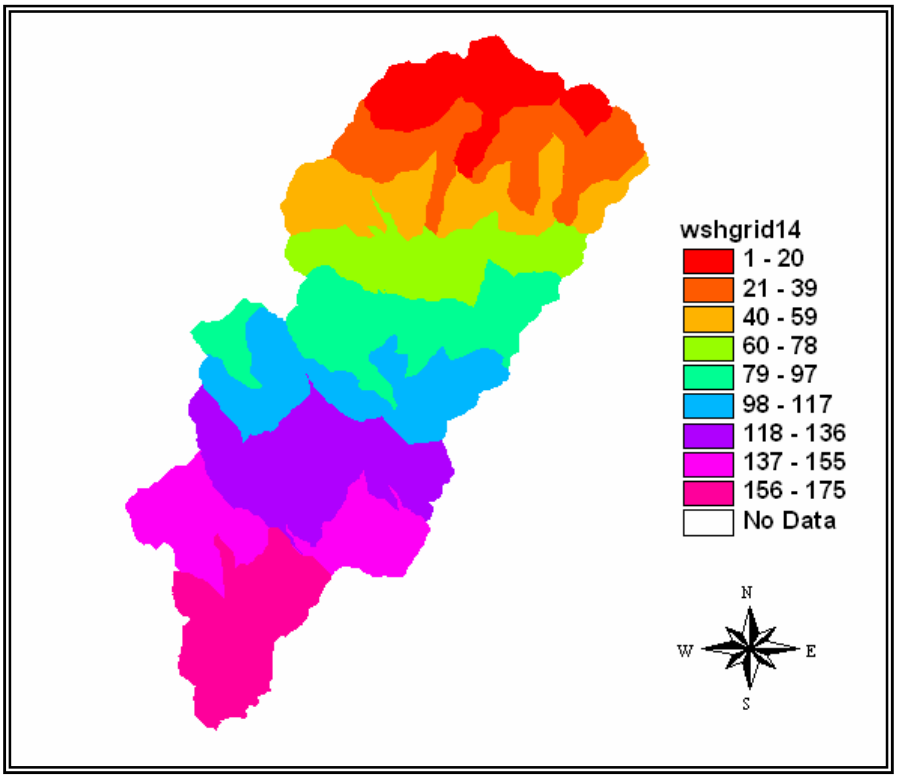

Figure 8.8 Watershed delineation for the Bostanli Basin.

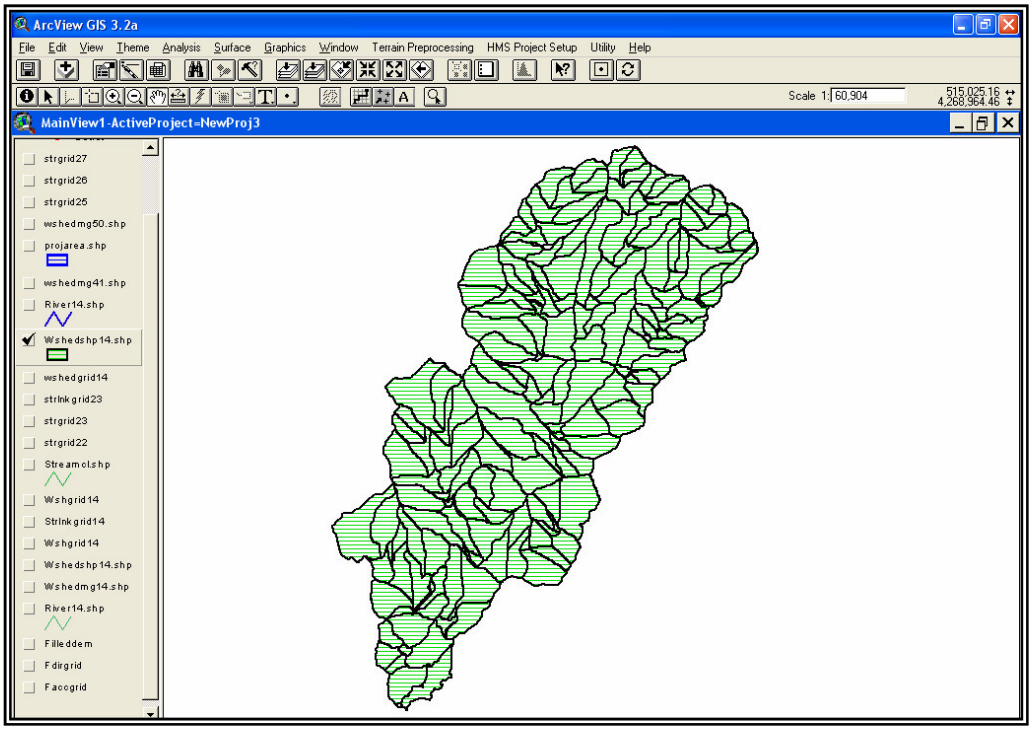

Figure 8.9 Watershed polygon processing for the Bostanli Basin.

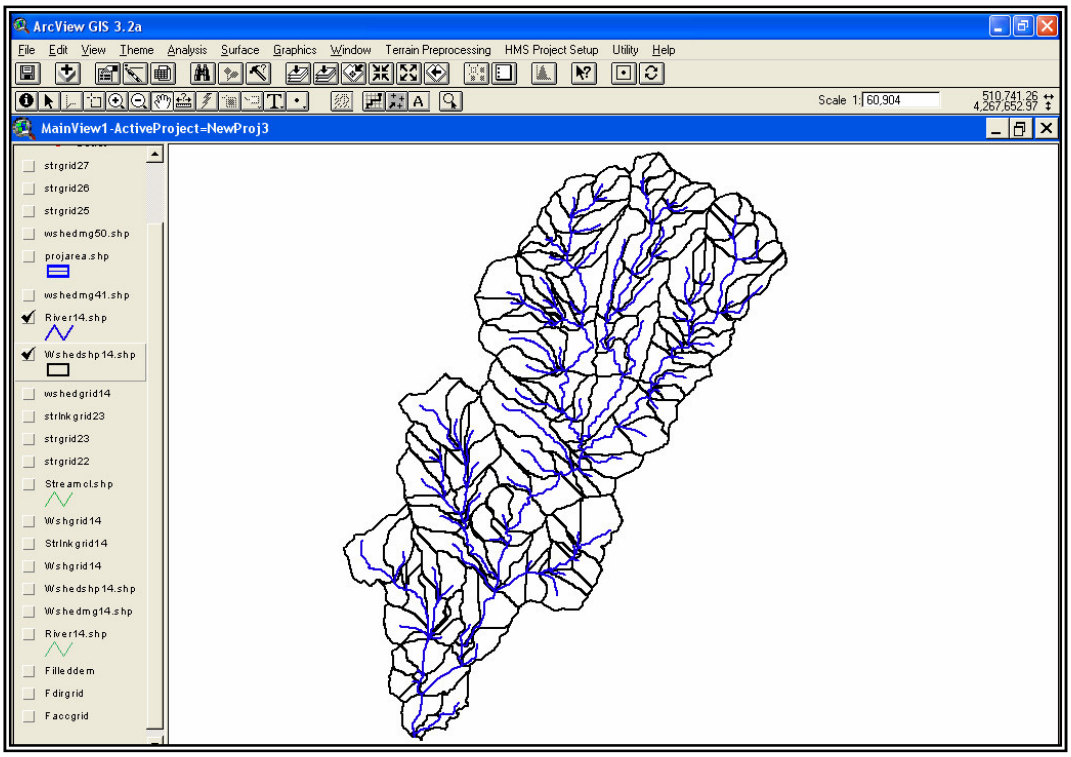

Figure 8.10 Stream segment processing for the Bostanli Basin.

Watershed Aggregation

In this step, the upstream subbasins are aggregated by using the "Watershed Aggregation" process at every confluence. The result in the form of a shapefile as "WshedMg50.shp" theme is shown in Figure 8.11.

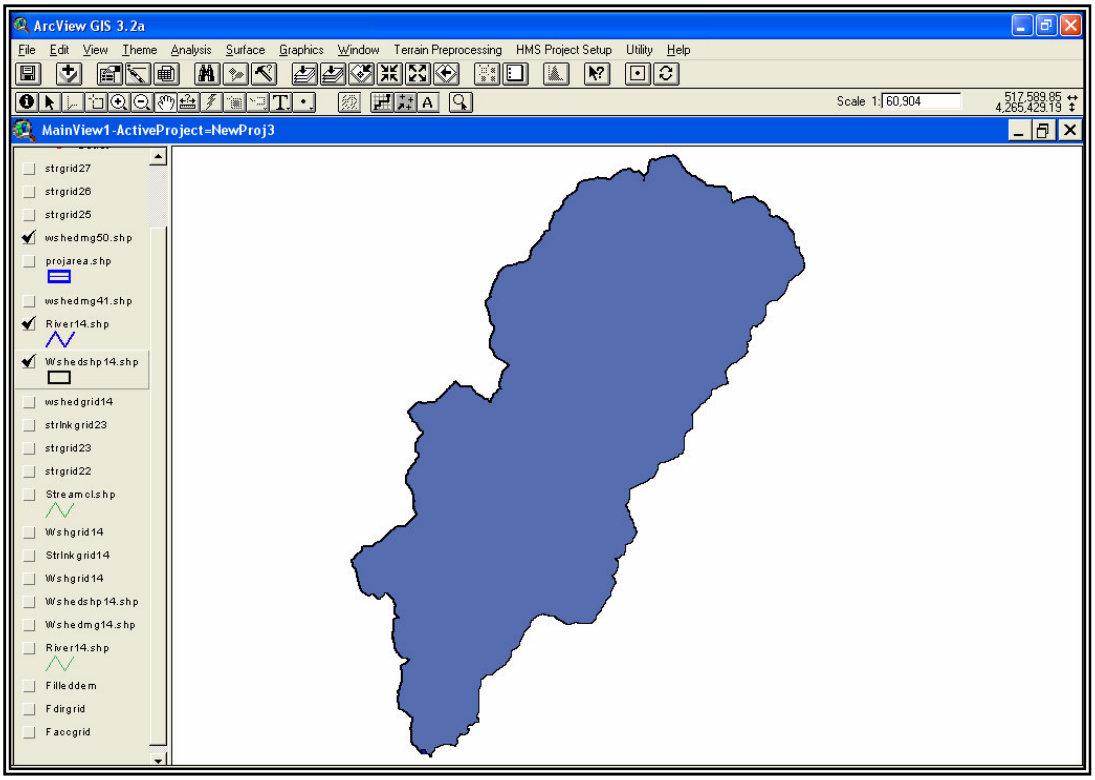

Figure 8.11 Watershed aggregation for the Bostanli Basin.

Full Processing Setup

Figure 8.12 shows the full processing setup screen used to address the themes required to complete the full processing. As can be seen from the figure, the DEM file, direction grid file, accumulation grid file, stream grid file, stream link grid file, raster and vector files for watersheds, river network vector file, and watershed aggregation result file are required for full processing.

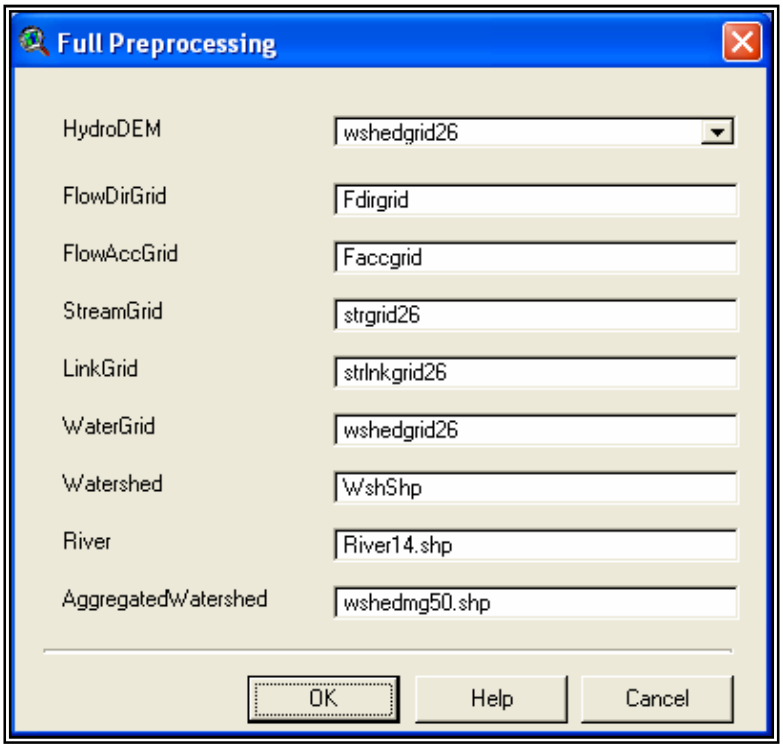

Figure 8.12. Full processing setup with theme names.

Hydrologic Model Setup

In the ProjView, which is named as "Bostanli", the data sets explained in the following sections are extracted and created for the specified study area. The extracted area includes the buffer zone in order to deal with the boundary conditions.

8.2.2 Hydrologic Processing

After terrain processing is performed in the MainView, the extracted data for the HMS model are generated and placed in the ProjView to allow revising of the subbasin delineation.

8.2.2.1 Basin processing

Basin merge processing is used to derive the subbasins to be considered in the HEC-HMS model for derivation of the flood hydrographs. The merged basin is shown in Figure 8.13.

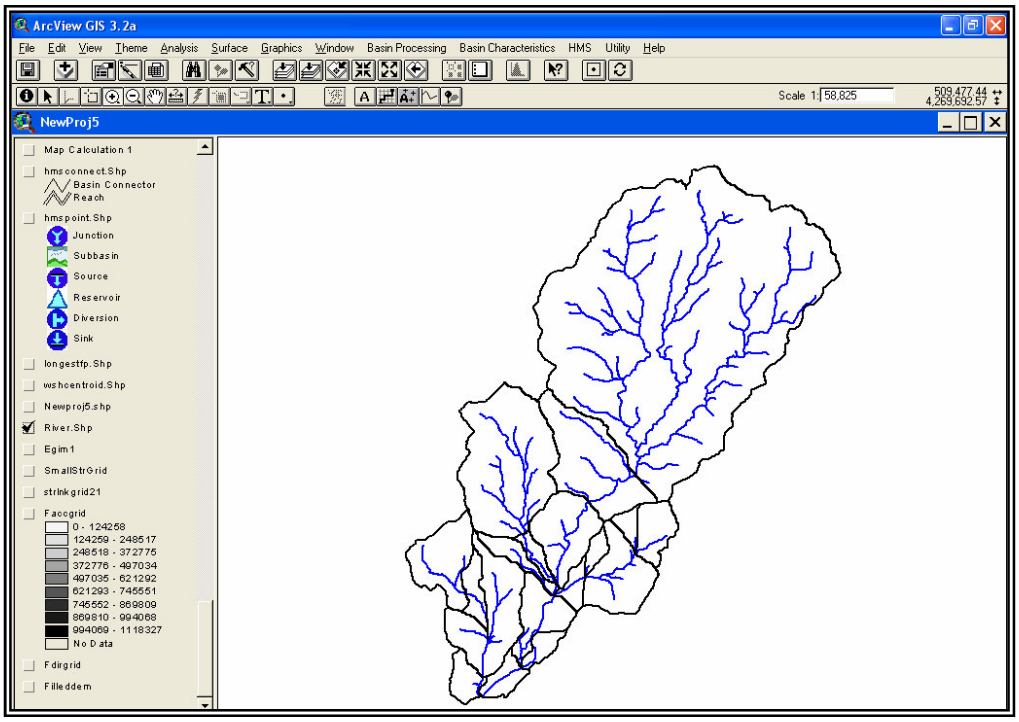

Figure 8.13 Merged subbasins.

River Length

The result of the river length computation is the “Riv_Length” column, that is added to the initial attribute table and that includes the length values in meters for this study.

River Slope

In this step, the upstream and downstream elevations of a river reach and its slope was computed and named as “us_Elv”, “ds_Elv”, and “Slp_Endpt” automatically.

Basin Centroid

The flow path method is used to locate the basin centroid. Through this method, the longest flow lengths are determined for the subbasins, and the centroids are placed approximately at the midpoints of these lengths. The results are shown in Figure 8.14.

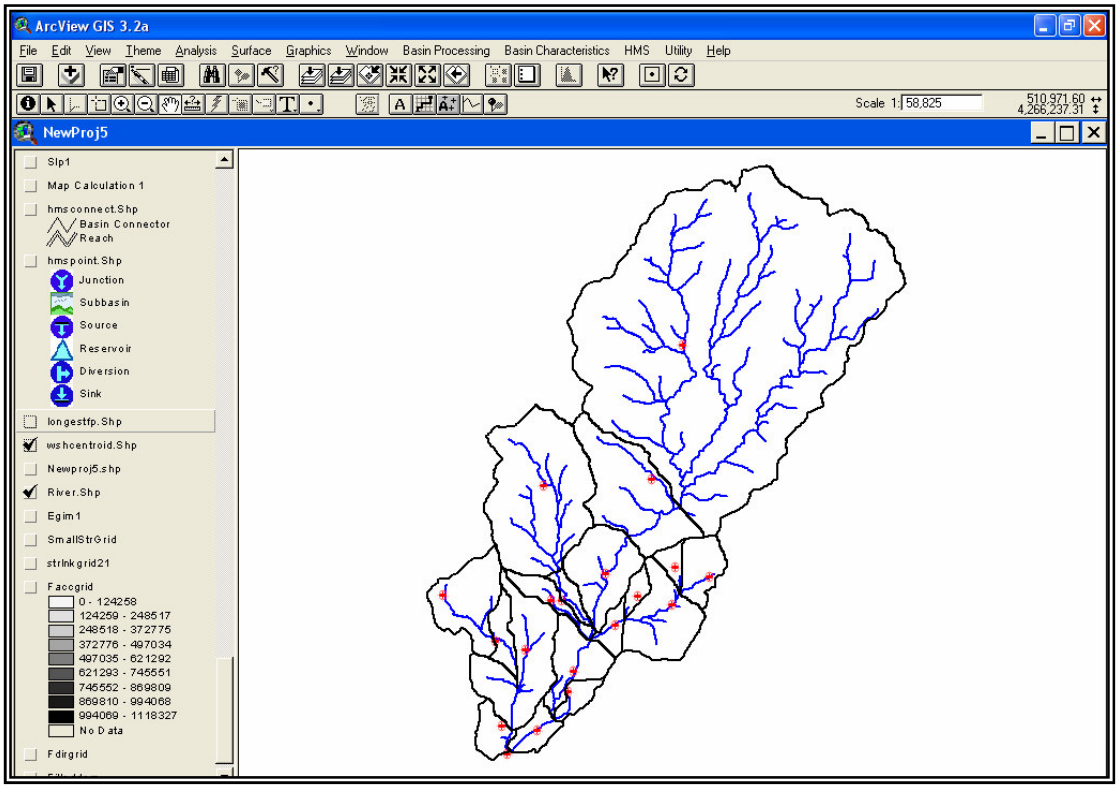

Figure 8.14 Basin centroids derived by using the flow path method.

Longest Flow Path

The longest flow path was already computed prior to the calculation of the basin centroid. The results are presented in Figure 8.15.

Centroidal Flow Path

The results of the centroidal flow path operation in the form of a separate layer (also as a shapefile called the "Centroidalfp.shp") with some linear features is shown in Figure 8.16. The lines in the figure represent the flow paths from the centroid to the outlet in each subbasin.

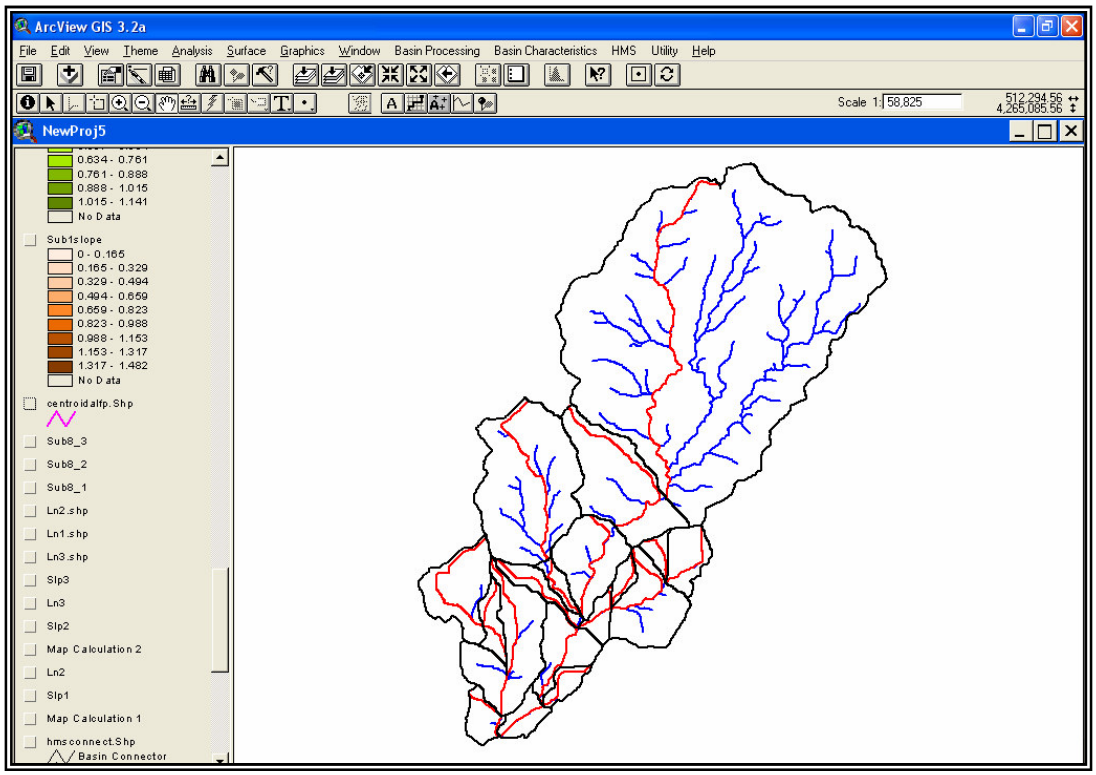

Figure 8.15 Longest flow path results.

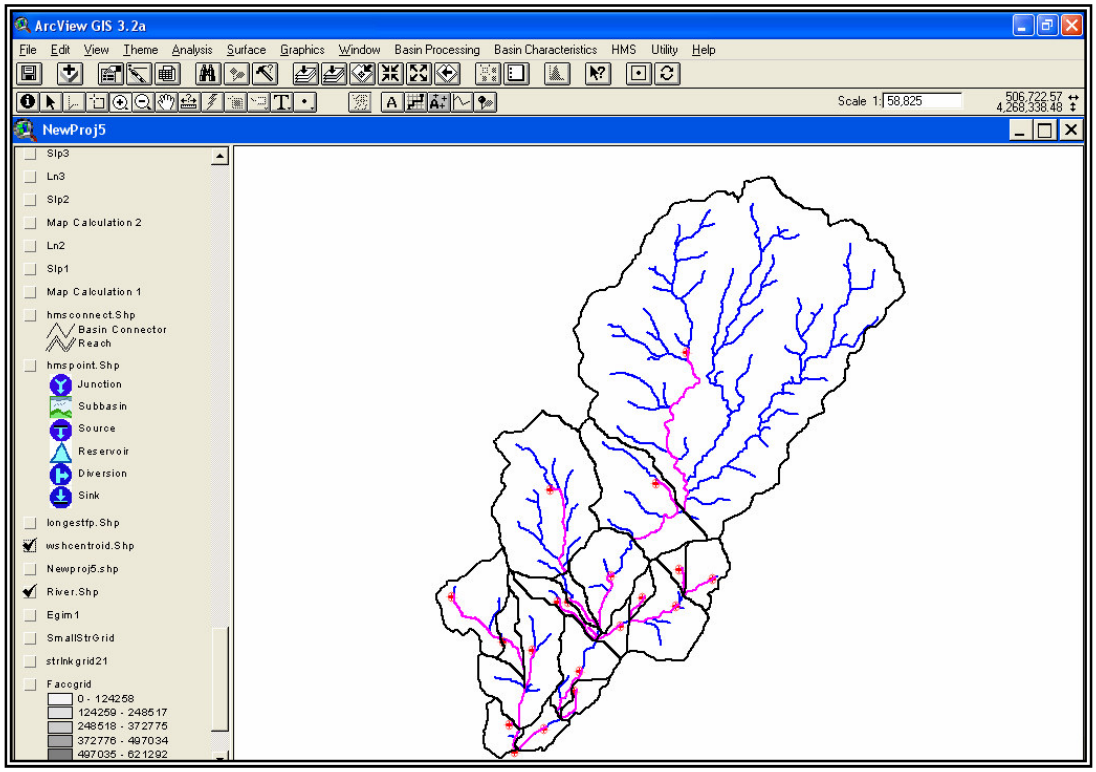

Figure 8.16 Centroidal flow paths.

8.2.2.2 Hydrologic Modeling System

The names of reaches and subbasins are generated automatically in this step of the total process.

Reach AutoName

The generated reach autonames are given in Figure 8.17.

RivId	Length	Riv_Length	Slp_Endpt	us_Elv	ds_Elv	Name
2	187	187.0	0.0962	783.4659	765.4838	R20
1	236	235.8	0.0951	787.9001	765.4838	R10
4	81	80.7	0.0977	765.4838	757.5945	R40
5	11	10.6	0.1317	758.9911	757.5945	R50
3	317	317.4	0.2951	713.1474	619.4780	R30
7	223	223.4	0.3233	691.7074	619.4780	R70
9	123	122.9	0.1609	767.0884	747.3149	R90
11	150	150.3	0.3162	794.8346	747.3149	R110
12	26	26.2	0.1494	747.3149	743.3998	R120
13	354	354.3	0.2337	826.2108	743.3998	R130
8	364	363.9	0.1689	595.0273	533.5671	R80
10	493	493.2	0.1742	619.4780	533.5671	R100
15	130	129.6	0.2459	765.9180	734.0548	R150
17	35	34.6	0.1845	740.4316	734.0548	R170
6	529	529.2	0.1482	757.5945	679.1624	R60
14	410	410.4	0.1565	743.3998	679.1624	R140
16	263	262.8	0.1517	533.5671	493.6960	R160
18	526	526.0	0.2332	616.3555	493.6960	R180
23	103	103.4	0.2536	696.0776	669.8538	R230
19	266	265.7	0.2416	734.0548	669.8538	R190

Figure 8.17 Reach autonames for the subbasins.

Basin AutoName

The subbasin autonames are given in Figure 8.18.

Attributes of WaterShd.Shp

Shape	Id	Gridcode	Area	WshId	TopoDone	Perimeter	Elevation	Name	Elevation_HMS	Area_HMS	CentroidalFL	CentroidalFl_HMS	L
Polygon	6	1	15317999.99	1	0	22080.00000	343.7175	R1100W10	343.717	15.318	3252.277	3252.277	
Polygon	165	97	2915125.000	97	0	9390.000000	321.4331	R1270W970	321.433	2.915	1560.881	1560.881	
Polygon	222	93	1834149.999	93	0	8500.000000	224.4427	R1190W930	224.443	1.834	1579.594	1579.594	
Polygon	235	132	165650.0000	132	0	2560.000000	206.5819	R1320W1320	206.582	0.166	450.563	450.563	
Polygon	249	123	1054749.999	123	0	5550.000000	86.4286	R1360W1230	86.429	1.055	1031.114	1031.114	
Polygon	253	135	1038750.000	135	0	5730.000000	110.8099	R1460W1350	110.810	1.039	883.762	883.762	
Polygon	257	130	500099.9999	130	0	3670.000000	184.2820	R1300W1300	184.282	0.500	616.703	616.703	
Polygon	275	142	155800.0000	142	0	2480.000000	166.4224	R1420W1420	166.422	0.156	500.845	500.845	
Polygon	280	129	185274.9999	129	0	3630.000000	104.7030	R1290W1290	104.703	0.185	706.911	706.911	
Polygon	281	138	996274.9999	138	0	6120.000000	233.4279	R1510W1380	233.428	0.996	1131.396	1131.396	
Polygon	285	152	307524.9999	152	0	4180.000000	58.7921	R1540W1520	58.792	0.308	875.269	875.269	
Polygon	310	143	1454824.999	143	0	9300.000000	47.6938	R1650W1430	47.694	1.455	1319.013	1319.013	
Polygon	314	148	214424.9999	148	0	2880.000000	69.8553	R1480W1480	69.855	0.214	505.165	505.165	
Polygon	317	166	215274.9999	166	0	2900.000000	35.9513	R1660W1660	35.951	0.215	597.058	597.058	
Polygon	348	168	301699.9999	168	0	4100.000000	17.1521	R1680W1680	17.152	0.302	572.015	572.015	
Polygon	350	169	308249.9999	169	0	3150.000000	22.4097	R1720W1690	22.410	0.308	544.234	544.234	
Polygon	356	173	199.9999999	173	0	100.0000000	12.6189	R1730W1730	12.619	0.000	12.500	12.500	
Polygon	0	134	316849.9999	176	0	4810.000000	113.9704	R1550W1760	113.970	0.317	0.000	0.000	
Polygon	0	134	675274.9999	174	0	5530.000000	43.6340	R1670W1740	43.634	0.675	0.000	0.000	

Figure 8.18 Subbasin autonames.

8.2.2.3 HMS Model Files

Mapping to HMS Units

By using the unit conversion operation, three columns are added to the stream attribute table and six columns are added to the subbasin attribute table as shown in Figures 8.19 and 8.20.

utes of River.Shp

RivId	Length	Riv_Length	Slp_Endpt	us_Elv	ds_Elv	Name	Riv_Length_HMS	us_Elv_HMS	ds_Elv_HMS
2	187	187.0	0.0962	783.4659	765.4838	R20	187.000	783.466	765.484
1	236	235.8	0.0951	787.9001	765.4838	R10	235.800	787.900	765.484
4	81	80.7	0.0977	765.4838	757.5945	R40	80.700	765.484	757.595
5	11	10.6	0.1317	758.9911	757.5945	R50	10.600	758.991	757.595
3	317	317.4	0.2951	713.1474	619.4780	R30	317.400	713.147	619.478
7	223	223.4	0.3233	691.7074	619.4780	R70	223.400	691.707	619.478
9	123	122.9	0.1609	767.0884	747.3149	R90	122.900	767.088	747.315
11	150	150.3	0.3162	794.8346	747.3149	R110	150.300	794.835	747.315
12	26	26.2	0.1494	747.3149	743.3998	R120	26.200	747.315	743.400
13	354	354.3	0.2337	826.2108	743.3998	R130	354.300	826.211	743.400
8	364	363.9	0.1689	595.0273	533.5671	R80	363.900	595.027	533.567
10	493	493.2	0.1742	619.4780	533.5671	R100	493.200	619.478	533.567
15	130	129.6	0.2459	765.9180	734.0548	R150	129.600	765.918	734.055
17	35	34.6	0.1845	740.4316	734.0548	R170	34.600	740.432	734.055
6	529	529.2	0.1482	757.5945	679.1624	R60	529.200	757.595	679.162
14	410	410.4	0.1565	743.3998	679.1624	R140	410.400	743.400	679.162

Figure 8.19 River attribute table populated with fields of HMS units.

Attributes of WaterShd.Shp

Elevation_HMS	Area_HMS	CentroidalFL	CentroidalFl_HMS	DSElv	Slp_EndPt	Slp_1085	LongestFL	USElv	LongestFl_HMS	USElv_HMS	DSElv_HMS
343.717	15.318	3252.277	3252.277	151.9903	0.100	0.106	6504.554	800.0000	6504.554	800.000	151.990
321.433	2.915	1560.881	1560.881	141.6023	0.153	0.178	3121.762	620.0000	3121.762	620.000	141.602
224.443	1.834	1579.594	1579.594	115.7566	0.169	0.149	3159.188	651.0000	3159.188	651.000	115.757
206.582	0.166	450.563	450.563	122.3564	0.224	0.238	901.127	324.0000	901.127	324.000	122.356
86.429	1.055	1031.114	1031.114	57.2403	0.116	0.107	2062.229	297.0000	2062.229	297.000	57.240
110.810	1.039	883.762	883.762	74.4514	0.143	0.143	1767.523	328.0000	1767.523	328.000	74.451
184.282	0.500	616.703	616.703	121.7040	0.230	0.225	1233.406	406.0000	1233.406	406.000	121.704
166.422	0.156	500.845	500.845	74.7008	0.238	0.261	1001.690	313.0000	1001.690	313.000	74.701
104.703	0.185	706.911	706.911	57.2321	0.084	0.084	1413.823	176.0000	1413.823	176.000	57.232
233.428	0.996	1131.396	1131.396	62.2914	0.147	0.166	2262.792	394.0000	2262.792	394.000	62.291
58.792	0.308	875.269	875.269	26.1909	0.146	0.139	1750.538	282.0000	1750.538	282.000	26.191
47.694	1.455	1319.013	1319.013	17.2375	0.133	0.130	2638.026	367.0000	2638.026	367.000	17.238
69.855	0.214	505.165	505.165	53.1790	0.084	0.063	1010.330	138.0000	1010.330	138.000	53.179
35.951	0.215	597.058	597.058	24.4570	0.132	0.126	1194.117	182.0000	1194.117	182.000	24.457
17.152	0.302	572.015	572.015	12.1187	0.017	0.020	1144.031	32.0000	1144.031	32.000	12.119
22.410	0.308	544.234	544.234	12.2455	0.083	0.097	1088.467	103.0000	1088.467	103.000	12.246
12.619	0.000	12.500	12.500	12.0723	0.077	0.053	25.000	14.0000	25.000	14.000	12.072
113.970	0.317	0.000	0.000	53.1074	0.170	0.158	1797.939	359.0000	1797.939	359.000	53.107
43.634	0.675	0.000	0.000	0.0000	0.000	0.000	0.000	0.0000	0.000	0.000	0.000

Figure 8.20 Watershed attribute table populated with fields of HMS units.

HMS Data Check

As required by the model, several checks are performed on the data obtained throuh preprocessing operations on HEC-GeoHMS to guarantee their accurate use in the HEC-HMS model. After completing the full check and receiving were no error reports, it has been ensured that all the preprocessing operations have been properly executed so that the end results can be used in the HEC-HMS model (Figure 8.21).

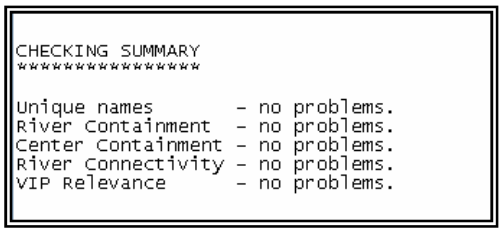

Figure 8.21 HMS data check summary.

HEC-HMS Basin Schematic and HMS Legend

The GIS representation, namely the HMS basin schematic, of the hydrologic basin model with basin elements and their connectivity is obtained as shown in Figure 8.22. In this step, the point shapefile, "HMSPoint.shp", and the line shapefile, "HMSConnect.shp" are created.

Background Map File

The background map file, including the geographic information of the subbasin boundaries and stream alignments, is stored in an ASCII text file. A part of the resulting background map file in ASCII format is given in Figure 8.23.

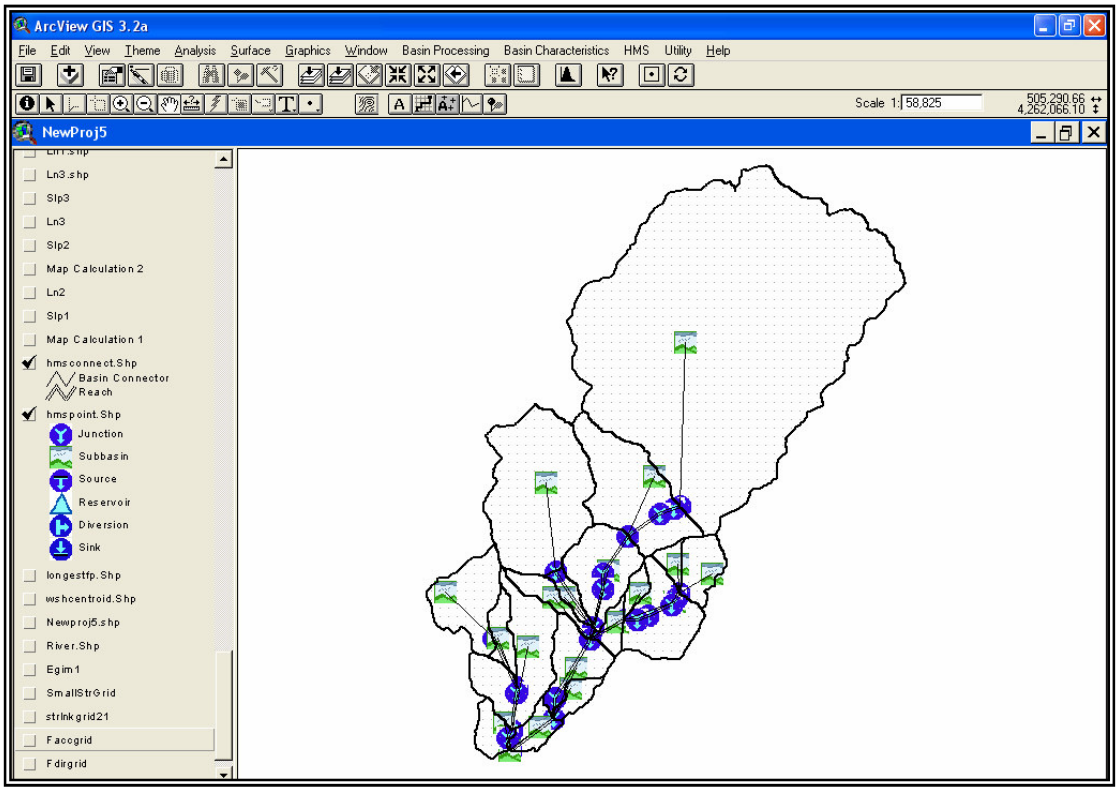

Figure 8.22 HMS schematic with symbols.

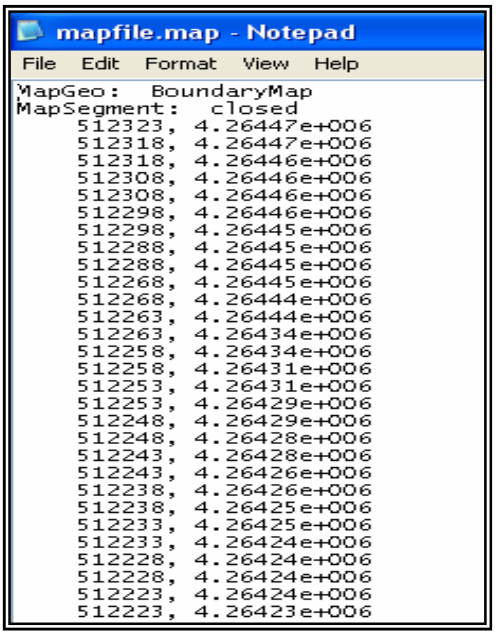

Figure 8.23 HMS background map file for the Bostanli Basin.

8.3 Importing Input Files to the HMS Model

The derived basin model and the background map file are exported into the HEC-HMS model so that the study area, its boundaries and subbasin areas are visualized; and furthermore, some required data are entered automatically by this procedure.

The resulting basin model with the background map is shown in Figure 8.24.

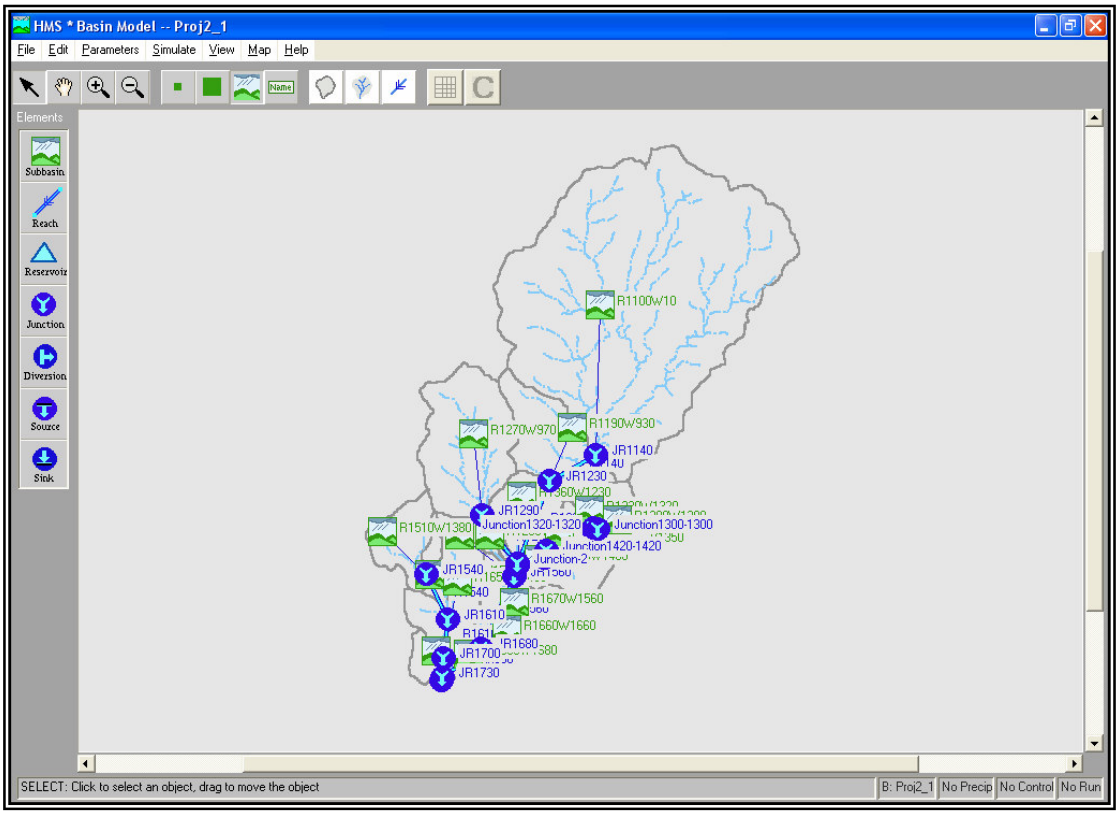

Figure 8.24 HMS basin model schematic.

8.4 Computation of CN values

In order to obtain averaged representative CNs for single subbasins, firstly, unique soil group-land cover polygons over the whole basin area were identified. In doing this, the primary soil groups were defined based on such soil characteristics as texture, depth and stoneness. As we did not have a well-defined land use/land cover map and also as

the upper part of the basin area under investigation was free of the built-up and agricultural land, already available NDVI map have been utilized to represent the vegetation cover in that area. Then, the soil type-land cover combination polygons were defined and corresponding CNs were assigned to each unit cell area within the basin. And finally, representative CNs for subbasins were obtained by using the method of averaging based on the defined formula. While Figure 8.25 shows the NDVI, soil map and computed grid of CN values for the Bostanli Basin, the computed CN values for each subbasin area are given in Table 8.2.

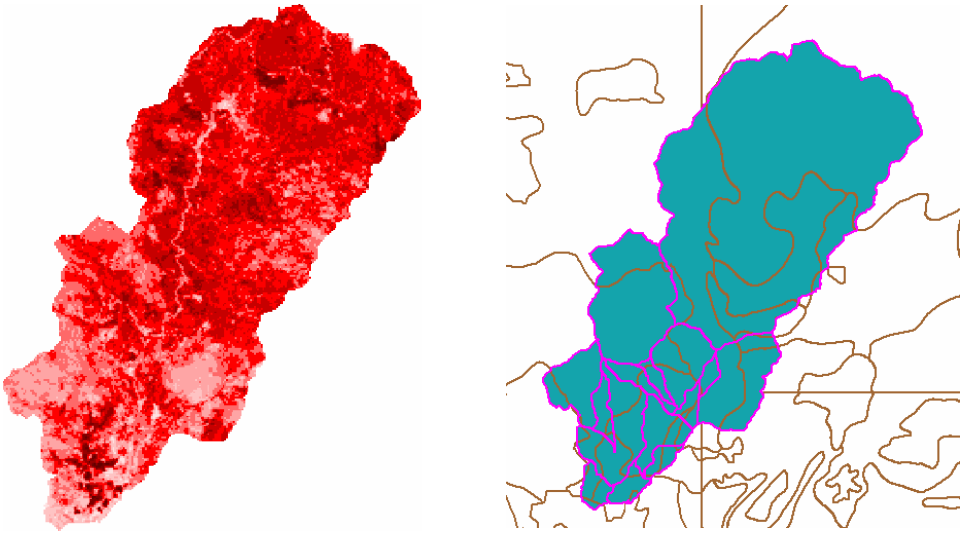

(a) (b)

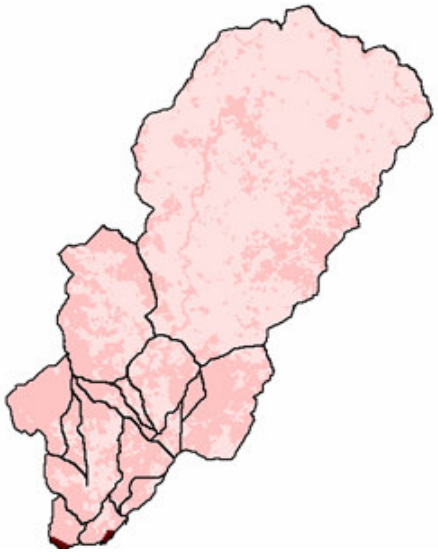

Table 8.2 CN values of the basin.

Subbasin Name	CN values	Subbasin Name	CN values
SUB01	73.797	SUB10	76.579
SUB02	73.977	SUB11	75.998
SUB03	75.212	SUB12	76.723
SUB04	75.073	SUB13	75.827
SUB05	75.982	SUB14	75.302
SUB06	75.147	SUB15	76.091
SUB07	75.133	SUB16	75.910
SUB08	76.872	SUB17	78.404
SUB09	75.471	SUB18	77.045

Figure 8.25 (a) NDVI, vegetation cover, (b) soil map of the Bostanli basin and (c) computed CN grid.

8.5 Application of Clark's Unit Hydrograph

In this study, the digital elevation model of the Bostanli Basin is used to determine the time-area diagram. First, the directions of flow from each cell are determined, and then, the travel distances of flow from each cell to the basin outlet are computed for each single 5mx5m cell. The values of these travel distances are then converted to the travel time values. Since each cell in the study area ha dimensions of 5m x 5m, the cumulative number of cells gives the corresponding area when multiplied by 25 m^2 (single cell area) to derive the time-area diagram.

Flow Length Grid obtained from the already derived flow accumulations is given in Figure 8.26. Tc values are also computed by using the relevant equations given in Chapter Three.

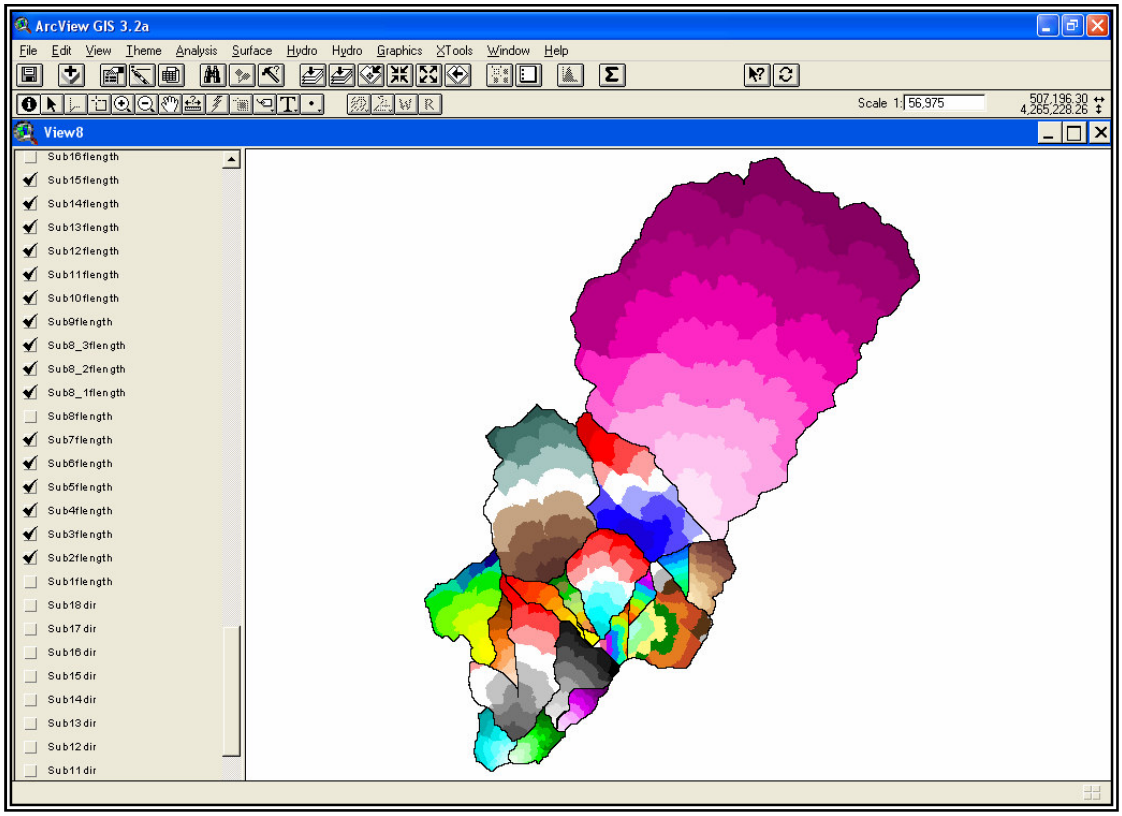

Figure 8.26 Flow length grid.

After the Travel Times Grid (TtGrid) (Figure 8.27) is determined, the time-area diagram is obtained by using this grid theme. For this purpose, the diagrams of the TtGrid are derived for the minimum time interval. At this point, it may be noted that a small interval gives a more detailed diagram that resembles complex hydrographs, while the shape of the diagram looks like a single peaked hydrograph if the interval is sufficiently enlarged. IUH can be derived if the selected time interval is infinitesimal. However, as it is not simple to obtain the diagram of TtGrid with infinitesimal intervals, the smallest possible computation interval is selected, considering all factors mentioned above to derive the time-area diagrams of all subbasins in the study area.

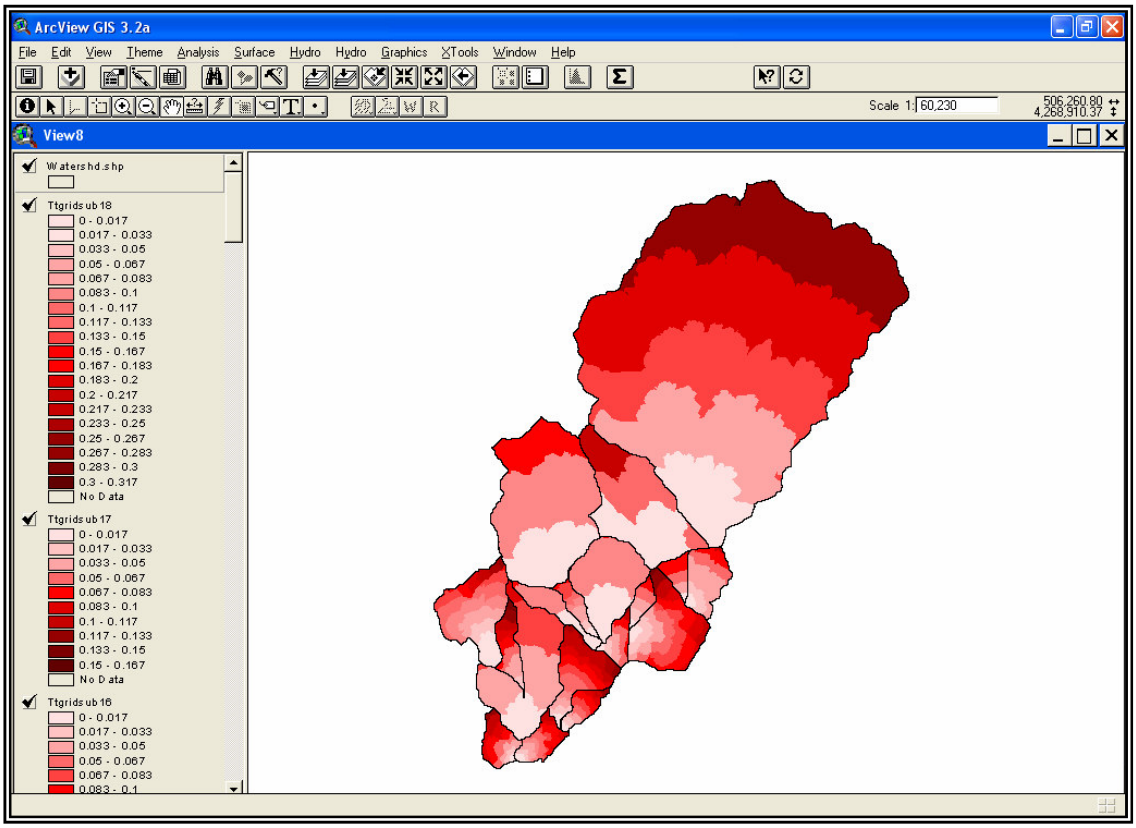

Figure 8.27 TtGrid of the Bostanli Basin.

In the TtGrid diagram, time values are on the abscissa and the counts of cells are on the ordinate. The time-area diagram with these coordinates is computed from TtGrid by converting the counts of cells to areas through multiplication by 25 m^2 for 5mx5m grid

cell dimensions. As an outcome of these computations, the diagrams for each subbasin in Bostanli Basin are obtained as given in Figure 8.28 for the “subbasin 16”.

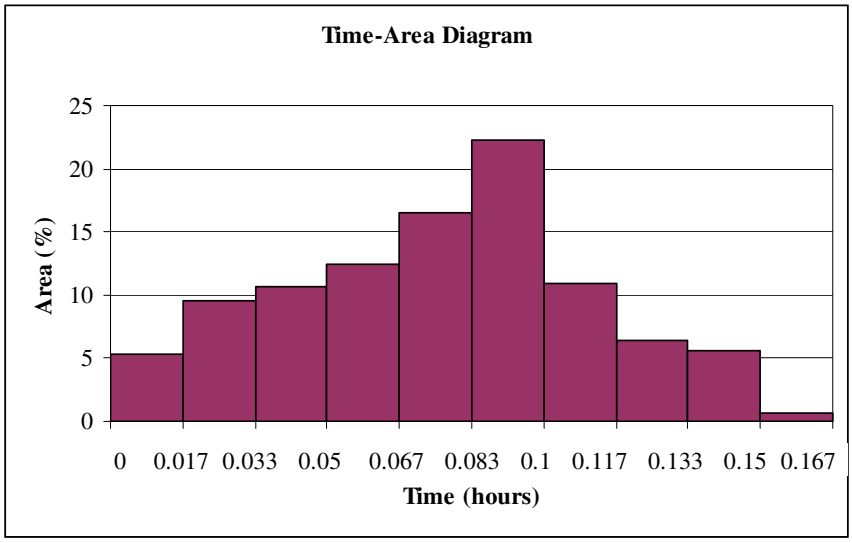

Figure 8.28 Time-area diagram of the subbasin 16.

Since Equation 4.24 is suitable only for gauged streams, it has not been possible to use it in this study. Instead, Equation 4.26 is employed to determine the value of K, taking the constant “b” value as 0.02. After the required parameters are obtained, the storage coefficients are determined by substituting them into Equation 4.26

By routing the time-area diagram through the linear reservoir, the instantaneous hydrographs of subbasins are developed. The 5 minute-unit hydrograph is derived by averaging two instantaneous unit hydrographs which are Δt time step apart (Figure 8.29).

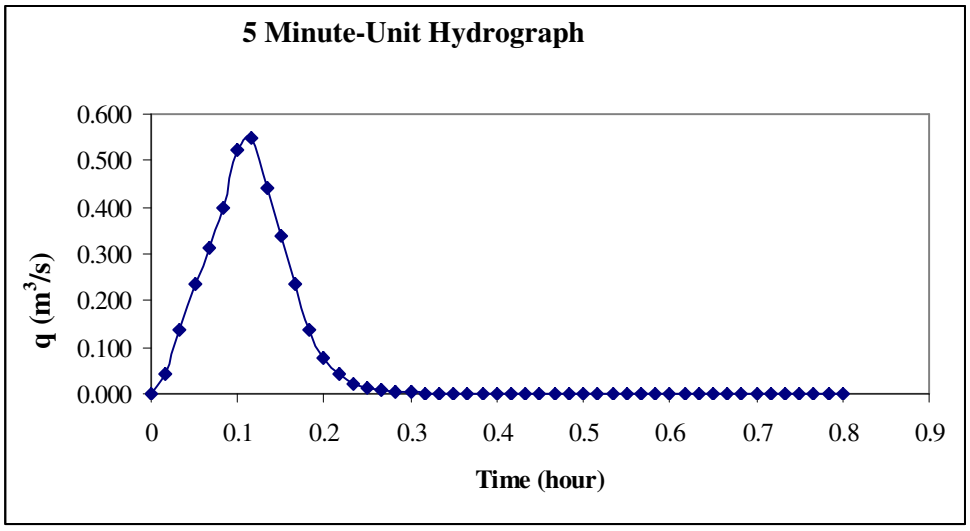

Figure 8.29 5 minute-final unit hydrograph of subbasin 16.

8.6 HEC-HMS Model Use

For the basin model of HMS, the SCS Curve Number method is used to determine loss rates. The CN values computed by utilizing some GIS operations for individual subbasins are entered manually in the specified fields.

For precipitation-runoff transformation, the Clark Synthetic Unit Hydrograph Method is selected for purposes of this study due to the availability of detailed spatial information in the study area. After the unit hydrographs are determined in each subbasin, the User Defined Unit Hydrograph method of HEC-HMS is selected, and the computed unit hydrographs are entered.

The Muskingum-Cunge method is used for the channel routing process. Since the required information on this method is based solely on channel geometry, the input data, which are assumed to be average along the river reach are obtained by using the GIS data sets and the derived maps. For example, the average slope of a reach is computed by multiplying the slope map with the length of that reach.

In this application, the base flow is assumed to be zero for all subbasins. Since hydraulic structures can not be added automatically in the GIS basin file, they need to be inserted manually. Thus, Bostanli Dam is added to the basin model by the use of the "drag and drop" capability of the HEC-HMS model, and its characteristics are entered manually. Afterwards, the connections of the Bostanli Dam with some other basin elements are supplied. Since the existence of short reaches make the model unnecessarily complex, it is preferred to remove these reaches and reconnect them to the closest hydrologic element. The storage specification alternatives are selected for flood routing in Bostanli Dam.

In the meteorological model of the Bostanli Basin, precipitation values on the 3rd and the 4th of November, 1995, recorded at Guzelyali meteorological station in Izmir, and the instantaneous intensity hyetographs for recurrence intervals of 100-years and 500-years are used to create different scenarios to both determine the runoff hydrograph for an observed rainfall record and compare this hydrograph and its peak value to the hydrographs obtained by using design hyetographs. A suitable simulation time is selected for hypothetical scenarios, and the computational time interval is set to five minutes for all scenarios. This stage then finalizes the preparation of the modeling.

After all data required for the HEC-HMS model are complemented, the model is run for the three conditions below, that differ according to the existence and nonexistence of the Bostanli Dam.

1) using the storm observed in 1995 under current conditions
2) using a 100-year storm under current conditions
3) using a 500-year storm under current conditions

After the model is run for these 3 conditions, the runoff hydrographs are obtained at the desired locations. The figures from 8.30 to 8.32 present the hydrographs at the outlet of the Bostanli Basin with the precense of the Bostanli Dam, while figures from 8.33 to 8.35 indicate the hydrographs for the basin outlet but this time without considering the dam.

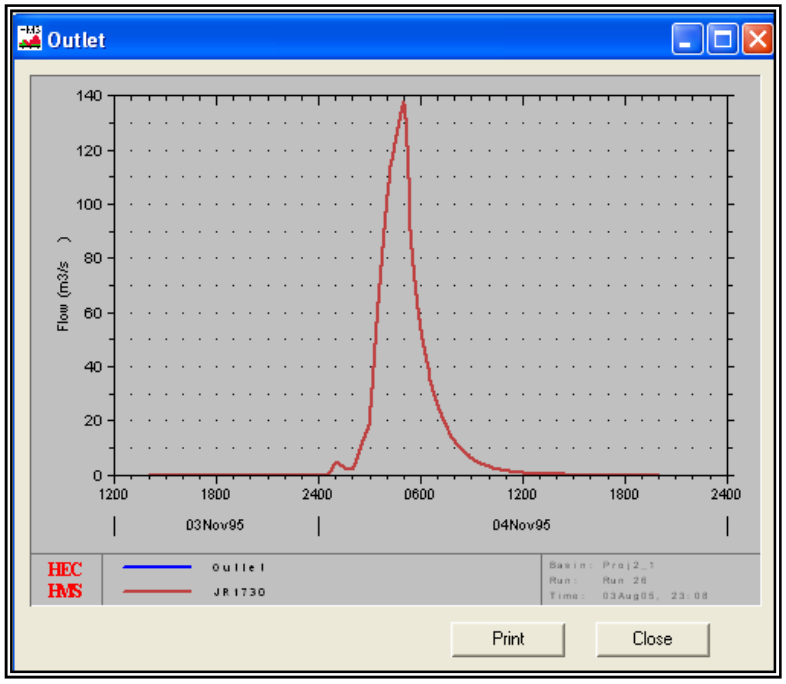

Figure 8.30 Output hydrograph at the basin outlet for 1995 storm for the "without-the-dam" scenario.

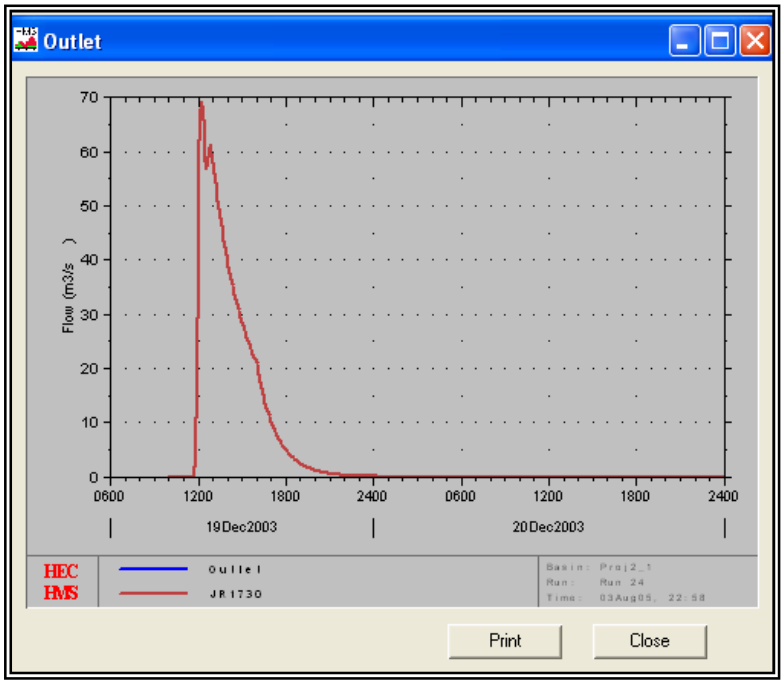

Figure 8.31 Output hydrograph for T=100 years at the basin outlet for the "without-the-dam" scenario.

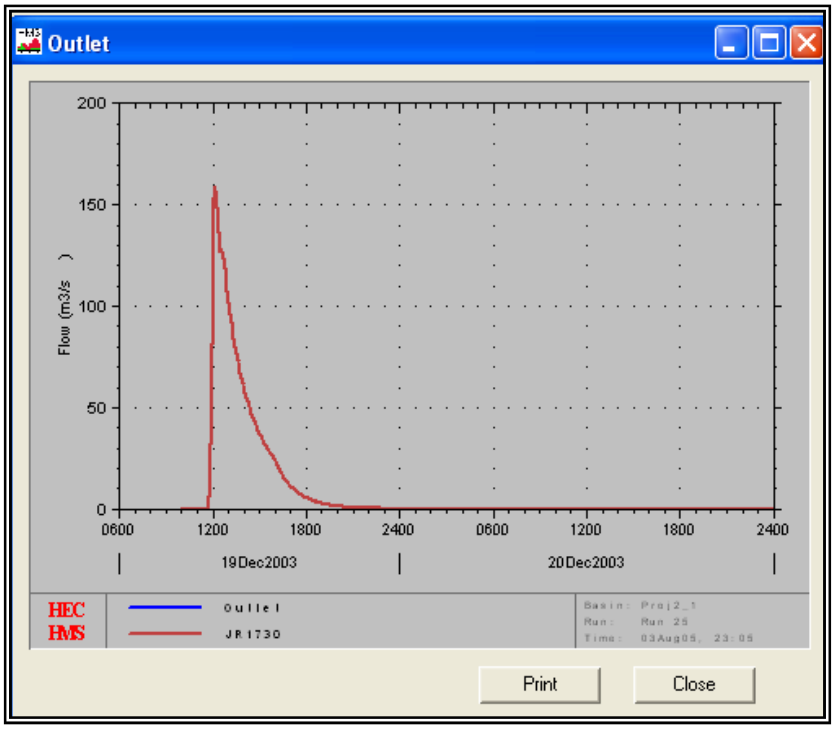

Figure 8.32 Output hydrograph for T=500 years at the basin outlet for the "without-the-dam" scenario.

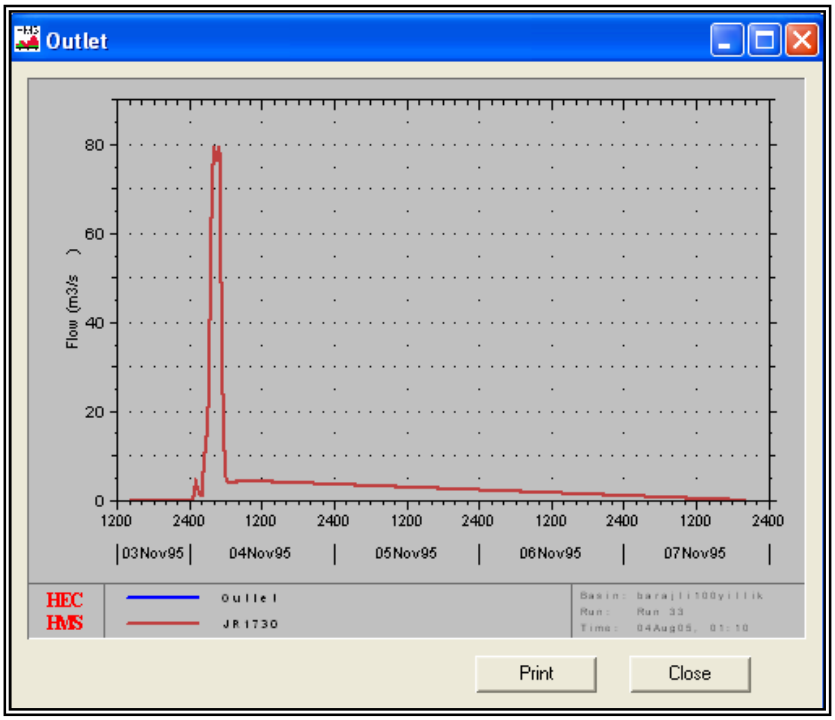

Figure 8.33 Output hydrograph at the basin outlet for 1995 storm for the "with-the-dam" scenario.

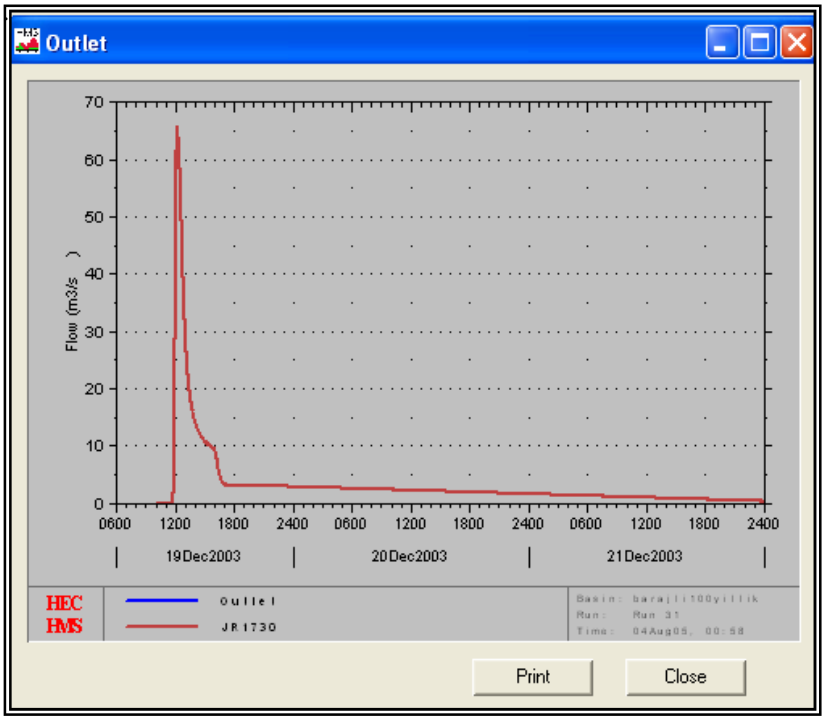

Figure 8.34 Output hydrograph for T=100 years at the basin outlet for "with-the-dam"scenario.

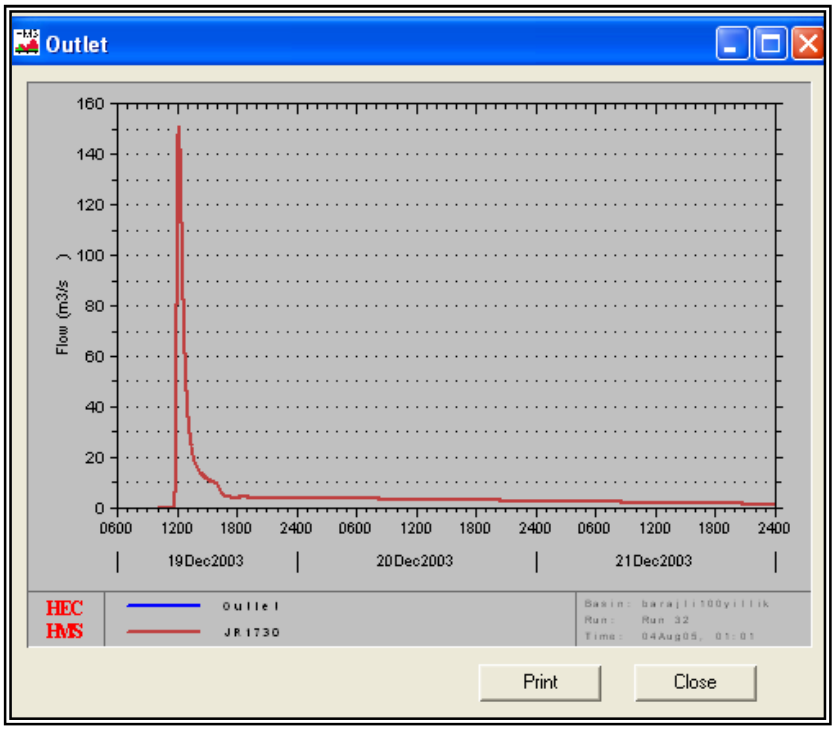

Figure 8.35 Output hydrograph for T=500 years at the basin outlet for "with-the-dam dam" scenario.

Flood peak discharges for each scenario are given in Table 8.3.

Table 8.3 Flood peak discharges for each scenario.

Scenarios	**1995 storm with the dam**	**1995 storm without the dam**	**T=100 with the dam**	**T=100 without the dam**	**T=500 with the dam**	**T=500 without the dam**
Flood peak (m^3/s)	79.384	137.33	65.531	68.89	150.70	158.66

The results of this study show that Bostanli Dam reduces the flood peak for the 1995 storm almost by half. However, the effect of the dam can not be seen so much for the other scenarios. Although the effect of the Bostanli Dam can not be ideally seen in these diagrams, outputs of the HEC-HMS model show that the dam has performed its expected function. However; the already selected two design storms of identical 6-hour durations, but with 100-year and 500-year recurrence intervals, seem to have produced much bigger flood peaks in the other subbasins compared to recorded storm in 1995. In addition, it can be seen that the flood that is based on the recorded storm has been attenuated in the subbasins unlike the floods from the design storms as an expected result of the duration difference.

CHAPTER NINE
APPLICATION OF THE HEC-RAS MODEL AND ITS HEC-GEORAS EXTENSION

For the hydraulic modeling analysis in the study, the lower part of the Bostanli Basin, which mainly consists of highly urbanized areas, is selected to keep the analyses parallel to those realized in hydrological modeling. The outputs of the HEC-HMS in the form of computed hydrographs have then became inputs for the HEC-RAS modeling part.

The first step in the application of the HEC-RAS model is to develop the Digital Terrain Model (DTM) and then to use the HEC-GeoRAS extension to create the import file to be used in the HEC-RAS. Correspondingly, this import file is prepared and imported into the HEC-RAS platform to perform the necessary hydraulic simulations both for the steady and the unsteady conditions. Finally, the floodplain maps that represent the actual results of the hydraulic simulations under several scenarios are derived after exporting the output files of the HEC-RAS to the HEC-GeoRAS and utilizing some post-processing operations there. The following sections give some detailed information about these applications.

9.1 Digital Terrain Model

In HEC-RAS, a DTM is required to obtain the cross-sectional geometry data related to the stream channel considered. HEC-GeoRAS, the extension for Arcview designed to process the geospatial data before and after hydraulic modeling, needs this DTM in the form of a Triangulated Irregular Network (TIN) model. The TIN model represents both the channel bottom geometry and the adjacent floodplain area. The data on the channel cross-section geometry are generally extracted from the TIN and then revised by a series of minor corrections based on the in-situ measurements. As the channel geometry normally dictates the flow in river systems, the TIN model to be utilized prior to the

hydraulic computations should be precise enough to allow the most accurate determination of the channel geometry and the surrounding landform.

In this study, the TIN model is created from point elevation measurements as well as from some linear features either in the form of elevation contours or polygonal boundaries with some recorded elevation values. A number of pre-defined digital maps are utilized to extract both the points with elevation records and the line objects that are composed of a series of points with their corresponding elevation values (Figure 9.1).

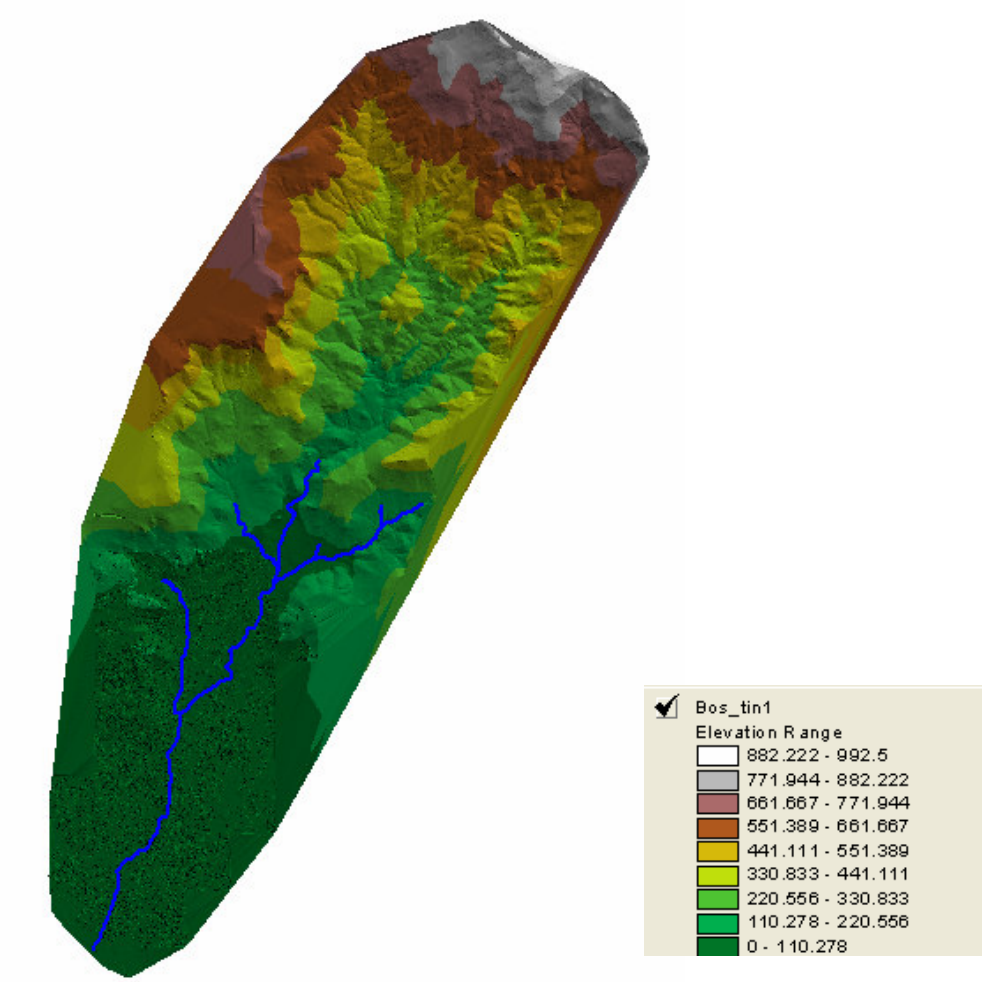

Figure 9.1 The TIN model obtained from point and line objects with elevation data.

One major difficulty in generating the TIN based terrain model for the Bostanli Basin has been the quite long time required for creating and loading the model prior to the main operations. Since the TIN has the form of a mesh of triangular surfaces consisting of 6458851 triangles and 3229450 nodes, loading could be completed in about 30 minutes.

9.2 Derivation of Input Files Via HEC-GeoRAS

First, RAS themes are created to develop the necessary import file for the HEC-RAS. These themes are summarized below.

9.2.1 Creation of RAS Themes

The actual geometric data development and extraction processes are fulfilled in this step. The following themes are created for this purpose:

Stream Centerline

As the stream centerline has been shown in the data provided by IZSU, it is directly utilized in the analyses. The stream centerline theme is copied from the *stream_y1.shp* theme and saved as *streamctbl.sh*p. However, some errors in the digitized stream line had to be eliminated for proper use of the stream data. For example, the direction of digitizing the lines in the HEC-GeoRAS is very important; thus, it has been necessary to examine all the lines constituting the major part of the stream with its reaches to arrive at correct digitizing directions. For this purpose, the improper directions have been reversed by using the FLIP command in the HEC-GeoRAS, and the lines which belong to a single reach but which originally are composed of many line segments have been merged, as required by HEC-GeoRAS. Using the *River ID* tool, each section of the stream centerline is defined with a *Stream_ID* and a *Reach_I*D. Figures 9.2 and 9.3 show the stream centerline theme and the stream centerline theme table, respectively.

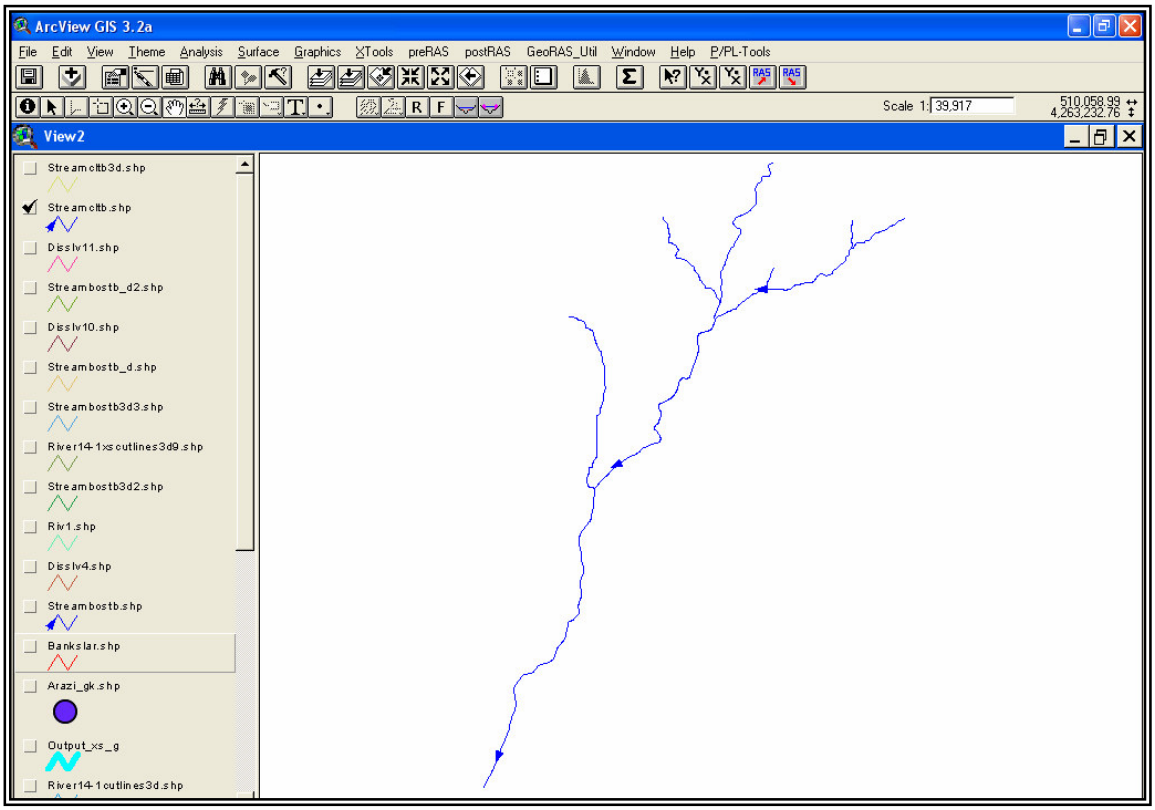

Figure 9.2 Stream centerline theme of the Bostanli River Basin.

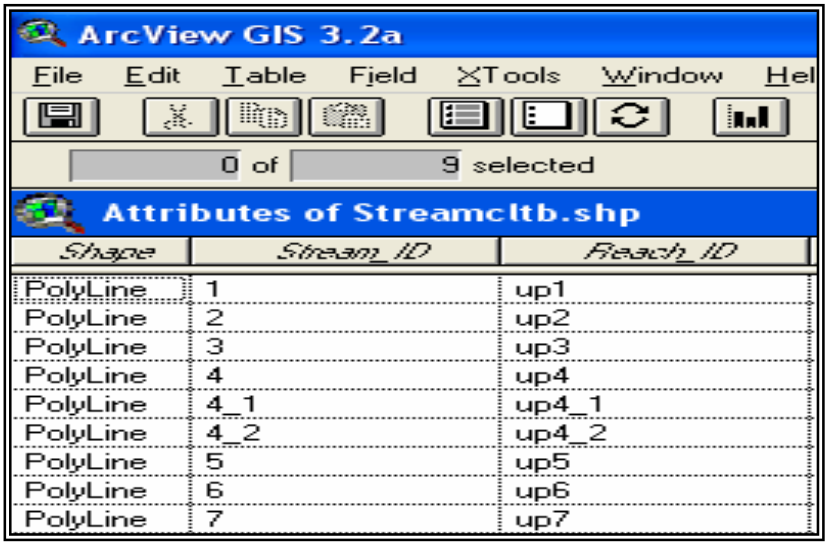

Shape	Stream_ID	Reach_ID
PolyLine	1	up1
PolyLine	2	up2
PolyLine	3	up3
PolyLine	4	up4
PolyLine	4_1	up4_1
PolyLine	4_2	up4_2
PolyLine	5	up5
PolyLine	6	up6
PolyLine	7	up7

Figure 9.3 Table of stream centerline theme for the Bostanli River Basin.

Main Channel Banks

Main channel banks of the Bostanli River are digitized using the IZSU data (Figure 9.4).

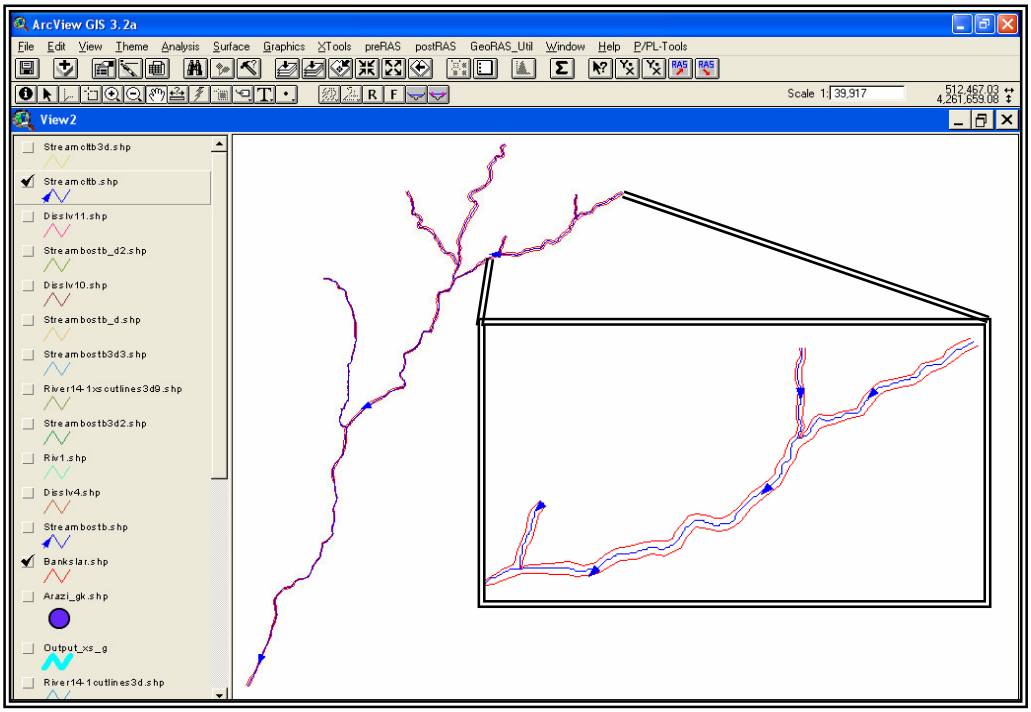

Figure 9.4 Main channel banks theme of Bostanli River Basin.

Flow Path Centerlines

Flow paths are defined for the stream centerline, the left and the right flood plains. Using the *Label flowpaths* tool, the left and right overbank flow paths are drawn in the upstream to downstream direction, and the center flow path is created by just copying the stream centerline theme and renaming it as *flowpath.sh*p (Figure 9.5).

Crosssectional Cutlines

The cross-section cutlines are placed at the points where the river cross sections change and also at all other important sections. The locations of the cross-sections are

drawn approximately at points where the field survey data for the channels exist. This is either to obtain the profile from scratch or to improve some available profile information by further extending the lines. Another point considered for locating the cross-sectional cutlines has been to place them systematically just before and after any existing hydraulic structure and in a systematic way such that they will not cross each other. In the field study, the locations of the existing culverts and bridges were measured by using a GPS (Geographical Positioning System), and their X and Y coordinates were then transferred into the ArcView software system as "Arazi_gk.shp" theme. The purpose here is to check whether all the cross-sectional cutlines are placed accurately before and after the hydraulic structures. The locations of the weirs were obtained from a publication on the weirs on Izmir streams (IZSU, 2004). Furthermore, even though the cross section points in the digital map of IZSU did not cover the entire area, they were used just to get an idea about the positions of cross-sectional cut lines. Figure 9.6 shows the GPS points, the cross-section points, and the cross-sectional cutlines drawn only for a part of the basin, while Figure 9.7 indicates all of the cross-sectional cut lines existing in the basin.

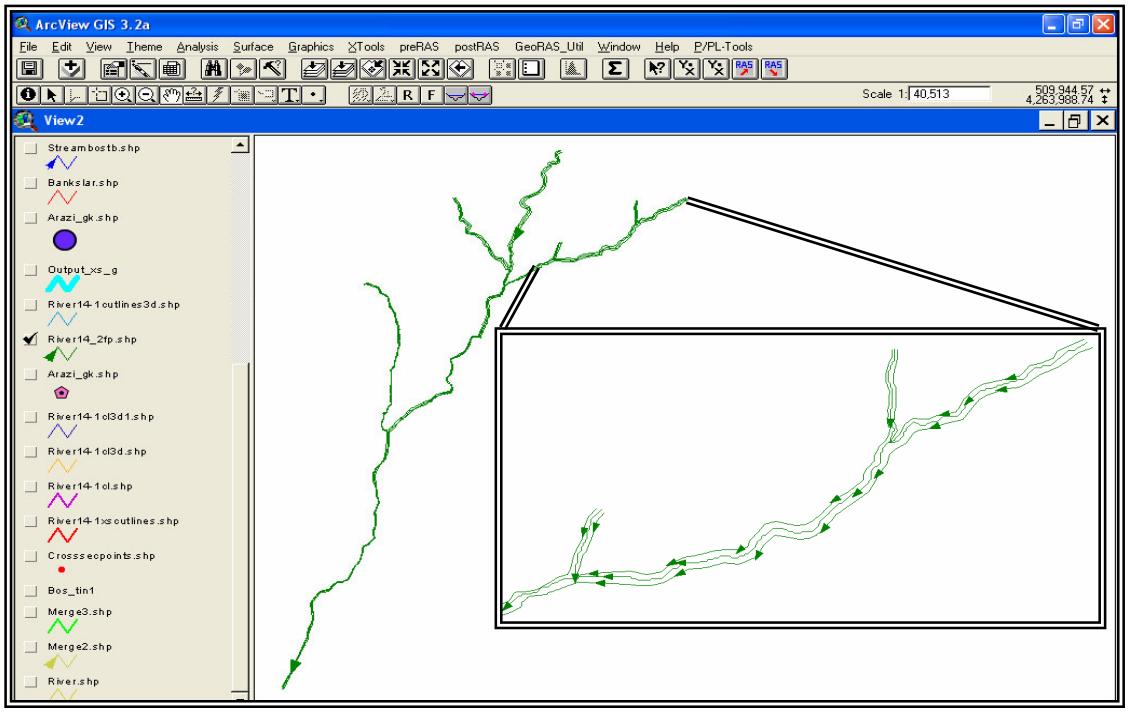

Figure 9.5 Flow paths (left, right and channel) theme of Bostanli River Basin.

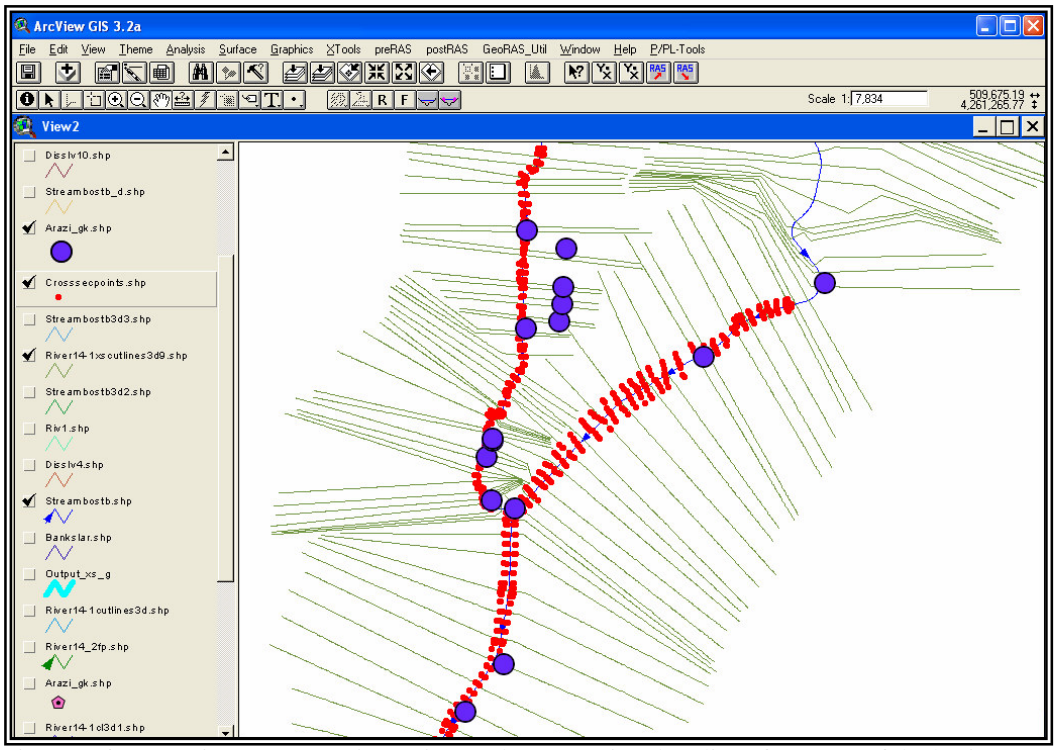

Figure 9.6 GPS points, cross section points and crosssectional cutlines for a part of the basin.

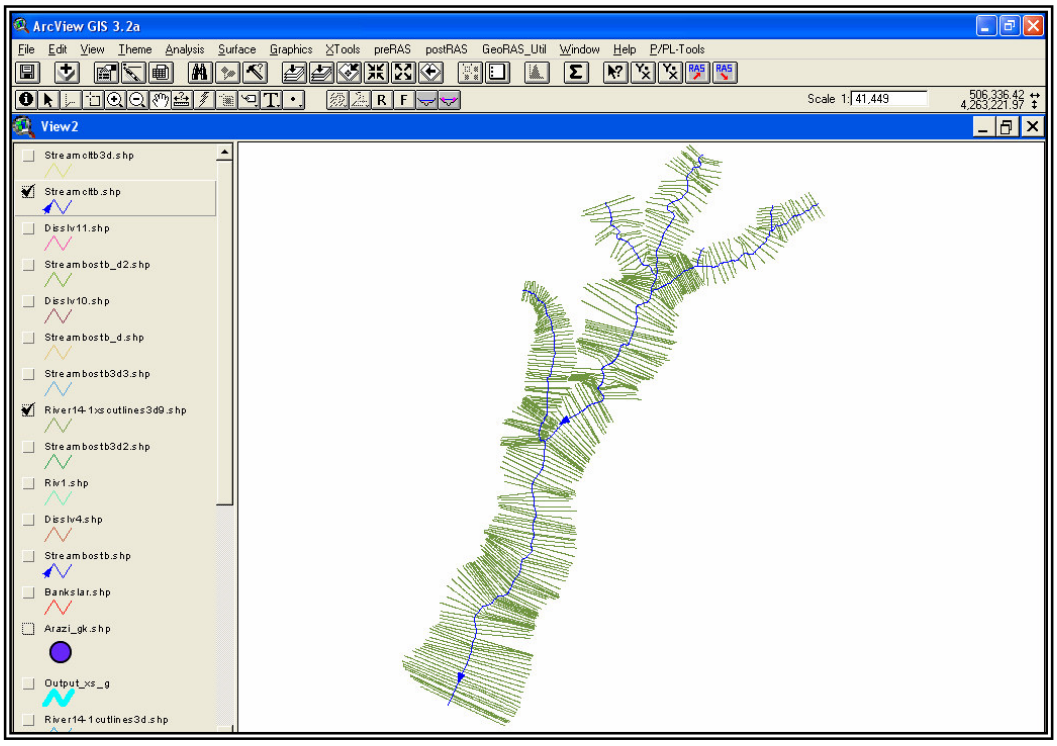

Figure 9.7 Crosssectional cut lines theme on Bostanli River Basin.

Theme Setup

The role of each input theme created is specified in the Theme Setup before performing any computation on the themes (Figure 9.8)

Centerline Completion

- Lengths/Stations

All river lengths are computed along the stream centerline. Fields *from_ST* (downstream endpoint) and *to_ST* (upstream endpoint) are automatically added to the Stream Centerline theme by the program (Figure 9.9).

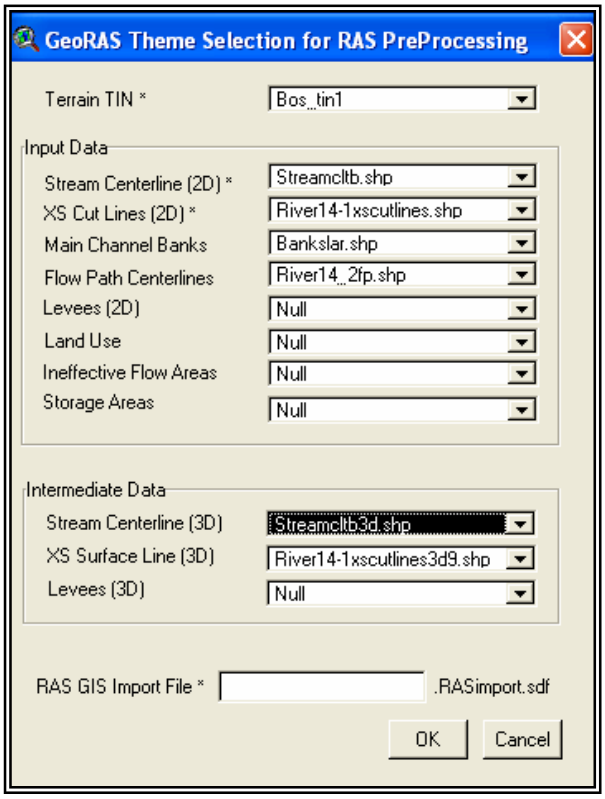

Figure 9.8 Theme Setup for Bostanli River Basin.

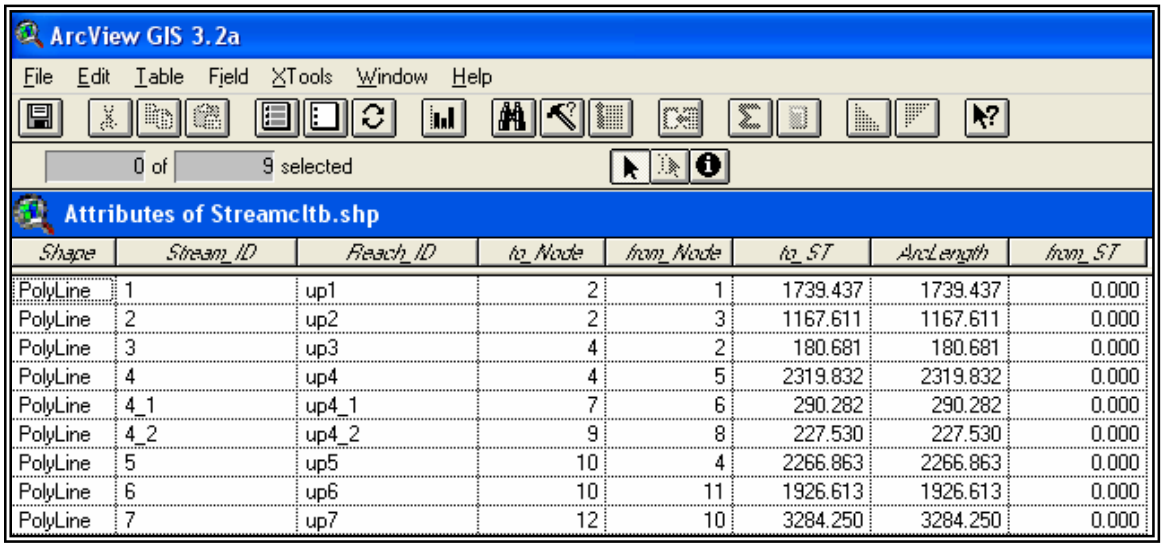

Shape	Stream_ID	Reach_ID	to_Node	from_Node	to_ST	ArcLength	from_ST
PolyLine	1	up1	2	1	1739.437	1739.437	0.000
PolyLine	2	up2	2	3	1167.611	1167.611	0.000
PolyLine	3	up3	4	2	180.681	180.681	0.000
PolyLine	4	up4	4	5	2319.832	2319.832	0.000
PolyLine	4_1	up4_1	7	6	290.282	290.282	0.000
PolyLine	4_2	up4_2	9	8	227.530	227.530	0.000
PolyLine	5	up5	10	4	2266.863	2266.863	0.000
PolyLine	6	up6	10	11	1926.613	1926.613	0.000
PolyLine	7	up7	12	10	3284.250	3284.250	0.000

Figure 9.9 Stream centerline theme derived after the lengths/stations process.

- Centerline Topology

In this process, the centerline topology is developed to derive the connectivity and the orientation of the river network by using the information provided in the stream centerline theme.

- Centerline Z Extract

3D shapefile (also known as 2.5D in common GIS terminology) of the stream centerline (originally in 2D) is created by the *Centerline Z Extract* function. The result of this process is given in Figure 9.10.

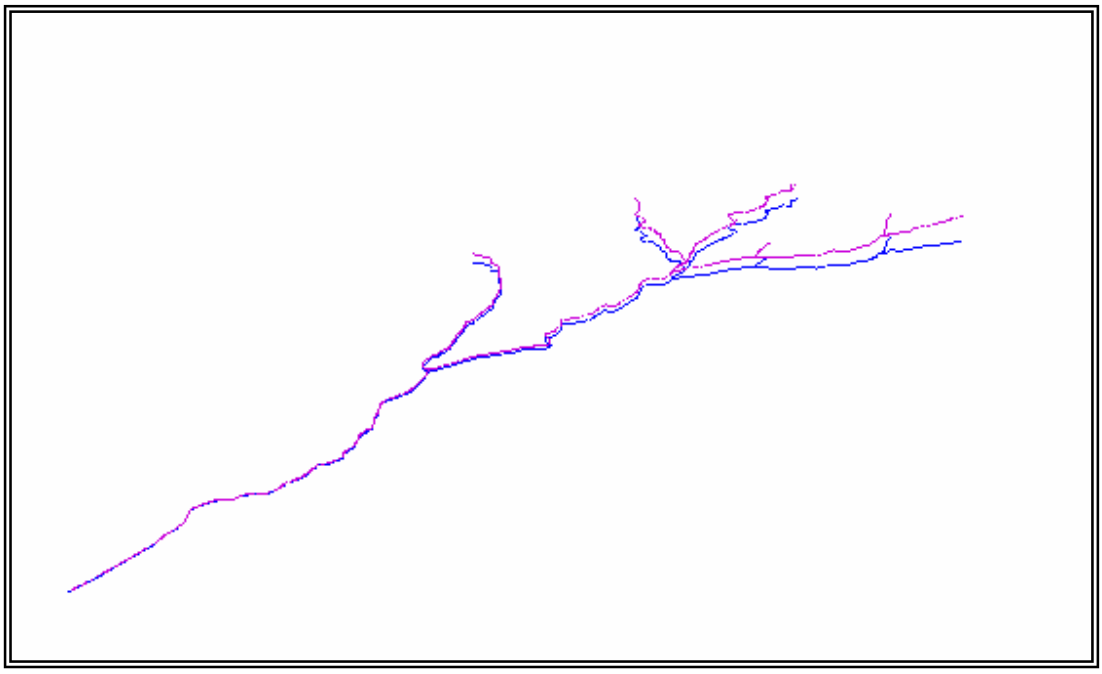

Figure 9.10 3D Shapefile of the stream centerline theme.

XS Attributing

All attributes (including river and reach names, stationing, bank stations, and reach lengths) are added to the *Cross-Section Cut Line* shapefile by using this function.

XS Elevations

Similar to the operation for the centerline, 3D shapefile of the cross-section cut line theme is created from the 2D theme by using the *XS Elevations* function.

9.2.2 Generating the RAS GIS Import File

All the data required to generate the RAS GIS Import File, consisting of the Stream Centerline (2D), XS Cut Lines (2D), Main Channel Banks, Flow Path Centerlines as Input Data; and Stream Centerline (3D), XS Surface Line (3D) as Intermediate Data are

defined here. Among the other required data were the Terrain TIN and the name of the RAS GIS Import file. After completing the full definition for data requirements, the RAS GIS Import File is created by just pressing the OK button in the bottom right corner of the theme selection window (Figure 9.11).

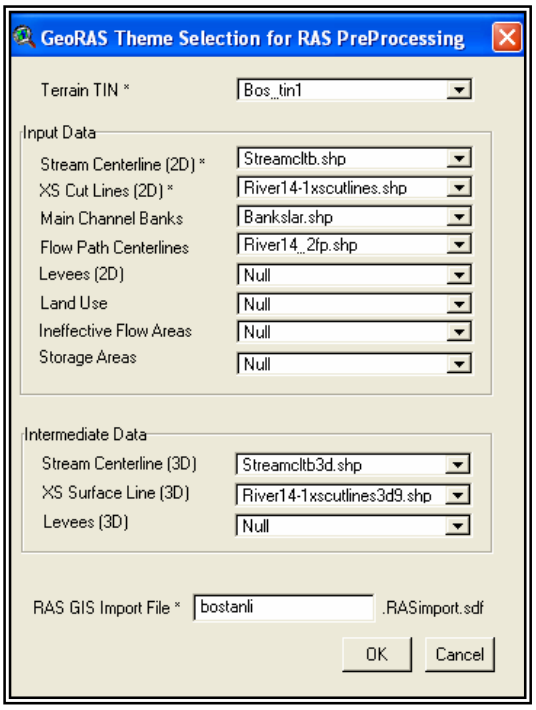

Figure 9.11 RAS-GIS import file generation window.

9.3 HEC-RAS Modeling

9.3.1 Importing Input Files to the HEC-RAS Model

As the HEC-RAS GIS import file has been ready to be introduced into the geometry data editor, the import file, namely Bostanli.sdf, is imported into the HEC-RAS model as geometric data, where the river network and cross-sectional cutlines are shown schematically. Their attribute information, such as the reach names, X, Y and Z values

for the reaches, are entered automatically in this way (Figure 9.12). The resulting geometric model is shown in Figure 9.13.

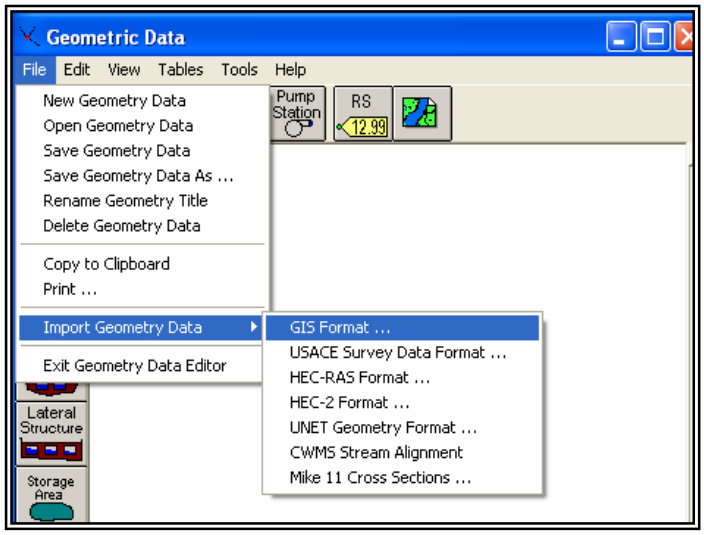

Figure 9.12 Geometric data importing process.

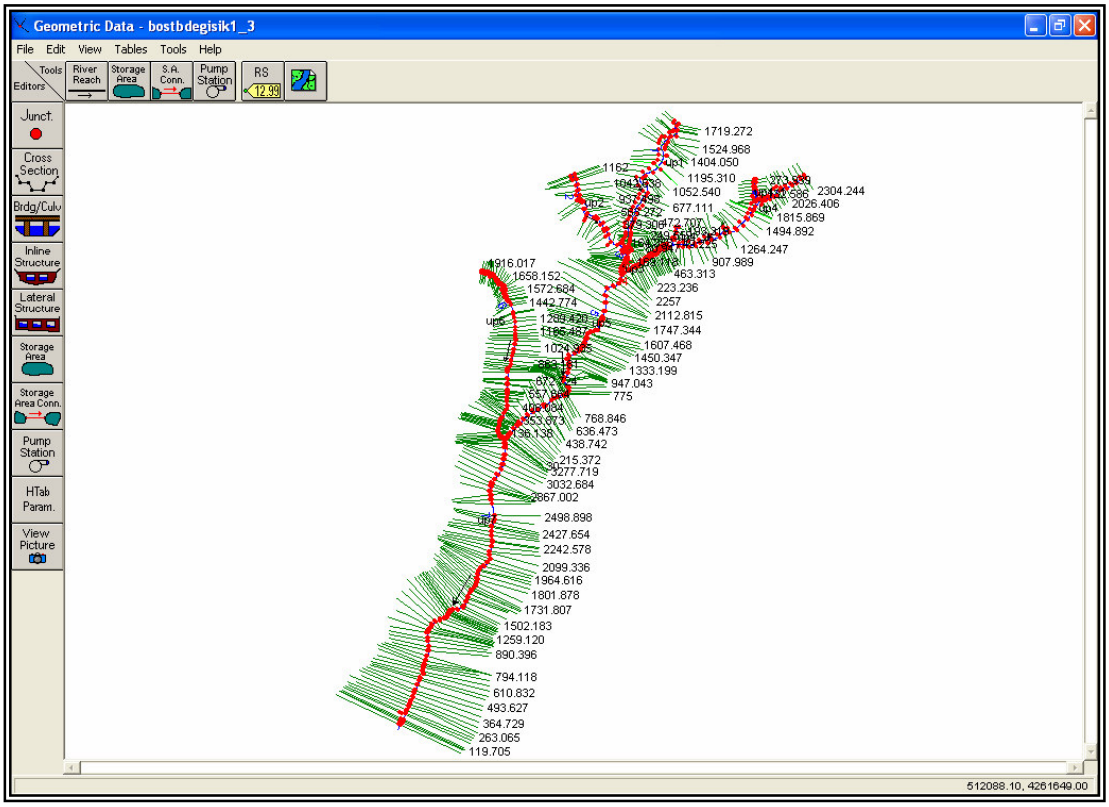

Figure 9.13 Resulting geometric model of Bostanli Basin.

9.3.2 HEC-RAS Model Use

At the hydraulic computation stage, scenarios are created, based on the steady and the unsteady conditions. These scenarios are developed, regarding the existence of the Bostanli Dam, the existence of the weir, and the precipitation values with the return periods of 100 years and 500 years. Observed precipitation records at Guzelyali meteorological station are also considered. Table 9.1 shows the list of scenarios, where some abbreviations for the defined scenarios are also included. In the analysis of the unsteady flow, only one scenario, indicated as A1_U, is examined, where a hypothetical storm with a 100-year return period and the existing weirs are considered by excluding the original dam.

Table 9.1 List of scenarios applied in the study for steady flow analysis.

	With Dam		**Without Dam**	
Steady Flow	**With Weir**	**Without Weir**	**With Weir**	**Without Weir**
100-year return period	A1_S	A3_S	D1_S	D3_S
500-year return period	B1_S	B3_S	E1_S	E3_S
Observed rainfall	C1_S	C3_S	F1_S	F3_S

9.3.2.1 Plan Data

Each scenario is applied in the same project but on different plan data, where the geometry and the flow are defined individually.

9.3.2.2 Geometry Data

In the Bostanli Basin, it is proper to use some available elevation contour data, especially in the overbank areas, to define the terrain beyond the stream channels and to

utilize the original cross-section data only for the channel. Cross section data obtained from the field study are inserted manually into the geometry data derived by the HEC-GeoRAS in order to define the correct geometry (Figure 9.14). After the cross-sections are created, several hydraulic structures, such as culverts, bridges and weirs along the Bostanli River and its branches, are inserted into the HEC-RAS models. Then, their characteristics and some other required information are also entered by using the data collected from the field study (Figures 9.15 and 9.16). Detailed information on these hydraulic structures is provided in Appendix II. 15 culverts, 10 bridges, and 13 weirs are entered into the geometric model. Appropriate Manning's n values both for the channels and the floodplains are also entered to obtain the complete geometry models of the Bostanli River.

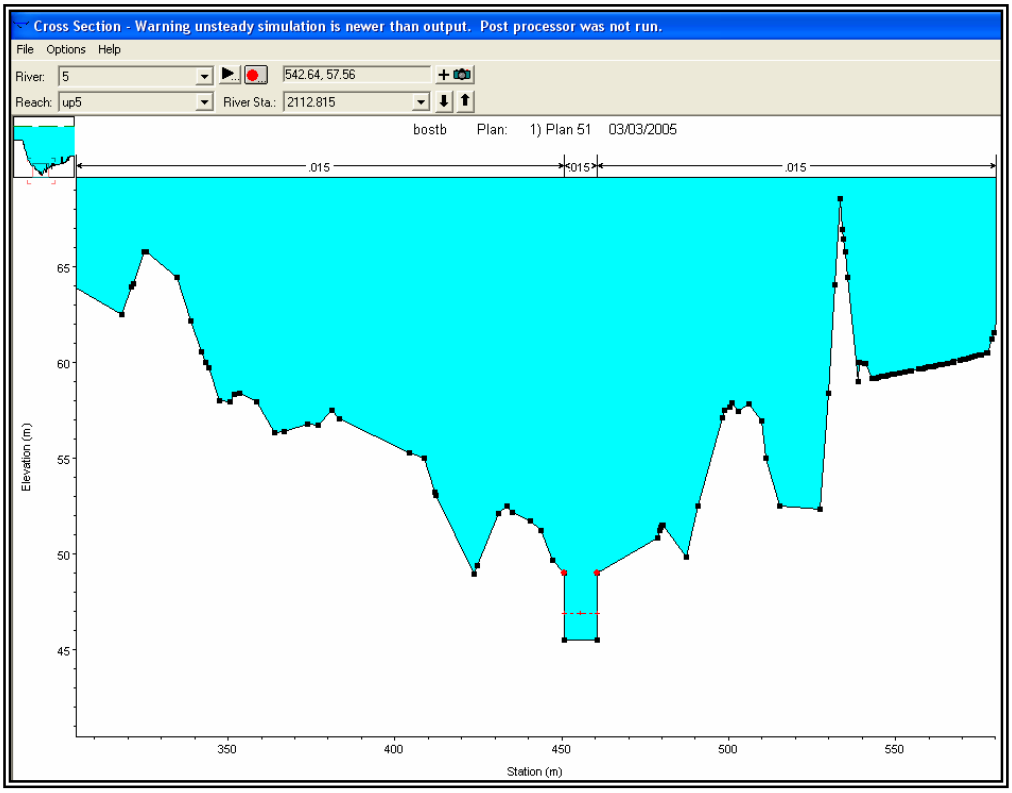

Figure 9.14 Cross-section data inserted into the HEC-GeoRAS geometry data.

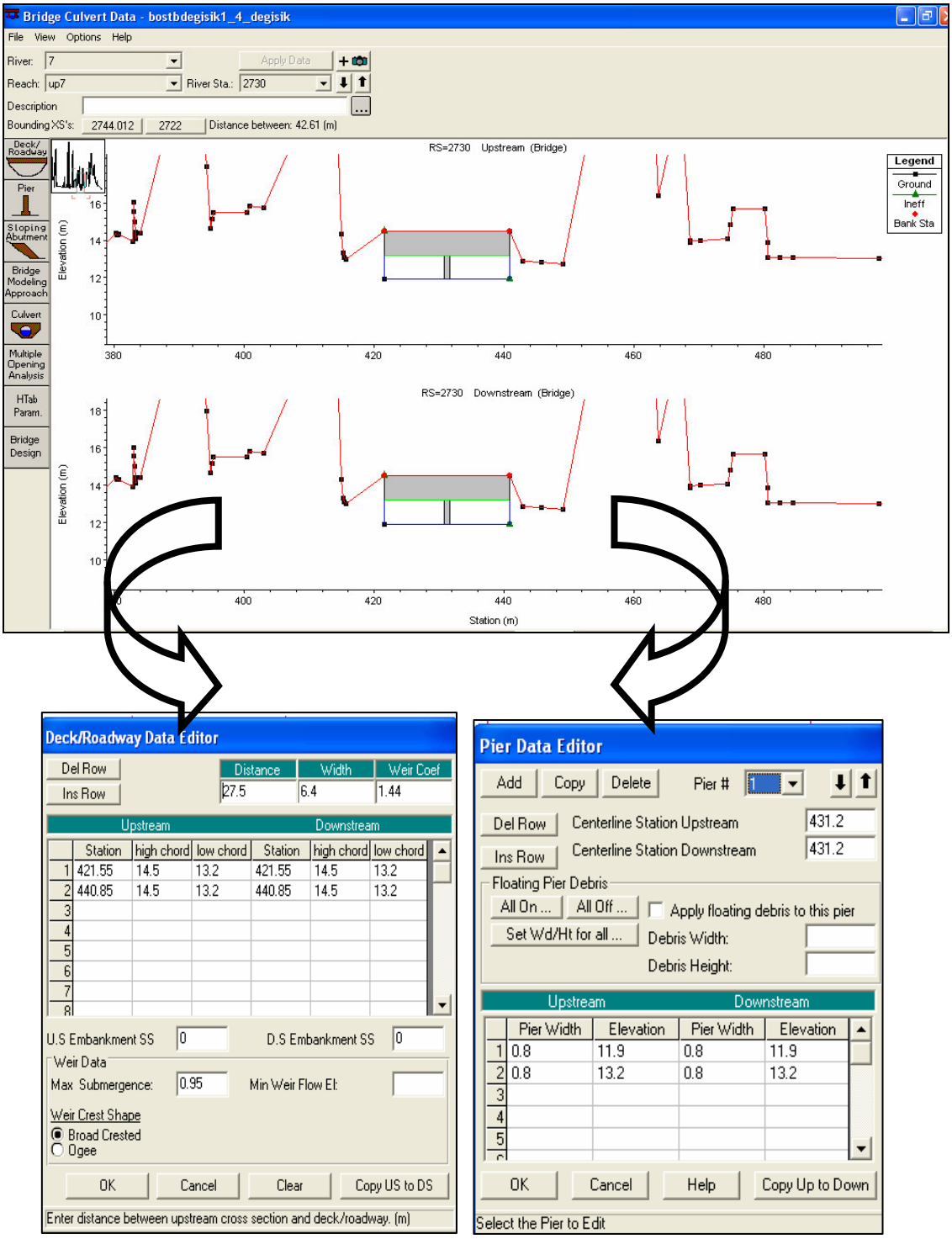

Figure 9.15 Data on the bridge at river station 2730 and its characteristics.

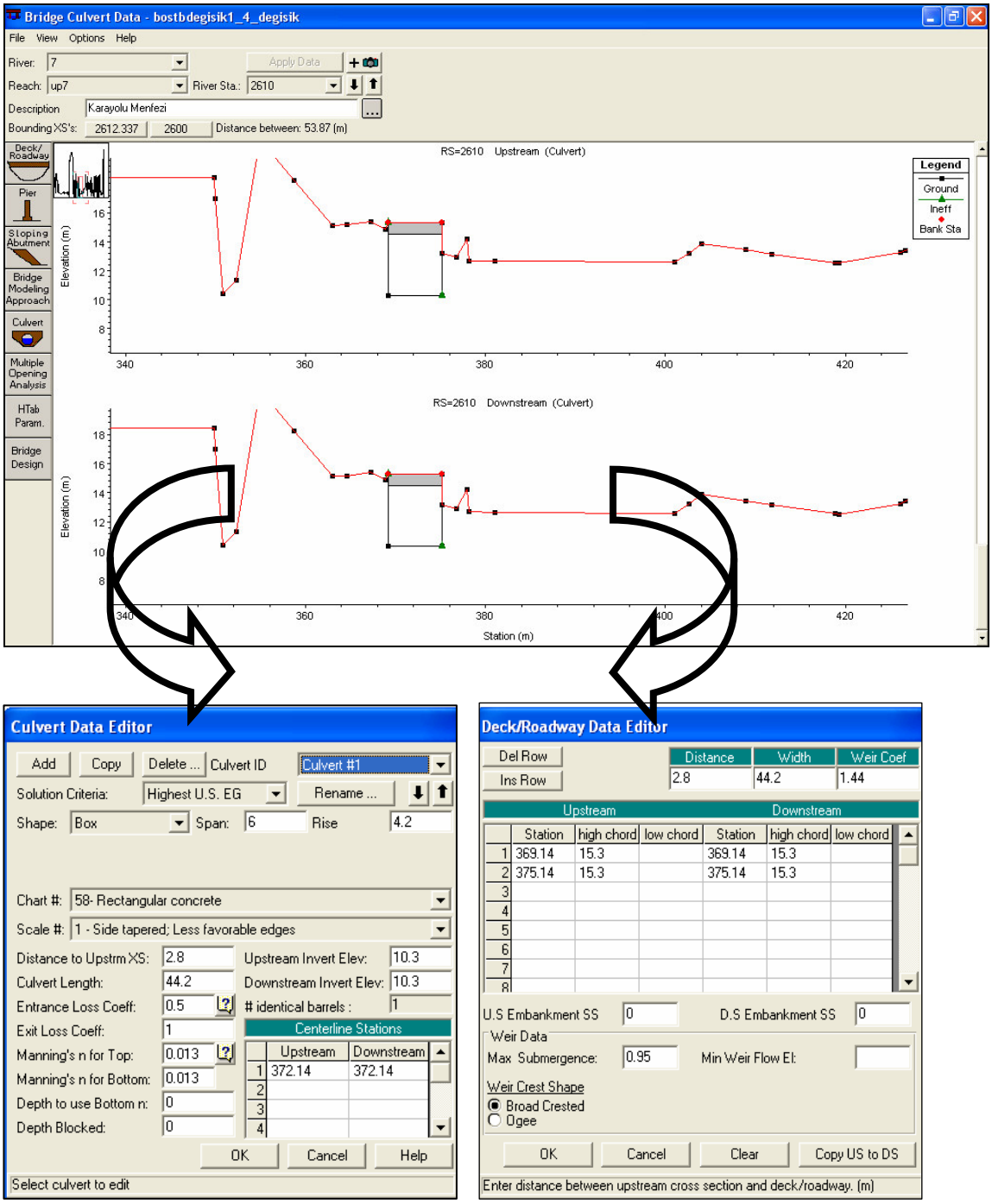

Figure 9.16 Data on the culvert at river station 2610 and its characteristics.

The geometric model presented in Figure 9.13 is used for the steady flow analysis; but the same model can not be applied to the unsteady flow computation. Hence, the

unsteady flow analysis was applied to only one tributary of the Bostanli River. There are many reasons that lead to such a solution:

- The case area is too large and complex to apply any unsteady flow analysis. When some previous examples and applications are carefully examined, it is noticed that the unsteady flow analysis has been utilized as a tool mostly for small sized regions.
- There are many hydraulic structures which can cause the model to be unstable. Although a culvert may have a simple structure, the hydraulics of the culvert may be quite complex. The culvert may or may not flow full, the exit may or may not be submerged, the flow regime may be subcritical or supercritical, and the culvert's capacity may be controlled by either the upstream or the downstream flow conditions (inlet or outlet control). The same culvert may switch from one condition to another as the discharge through the culvert changes. Because of all these conditions, correct modeling of culverts and the interpretation of the output can be a challenge.
- Unsteady flow simulation requires that the computation time interval is small, on the other hand, the number of cross-sections is excessive to reach accurate and reliable solutions. But, such a computation, especially for a complex model, is pretty tedious.

Because of the reasons mentioned above, the geometry models given in Figure 9.17 and Figure 9.18 are developed for the unsteady flow analyses for *up6* and *up3* reaches, respectively. The first one is an example of a complex model which includes weirs, culverts, and bridges, while the other is less complex, where no hydraulic structure exist. First, the geometry file for the steady flow analysis is saved with a different name. Then, by using the capabilities of the HEC-RAS model, the reaches, except *up6*, are deleted from the model, and the model is saved again so that the new geometry model including *up6* is formed. Later, the same procedure and the geometry model are applied for *up3*.

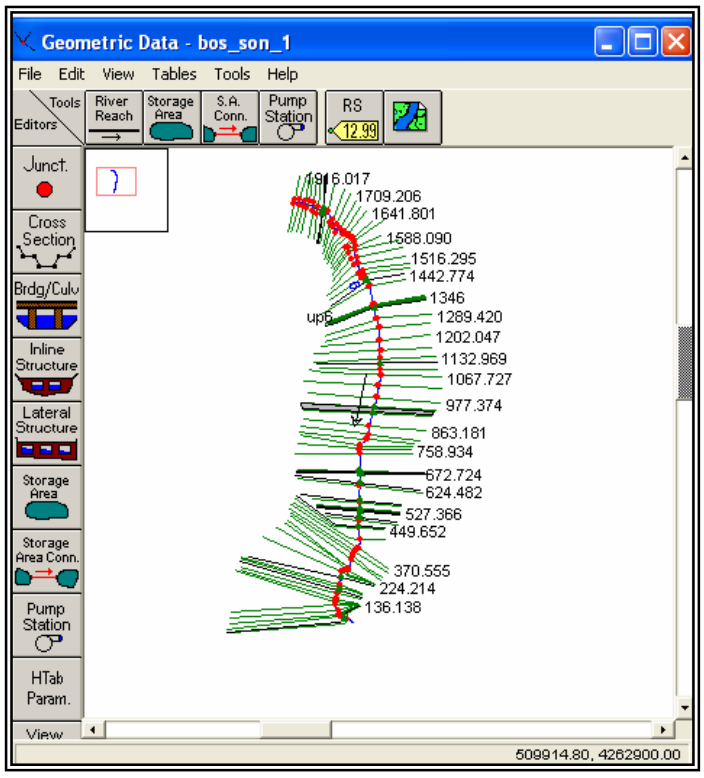

Figure 9.17 The geometry file of up6 for the unsteady flow analysis

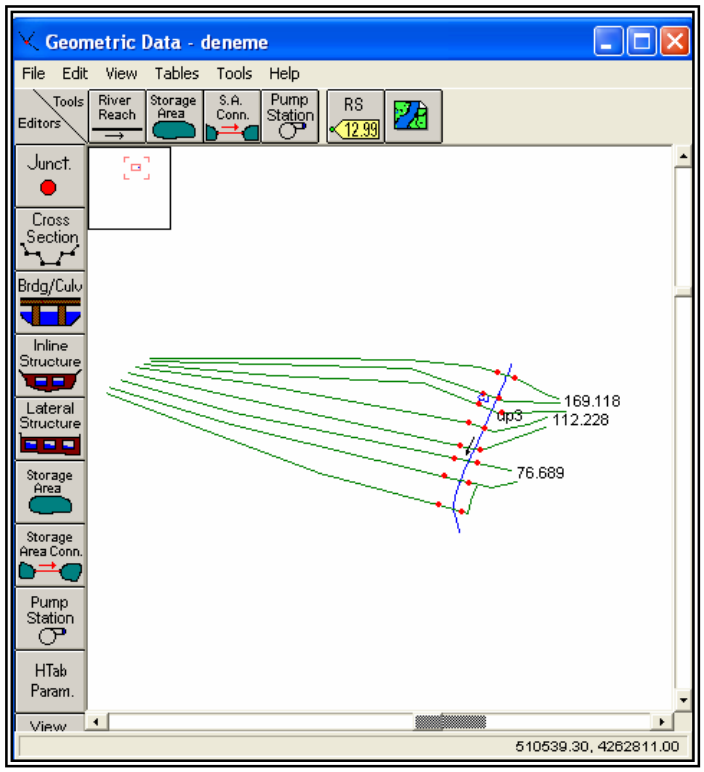

Figure 9.18 The geometry file up3 for the unsteady flow analysis.

Since there are lots of iterations between the cross sections, the model requires more cross sections on the reach to arrive at reliable results. In order to have additional cross sections, *XS interpolation* option under the *Tools* menu of the *Geometric Data Editor* is used. The editor has served two alternatives: first being the XS interpolation *within a reach,* and the second being the XS interpolation *between 2 XS's.* By selecting the option of *within a reach* and fixing the length between the cross-sections to 1 meter (the length of this space depends on the modeler), new cross sections presented in Figures 9.18 and 9.19 are developed.

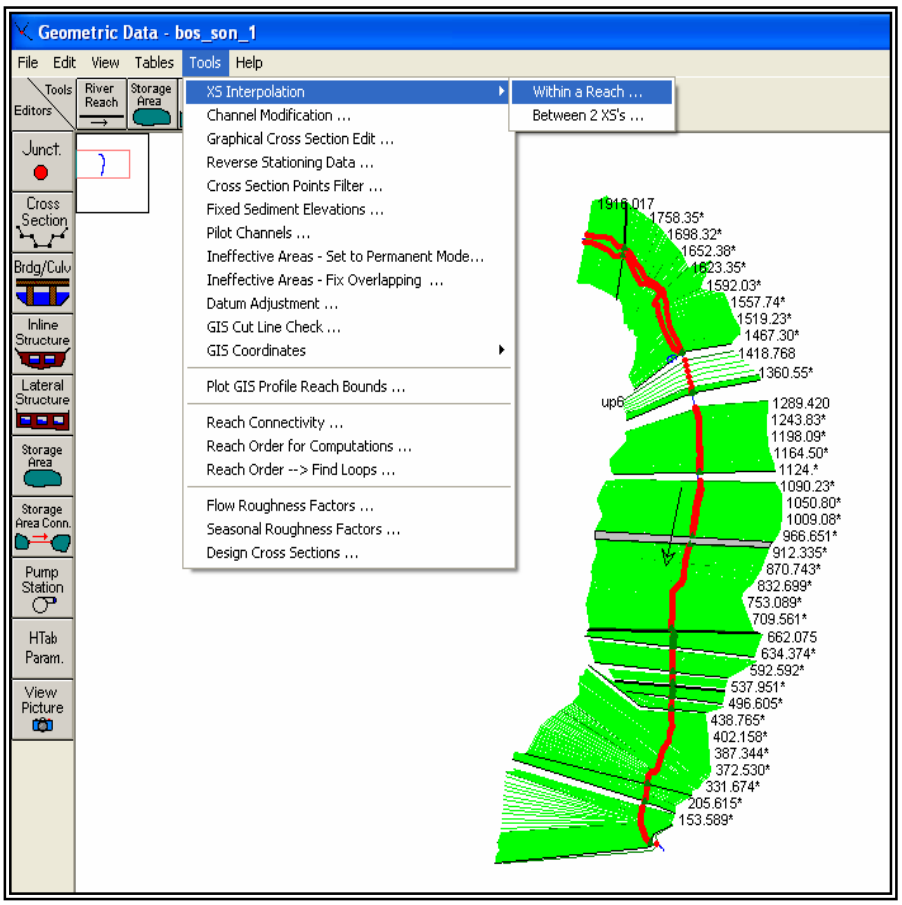

Figure 9.18 New cross sections for up6.

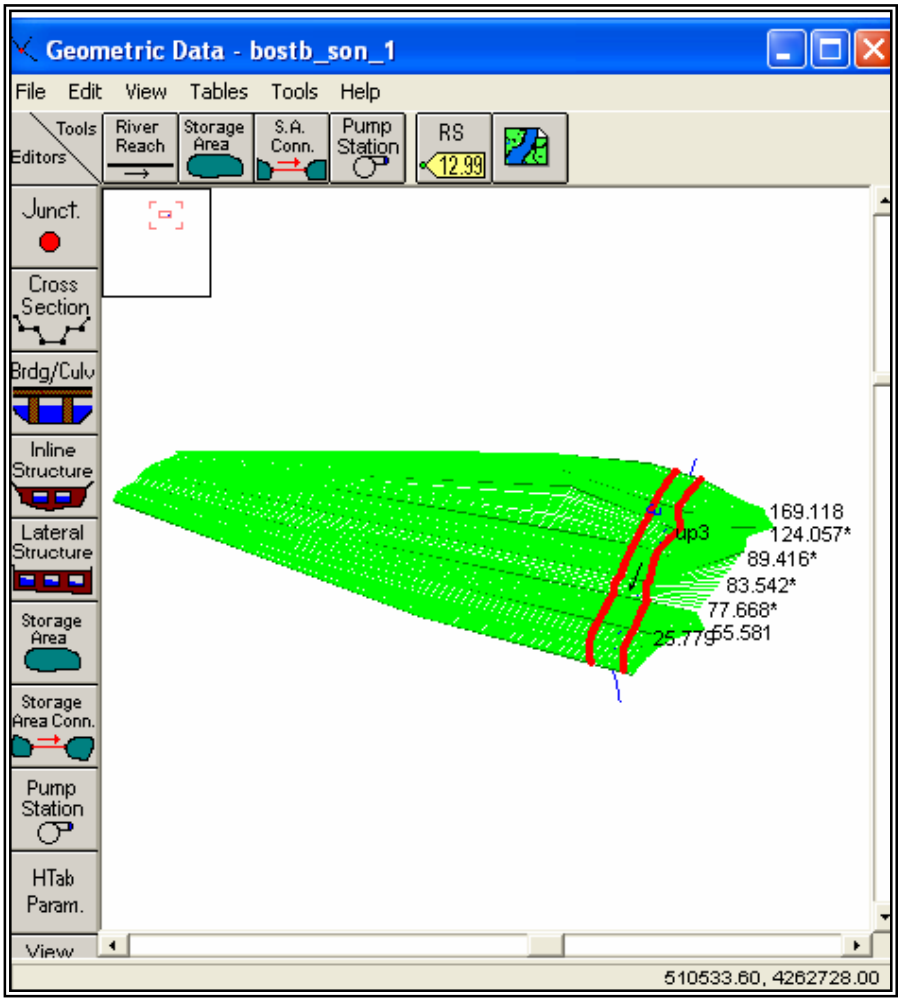

Figure 9.19 New cross sections for up3.

9.3.2.3 Flow Data

Flow rates for the steady and unsteady conditions are computed in the HEC-HMS model. In the steady flow analysis, only the flood peaks at specified sections are entered manually for all scenarios. Figure 9.20 shows the steady flow data used in the scenario A1_S.

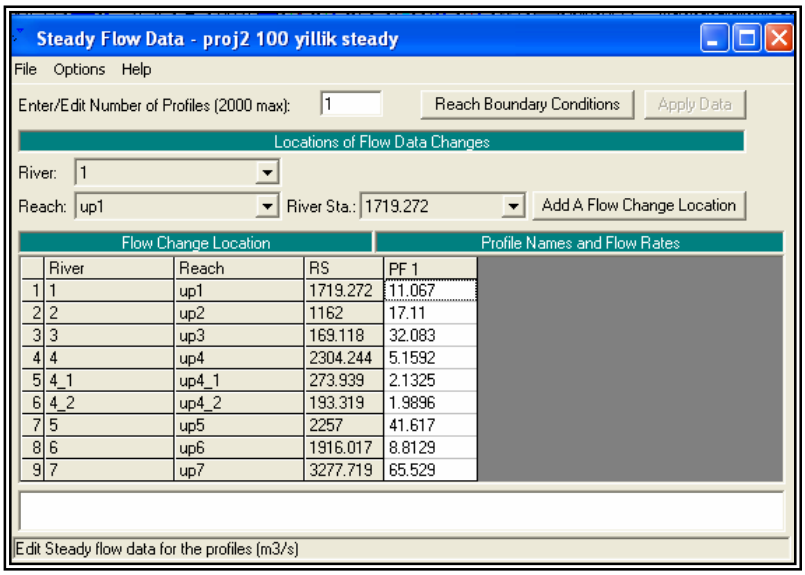

Figure 9.20 Flow data used in the scenario A1_S for steady flow analysis.

To prepare the unsteady flow data, the flow values used as a boundary condition in the unsteady analysis are imported directly from the HEC-HMS runs for each scenario. For the initial condition, the option of *enter initial flow distribution* is selected as an initial flow distribution method. After the first simulation, this method is changed with the *use a restart file* method to use this file in every iteration and to approach the reliable results. Boundary conditions are given in Figure 9.21, and Figure 9.22 shows how to import the flow values into the boundary condition table of A1_U for up6.

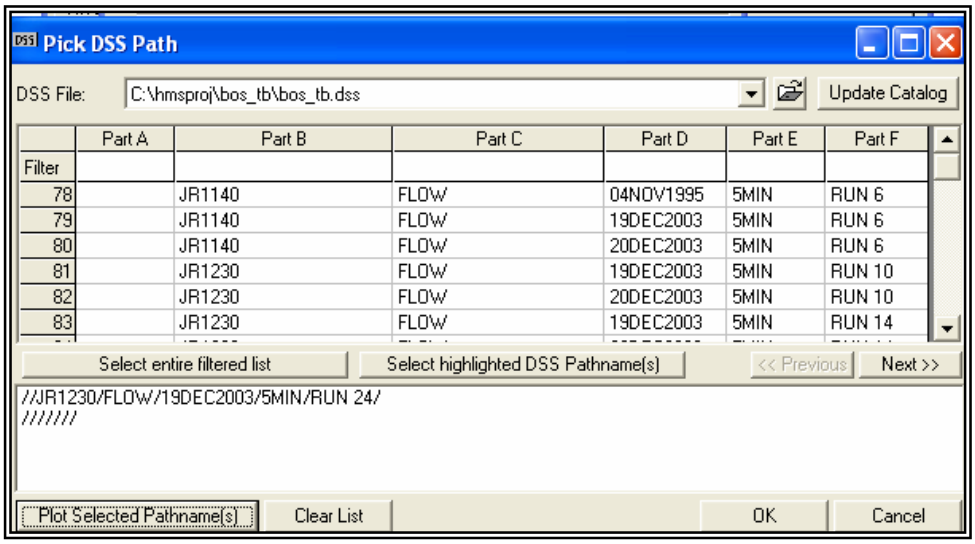

Figure 9.21 Importing flow values from HEC-HMS.

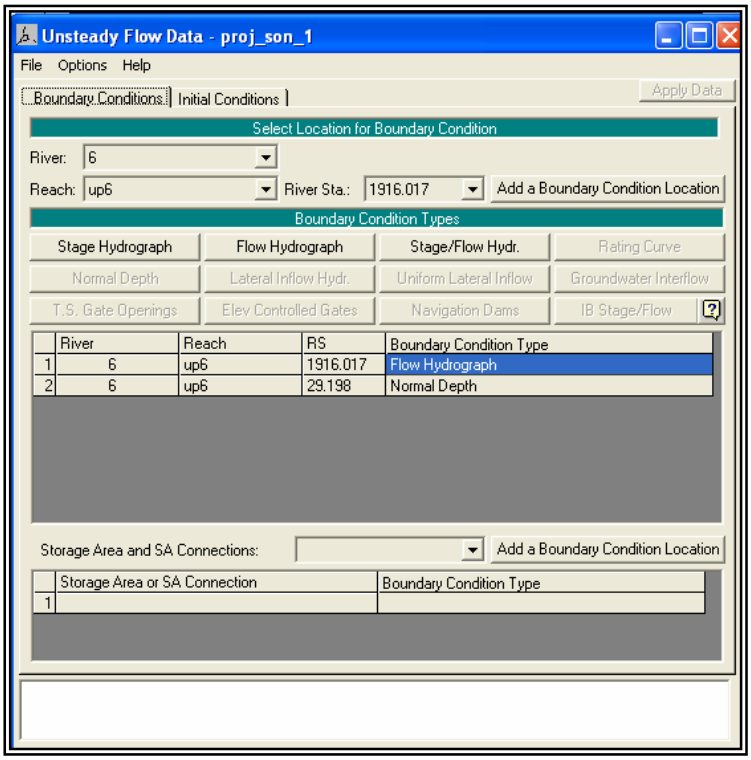

Figure 9.22 Flow values used in the scenario A1_U for unsteady flow analysis for up6.

After all inputs for steady and unsteady flow analyses are entered, the HEC-RAS program is run under previously defined scenarios. Steady and unsteady flow computation windows are not the same with regard to their required data. Some additional information, including computational time step, simulation date, and calculation options, is needed in the unsteady computation in contrast to the steady flow analysis. As examples for both computations, computation windows for A1_S and A1_U scenarios both for up6 are given in Figures 9.23 and 9.24, respectively.

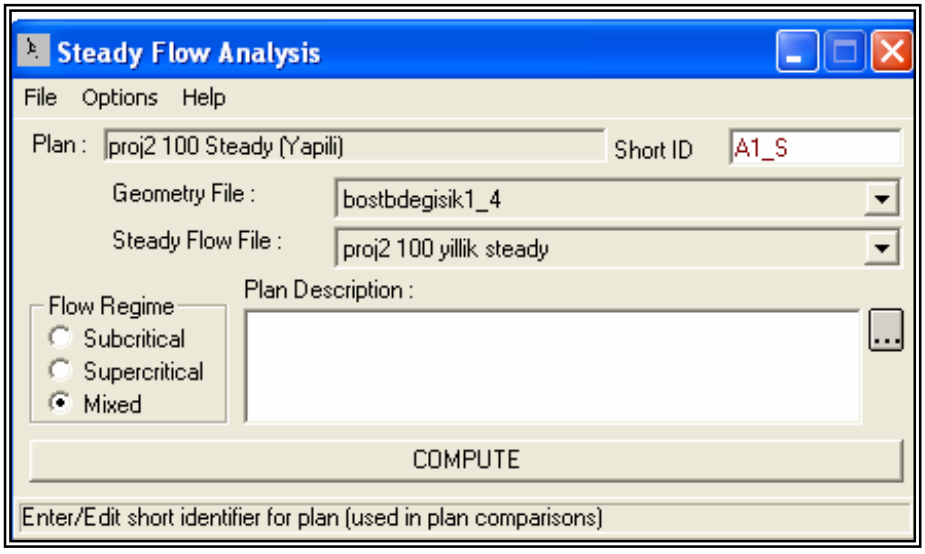

Figure 9.23 Computation window of steady flow analysis for scenario A1_S.

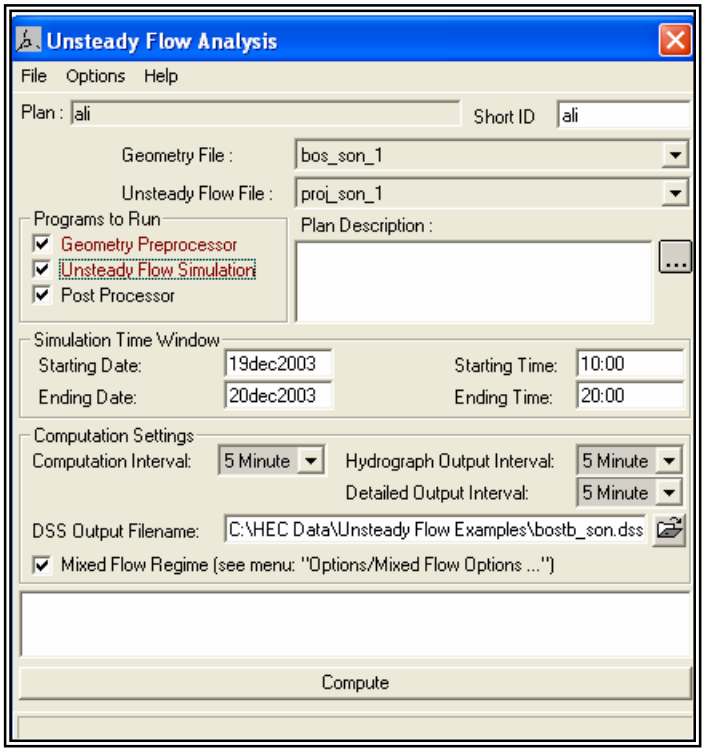

Figure 9.24 Computation window of unsteady flow analysis for scenario A1_U for up6.

9.3.3 Model Results

The HEC-RAS model results are obtained by using the post processing option in the HEC-RAS model. This process generally takes more time if the number of the cross sections and the hydraulic structures in the case area is high.

9.3.3.1 Steady Flow Analysis Results

As the HEC-RAS model has the capability of presenting the outputs in a variety of ways, water surface, critical elevation and energy grade elevation lines versus station graphics at the river station 12.293 next to the last culvert at the outlet are provided for two groups of scenarios (the first for A1_S, A3_S, B1_S, B3_S, C1_S and C3_S and the other for D1_S, D3_S, E1_S, E3_S, F1_S and F3_S) in Figures 9.25 and 9.26.

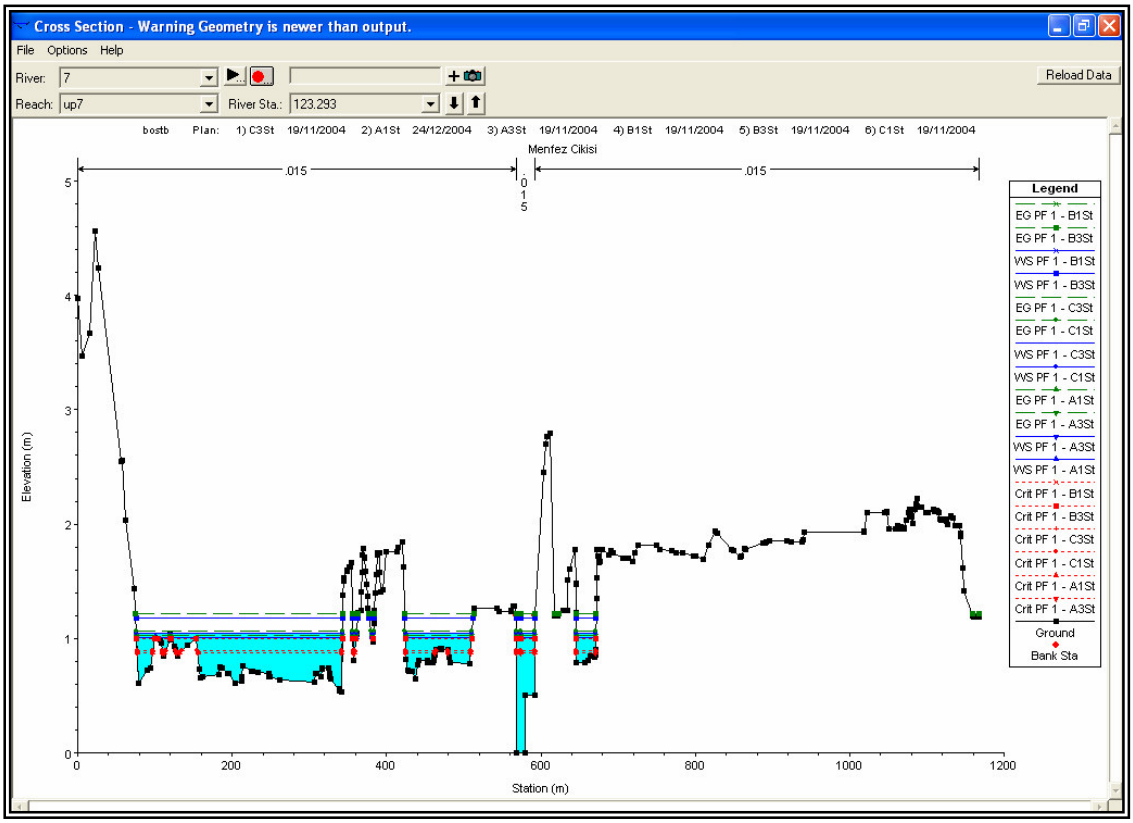

Figure 9.25 Water surface, critical elevation and energy grade elevation lines versus station for scenarios A1_S, A3_S, B1_S, B3_S, C1_S and C3_S.

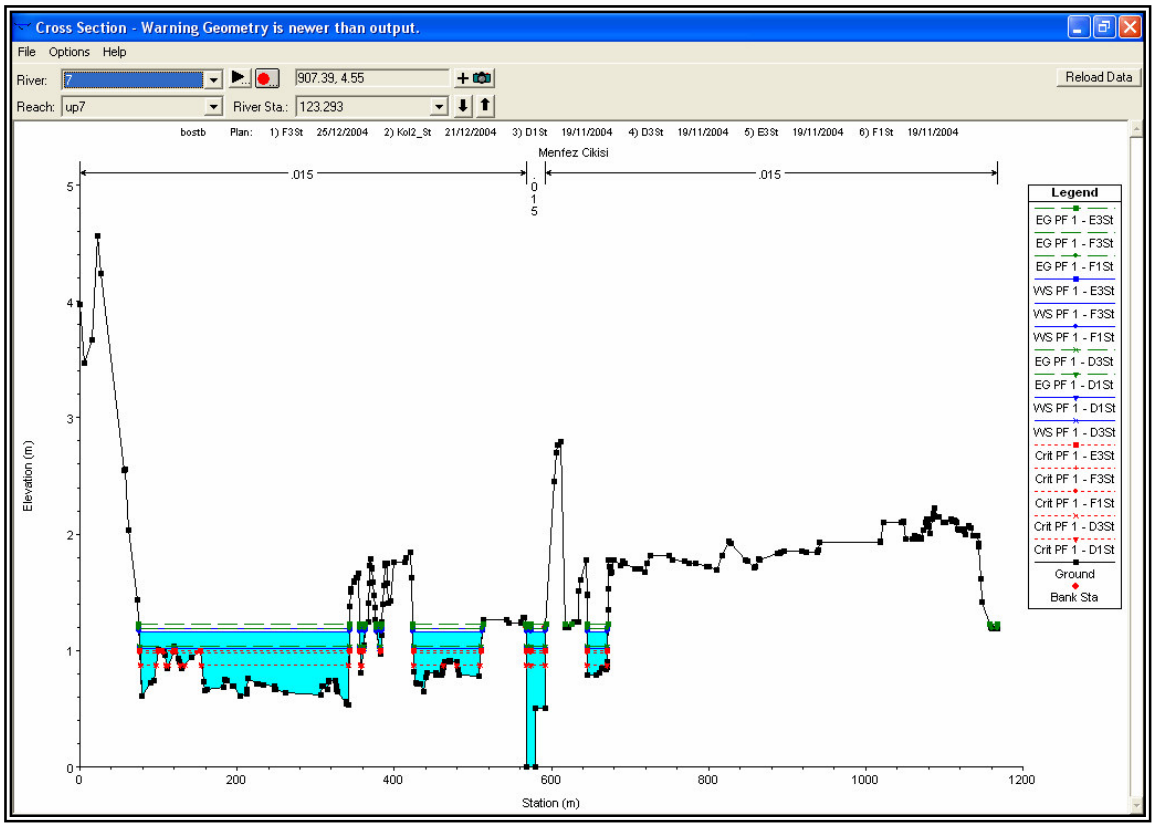

Figure 9.26 Water surface, critical elevation and energy grade elevation lines versus station for scenarios D1_S, D3_S, E1_S, E3_S, F1_S and F3_S.

9.3.3.2 Unsteady Flow Analysis Results

The results of the unsteady analysis given in Figures 9.27 and 9.28 show the computed water levels on December 19 at 10:00, December 20 at 03:15, and December 20 at 20:00, as well as the maximum level at the river station 40, which carries one of the culverts, and the same at the river station 1892.41 which is at the upstream part of reach *up6*.

In addition, Figure 9.29 shows the computed water levels for up3 at the first river station, 169.118, on the dates and the times given above.

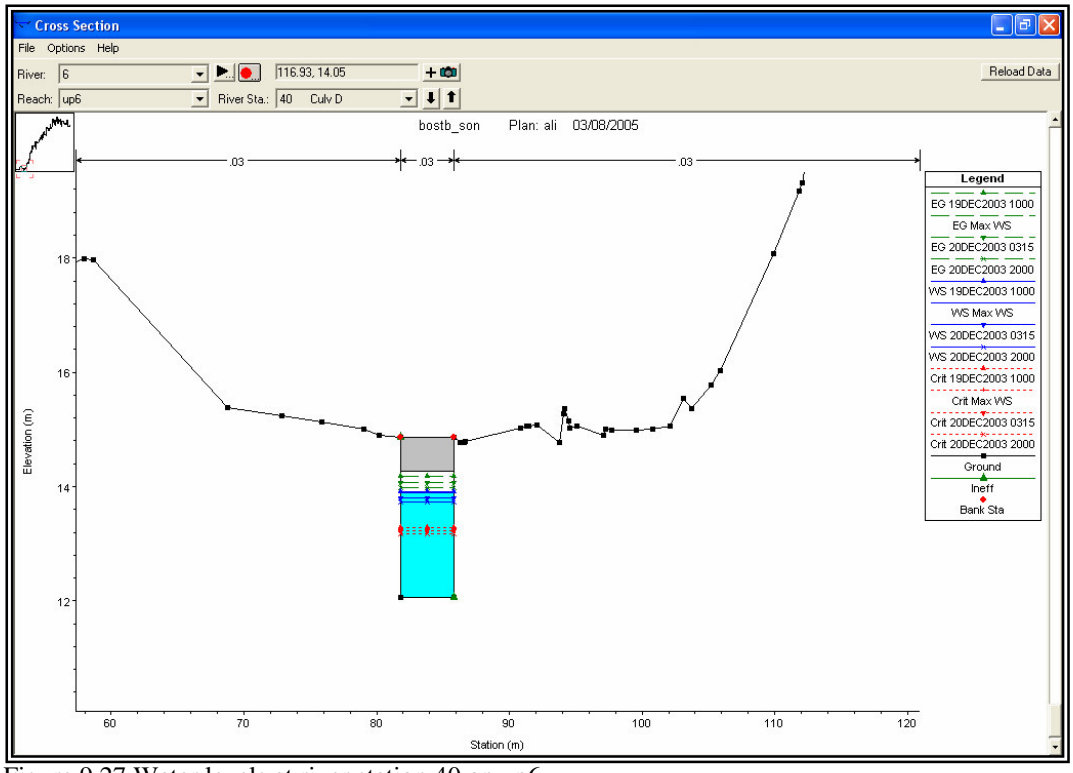

Figure 9.27 Water levels at river station 40 on up6.

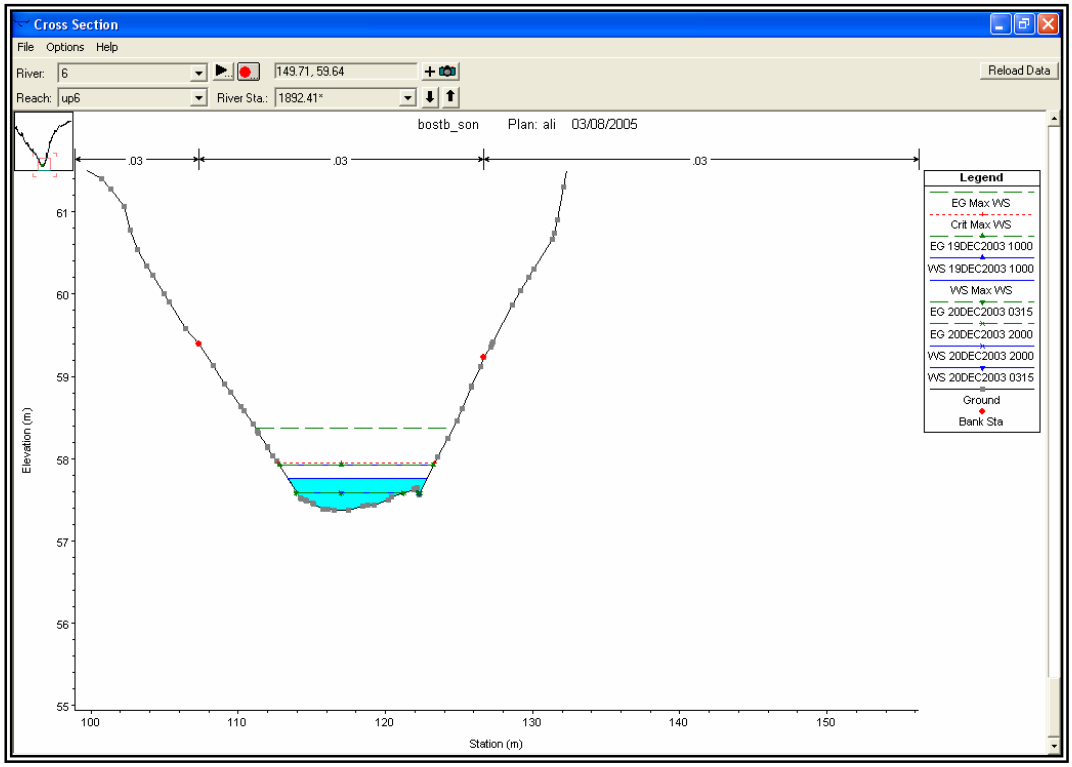

Figure 9.28 Water levels at river station 1892.41 on up6.

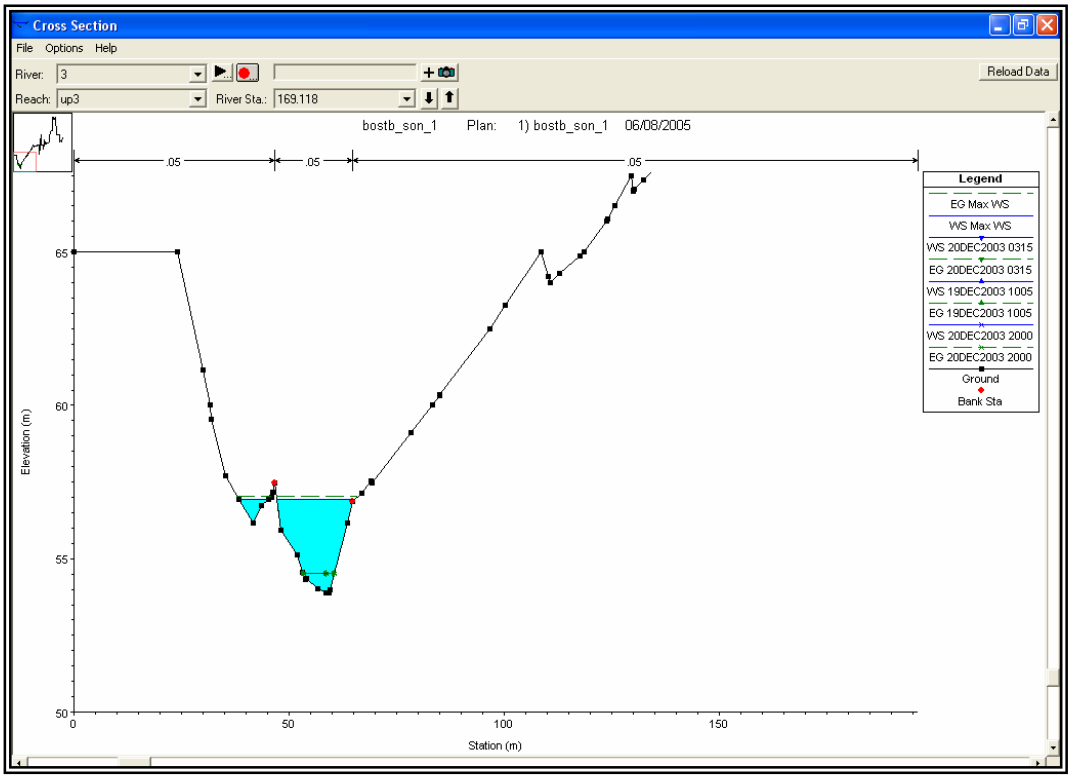

Figure 9.29 Water levels at river station 169.118 on up3.

CHAPTER TEN
RESULTS

This chapter discusses the overall results of the research on the application of the floodplain delineation process. Since there are no hydrologic gaging stations in the Bostanli Basin, the flow model could not be calibrated properly; the accuracy of the model could not be validated, either. Without validation of the model, the study results can only be evaluated qualitatively to assess the efficiency of flood modeling technologies as used and developed in this study.

10.1 Delineation of Floodplain Areas

After performing the steady and unsteady flow computations as described in the previous chapter, the HEC-RAS model results were visualized under different conditions and scenarios by using the visualization feature of the HEC-GeoRAS. The postRAS menu in the HEC-GeoRAS extension is user-friendly and capable of processing multiple water surface profiles simultaneously, allowing the user to observe and compare the effects of different storm return periods on the surrounding terrain at one time. Thus, the water surface TIN and the floodplain delineation themes were created properly to evaluate the results of the research.

Floodplain visualization was provided first by creating the export file from the results of the HEC-RAS model in a process performed by the HEC-RAS model itself. The difference between the export files of both steady and unsteady analyses is in the character of the defined flow. While the flow values change with respect to time in the unsteady analysis and the water surface profiles are computed separately for each time step, there is only one water surface profile for the steady flow analysis. In addition, the available velocity distribution and geometry related information may also be included in the export file. Figure 10.1 shows the export file development window utilized in the study for the scenario A1_U and for the reach *up6*.

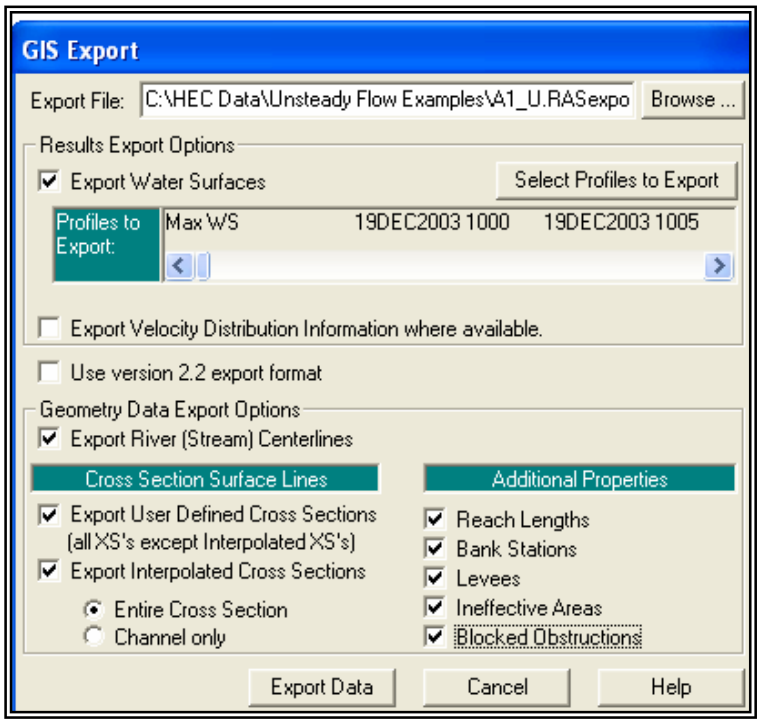

Figure 10.1 Development of the export file.

Second, the postprocessing procedure which mainly helps to display the floodplain areas was carried out by using the HEC-GeoRAS. Chapter 6 gives the detailed information about this process. By selecting and entering the required information, "Theme Setup" was performed as indicated in Figure 10.2.

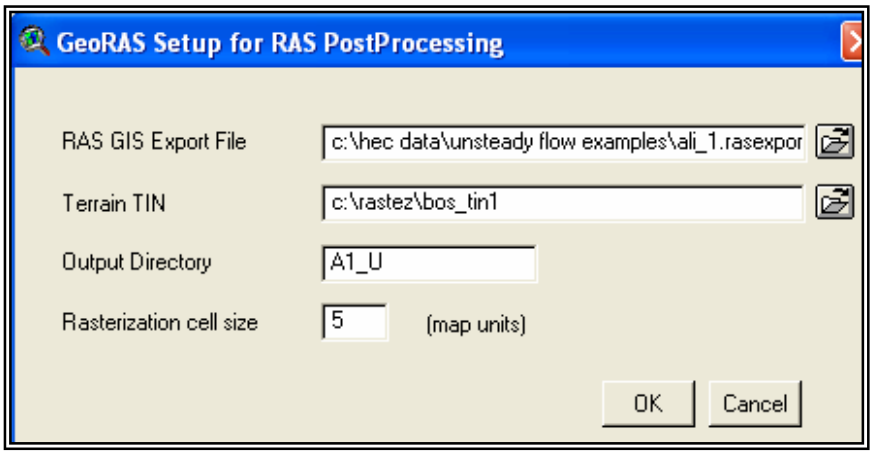

Figure 10.2 Performing Theme Setup.

Next, a new window which is automatically named by the “output directory” in the setup process is created in the ArcView software, and then the GIS export file was read by the system to convey the required themes for floodplain generation into this new view (Figure 10.3).

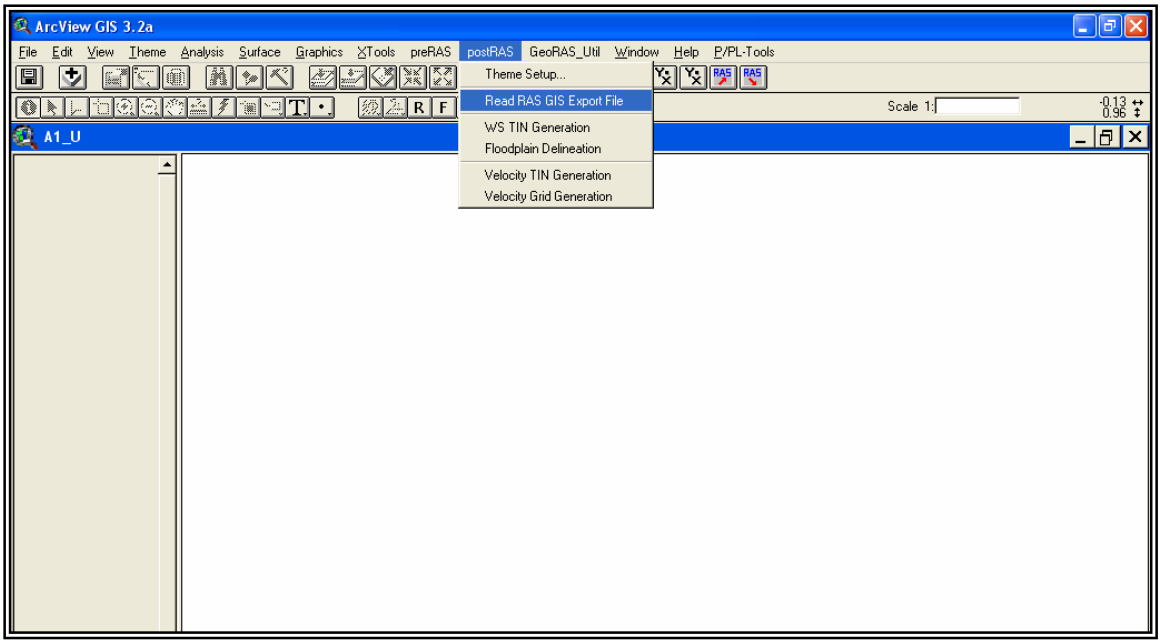

Figure 10.3 Reading RAS GIS export file.

Following the generation of the water surface TIN, floodplains are delineated in a process that is applied to all scenarios. In order to make the results more meaningful, the buildings in the area are also displayed as an individual theme over the floodplain areas to call more attention to areas under risk. For this purpose, buildings, which were originally in the polygon format, are picked from the digital map and saved as “evler_poly” theme to be visualized over the floodplain areas.

10.2 Steady Flow Model Results

Figures 10.4 to 10.15 indicate the floodplain areas obtained from each scenario.

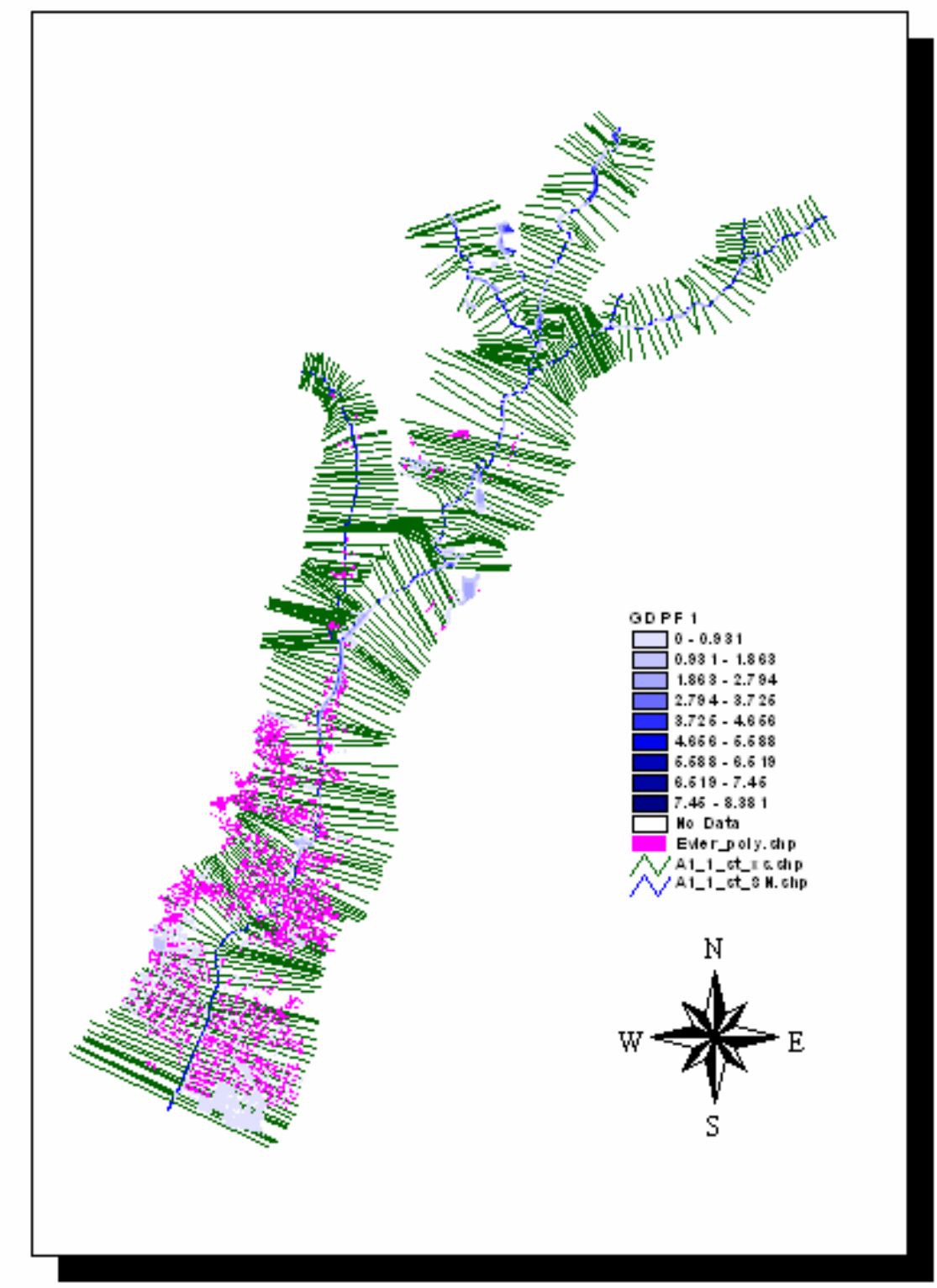

Figure 10.4 Floodplain areas for scenario A1_S.

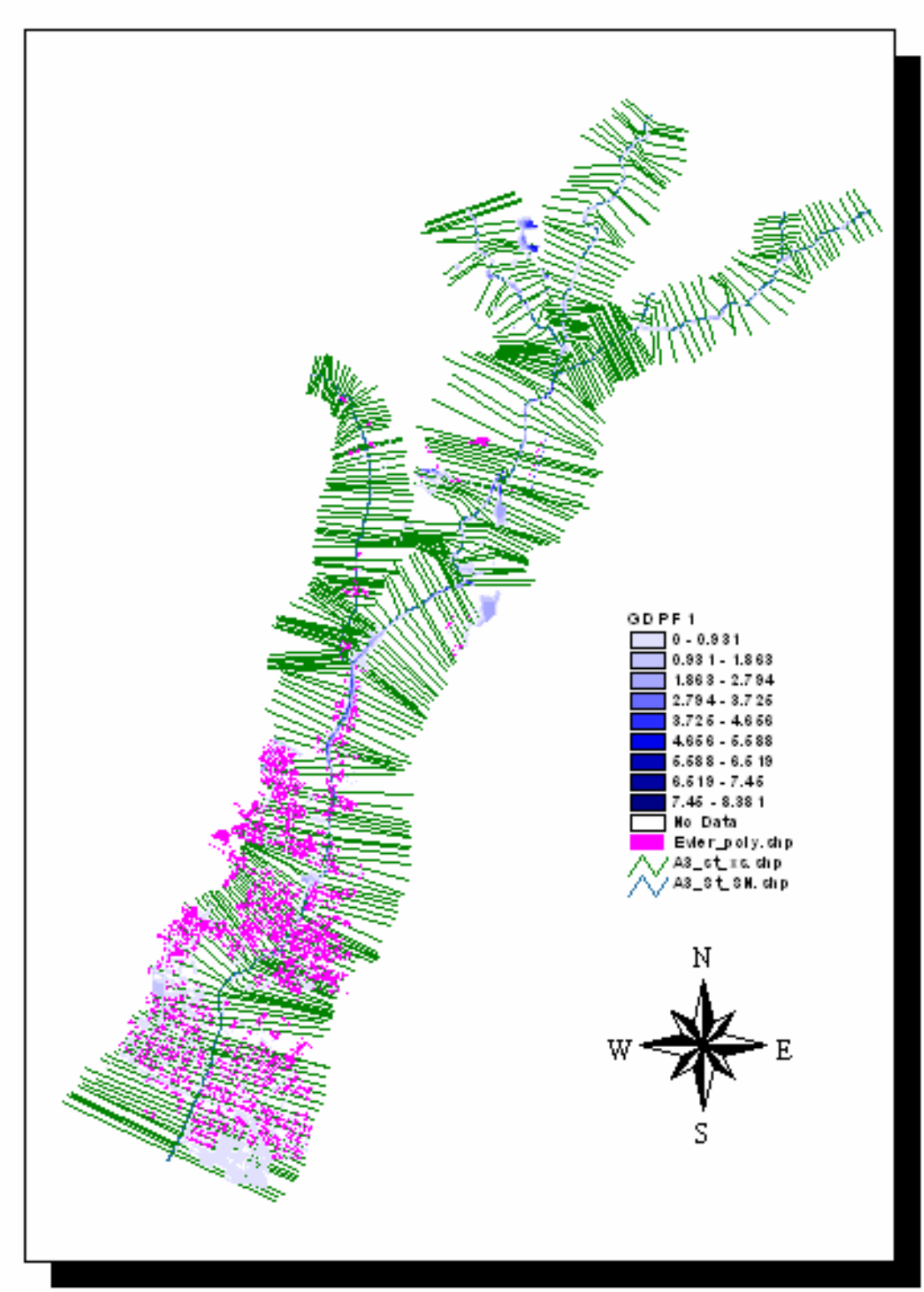

Figure 10.5 Floodplain areas for scenario A3_S.

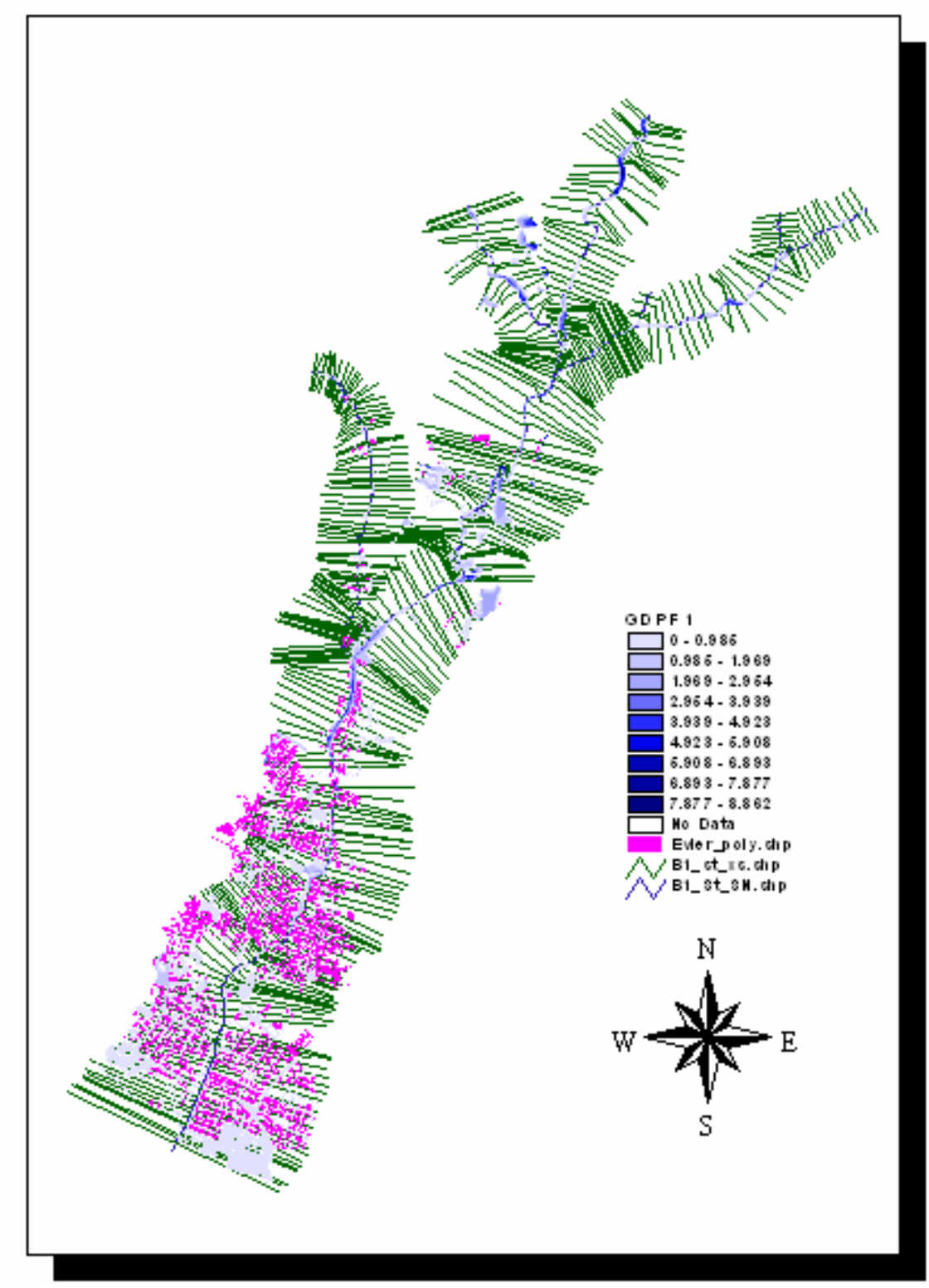

Figure 10.6 Floodplain areas for scenario B1_S.

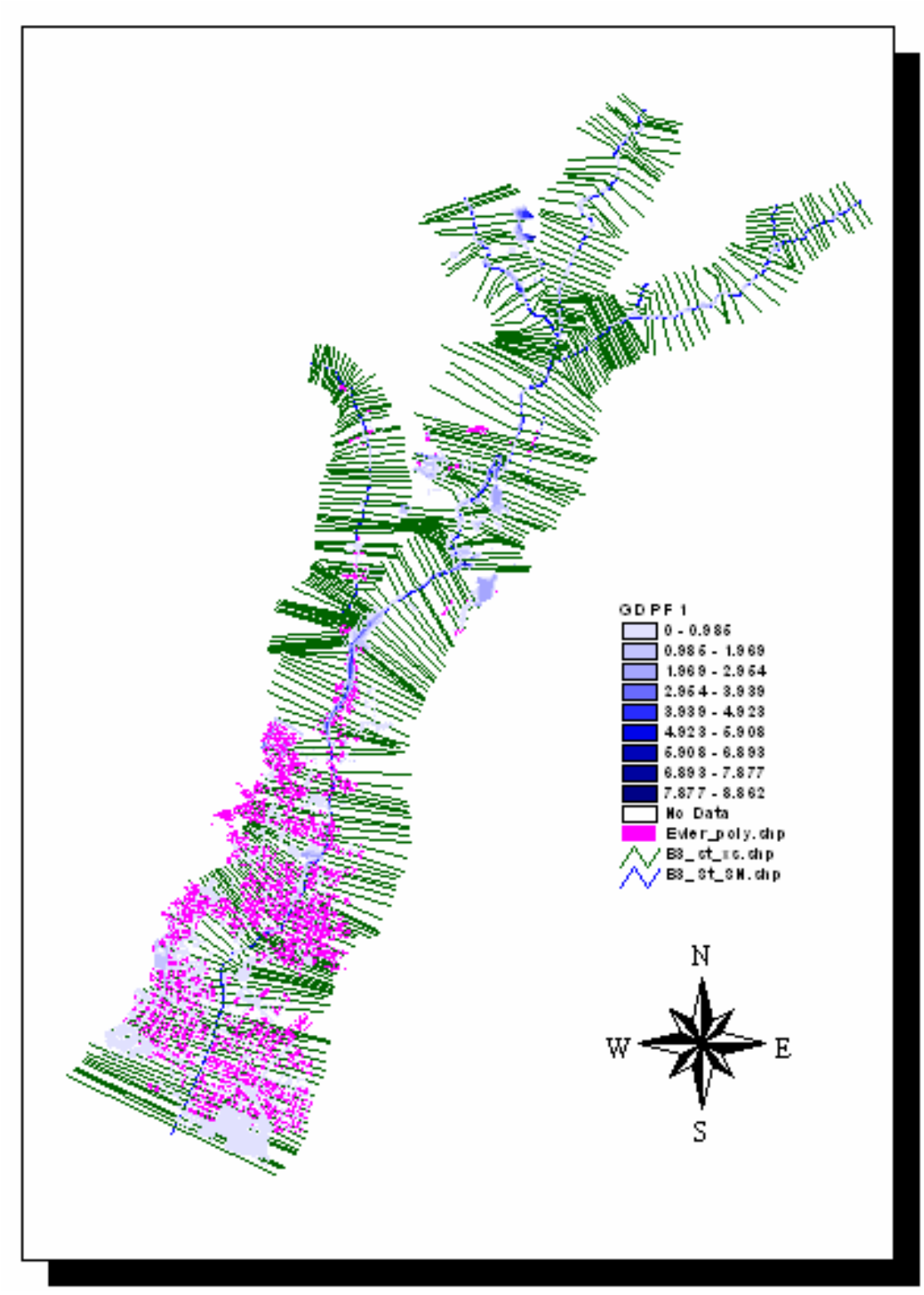

Figure 10.7 Floodplain areas for scenario B3_S.

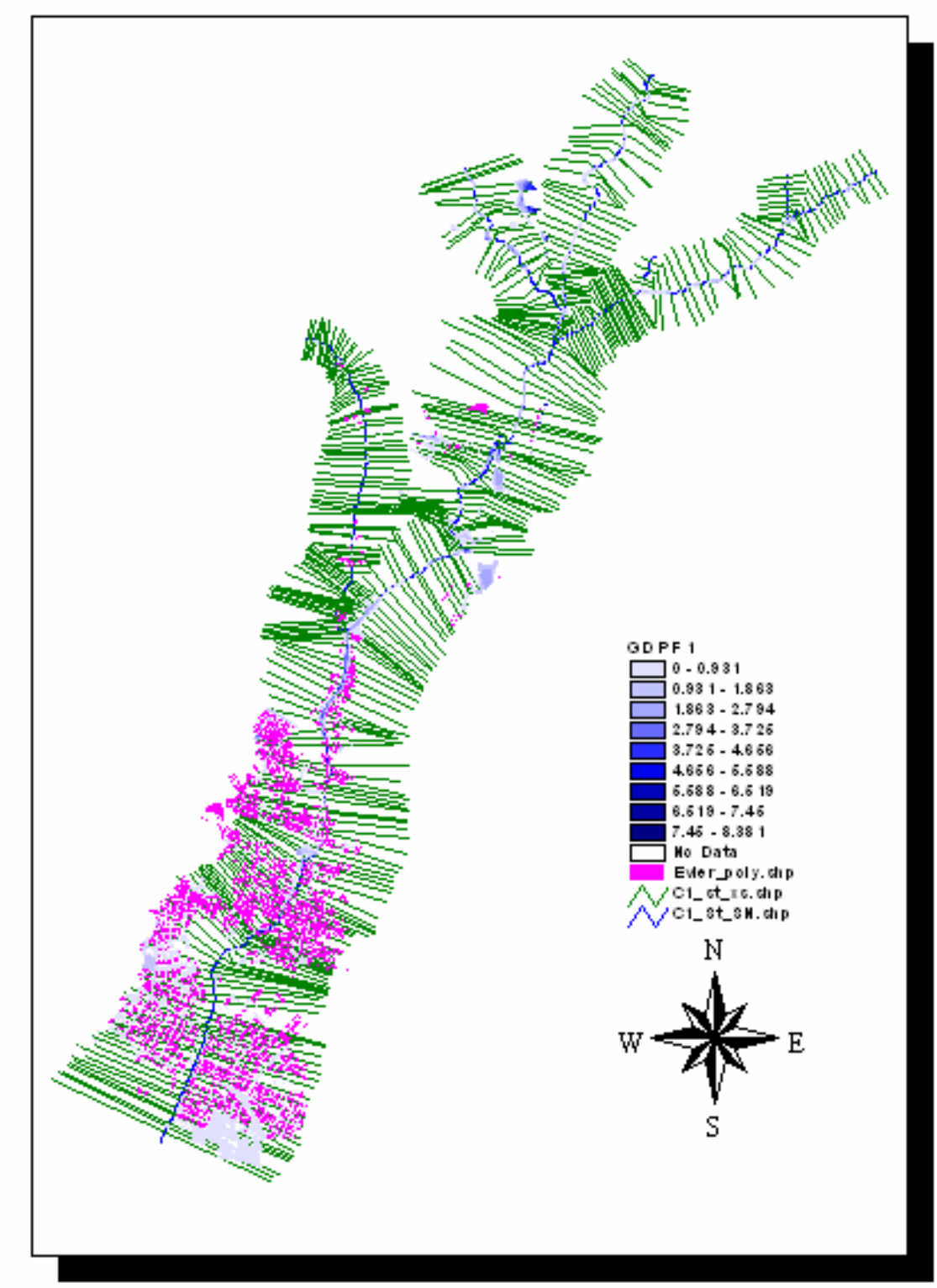

Figure 10.8 Floodplain areas for scenario C1_S.

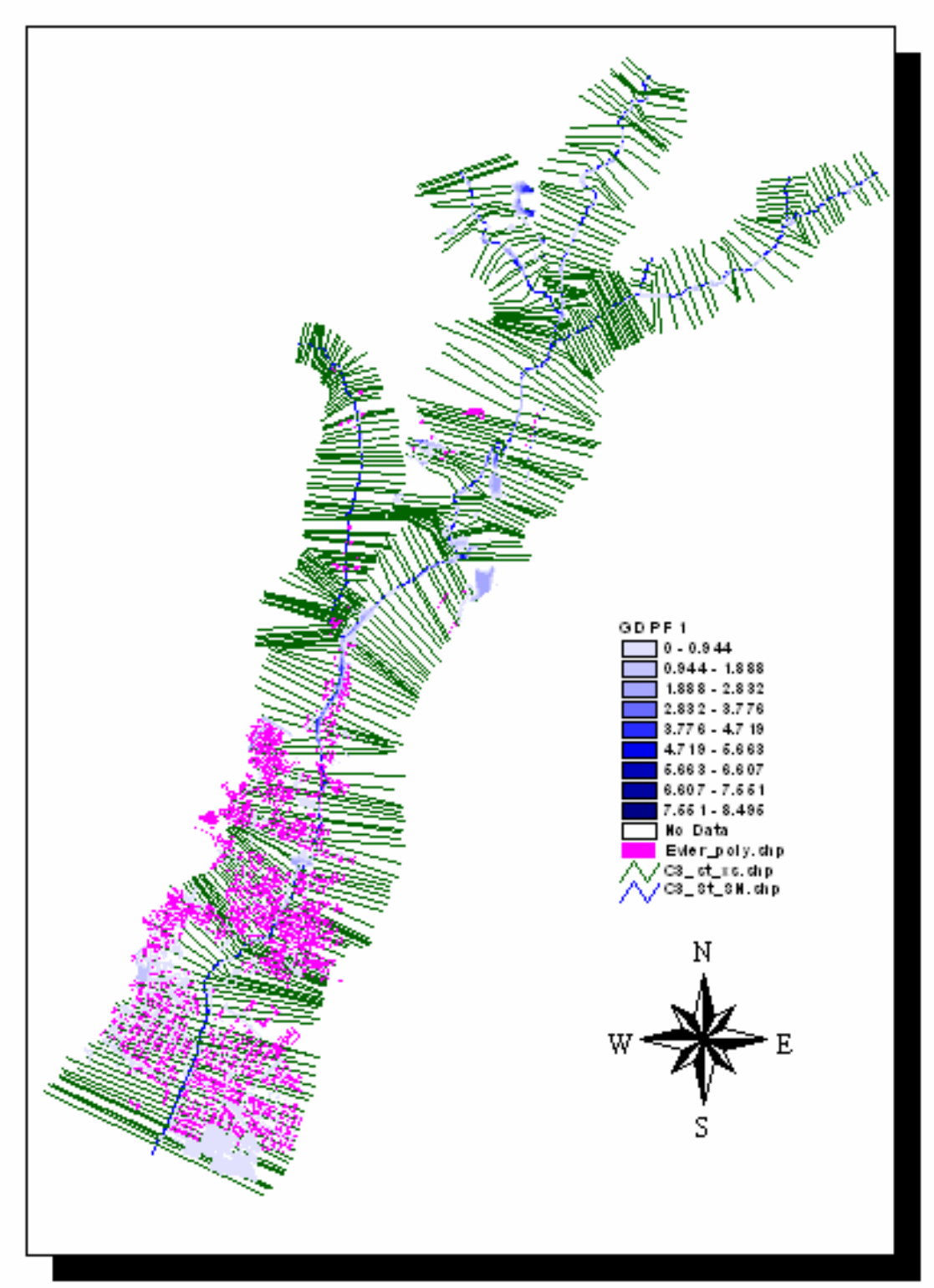

Figure 10.9 Floodplain areas for scenario C3_S.

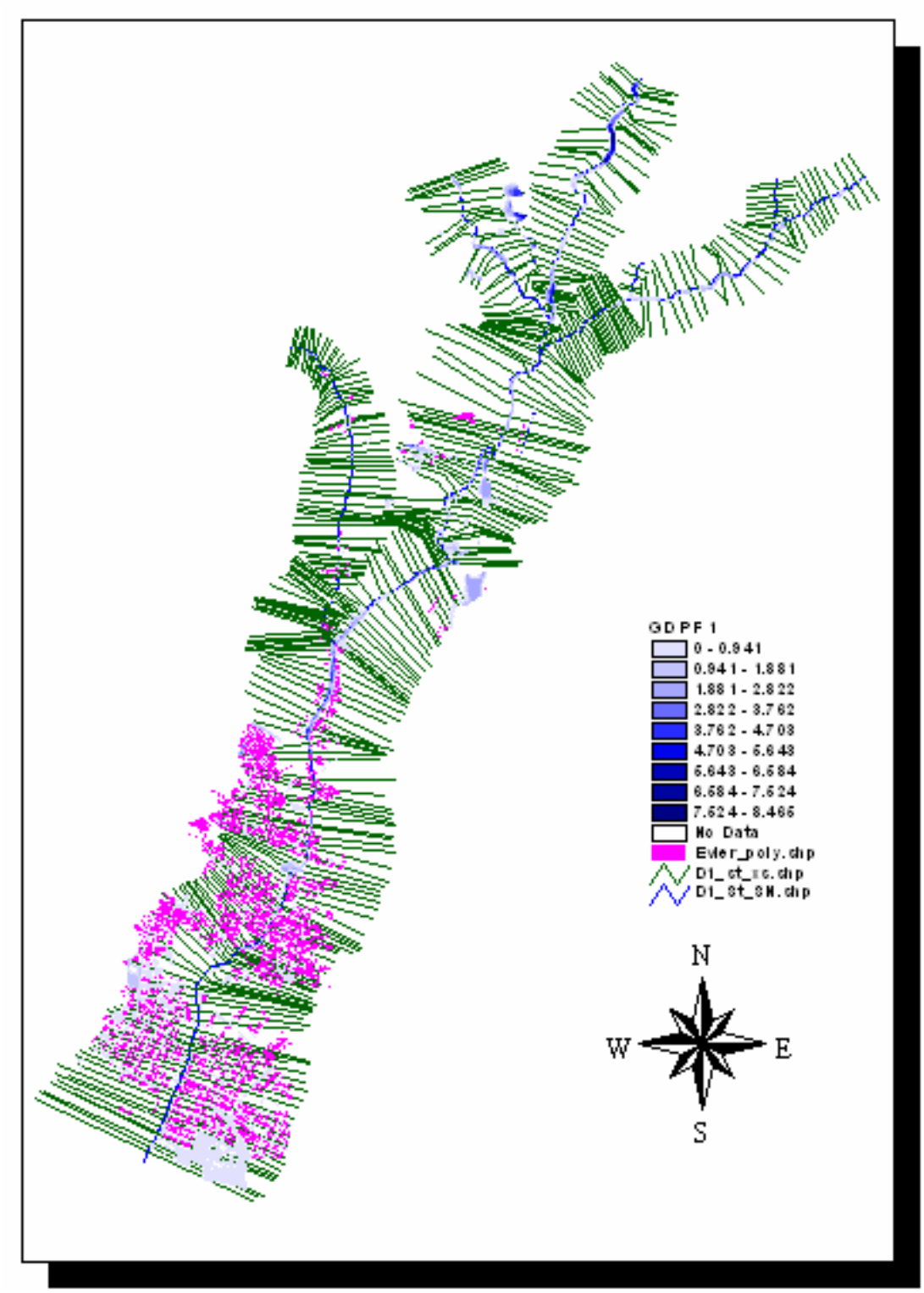

Figure 10.10 Floodplain areas for scenario D1_S

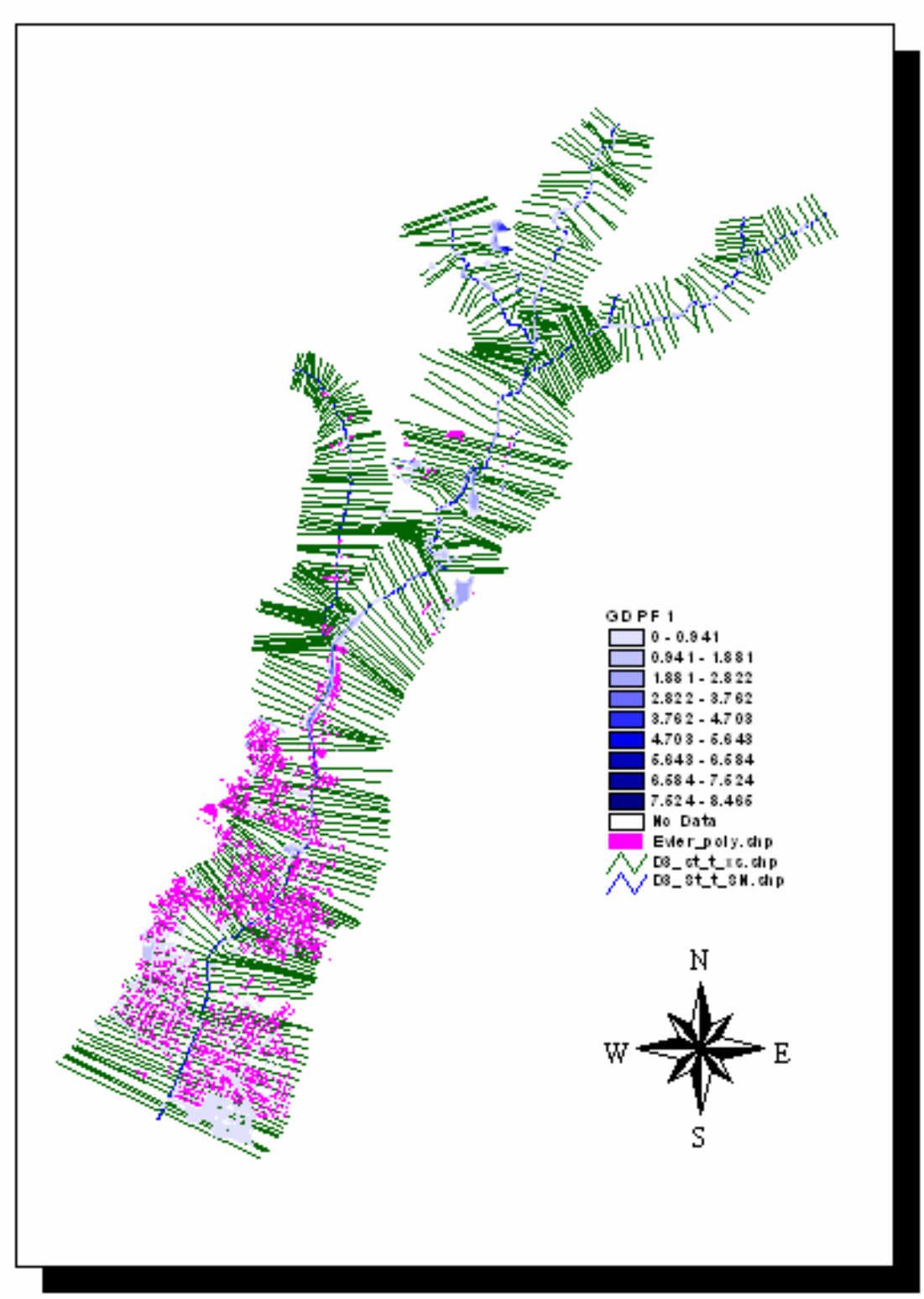

Figure 10.11 Floodplain areas for scenario D3_S.

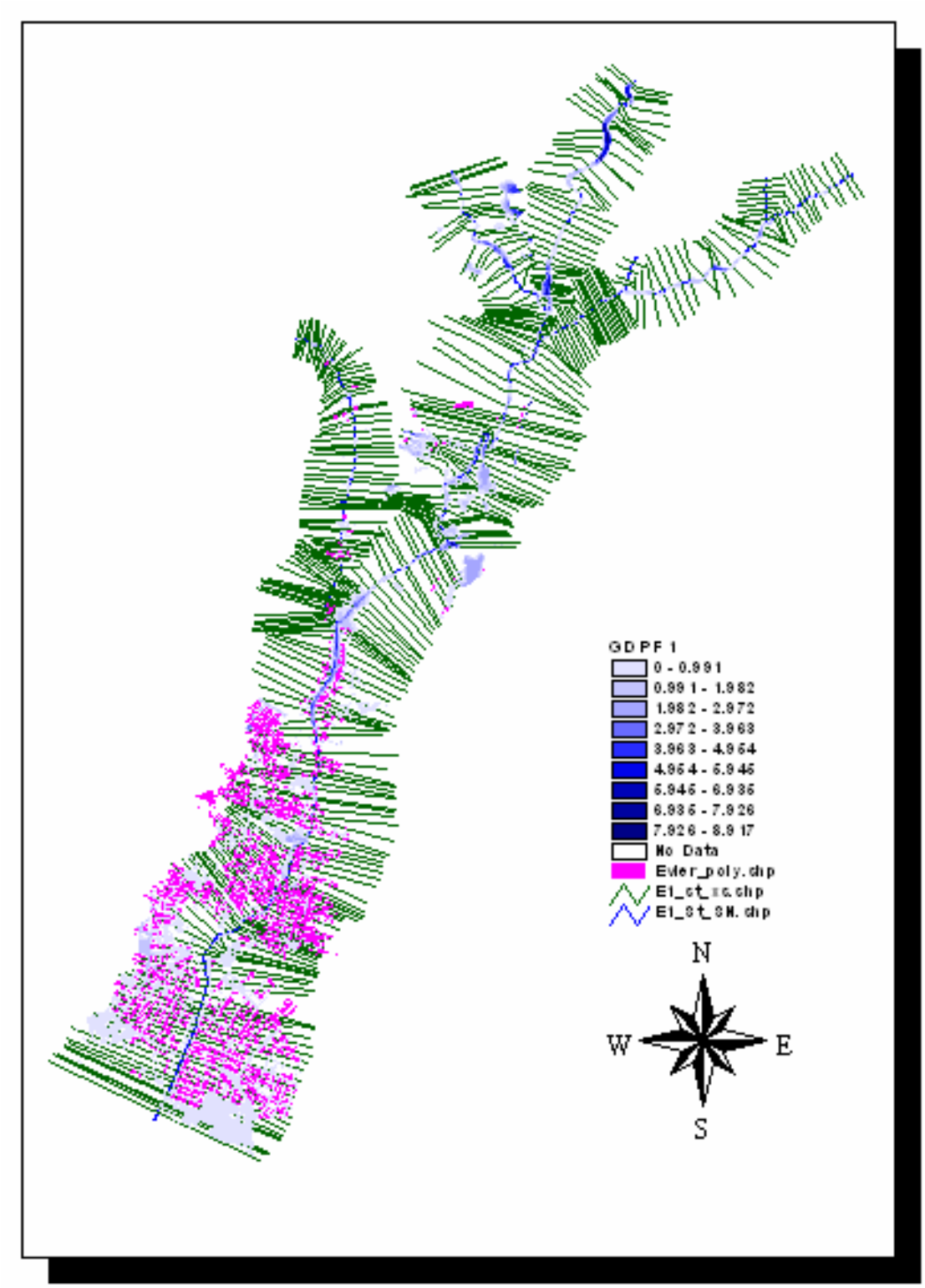

Figure 10.12 Floodplain areas for scenario E1_S.

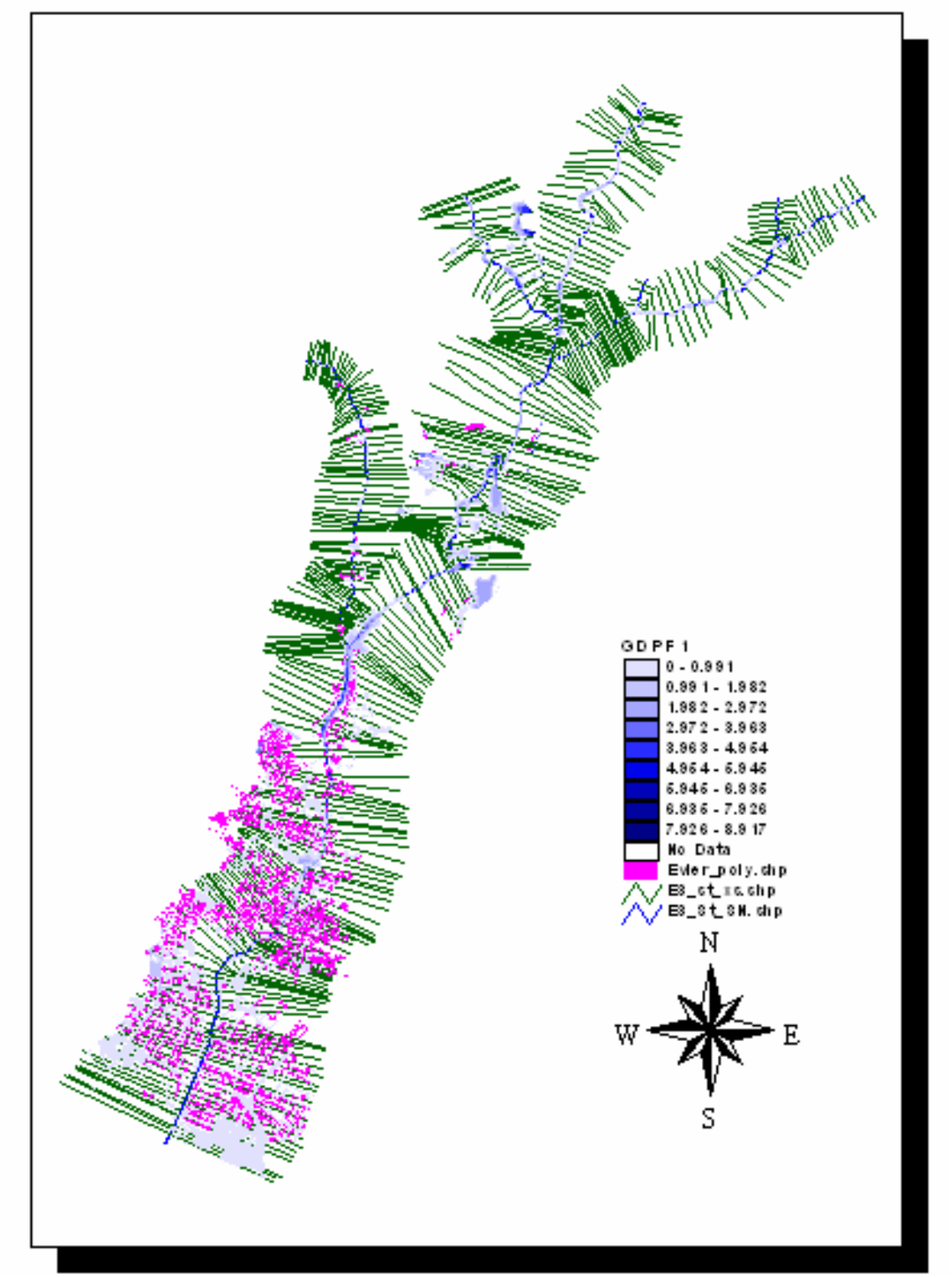

Figure 10.13 Floodplain areas for scenario E3_S.

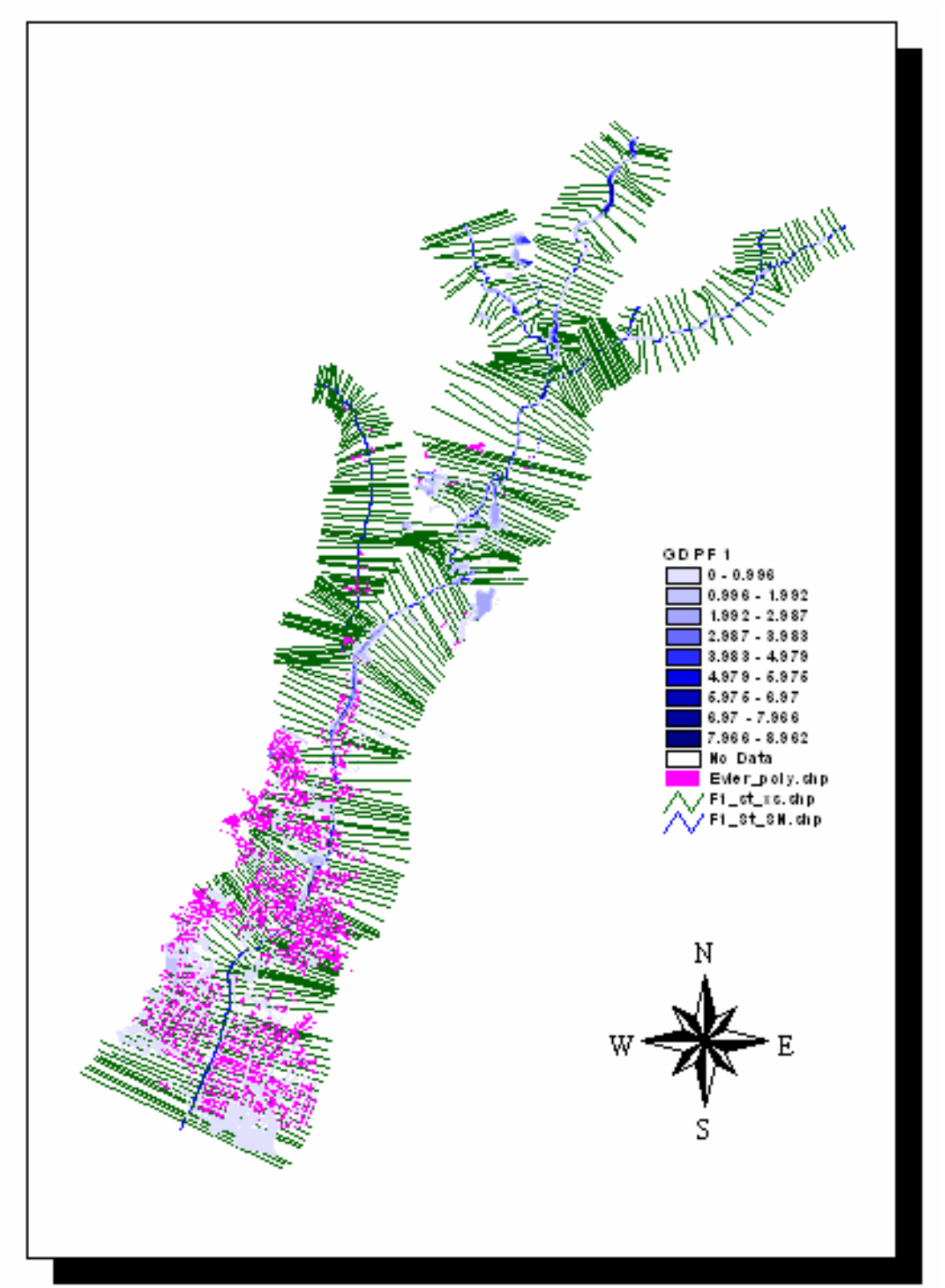

Figure 10.14 Floodplain areas for scenario F1_S.

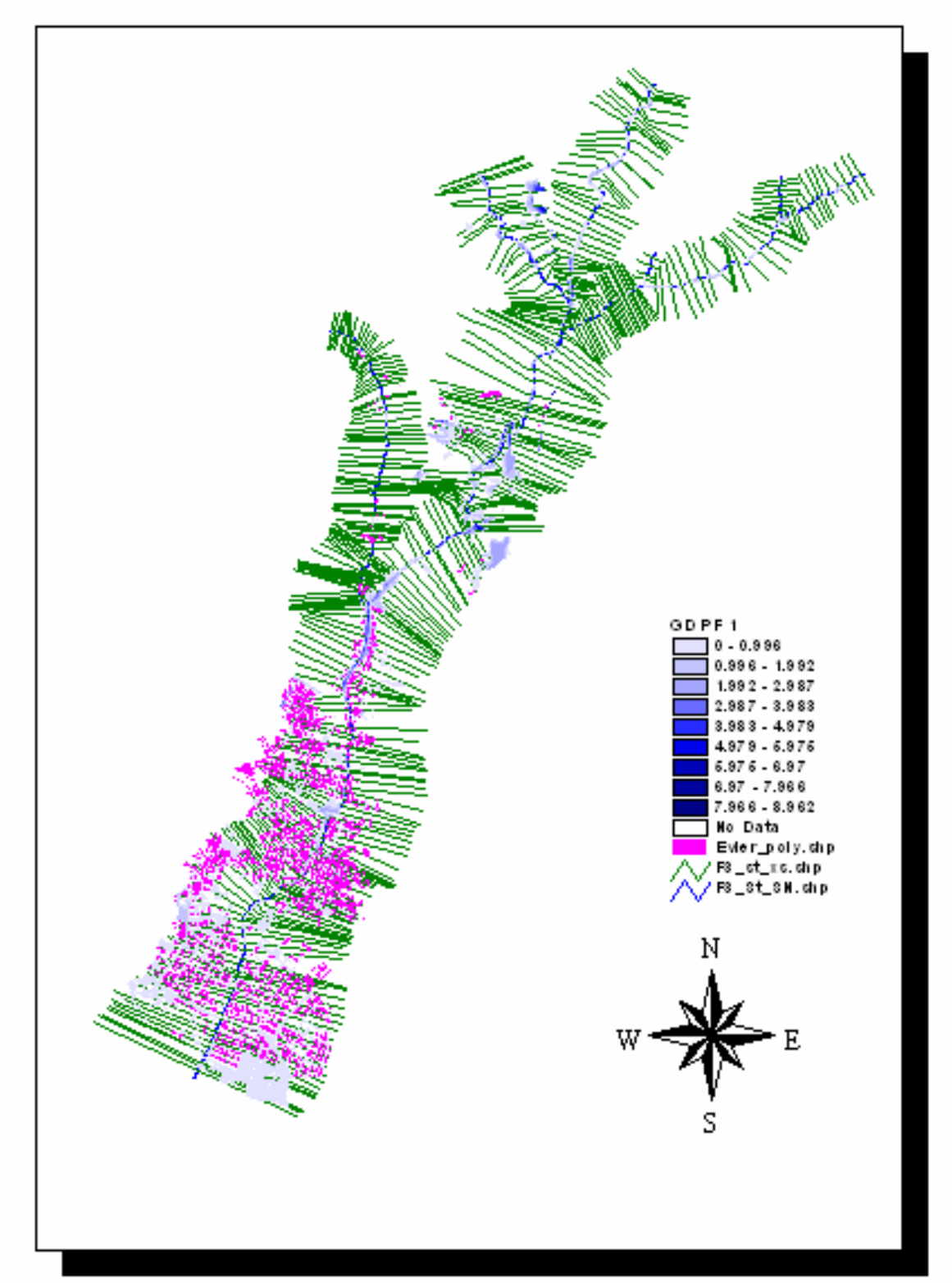

Figure 10.15 Floodplain areas for scenario F3_S.

Even though the above presented figures may seem to be quite similar to each other, it can be easily noticed that the floodplain areas corresponding to the floods with high return periods cover much larger areas over the land surface. Furthermore, the retention effect of the Bostanli dam is quite uncertain especially in the case of precipitation with a 500-year return period. It is also noticeable that the dykes have quite remarkable effects in mitigating the flooding effects, but the culverts, especially located in the interior parts, need re-examination for their functionalities. Despite the fact that the computed water level is not so high (at about 15-20 cm. levels) in the downstream part of the basin, it may be stated that the floodplain areas are expected to cover most of these highly urbanized areas. In Appendix 3, floodplain and water depth maps are given for the downstream part of the study area for each steady flow scenario.

Regarding the stream channels, even though it has not been possible to compare the existing situation with the previous conditions due to the inavailability of past information, it can be stated that the region is not under a high flooding risk as a result of the performed prevention measurements, but there still exists a threat especially in the upper areas where the stream channels get connected.

10.3 Unsteady Flow Model Results

The model results of the unsteady flow analysis are given in Figure 10.16 for *up6* and in Figure 10.17 for up3. It should be noted that these floodplain areas were created regarding a 0.2-meter water surface computational tolerance, which is more than the model default value. Figures 10.16 and 10.17 exhibit the floodplains for the maximum water level. Figure 10.18 shows X-Y-Z perspective plot of up3 with calculated water surface.

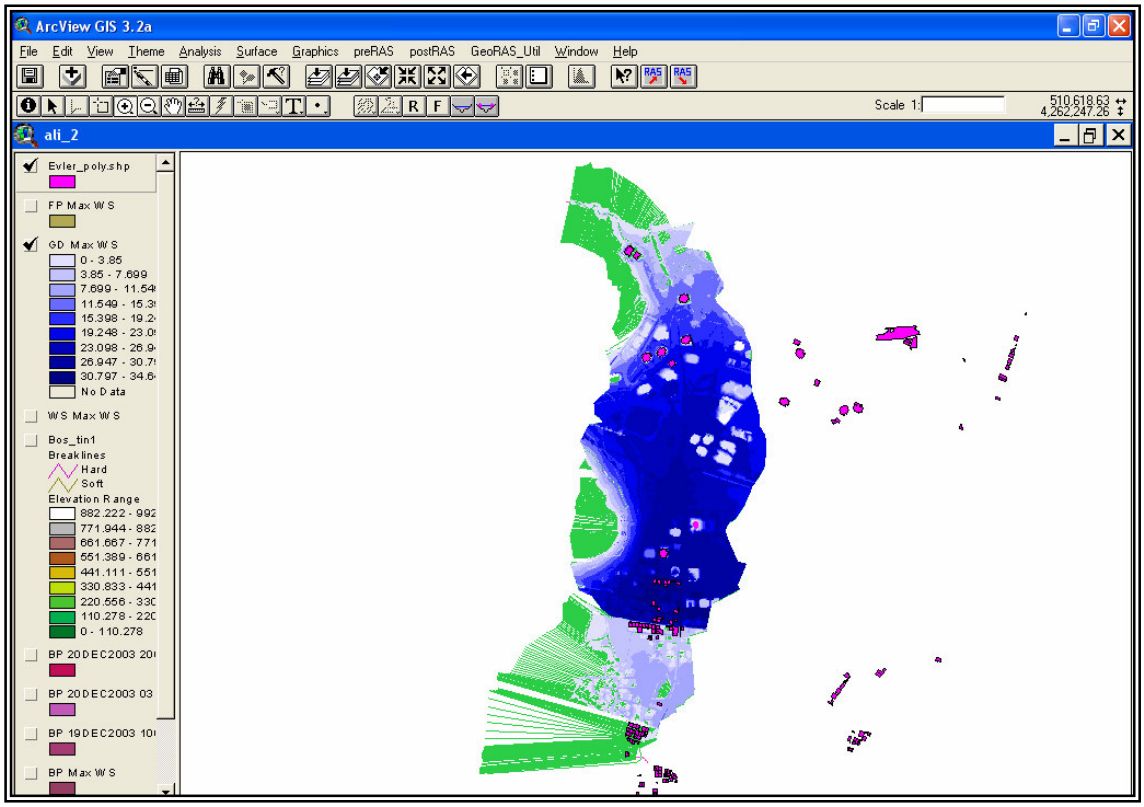

Figure 10.16 Floodplain areas on up6 for scenario A1_U.

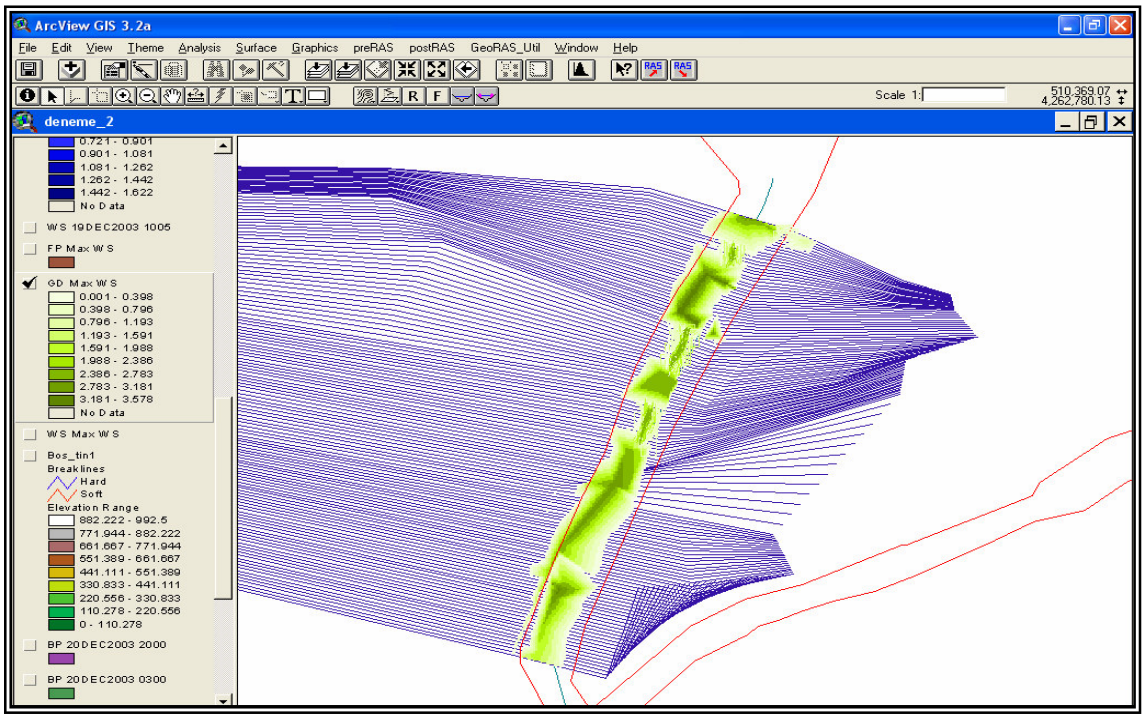

Figure 10.17 Floodplain areas on up3 for scenario A1_U.

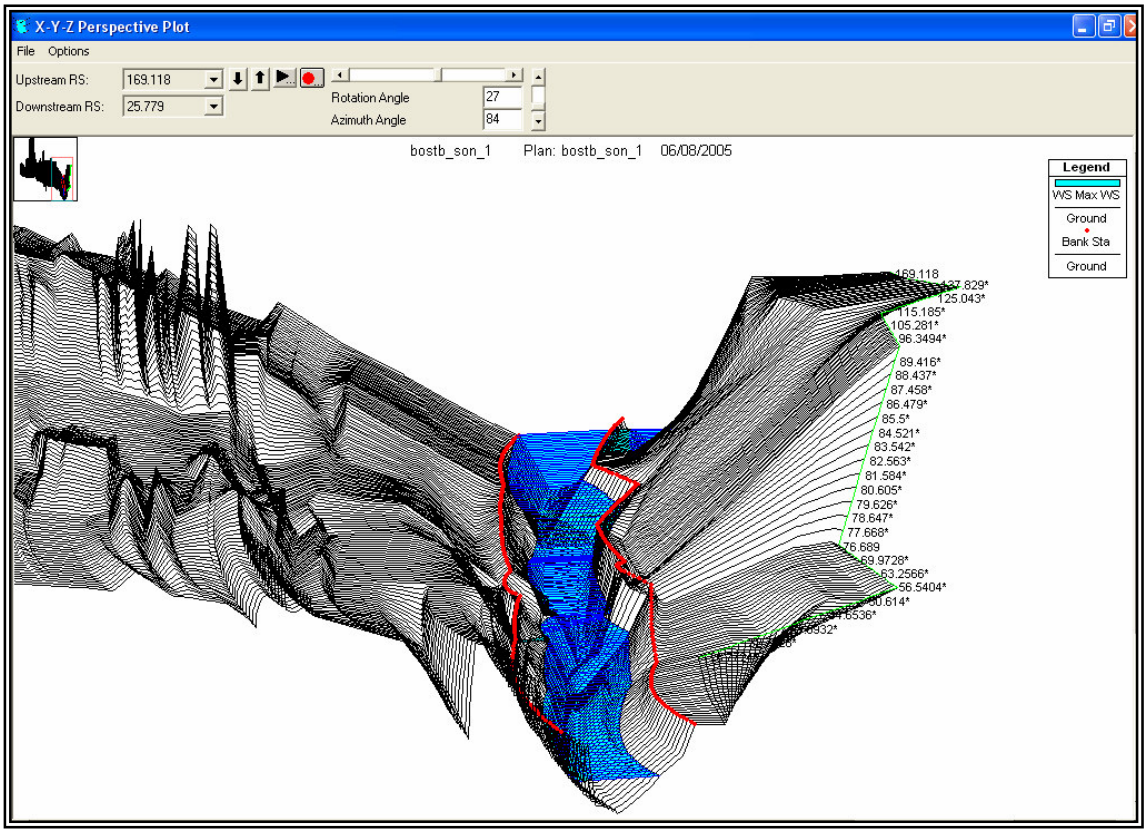

Figure 10.18 X-Y-Z Perspective plot of up3.

Figure 10.19 provides a comparison of the unsteady and steady flow analysis results obtained for the reach *up3*. The floodplain area obtained from D1_S scenario was selected to represent the steady flow outcomes. The blue-based color shows the flood plains for the steady flow, while the green-based color reflects the floodplain from the unsteady flow analysis.

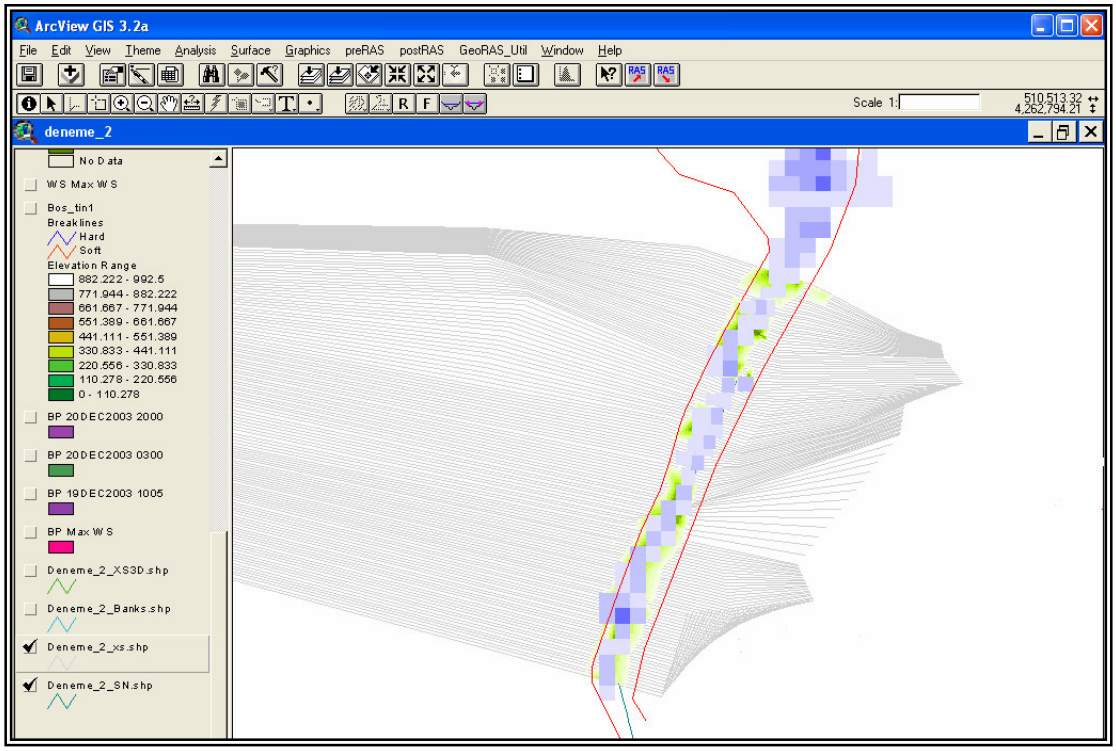

Figure 10.19 Comparison of the results of steady and unsteady flow analyses.

The floodplain areas obtained from the steady and unsteady analyses are shown together in order to check whether the results are as expected and compatible. Floodplains in Figure 10.16 cover a larger area than the floodplains of D1_S scenario, which was originally expected to be the opposite. This is simply because the unsteady flow model provides a maximum water stage height that is yet less than the stage height found from the steady flow model, where the peak discharges are considered to occur simultaneously everywhere, which, of course, is not the case in reality.

On the other hand, as seen from Figure 10.18, floodplains on *up3,* which is not as complex as *up6,* show quite harmonious results.

When the floodplain areas produced by in the unsteady model are considered, it is observed that the resulting areas for *up6* are somehow larger than expected. It should be noted that such a result may indeed be induced by the modeling operations where the

default computational tolerances were exceeded and where the model itself is much more sensitive to the quality of the utilized digital data. Here, a supplementary study may be proposed to thoroughly examine the detailed plans of the quite large number of hydraulic structures existing in the basin. The reason for obtaining more reasonable and acceptable results for the reach of *up3* (different from the case in *up6*), can be that the reach *up3* has a less complex shape, and there does not exist any hydraulic structure that requires more specialized analyses.

CHAPTER ELEVEN
CONCLUSION

Flood visualization techniques, which have been commonly used in flood-related research in both many European countries and also the USA, play an important role in flood management studies by providing a visual basis for explaining the results from hydraulic models to community members, decision makers, engineers, planners, and officials in a more comprehensive and user-friendly way. Furthermore, the integration of some well-known hydrologic and hydraulic models, like the USACE's HEC-HMS and HEC-RAS models, with a GIS has been widely welcomed in the engineering community.

This research provides important contributions to floodplain management studies in Turkey, as regards being the first application example to HEC-HMS, HEC-RAS and GIS integration. The results presented in this study indicate that terrain development, hydrologic and hydraulic modeling, and accurate floodplain delineation in the digital domain can be properly used in Turkey.

Conclusions that can be drawn from the successive implementation of GIS, hydrologic and hydraulic modeling tools for floodplain delineation can be summarized as explained in the following paragraphs.

In this study, three different steps were carried out for pre-processing of the hydrologic modeling phase, because of the lack of both meteorological and flow monitoring stations in the study area. These are;

- generation of design hyetographs
- determination of SCS curve numbers
- computation of Clark's synthetic unit hydrographs.

In the first step, design hyetographs were created in order to define the meteorology model of the HEC-HMS; and then, SCS CNs were calculated to be used in the loss rate determination. Afterwards, synthetic unit hydrographs were identified by using Clark's method to describe the transformation between the precipitation and the resulting runoff. As the last two operations were performed with the use of available spatially-distributed digital data about the physical characteristics of the basin, it can be said that entire hydrologic model is expected to give reliable solutions under several scenario considerations. Here, it should be noted that proper use of the available data is the most important determinant of the overall quality that is expected at the end of the hydrologic modeling process, as in all of the modeling studies in general; but GIS has become an inevitable tool to obtain trustworthy estimates in such a study.

In the second phase of the research for hydraulic modeling, three different difficulties faced through the modeling process can be mentioned: uncertainty in the full reliability of the digital terrain model (representativeness of the TIN model), limited data availability for channel geometry, and excessive number of hydraulic structures within the project area.

The type and resolution of the terrain data are the most critical factors affecting accurate floodplain delineation activities. In this current study, the gaps in the available terrain data have negatively affected the resulting terrain information and the subsequent floodplain map simply because both the hydrologic and the hydraulic models were to be developed purely on the basis of this data. Terrain data of a higher resolution would provide a better representation of the channel banks, and ultimately, of the extent of the floodplain. The TIN-based delineation method creates a more realistic delineation of flood levels from the terrain model (Snead, 2000). This type of delineation works well for smaller study areas because of its high resolution, but it may become cumbersome when the study area becomes larger.

Geometry data, which can also be extracted from TIN, should be confirmed with a suitable field work, as its quality is another important factor affecting the model outputs. Field study mostly becomes necessary in all floodplain management studies, especially when there is no accurate information about the existing hydralic structures or it is very limited.

On the other hand, hydraulic structures require an extensive study especially in the case of unsteady flow modeling. The unsteady flow algorithms are not as mathematically stable as the ones for steady flow. In these computations, for example, the flow simulation will terminate undesirably when a water stage height is computed at a value less than the streambed elevation. This type of problems does not necessarily arise from inaccurate mathematical computations; but simply due to the fact that natural systems do not always follow the rules of mathematics. In such cases, some interventions by the user will be required to guarantee proper operation of the model. Increasing the number of cross-sections in order to decrease the incremental step in the stage difference from element to element in the system, and/or decreasing the model's simulation time step should be considered among many others. Beyond all these computational performance considerations, the existence of hydraulic structures such as bridges and culverts in the study area would have an effect to amplify flood inundation through backwater effects from piers and abutments; thus, these structures would require an extensive analysis to determine the optimum modeling method

Another consequence from the study is about the selection of the most suitable type of modeling, either steady or unsteady. Unlike the steady flow models, the unsteady models can express the effects of flood duration, which is also an important factor in flood prevention planning. However, using unsteady flow models for flood visualization is more complicated and lengthy, depending on the size of the study area. Especially, inaccurate or incomplete data sources can affect the model results in addition to many factors. The amount of the required stream geometry data can become very substantial as the size of the stream network increases. It is preferable to choose a modeling method

that gives reliable and accurate solutions for the study area.. Many factors can affect the model developing process for unsteady flow models while they are not an issue for steady flow models. In that case, the HEC-RAS model becomes easier to develop, and the HEC-HMS data can be incorporated into the HEC RAS model easily. Once the terrain model is created, the process of developing flood maps with the HEC-GeoRAS extension becomes much simpler.

As it is widely accepted, this study also proves that data exchange capabilities between the HEC-HMS and HEC-RAS models, which allow, for example, importing the runoff hydrographs from the HEC-HMS model into the HEC-RAS model, minimizes data processing in such a way that becomes quite important especially in unsteady flow simulations.

At the end of all hydrologic and hydraulic studies performed within this current study, it has been possible to obtain a series of project-specific conclusions such that the improvements in the Bostanli Basin have proved to be quite sufficient in upper parts where the share of the built-up land is comparably low, but there still exist some risk in the river reach connections. In the lower part of the basin area where urbanization effect is much higher, the study has given some results that mainly differ under different scenario considerations. Here, it should be noted that stormwater drainage systems which will decrease the flooding effect in these lower parts have not been taken into consideration within the scope of this study.

The study performed on the example of Bostanli Basin can be further extended to other river basins surrounding the city of Izmir to make an efficiency analysis for the improvements carried out by local water authorities and even more to find out the problematic areas which still need further improvement. It becomes also possible to obtain digital floodplain maps for the city of Izmir and its surroundings with the help of a similar study through the use of sufficient amount of data that will allow integrated assessments on HEC-HMS, HEC-RAS and a stormwater management model.

Following the determination of most probable floodplain areas, it would become possible to define floodplain management strategies for the city of Izmir and further develop a management plan. It should also be noted that with the help of close cooperation and mutual information exchange between research institutes and local authorities, it will be quite effective to display the results from all these modeling and management studies on internet platform to increase public awareness on possible dangers.

REFERENCES

Abbott, M.B.(1979). *Computational hydraulics: Elements of the theory of free surface flows*. London: Pitman.

Alamilla, S., Novotny, V., & Bartosova, A. (2001). *GIS based approach to floodplain delineation and flood risk estimation applied to the Oak Creek Watershed*, Technical Report No:10, Institute for Urban Environmental Risk Management, Marquette University, Milwaukee. Retrieved June 12, 2003, from ProQuest Digital Dissertations database.

Anderson, D.J. (2000). *GIS-based hydrologic and hydraulic modeling for floodplain delineation at highway river crossing*, MSc Thesis, The University of Texas, Austin. Retrieved June 10, 2003, from ProQuest Digital Dissertations database.

Andrysiak, P.B. & Maidment, D. (2000). *Visual floodplain modeling with geographic information systems*, CWR Online Report 00-4, Center for Research in Water Resources, The University of Texas, Austin.

Azagra E., Olivera F., & Maidment, D. (1999). *Floodplain visualization using TINs,* CWR Online Report 99-5, Center for Research in Water Resources, The University of Texas, Austin.

Beavers, M.A. (1994). *Floodplain determination using HEC-2 and geographic information system*s. MSc Thesis, Department of Civil Engineering, The University of Texas at Austin. Retrieved June 14, 2003, from PreQuest Digital Dissertation database.

Bedient, P.B., & Huber, W.C. (2002). *Hydrology and floodplain analysis* (3rd ed.). USA: Prentice Hall.

Benavides, J.A. (2001). *Information technologies in water resources: Modeling flood control alternatives for the Clear Creek Watershed within a GIS framework*, MSc. Thesis, Rice University, Houston, Texas. Retrieved June 14, 2003, from ProQuest Digital Dissertations database.

Benzeden, E.(2000). *Hydrology of floods*, Lecture Notes, Izmir, Turkey.

Bukey, B. (2000). *Ege Bölgesindeki sağanak yağışlar için şiddet-süre-tekerrür bağıntılarının modellenmesi*, DEÜ Mühendislik Fakültesi İnşaat Mühendisliği Bölümü, Hidroloji ve Su Yapıları Bitirme Projesi, No: 203 Yöneten: Prof. Dr. Ertuğrul Benzeden, İzmir, Türkiye.

Burby, R. J. and French, S. P. (1981). Coping with floods: The land-use management paradox, *J. American Planning Association,* 47(3).

Chang, T.J, Hsu, M.H., Teng, W.H., & Huang, C.J. (2000). A GIS-assisted distributed watershed model for simulating flooding and inundation. *Journal of the American Water Resources Association, 36* (5), 975-988.

Clark, C.O. (1945). Storage and the unit hydrograp, *Transactions of the American Society of Civil Engineers*, 110, 1419–1446.

Chow, V.T. (1959). *Open-channel hydraulics* (International student ed.). New York: McGraw-Hill Book Company.

Chow, V.T., Maidment, D.R., & Mays, L.W. (1988). *Applied hydrology*. McGraw-Hill Book Company: New York.

Correia, N.F., Saraiva, M.G., Silva, N.F., & Ramos I.. (1999). Floodplain management in urban developing areas: Part I. Urban growth scenarios and land-use controls. *Water Resources Management*,13, 23-37.

Djokic, D., Beavers, M.A., & Deshakulakarni, C.K. (1994). *ARC/HEC2: an ARC/INFO - HEC-2 interface*. Proceedings of the 21st Annual Conference on Water Policy and Management: Solving the Problems. American Water Resources Association, ASCE, 41-44.

ESRI (Environmental Systems Research Institute). (1999). *ArcView GIS Extensions*. Retrieved October 26, 1999 from http://www.esri.com/software/arcview/extensions/index.html.

Evans T.A. (1998). *GIS data exchange for the Hydrologic Engineering Center's hydraulic and hydrologic models,* International Water Resources Engineering Conference Proceedings, ASCE, 786-789.

FEMA (Federal Emergency Management Agecy). (2004). *Map modernization objective: automated hydrology and hydraulics (H&H).* Retrieved April 10, 2005 from http://www.fema.gov/fhm/mm_ahh9.shtm

Fordham, M. H. (1992). *Choice and constraint in flood hazard mitigation: The environmental attitudes of floodplain residents and engineers*, PhD Thesis, Middlesex Polytechnic, School of Geography and Planning, in collaboration with the National Rivers Authority Thames Region.

Gonzales, N. S. (1999). *Two-dimensional modeling of the Red River floodway*, MSc Thesis, Department of Civil and Geological Engineering, University of Manitoba, Canada. Retrieved June 14, 2003, from ProQuest Digital Dissertations database.

Hacisuleyman, H.(2003). *Ege Bölgesi örneğinde şiddet-süre ilişkilerinin tekerrür aralığı ile değişimi*, DEÜ Mühendislik Fakültesi İnşaat Mühendisliği Bölümü, Hidroloji ve Su Yapıları Bitirme Projesi, No: 252 Yöneten: Prof. Dr. Ertuğrul Benzeden, İzmir, Türkiye.

Halley MC, White SO, & Watkins EW. (2000). *ArcView GIS Extension for Estimating Curve Numbers*, 2000 ESRI International User Conference, June 26-30, 2000 ESRI International User Conference Proceedings, USA.

Handmer, J. (1995). *Cooperation, coercion, capacity and commitment: Key concepts in floodplain management*, International Conference Flood Protection of Towns – Ideas and Experiences, Krakow, Poland.

HEC (1996). *Engineering and design - Hydrologic aspects of flood warning - preparedness programs*, ETL 1110-2-540. Retrieved September 30, 1996 from http://www.usace.army.mil/inet/usace-docs/eng-tech-ltrs/etl1110-2-540.

HEC (Hydrologic Engineering Center). (1997). *HEC-RAS river analysis system: Hydraulic reference manual*. Davis, CA: Hydrologic Engineering Center.

HEC (Hydrologic Engineering Center) (2000). *HEC geospatial hydrologic modeling extension (HEC-GeoHMS)*. USA: U.S. Army Corps of Engineers Hydrologic Engineering Center.

HEC (Hydrologic Engineering Center). (2001a). *HEC-HMS: Hydrologic modeling system user's manual.* Davis, CA: Hydrologic Engineering Center.

HEC (Hydrologic Engineering Center). (2001b). *HEC-RAS: River analysis system user's manual.* . Davis, CA: Hydrologic Engineering Center.

HEC (Hydrologic Engineering Center) (2002). *HEC- GeoRAS An extension for support of HEC-RAS using ArcView (v 3.1),* User's manual. USA: U.S. Army Corps of Engineers Hydrologic Engineering Center.

Henderson , F. M.(1996). *Open channel flow*. London: MacMillan.

HydroGIS-CD. (2001). *HEC-RAS, HEC-HMS, HEC-GeoRAS, and HEC-GeoHMS,* Houston, Texas: Dodson&Associates Inc.

IZSU (Izmir Su ve Kanalizasyon İdaresi Genel Müdürlüğü). (2004). *İzmir dereleri, bendler*. Izsu: İzmir.

Keifer, C.J., & Chu, H.H. (1957). Synthetic storm pattern for drainage design, *J. Hyd. Div.*, Am. Soc. Civ. Eng., 83 (HY4), 1-25.

Klotz D., Strafaci A., Hogan A., & Dietrich K.(Eds.) (2003). *Floodplain modeling using HEC-RAS* (1th ed.). USA: Haestad Press.

Linsley, R.K., Kohler, M.A., & Paulhus, J.L.H. (1998). *Hydrology for engineers* (SI metric Ed.). Singapore: McGraw Hill Book Company.

Lopcu, Y. (2004). *İzmir örneginde anlık şiddet yöntemiyle yağış hiyetografı çıkarılması*, DEÜ Mühendislik Fakültesi İnşaat Mühendisliği Bölümü, Hidroloji ve Su Yapıları Bitirme Projesi, No: 270 Yöneten: Prof. Dr. Ertuğrul Benzeden, İzmir, Türkiye.

Muccklestoń, K. (1972). *Problems of Ordering Flood Plain Occupanc*y, Oregon State University.

Noman, N.S. (2001). *An integrated approach for automated floodplain delineation from digital terrain models*, PhD. Thesis, Department of Civil and Environmental Engineering, Brigham Young University. Retrieved June 11, 2003, from ProQuest Digital Dissertations database.

Olivera F., & Maidment, D. (1999). *System of GIS-based hydrologic and hydraulic applications for highway engineering: Summary report*, Center for Transportation Research, The University of Texas, Austin.

Olivera, F. & D. Maidment. (2000). GIS tools for HMS modeling support. In *Hydrologic and hydraulic modeling support.* Redlands, CA: ESRI Press.

Onusluel G, Gul A. (2004). *Utilization of geographic infromation tools in water resources related studies*. EWRA Symposium on Water Resources Management: Risk and Challenges for the 21st Century, Sep. 2-4 , 2004 Conference Proceedings, Izmir, Turkey.

Parker, D. J. (1981). *Flood Mitigation through non-structural measures: A critical appraisa*l, International Conference on Flood Disasters, New Delhi, India.

Pilgrim DH, & Cordery I. (1993). Flood runoff. In *Handbook of hydrology* (9.1-10.1) USA: McGraw-Hill Inc.

Platt, R.H., & Mc Mullen, G.M. (1980). *Past-flood recovery and hazard mitigation: Lessons from the Massachusetts Coast*. Publication No:115. Water Resources Research Center, University of Massachusetts, Amherst.

Prasuhn, A.L. (1992). *Fundamentals of hydraulic engineering*. New York: Oxford University Press.

Rossi, G., Harmancioglu, N., & Yevjevich, V. (Eds.). (1992). *Coping with floods*. Series E: Applied Sciences (257), Netherlands: Kluwer Academic Publishers.

Saraiva, M. G. (1995). *The river as landscape: Management of river corridors in the framework of land-use planning*, PhD Dissertation, Instituto Superior de Agronomia, Universidade Técnicade Lisbon.

SCS (U.S. Soil Conservation Service). (1985). *National engineering handbook.* U.S. Department of Agriculture: Washington.

Shrestha, R. R. (2000). *Application of GIS and numerical modeling tools for floodplain modelling and flood risk assessment of Babai River in Nepal*. Retrieved October 26, 2000, from http://www.geocities.com/rajesh_rajs/Abstract.html.

Smith, K. (1992). *Environmental hazards assessing risk and reducing*. London: Routledge.

Snead, D.B. (2000). D*evelopment and application of unsteady flood models using geographic information systems*, MSc Thesis, The University of Texas, Austin. Retrieved June 10, 2003, from ProQuest Digital Dissertations database.

Tate, E. (1999). *Floodplain mapping using HEC-RAS and ArcView GIS,* CRWR Online Report 99-1, Center for Research in Water Resources, Bureau of Engineering Research, The University of Texas at Austin.

Tempo Altyapi. (2000). *Planning report on ımprovement project of the Bostanli River in Karsiyaka District*, Izmir.

Usul, N., & Yilmaz, M. (2002). *Estimation of instantaneous unit hydrograph with Clark's techniques in GIS*, 2002 ESRI International User Conference, July 8-12, 2002 ESRI International User Conference Proceedings, USA.

Wanielista, M., Kertsen, R., & Eaglin, R. (1997). *Hydrology water quantity and quality control* (2nd ed.). USA: John Wiley and Sons Inc.

Ward, A. D., & Elliot W. (Eds.). (1995). *Environmental hydrology*, New York: Lewis Publishers.

Yang, C.R., & Tsai, C.T. (2000). Development of a GIS-based flood information system for floodplain modeling and damage calculation. *Journal of the American Water Resources Association*, *36* (3), 567-577.

Yevjevich, V. (1992). Classification and description of flood mitigation measures. In *Coping with floods*. Series E: Applied Sciences-Vol.257, (573-585). Netherlands: Kluwer Academic Publishers.

Yu, Z. (2002). *Course online notes on principles of hydrology*, University of Nevada Las Vegas, USA. Retrieved November 1, 2002, from http://hydro.nevada.edu/courses/gey711/week06.pdf.

APPENDICES

APPENDIX I

PROGRAM DEVELOPED FOR DERIVATION OF INSTANTANEOUS INTENSITY HYETOGRAPHS

```
Public SD As Integer, ZD As Integer

Private Sub CommandButton1_Click()

Dim dx As Double, i As Integer
    If SD = 1 Then
    dx = Range("B12").Value
    fark = Range("b10").Value
    r = Range("B6").Value
    a = Range("G4").Value
    b = Range("e4").Value
    D = Range("f4").Value
    D = Range("b8").Value
    dt = Range("H4").Value
    S = 0

For i = 1 To (Range("B9").Value) / dx
    cl$ = "B" + Trim(Str(i + 15))
    Range(cl$).Select
    ActiveCell.Value = i * dx
    cll$ = "c" + Trim(Str(i + 15))
    If ActiveCell.Value <= Range("B10").Value Then
    Range(cll$).Select
    ActiveCell.Value = fark - (i * dx)
    Else
    Range(cll$).Select
    j = j + 1
    ActiveCell.Value = (j * dx)
    End If

    clll$ = "d" + Trim(Str(i + 15))
    If Range(cl$).Value <= D * 60 * r Then
```

```
    Range(clll$).Select
    ActiveCell.Value = (a * (((Range(cll$).Value / r) + D) ^ -b)) * (1 - ((b *
    Range(cll$).Value / r) / ((Range(cll$).Value / r) + D)))
    Else
    Range(clll$).Select
    ActiveCell.Value = (a * (((Range(cll$).Value / (1 - r)) + D) ^ -b)) * (1 - ((b *
    Range(cll$).Value / (1 - r)) / ((Range(cll$).Value / (1 - r)) + D)))
    End If

    cllll$ = "e" + Trim(Str(i + 15))
    Range(cllll$).Select
    ActiveCell.FormulaR1C1 = "=((RC[-1]+R[-1]C[-1])/2)*(R12C2/60)"
Next i

For k = 1 To (Range("B9").Value) / dt
    clllll$ = "G" + Trim(Str(k + 14))
    Range(clllll$).Select
    ActiveCell.Value = k * dt
Next k

    i = 1
    For j = 1 To (Range("B9").Value) / dx
cllllll$ = "H" + Trim(Str(j + 14))
Range(cllllll$).Select

        For i = i To ((Range("B9").Value) / dx) + 1
    cl$ = "B" + Trim(Str(i + 14))
    cllll$ = "e" + Trim(Str(i + 14))
    If Range(cl$).Value <= dt Then
    S = S + Range(cllll$).Value
    Else
    ActiveCell.Value = S / Range("H4").Value
```

```
    GoTo 10
    End If
    If i = ((Range("B9").Value) / dx) + 1 Then ActiveCell.Value = S /
    Range("H4").Value
        Next i

10 dt = Range("h4").Value + dt
i = i
S = 0
    Next j

 Else
MsgBox "Bu islemden once -Islemleri temizle- butonuna Basiniz!!!"
End If
SD = 0
ZD = 1
End Sub

Private Sub CommandButton2_Click()
Dim dx As Double, i As Integer
dx = Range("B12").Value

    For i = 1 To 10000
cl$ = "B" + Trim(Str(i + 15))
Range(cl$).Select
If ActiveCell.Value = 0 Then GoTo 20
ActiveCell.Clear
cll$ = "c" + Trim(Str(i + 15))
Range(cll$).Select
ActiveCell.Clear
clll$ = "d" + Trim(Str(i + 15))
Range(clll$).Select
```

```
ActiveCell.Clear
clllll$ = "e" + Trim(Str(i + 15))
Range(clllll$).Select
ActiveCell.Clear
cllllll$ = "g" + Trim(Str(i + 14))
Range(cllllll$).Select
ActiveCell.Clear
clllllll$ = "h" + Trim(Str(i + 14))
Range(clllllll$).Select
ActiveCell.Clear
    Next i


20 SD = 1
End Sub
```

APPENDIX II
HYDRAULIC STRUCTURES ON THE BOSTANLI RIVER

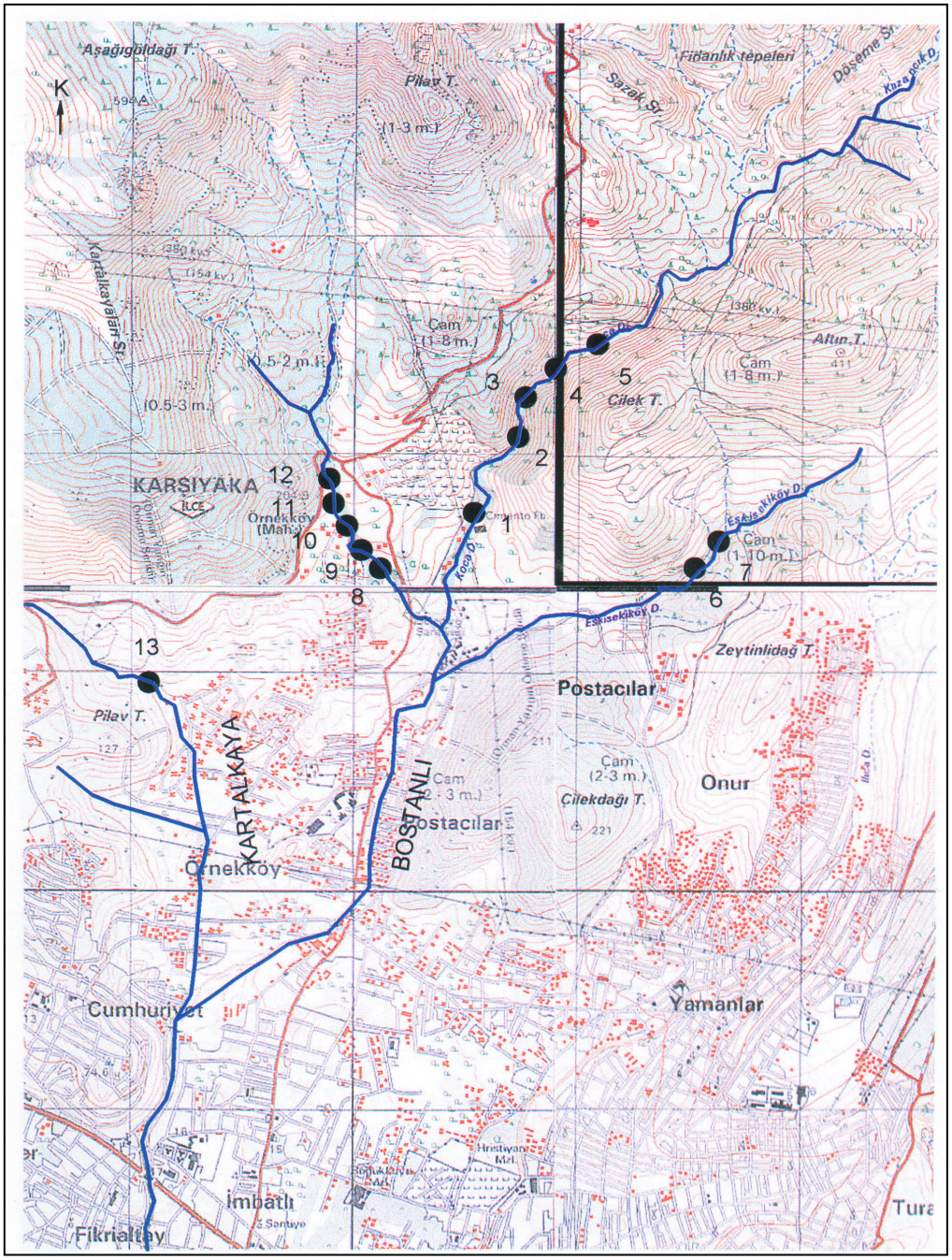

Figure A.1 Locations of weirs in Bostanli Basin.

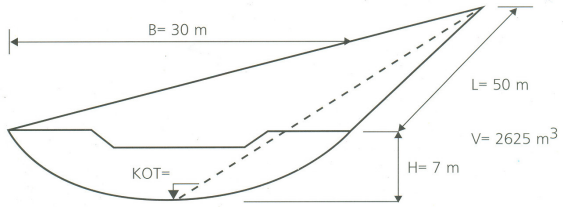

Figure A.2 Weir with number 1 and its characteristics.

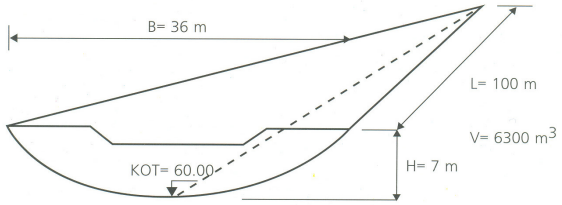

Figure A.3 Weir with number 2 and its characteristics.

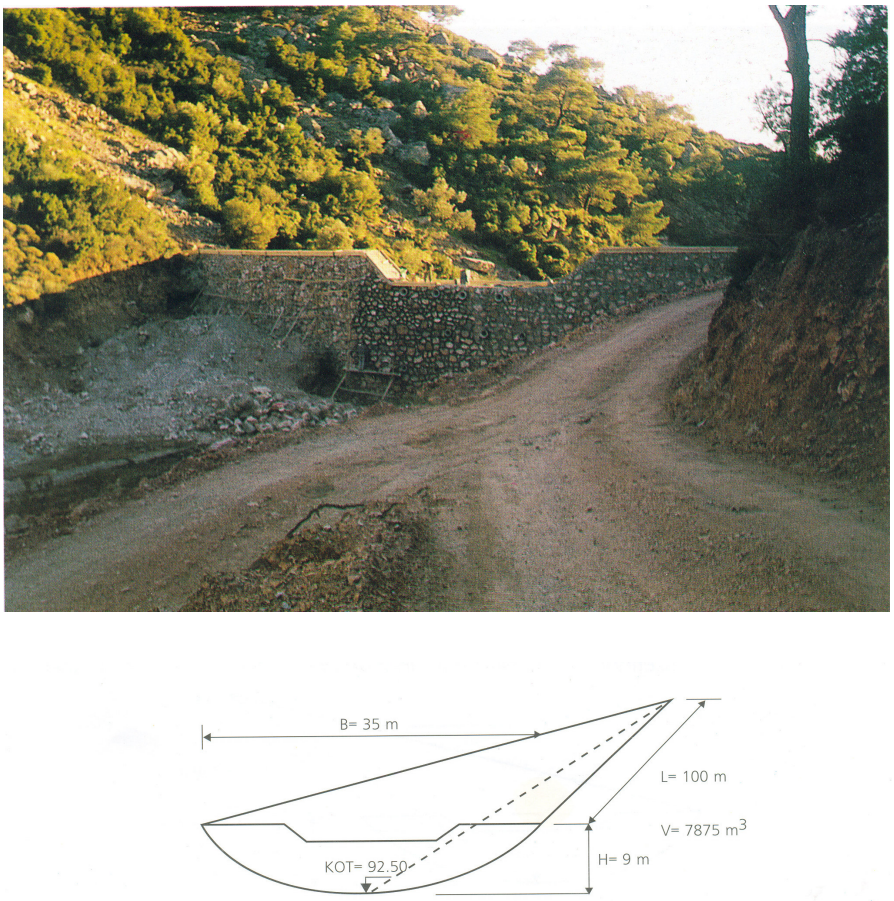

Figure A.4 Weir with number 3 and its characteristics.

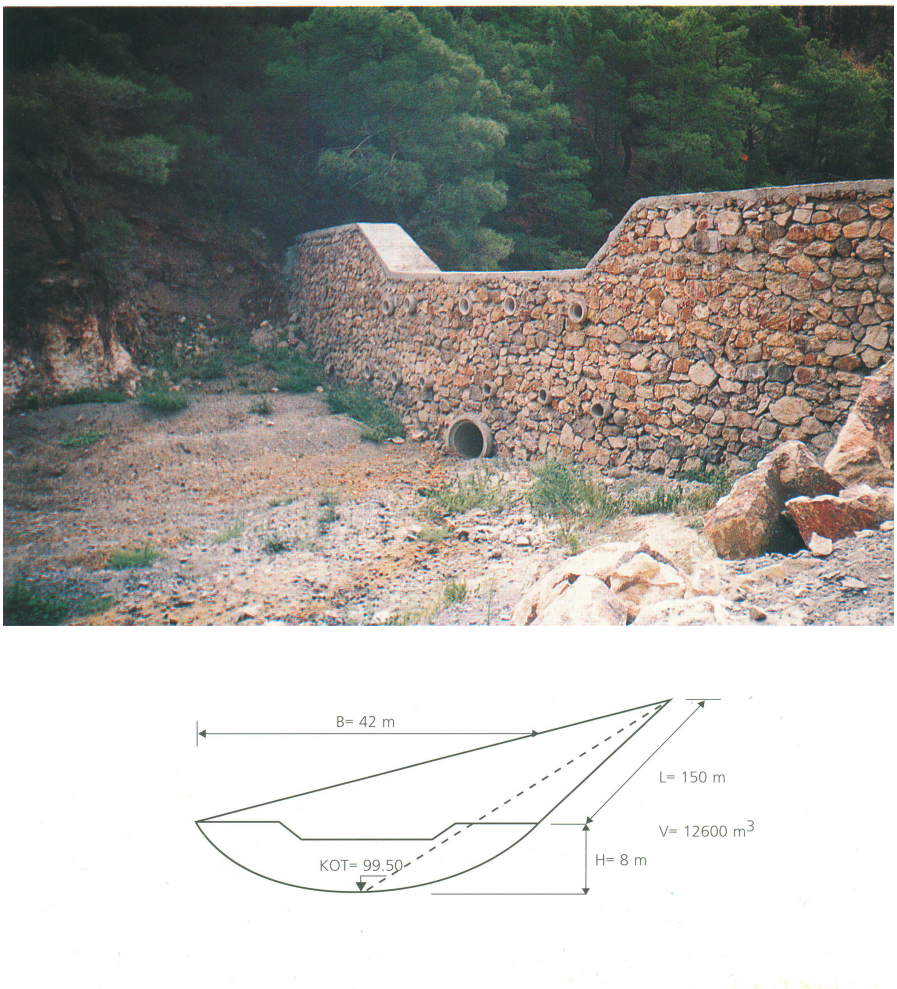

Figure A.5 Weir with number 4 and its characteristics.

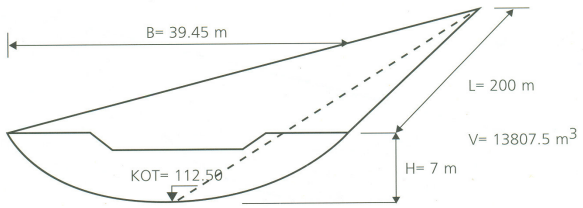

Figure A.6 Weir with number 5 and its characteristics.

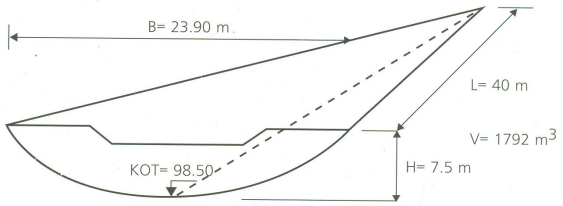

Figure A.7 Weir with number 6 and its characteristics.

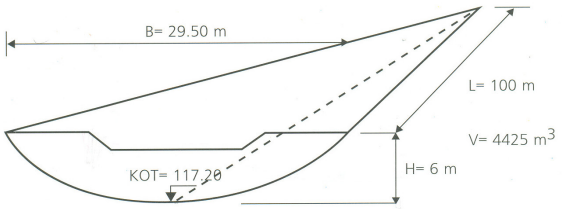

Figure A.8 Weir with number 7 and its characteristics.

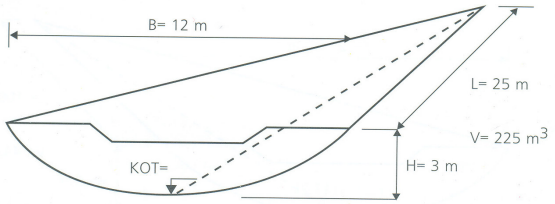

Figure A.9 Weir with number 8 and its characteristics.

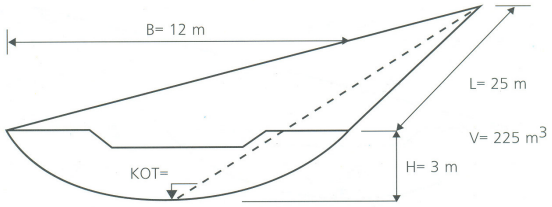

Figure A.10 Weir with number 9 and its characteristics.

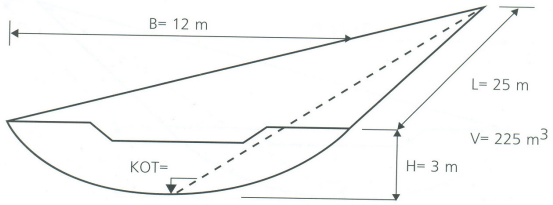

Figure A.11 Weir with number 10 and its characteristics.

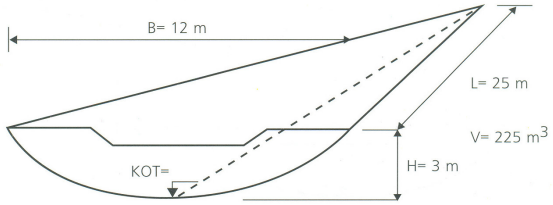

Figure A.12 Weir with number 11 and its characteristics.

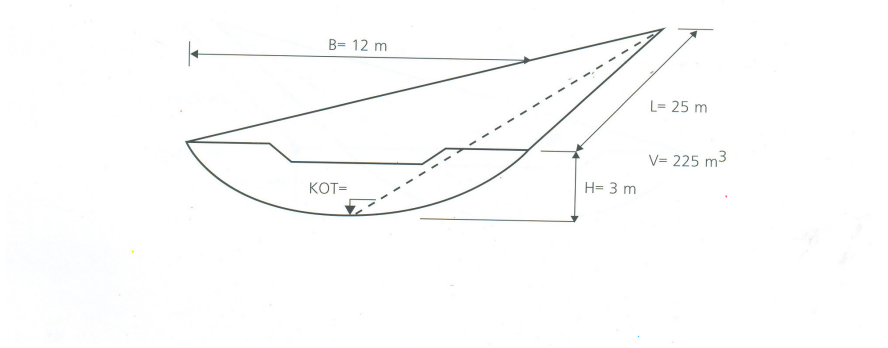

Figure A.13 Weir with number 12 and its characteristics.

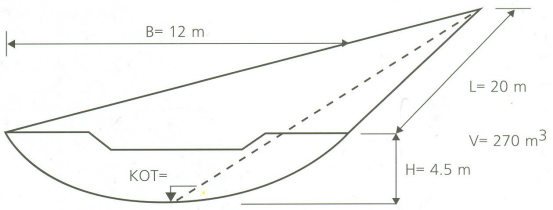

Figure A.14 Weir with number 13 and its characteristics.

Figure A.15 Front view from the outlet.

Figure A.16 Back view from the outlet.

Figure A.17 Bridge on the main stream.

Figure A.18 Bridge on the main stream.

Figure A.19 Culvert on the main stream.

Figure A.20 Bridge on the main stream.

Figure A.21 Bridge on the junction.

Figure A.22 Front view of a bridge on Kartalkaya River.

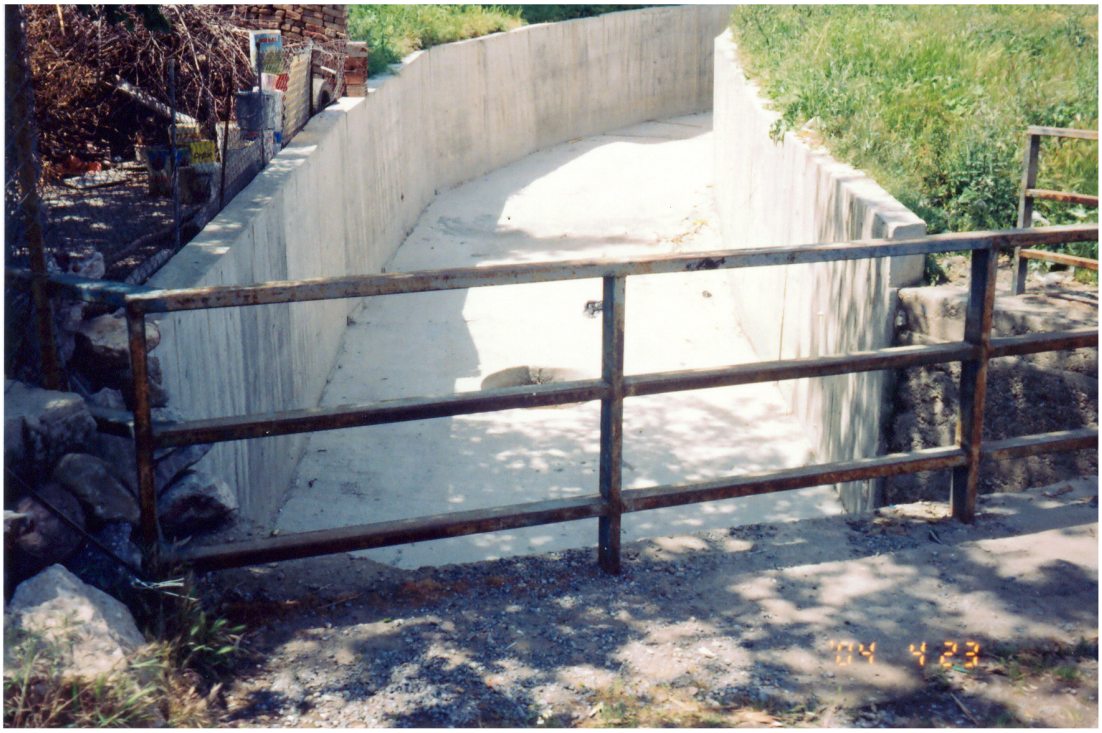

Figure A.23 Back view of a bridge on Kartalkaya River.

Figure A.24 Culvert on Kartalkaya River.

Figure A.25 Culvert on Kartalkaya River.

Figure A.26 Culvert and on Kartalkaya River.

Figure A.27 Culvert on Eskisekikoy River.

Figure A.28 Culvert on Eskisekikoy River.

Figure A.29 Bridge on the main stream.

Figure A.30 Culvert on Koca River.

Figure A.31 Weirs on Koca River.

APPENDIX III
WATER DEPTH & FLOODPLAIN MAPS

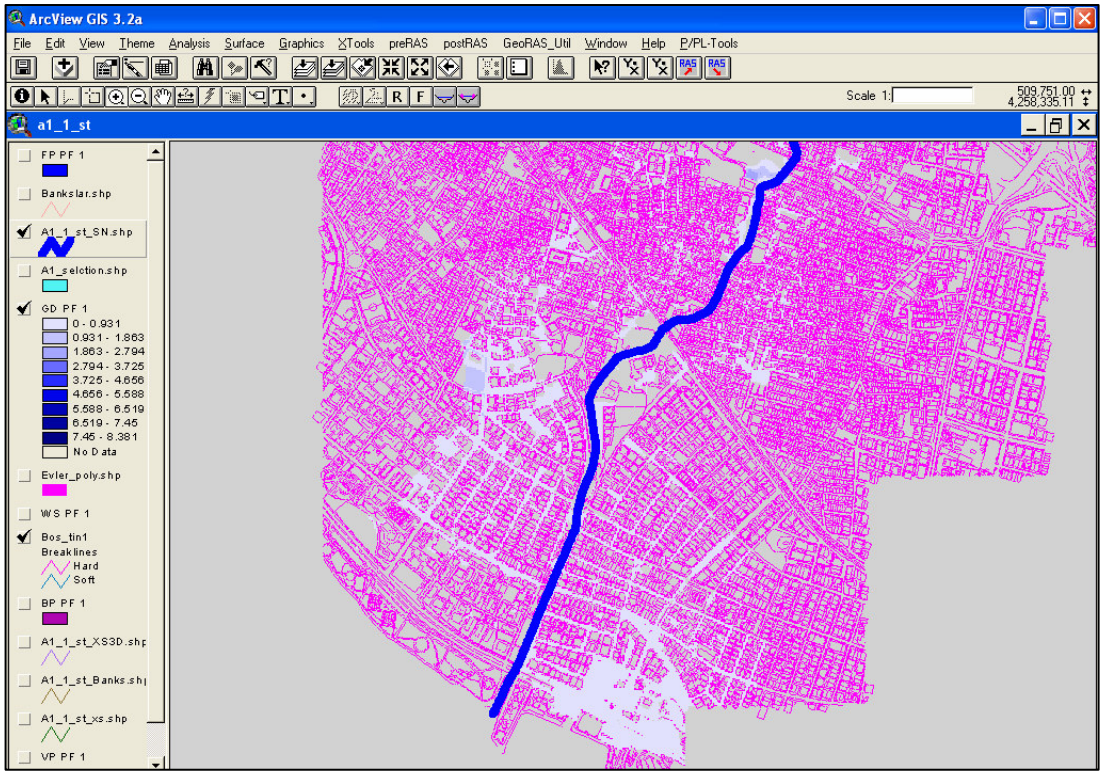

Figure B.1 Water depth map for scenario A1_S.

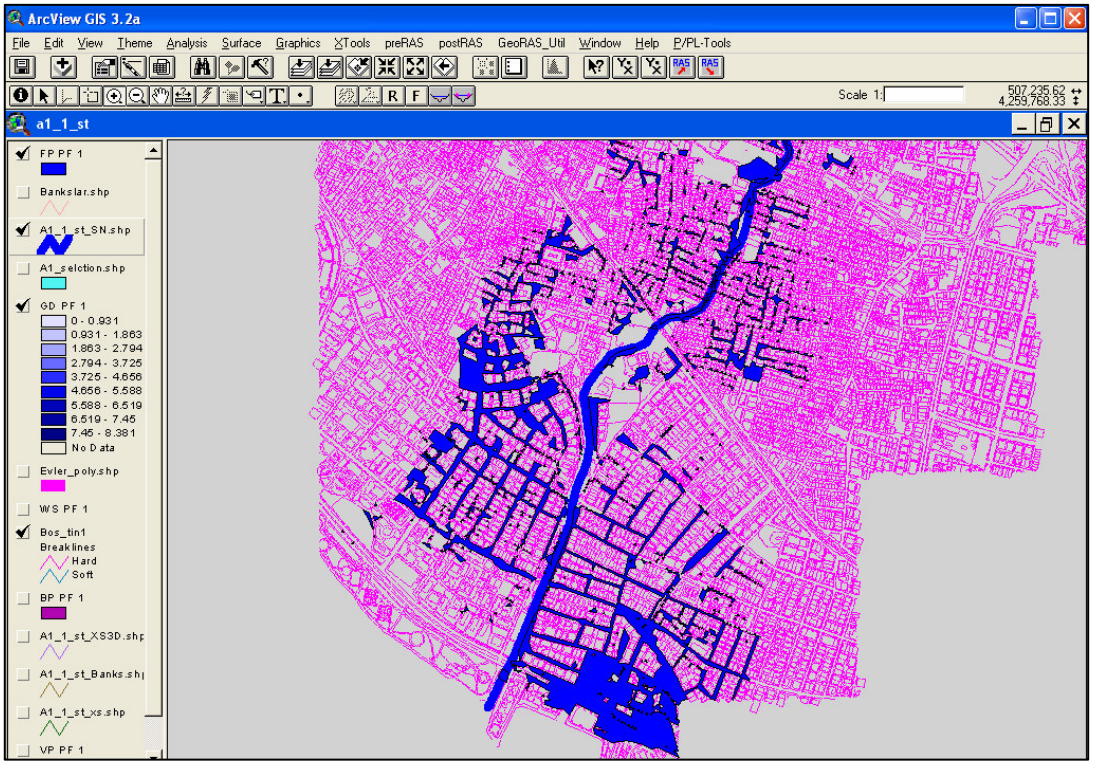

Figure B.2 Floodplain map for scenario A1_S.

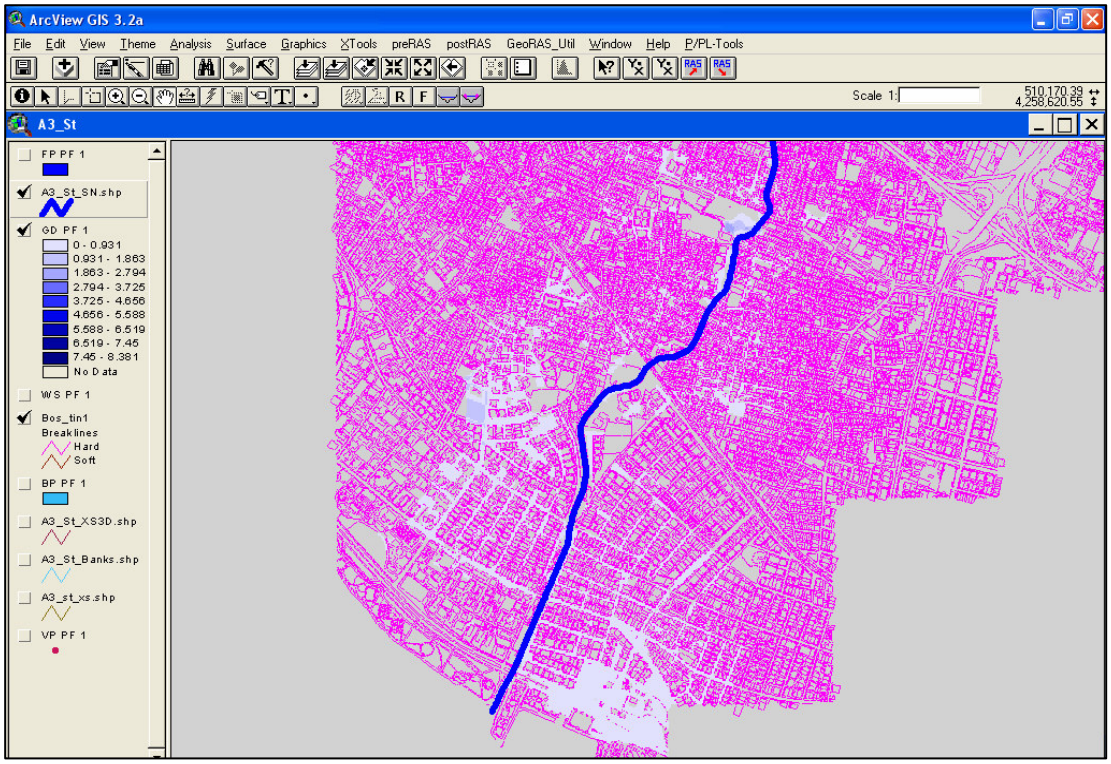

Figure B.3 Water depth map for scenario A3_S.

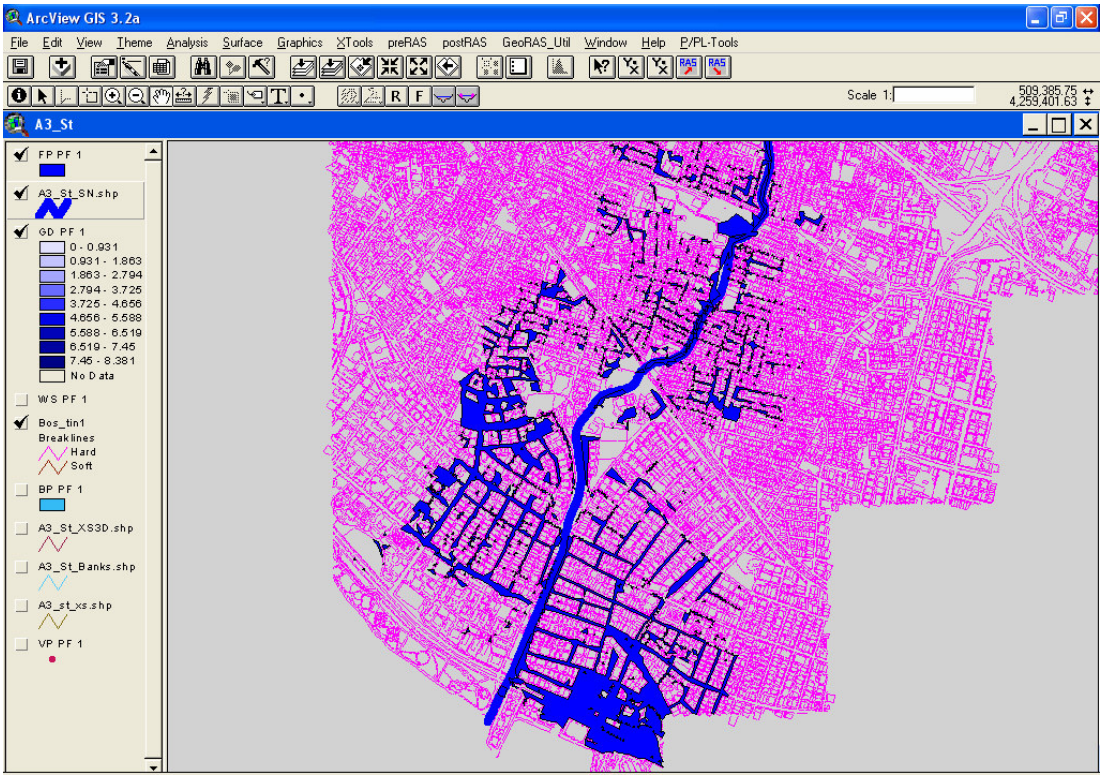

Figure B.4 Floodplain map for scenario A3_S.

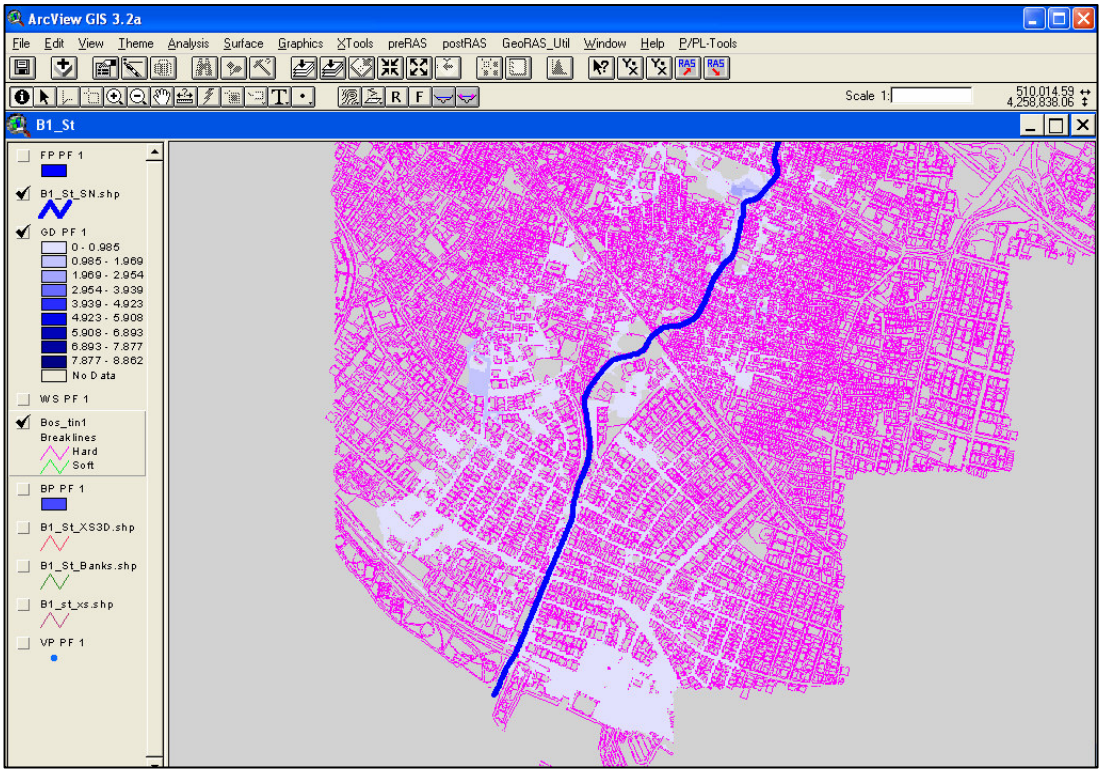

Figure B.5 Water depth map for scenario B1_S.

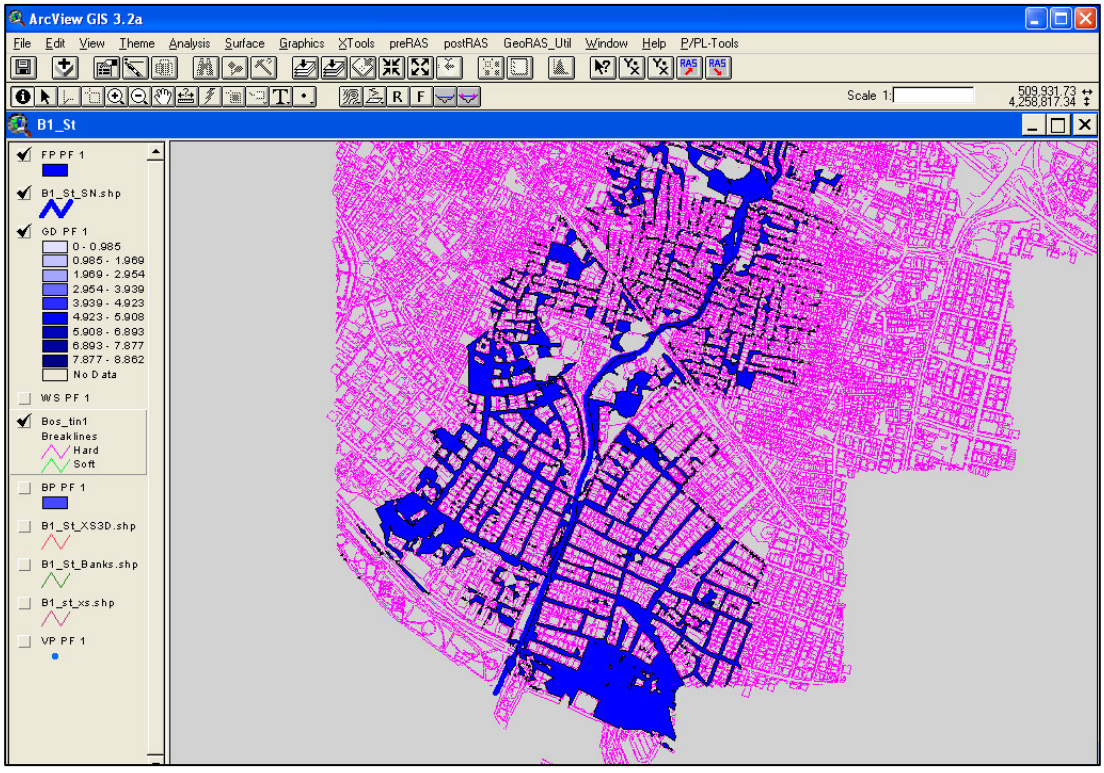

Figure B.6 Floodplain map for scenario B1_S.

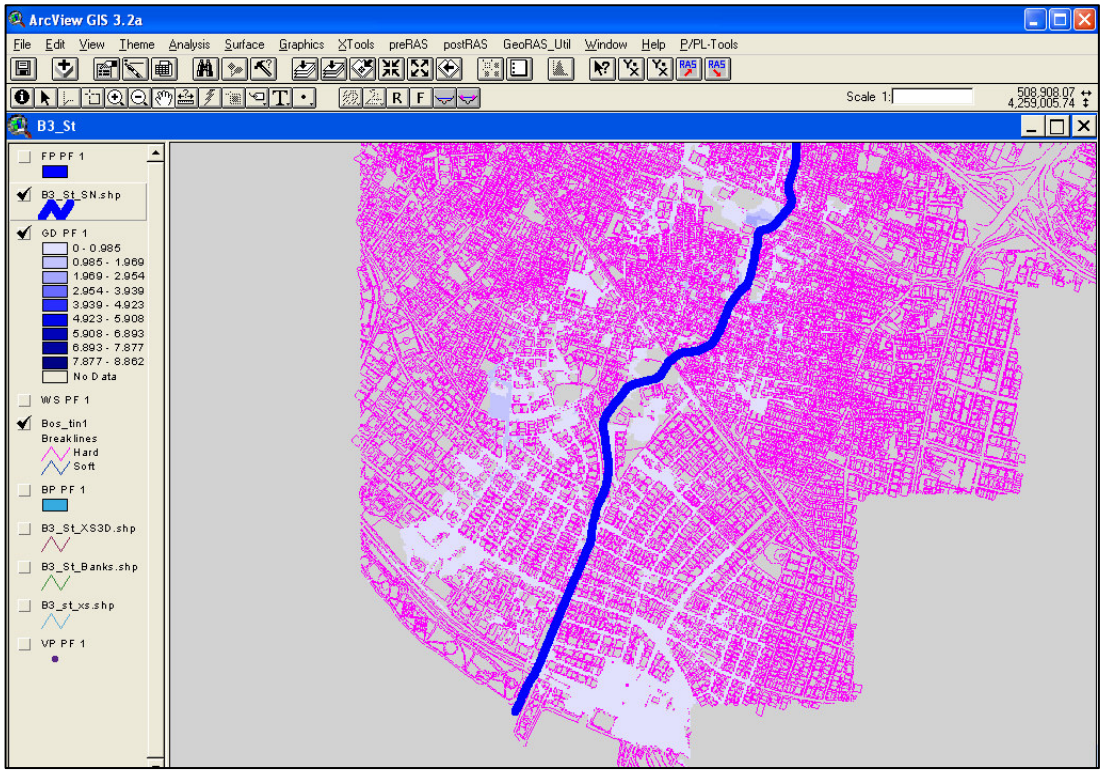

Figure B.7 Water depth map for scenario B3_S.

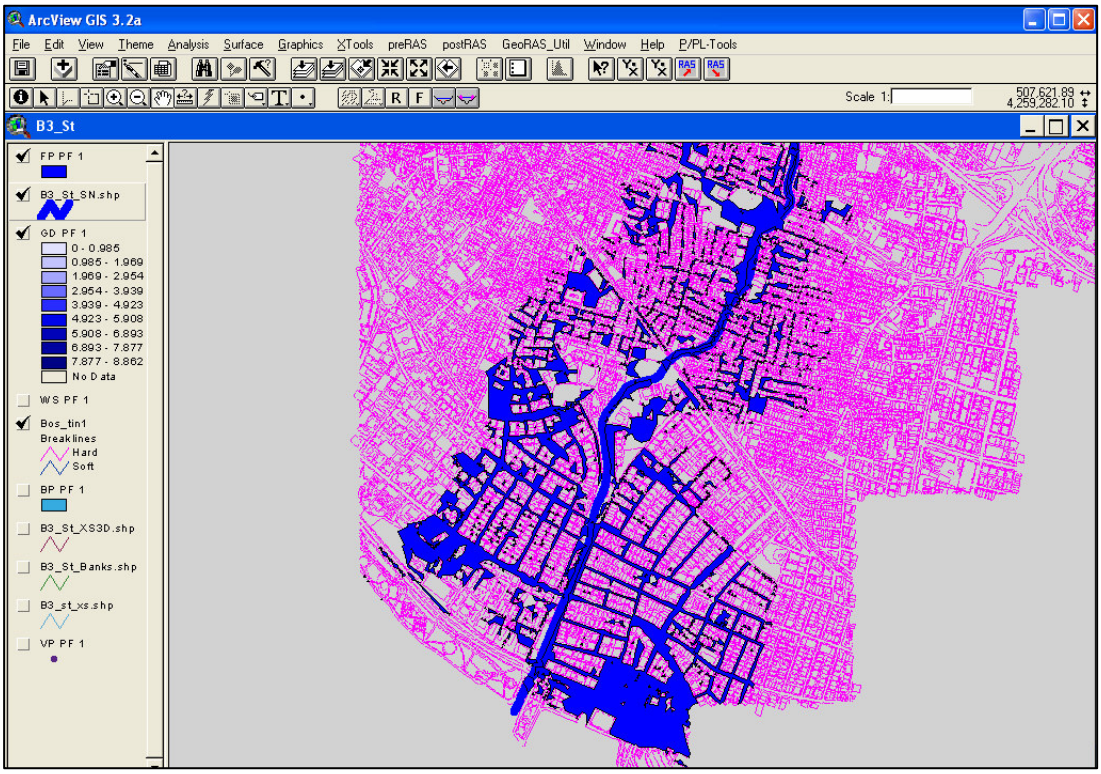

Figure B.8 Floodplain map for scenario B3_S.

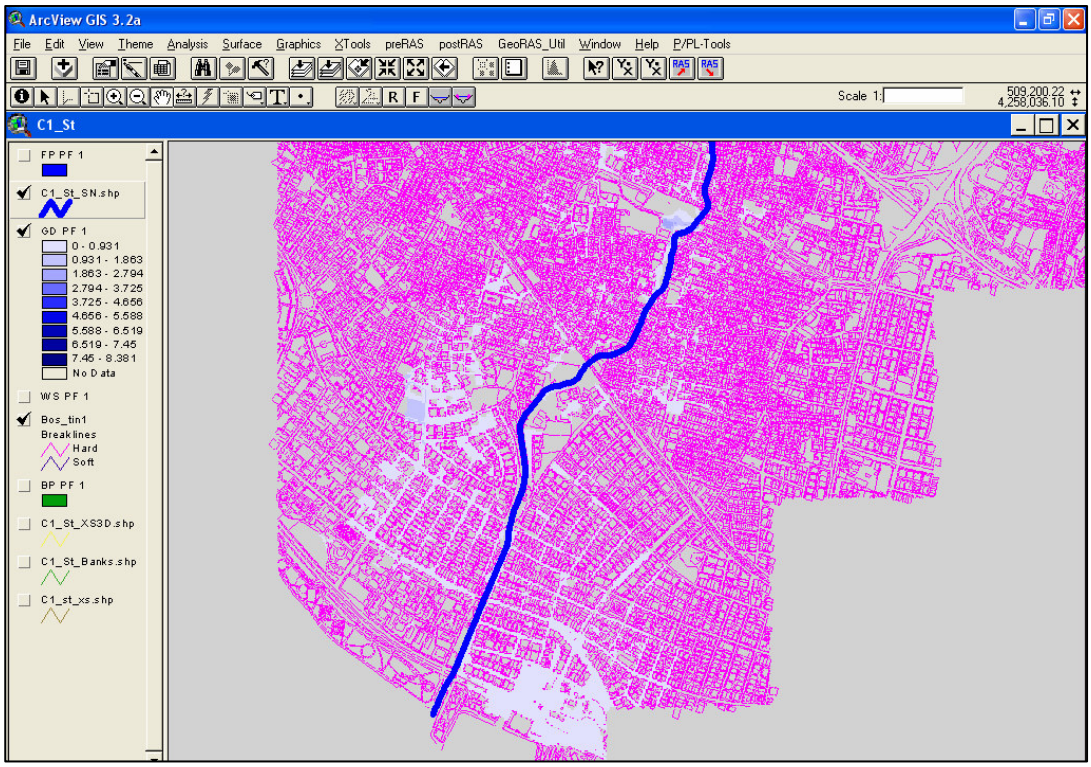

Figure B.9 Water depth map for scenario C1_S.

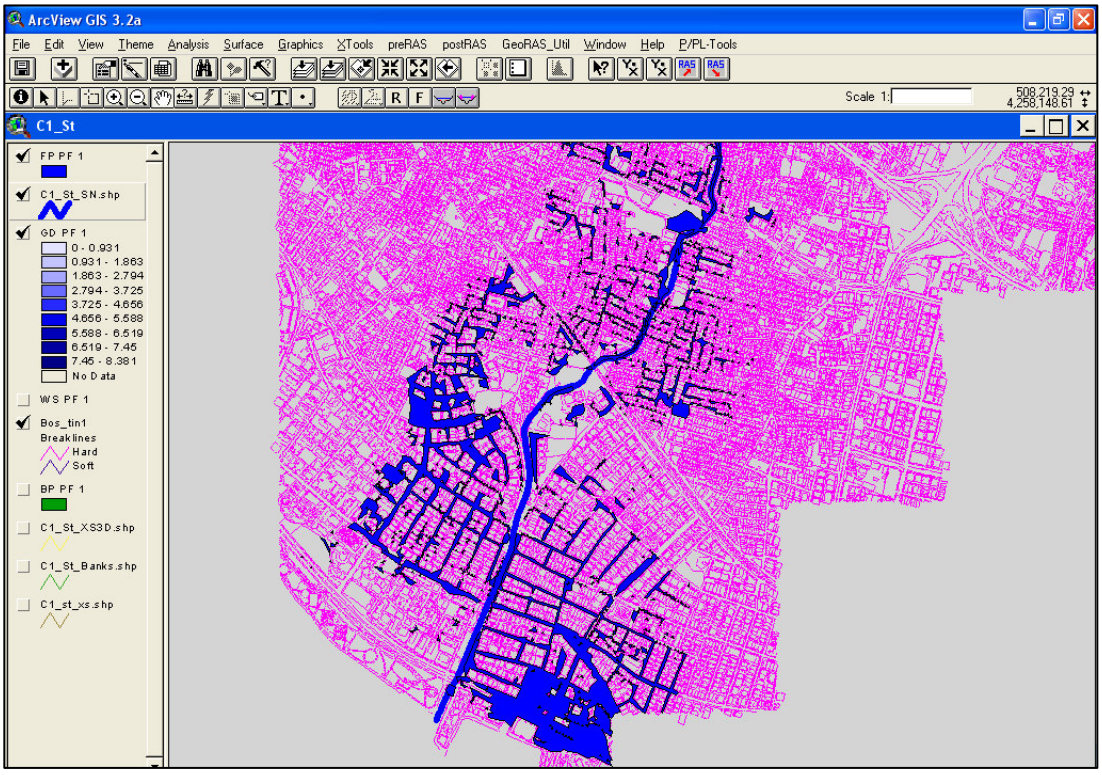

Figure B.10 Floodplain map for scenario C1_S.

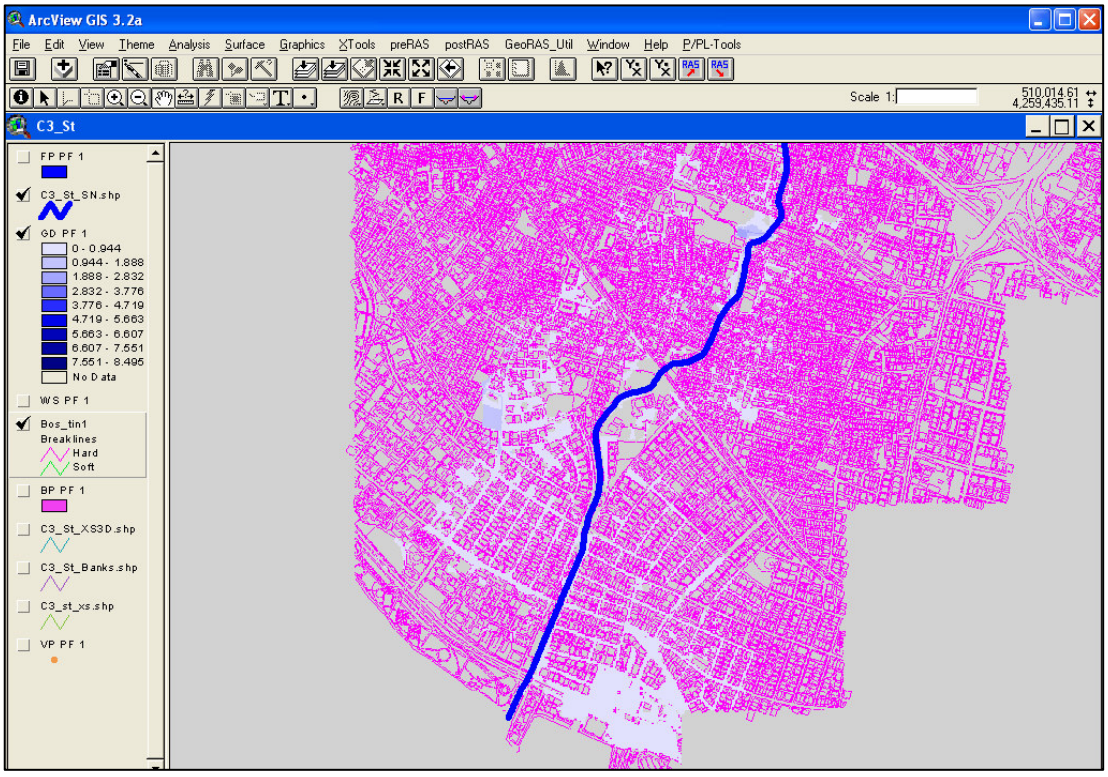

Figure B.11 Water depth map for scenario C3_S.

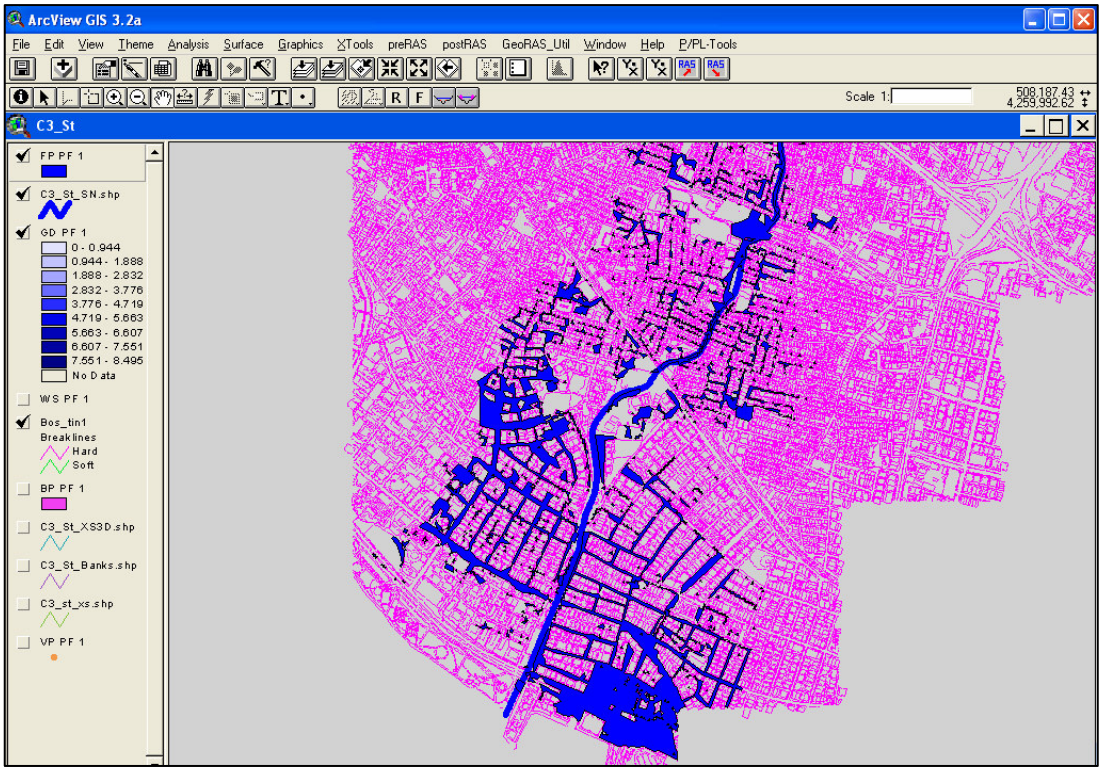

Figure B.12 Floodplain map for scenario C3_S.

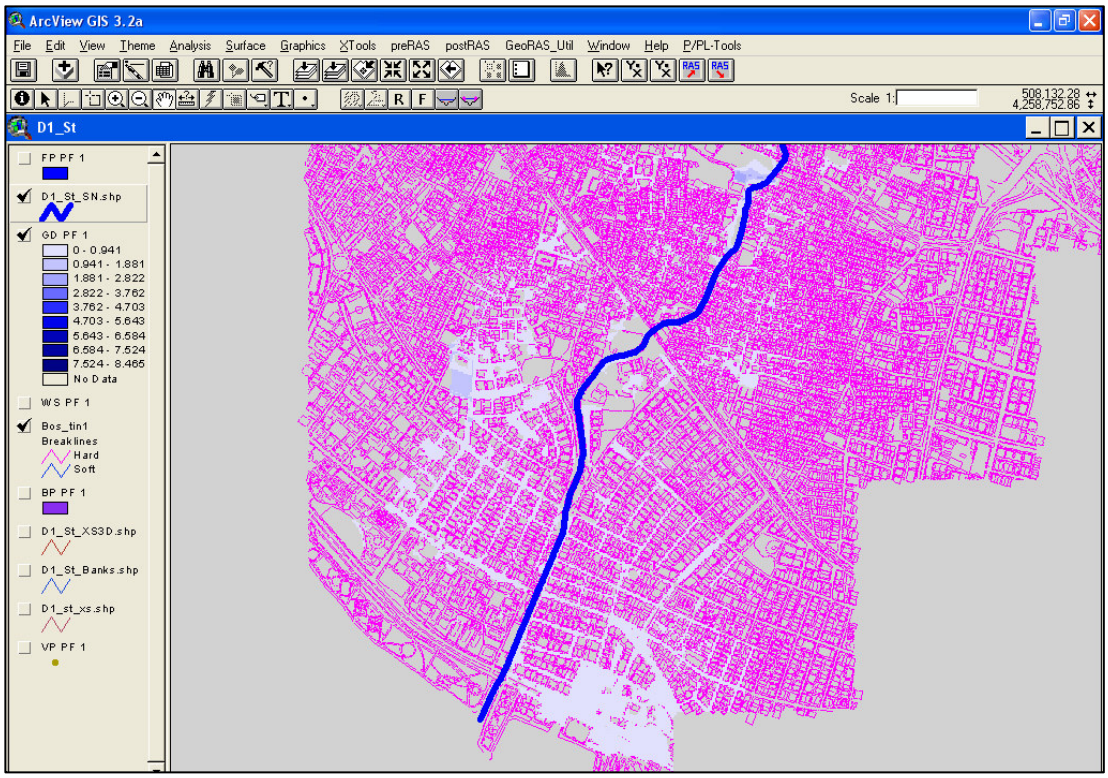

Figure B.13 Water depth map for scenario D1_S.

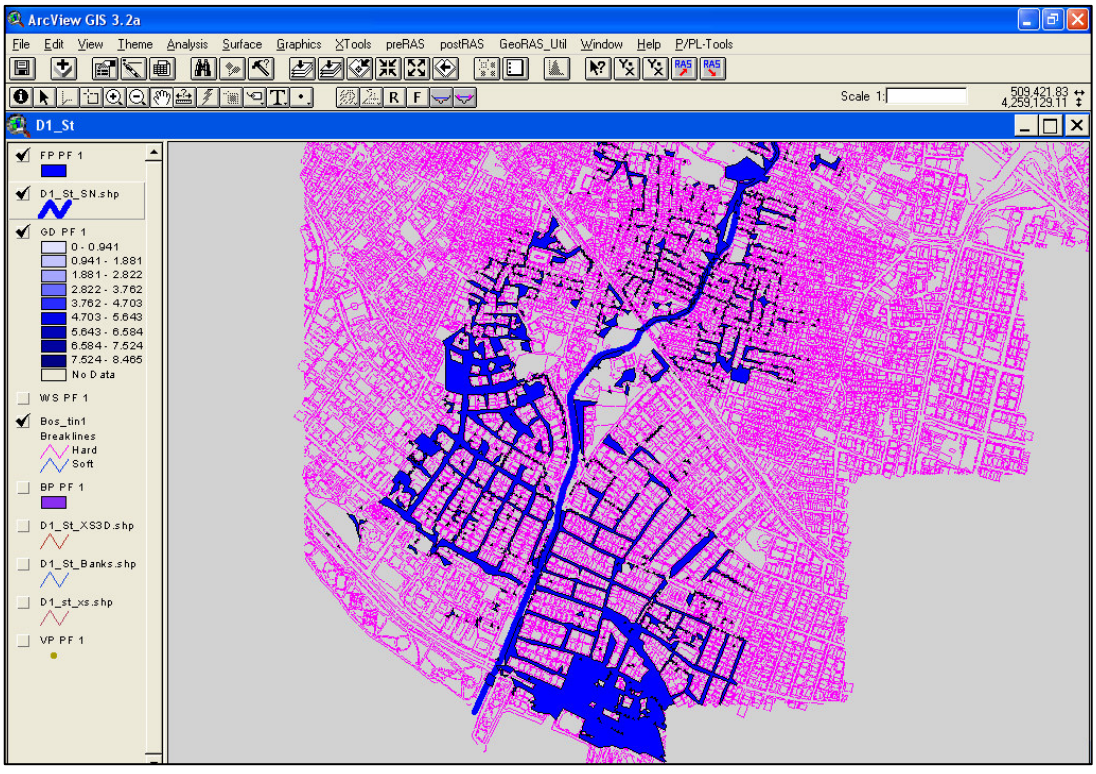

Figure B.14 Floodplain map for scenario D1_S.

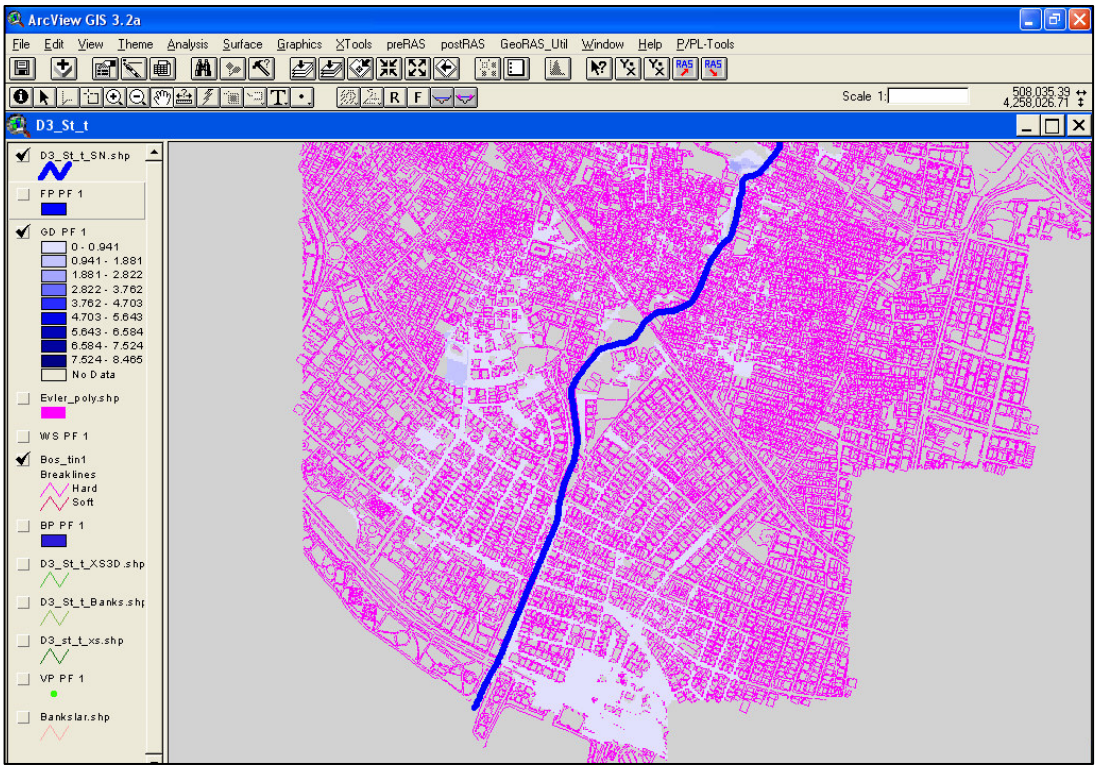

Figure B.15 Water depth map for scenario D3_S.

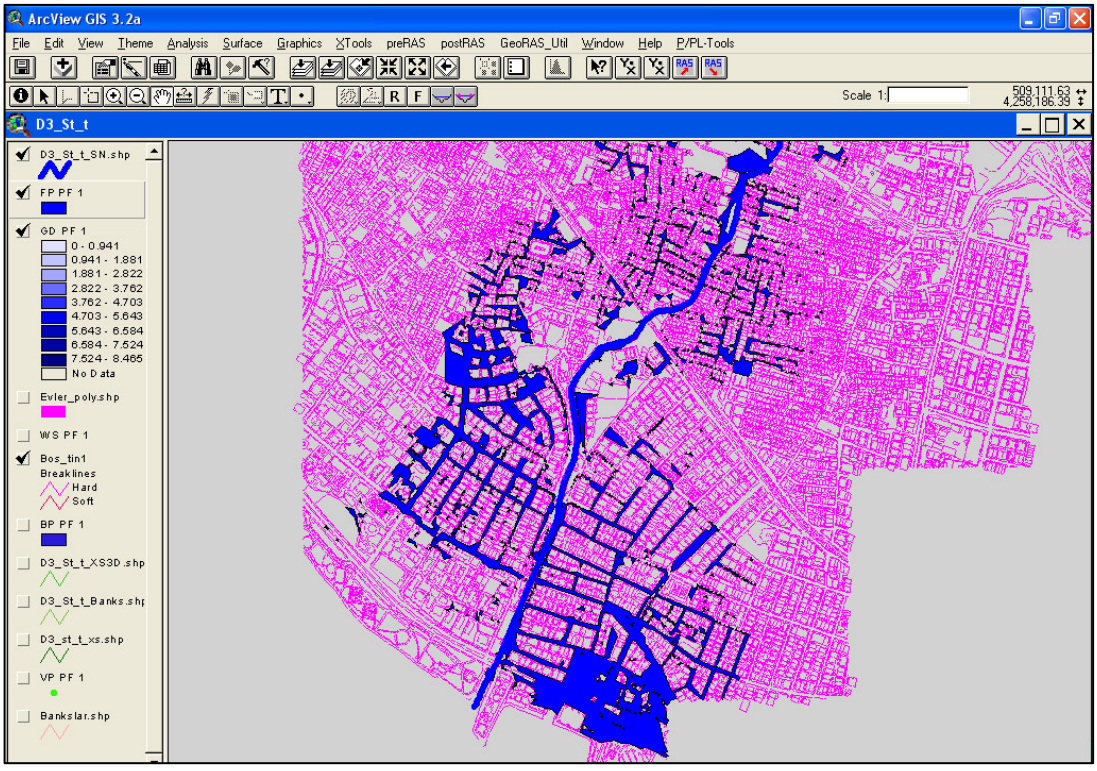

Figure B.16 Floodplain map for scenario D3_S.

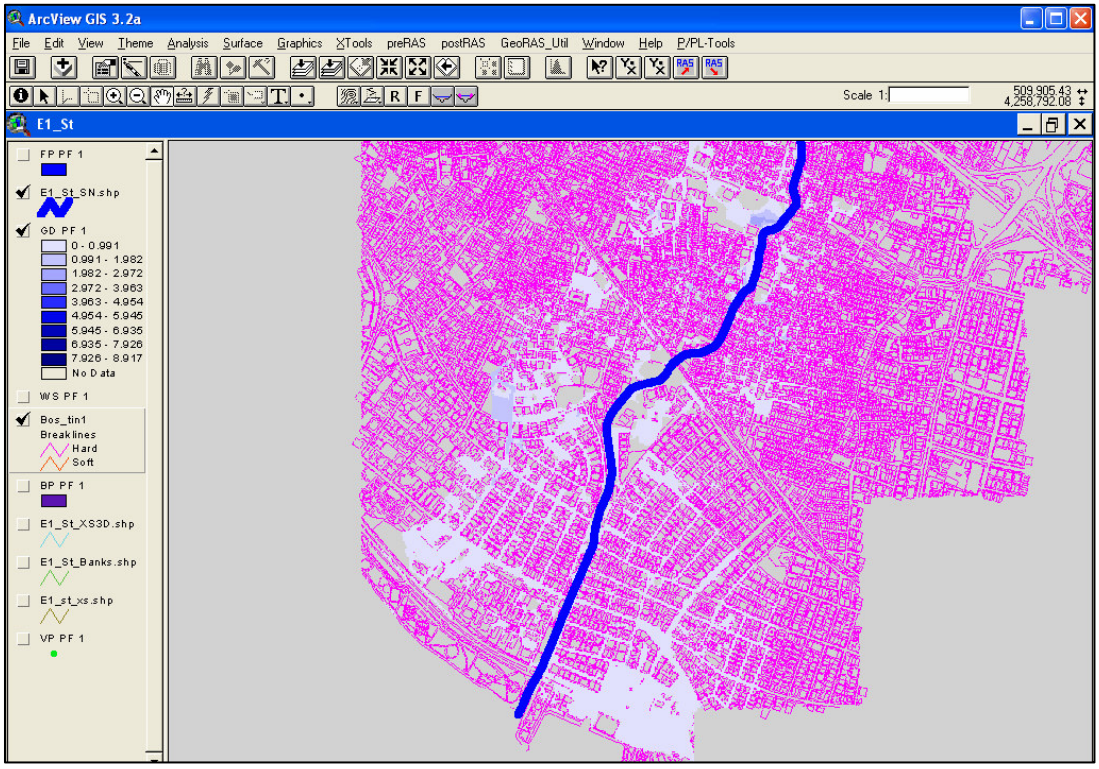

Figure B.17 Water depth map for scenario E1_S.

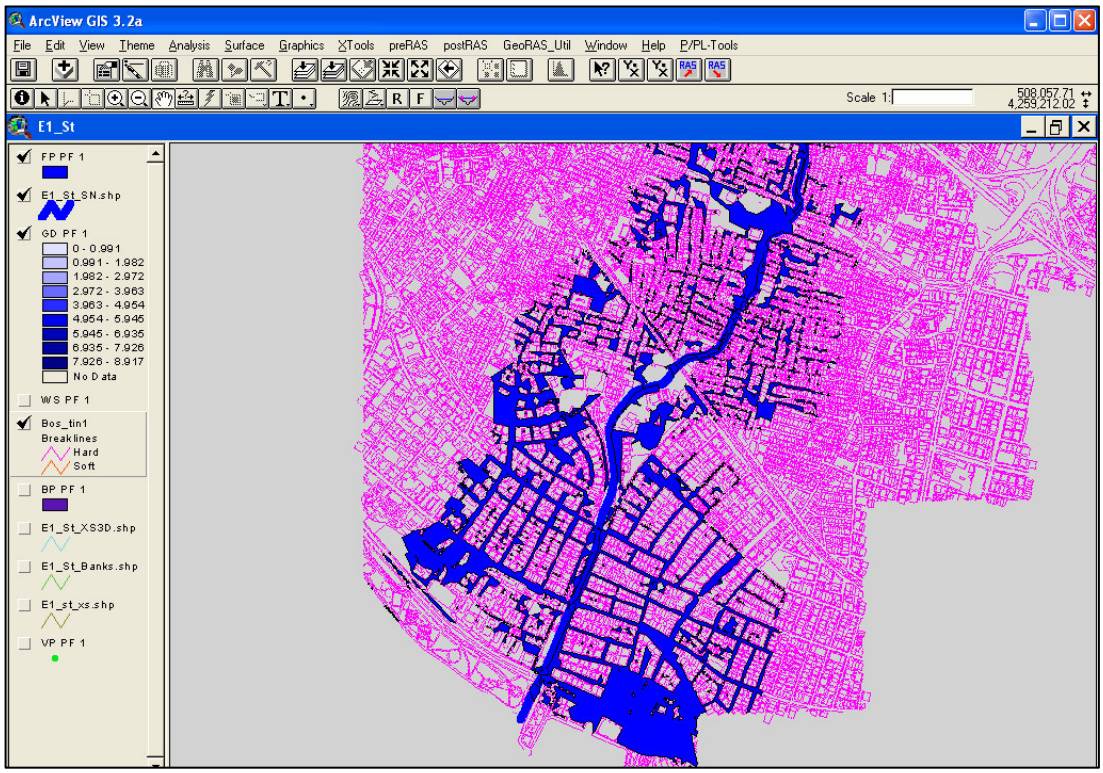

Figure B.18 Floodplain map for scenario E1_S.

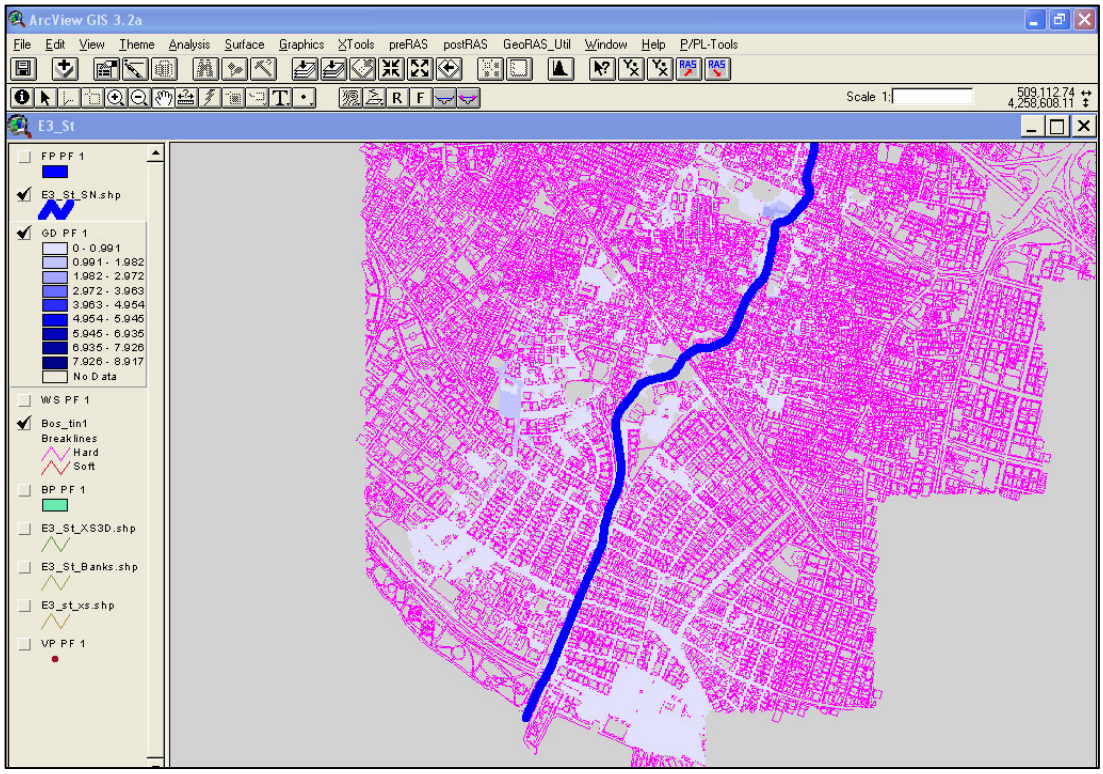

Figure B.19 Water depth map for scenario E3_S.

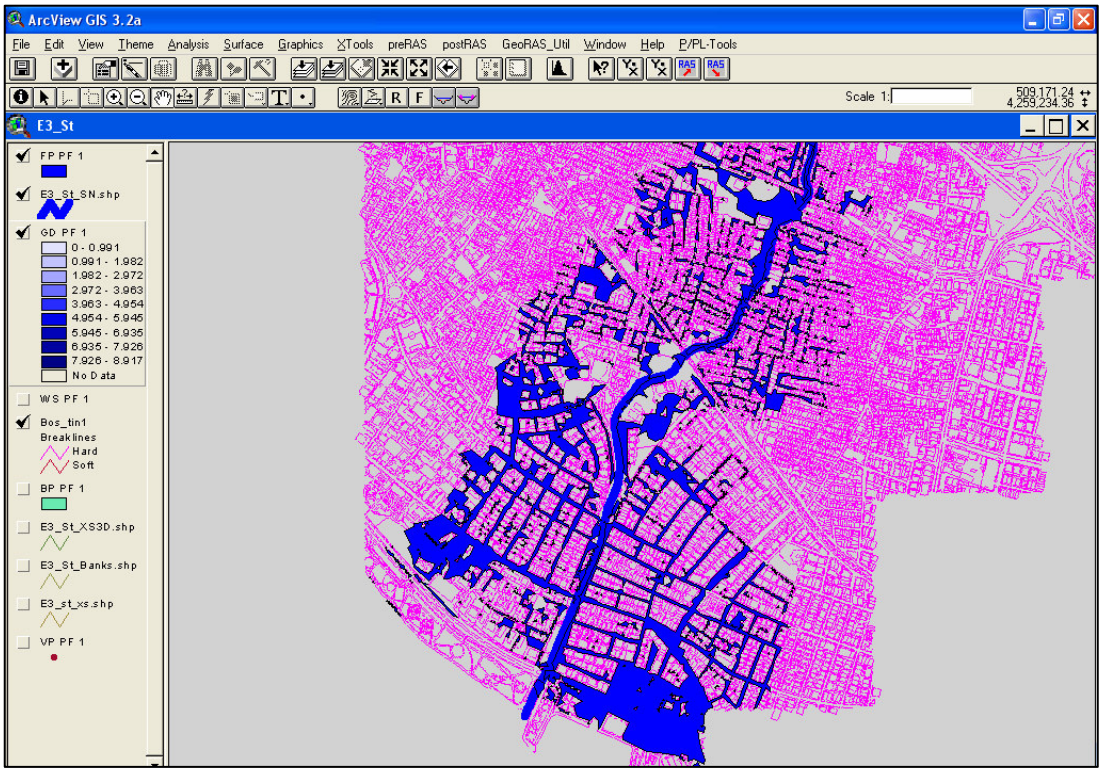

Figure B.20 Floodplain map for scenario E3_S.

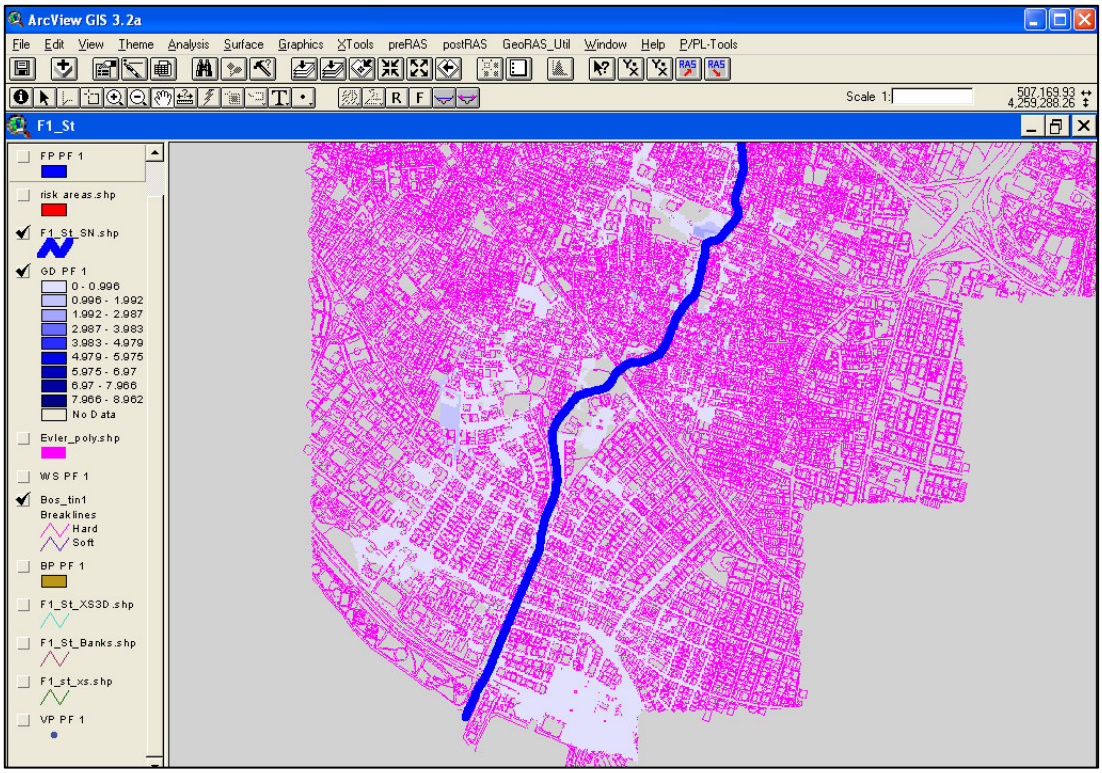

Figure B.21 Water depth map for scenario F1_S.

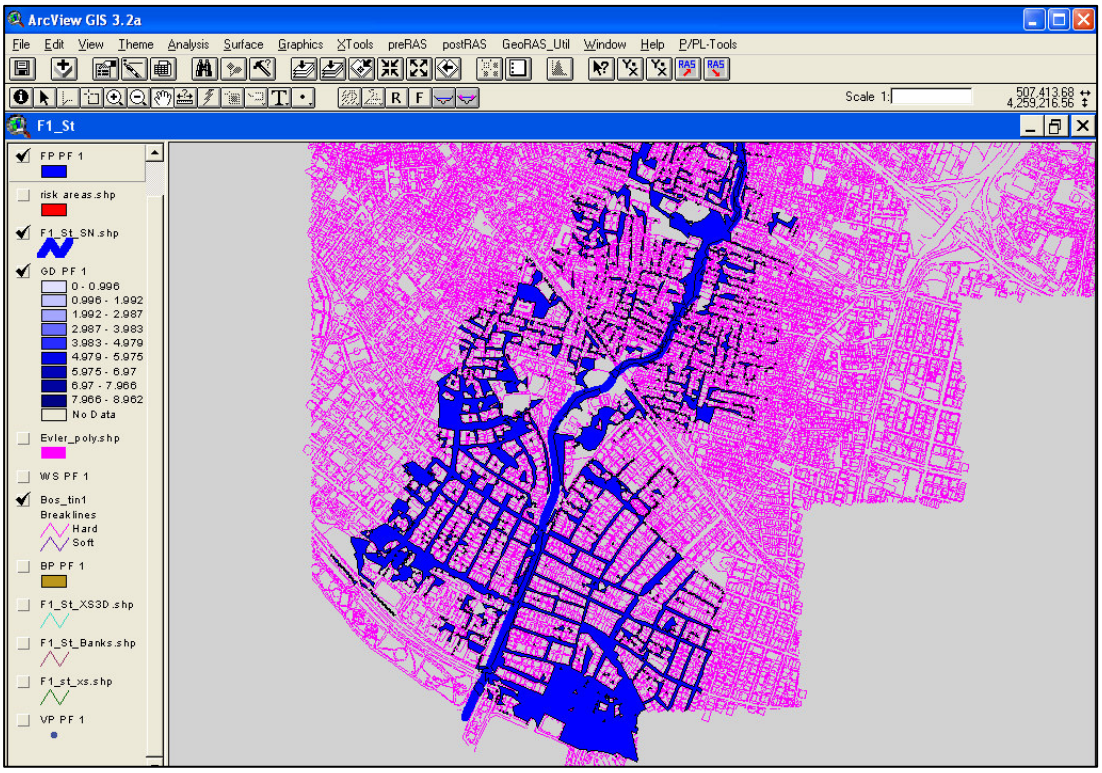

Figure B.22 Floodplain map for scenario F1_S.

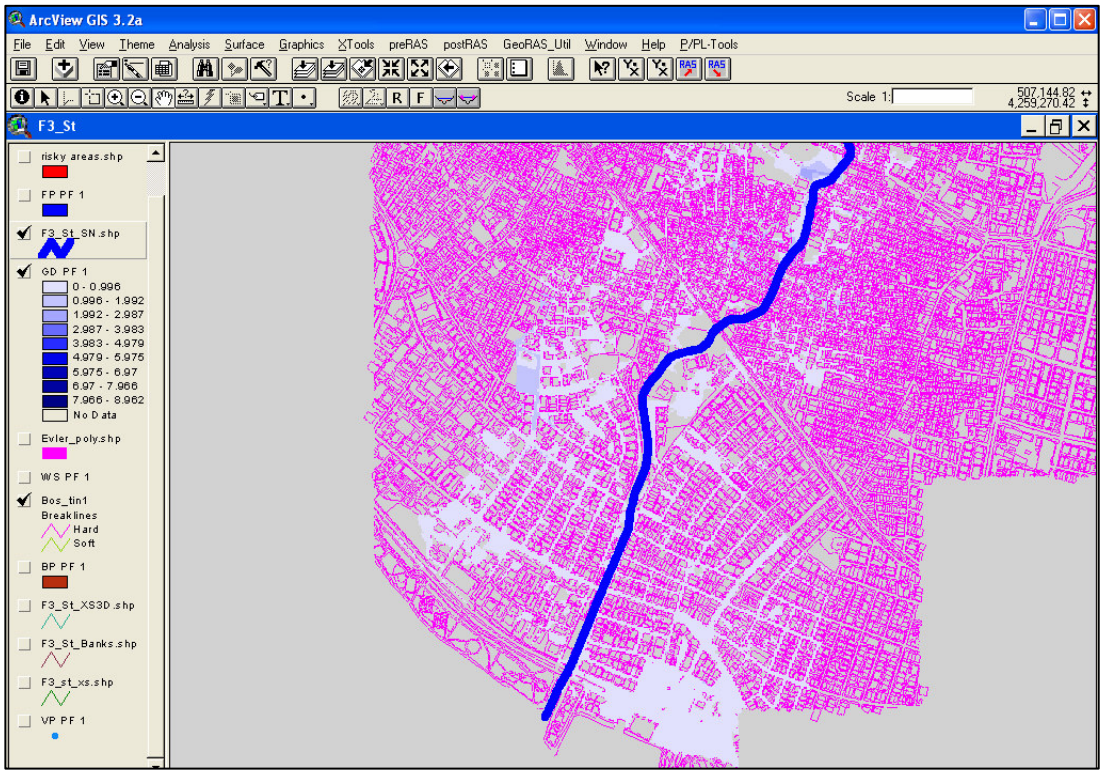

Figure B.23 Water depth map for scenario F3_S.

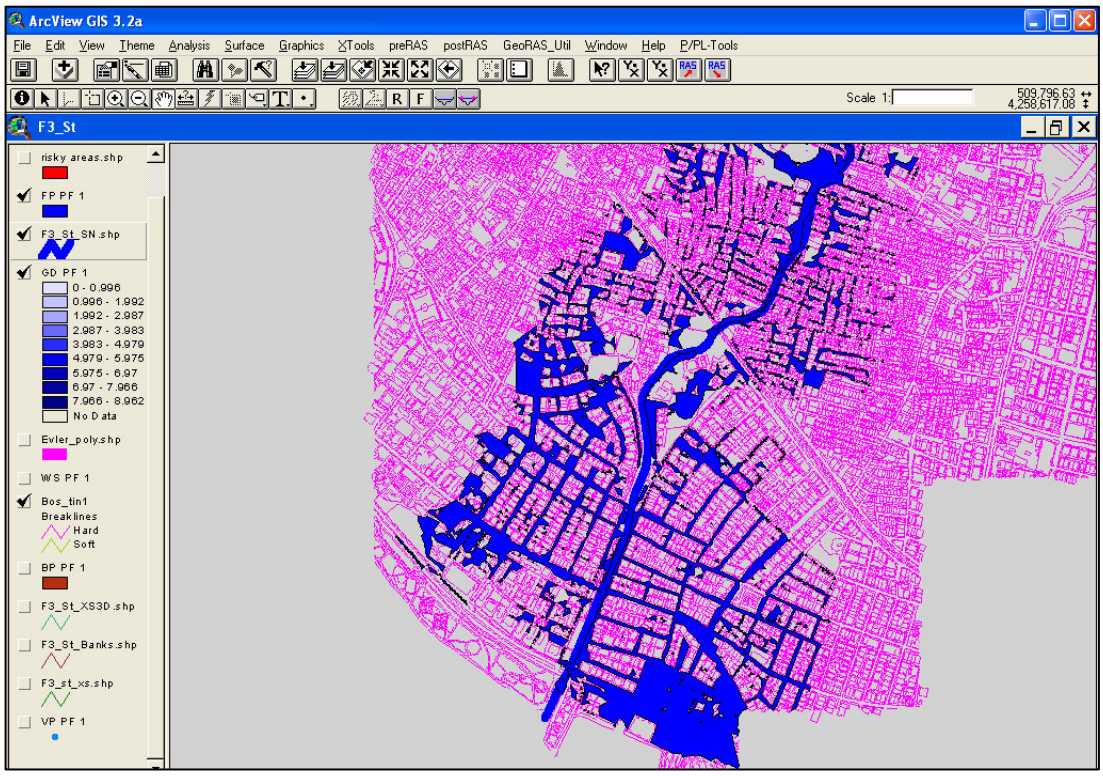

Figure B.24 Floodplain map for scenario F3_S.